Distributed State Estimation and Cooperative Path-Following Under Communication Constraints

THÈSE N^{O} 8626 (2018)

PRÉSENTÉE LE 28 MAI 2018

À L'ÉCOLE POLYTECHNIQUE FÉDÉRALE DE LAUSANNE
À LA FACULTÉ DES SCIENCES ET TECHNIQUES DE L'INGÉNIEUR
LABORATOIRE D'AUTOMATIQUE 3

ET

À L'INSTITUTO SUPERIOR TÉCNICO (IST) DA UNIVERSIDADE DE LISBOA

PROGRAMME DOCTORAL EN ROBOTIQUE, CONTRÔLE ET SYSTÈMES INTELLIGENTS
ET
DOUTORAMENTO EM ENGENHARIA ELECTROTÉCNICA E DE COMPUTADORES

POUR L'OBTENTION DU GRADE DE DOCTEUR ÈS SCIENCES (PhD)

PAR

Francisco FERNANDES CASTRO REGO

acceptée sur proposition du jury:

Prof. J. Santos-Victor, président du jury
Prof. C. N. Jones, Prof. A. M. dos Santos Pascoal, directeurs de thèse
Prof. F. M. Ferreira Lobo Pereira, rapporteur
Prof. A. Seuret, rapporteur
Prof. J. M. Lage de Miranda Lemos, rapporteur

TÉCNICO LISBOA

ÉCOLE POLYTECHNIQUE FÉDÉRALE DE LAUSANNE

Suisse
2018

To my family and friends.

Abstract

The main topics of this thesis are distributed estimation and cooperative path-following in the presence of communication constraints, with applications to autonomous marine vehicles. To this end, we study algorithms that take explicitly into account the constraints imposed by the communication channel, either by reducing the total number of messages per unit of time or quantizing the information with a reduced number of bits and transmitting it at a fixed rate.

We develop a cooperative path following (CPF) algorithm with event-triggered communications and show both through simulations and sea trials with Medusa-class marine vehicles that the self-triggered cooperative path-following algorithm proposed yields adequate performance for formation control of autonomous marine vehicles, while reducing substantially the communications among the vehicles. By exploiting tools from quantized consensus theory, we also provide a method for cooperative path-following with quantized communications, and an algorithm for distributed estimation and control with quantized communications. The performance of the resulting systems is illustrated in simulations.

A new methodology for the design of distributed estimators for linear systems is proposed that yields guaranteed stability in the case of collectively observable systems. The resulting algorithm only requires the broadcasting of each node's state estimate at each discrete time instant. We show via simulations that for some particular conditions the algorithm has a lower estimation error norm than other methods that use the same bandwidth and yields stable estimation errors for unstable systems.

This thesis also proposes a distributed estimation and control algorithm with progressive quantization. We show that with an appropriate parameter choice and given that the system is collective detectable, the algorithm proposed yields a bounded estimation error and state for every agent, with bounds proportional to the process and measurement noise of the system. Finally, it is shown in tests with model cars that distributed estimation with quantized consensus is a feasible strategy for formation control using only range measurements between the vehicles.

Key words: Distributed state estimation; Cooperative path-following; Quantized consensus; Event-triggered communications; Input-to-state stability

Resumo

Os principais tópicos desta tese são estimação distribuída de estados e seguimento de caminho cooperativo na presença de restrições de comunicação, com aplicações em veículos marítimos autónomos. Para este fim, estudamos algoritmos que tomam em consideração explicitamente as restrições impostas pelo meio de comunicação, seja reduzindo o número total de mensagens transmitidas por unidade de tempo ou codificando a informação com um número reduzido de bits e transmitindo-a a uma velocidade fixa.

Desenvolvemos um algoritmo de seguimento de caminho cooperativo (CPF) com comunicações desencadeadas por eventos e mostramos através de simulações e ensaios no mar com veículos marítimos da classe Medusa que o algoritmo de seguimento de caminho com comunicações auto-desencadeadas proposto produz um desempenho adequado para o controlo de formações de veículos marítimos autónomos, enquanto reduz substancialmente as comunicações entre os veículos. Ao utilizar ferramentas da teoria de consenso quantizado, fornecemos também um método para seguimento de caminho cooperativo com comunicações quantizadas e um algoritmo para estimação de estados e controlo distribuídos com comunicações quantizadas. O desempenho dos sistemas resultantes é ilustrado através de simulações.

É proposta uma nova metodologia para o projeto de estimadores distribuídos para sistemas lineares com garantia de estabilidade no caso de sistemas colectivamente observáveis. O algoritmo proposto requer apenas a transmissão da estimativa do estado do sistema de cada nó, em cada instante de tempo discreto. Mostramos através de simulações que, para algumas condições particulares, o algoritmo produz uma norma do erro de estimação mais baixa do que outros métodos que usam a mesma largura de banda e produz erros de estimação estáveis em sistemas instáveis.

Esta tese também propõe um algoritmo de estimação e controlo distribuído com quantização progressiva. Mostramos que com uma escolha de parâmetros apropriada e dado que o sistema é coletivamente detectável, o algoritmo proposto produz um erro de estimação limitado em cada agente, com limites proporcionais às magnitudes da perturbação e ruído de medição do sistema, e estabiliza o sistema. Finalmente, é ilustrado com recurso a testes com automóveis de radiomodelismo que o algoritmo de estimação distribuída com recurso a consenso quantizado é uma estratégia viável para o controlo de formações utilizando apenas medidas da distância entre os veículos.

Palavras-chave: Estimação de estados distribuída; Seguimento de caminho cooperativo; Consenso quantizado; Comunicações desencadeadas por eventos; Estabilidade entrada-estado.

Résumé

Les principaux topiques de cette thèse sont l'estimation distribuée d'états et suivi de chemin coopératif avec la présence de contraintes de communication, avec des applications sur véhicules marins autonomes. Avec cet objective nous étudions des algorithmes que prennent en considération d'une façon explicite les contraintes imposées par le moyen de communication, soit en réduisant le total de messages transmises par unité de temps soit en codifiant l'information avec un nombre réduit de "bits" et la transmettre avec une vitesse constante.

Nous avons développé un algorithme de suivi de chemin coopératif (CPF) avec des communications déclenchées par évènements et nous avons montré avec des simulations et expériences avec des véhicules marins de classe Medusa que l'algorithme alternatif proposé de suivi de chemin avec des communications auto-déclenchées produit une adéquate performance pour le contrôle de formations de véhicules marins autonomes en même temps réduisant fortement les communications entre les véhicules. En utilisant des outils de la théorie de consensus "quantizé" nous présentons aussi une méthode pour le suivi de chemin coopératif avec communications "quantizées" et un algorithme d'estimation d'états et contrôle distribués avec communications "quantizées". La performance des systèmes développés est illustrée avec des simulations.

Une nouvelle méthodologie est proposée pour le projet d'estimateurs distribués pour systèmes linéaires qui produit une garantie de stabilité dans le cas de systèmes collectivement observables. L'algorithme proposé exige seulement la transmission de l'estimation de l'état du système en chaque nœud, en chaque instant de temps discret. Nous montrons avec des simulations que, pour certes conditions particulières, l'algorithme produit une norme de l'erreur d'estimation moins élevée que d'autres méthodes qu'utilisent le même largueur de bande et produit des erreurs d'estimation stables avec des systèmes instables.

Cette thèse propose aussi un algorithme d'estimation de contrôle distribué avec une "quantization" progressive. Nous montrons que, avec un adéquat choix de paramètre et quand le système est collectivement détectable, l'algorithme proposé produit un erreur d'estimation limité en chaque agent, avec des limites proportionnels aux magnitudes de perturbation et bruit de mesure du système, et stabilise le système. Finalement, avec des expériences avec des automobiles de radio modélisme, nous montrons que l'algorithme d'estimation distribuée basé sur le consensus "quantizé" est une stratégie viable pour le contrôle de formations en utilisant seulement la mesure des distances entre véhicules.

Mots clefs : Estimation distribuée d'états ; suivi de chemin coopératif ; Consensus "quantizé" ; communications déclenchées par évènements ; stabilité entrée-état.

Acknowledgements

First and foremost, I would like to thank my supervisors, António Pascoal, Pedro Aguiar and Colin Jones, from whom I learned a great deal throughout these years. Although they always allowed me to pursue my own ideas, it is worth reminding that this thesis is also, in a large proportion, a product of their guidance. They nudged me several times in what I now believe was the right direction, pushing me to be rigorous and, to the best of my abilities, to write in an accessible fashion. For this, and for trusting in my work, I am profoundly grateful.

It must also be mentioned that the years during which I performed this work were greatly rewarding because of the outstanding working environments I was in. During this period I have been at the Automatic Control Laboratory (LA) at École Polytechnique Fédérale de Lausanne (EPFL) and at the Dynamic Systems and Ocean Robotics (DSOR) laboratory at the Institute For Systems and Robotics (ISR) at Instituto Superior Técnico (IST). I would like tho thank all the members of both institutions, for all the technical discussions, collaborations, and the genuine friendship I found there.

Many of my colleagues at DSOR and LA, also contributed to this work in different capacities and deserve to be mentioned. João, Jorge, Luís, and Manuel, who provided invaluable technical and operational assistance for the MEDUSA experiments. Sérgio, Andrea, Ye and Hung with whom I had the pleasure of co-authoring publications. Amaury Soviche and Mathieu Bresciani, who joined us for semester and master projects and whose work made it into this thesis in some form. I must also thank all of those involved in the IST-EPFL Joint Doctoral Initiative that gave me this unique opportunity of studying in two great universities.

Since the life of a PhD student is not only work, I must thank also my friends who supported me during this period. I am happy to count everyone at LA and DSOR within this group. Special mentions go to the Aerospace clique composed by the Pedros (Fernandes and Gonçalves), Fred, Nuno, Éder and Simão, in Lisbon and to Ricardo and Barbara in Geneva. I am also very grateful for the support of José and Maria Turiel during all the period I was in Lausanne. I felt more portuguese there than I do here in Lisbon.

Last but definitively not least, I would like to thank my family, who have always supported me throughout these 30 years. My mother, who worry more than I do and made me aware of all the possible troubles down the road, and my father and sister who helped me to put those troubles in perspective. Elsa for not letting me ever be hungry and my son Francisco for his constant availability to solve any problems I had. My grandparents, who are the best role models one could ask, and my big extended family who is always present.

Lisbon, 5 December 2017 F. F. C. R.

Funding institutions

- Fundação para a Ciência e a Tecnologia through doctoral grant [SFRH/BD/51929/2012]
- European Union through project MORPH [EU FP7 ICT 288704]
- EPFL through discretionary funding for the LA3 salary envelope

Contents

List of Figures

Introduction Part I

1 Motivation

Motivated by advances in small embedded processors, sensors, and miniaturized actuators, the development of fleets of autonomous marine vehicles has been gaining momentum worldwide, bringing into sharp focus their potential to drastically improve the means available for ocean exploration and exploitation. It is envisioned that the use of multiple autonomous robotic vehicles acting in cooperation will drastically increase the performance, reliability, and effectiveness of automated systems at sea. Possible scientific and commercial missions include marine habitat mapping, geophysical surveying, and adaptive ocean sampling, to name but a few.

In this thesis we address a number of problems that arise in the cooperative operation of multiple marine vehicles due to the presence of bandwidth limitations, when only a limited amount of data are exchanged among multiple distributed systems or agents per unit of time. In particular, we focus on the topics of networked cooperative control and estimation for multiple vehicle operations. This issue is of paramount importance in practical applications, since lower bandwidth translates into lower energy consumption and, consequently, into increased operational autonomy. Bandwidth limitations are particularly stringent in underwater applications since communication between vehicles takes place over low bandwidth, short range communication channels that have intermittent failures, multi-path effects and delays.

In the field of cooperative marine vehicle motion control, a wide range of applications require the solution of the problem of cooperative path following (CPF). The latter consists of, given n autonomous vehicles and different spatial paths assigned to them, deriving control laws to drive and maintain the vehicles on their paths with desired speed profiles, holding a specified formation pattern. In the literature, Ihle et al. [2006], Ghabcheloo et al. [2009] offer a theoretical overview of the subject and introduce techniques to solve the CPF problem. Different solutions to the CPF and similar problems can be seen in Giulietti et al. [2000], Stilwell and Bishop [2000], Ogren et al. [2002], Jadbabaie et al. [2003], Moreau [2005], Ma and Zhang [2010], Dong [2011]. One of our objectives in this thesis is to solve the CPF problem while keeping the communication bandwidth low.

Another type of problem that we address is motivated by one of the most challenging mission scenarios at sea: underwater habitat mapping in complex 3D environments, where the flexible structure of a fleet of small autonomous underwater vehicles (AUVs) is preferable to a single well-equipped AUV. In this scenario, it is critical that a number of vehicles carrying different sensor suites and navigation equipment maneuver in formation at close range, cooperating towards the acquisition of environmental data. Meeting this objective requires that the vehicles be equipped with advanced systems for networked navigation and control. As an example, we cite a mission in shallow water where one or more surface vehicles (the anchor vehicles) are equipped with advanced sensor suites for absolute geo-referencing, such as GPS, so as to follow desired paths or maneuver along arbitrary trajectories in response to episodic events. It is up to the follower vehicles in the fleet to reach and maintain a desired formation with the anchors, effectively moving along at the same speed while acquiring relevant environmental data with complementary sensor suites. In practice, executing this type of mission without expensive inertial sensor suites requires the follower vehicles to maneuver into formation by relying on measurements of their distances to the leading vehicles and exchanging complementary data. This entails considerable difficulties underwater, as conventional communication and localization systems are unavailable and usually replaced by acoustic devices: acoustic modems that allow the exchange of data, and ranging devices that estimate distances by measuring time-of-flight of acoustic signals. These devices exhibit a number of constraints that are inherent to the medium, such as temporary communication losses, outliers in the range measurements, and low bandwidth of the acoustic communication systems. In practice, an important consequence of these limitations is the inability to measure or communicate frequently, with inter-sample times often in the range of seconds, making the problem of underwater range-based multiple vehicle formation keeping very challenging.

The example mission of underwater mapping mentioned above leads to one of the problems that we address in this thesis, where each vehicle is required to know its absolute position and those of the neighboring vehicles, while measuring ranges to neighbouring vehicles. This problem is referred to as cooperative navigation, and when applied to the problem of formation control it is named range-based formation control. The problem of cooperative navigation is contained within the larger scope of distributed state estimation, which will also be addressed in this thesis. Spawned by recent advances in wireless sensor networks (WSNs) and distributed sensing, there has been a flurry of activity on the topics of distributed state estimation and its interaction with control, see for example Olfati-Saber [2005], Khan and Moura [2007, 2008], Calafiore and Abrate [2009], Garin and Schenato [2010], Battistelli and Chisci [2014], Li et al. [2015b], Battistelli et al. [2015], Battistelli and Chisci [2016] and the references therein. These issues are at the core of a wide range of applications, from network localization to environmental monitoring, surveillance, object tracking, collaborative information processing, and traffic monitoring (see Akyildiz et al. [2002], Xu [2002], Bethke et al. [2007], Smith and Hadaegh [2007], Zavlanos [2008], Ghabcheloo et al. [2009], Bahr et al. [2009], Mesbahi and Egerstedt [2010], Aberer et al. [2010], Prathap et al. [2012], Soares et al. [2013], Rawat et al. [2014], Soares et al. [2015a,b] for an introduction to these issues).

Motivated by the examples and problems above, the main topic of this thesis consists of tackling bandwidth limitations in cooperative path-following or distributed estimation algorithms, either by reducing the total number of communications or by transmitting at a fixed rate a limited number of bits. To this end, we consider two methods which have as a common feature the fact that they rely on synchronized estimators between agents, that is, the transmitters estimate the data at the emitter end, and the emitter computes the same estimate using the exchanged information. For continuous-time signals, we consider event-triggered communications mechanisms aimed at reducing the total number of messages per unit time by transmitting only when the difference between a relevant estimated quantity and the real quantity reaches a given threshold. For discrete-time systems, we propose quantized communications with progressive quantization as a means to address explicitly bandwidth constraints. This is done by considering explicitly that a limited number of bits are transmitted at a fixed rate.

An important desired feature in estimation and control applications is that the observers and controllers derived yield input-to-state stable (ISS) systems, in the sense that given bounded process and measurement noise, the estimation error and the state of those systems are bounded, with bounds proportional to those of the process and measurement noise. The main analysis effort undertaken in this thesis consists of deriving ISS guarantees for all the control and estimation algorithms proposed.

2 Outline

The main theme of this thesis is distributed estimation and cooperative path-following under bandwidth limitations, and applications to autonomous underwater vehicles. For a better comprehension of the content in this work, the thesis is organized in seven parts.

The main research topics occupy three central parts, starting with distributed estimation, continuing with event-based communications applied to cooperative path-following, and finally considering quantized communications in the design of algorithms to solve the problems of cooperative path-following and distributed estimation. The thesis is organized as follows:

Part I: Introduction We briefly motivate the core research topics of this thesis, describe the outline, and set forth the contributions of this work.

Part II: Mathematical Background We describe the basic mathematical tools that will be used throughout this thesis, and also provide some results in the theory of standard and quantized consensus.

Part III: Distributed Estimation We provide an introduction and a literature survey on the topic of distributed state estimation of linear dynamical systems, and propose a new distributed state estimation method.

Part IV: Event-based Communications We address the problem of cooperative path-following with self-triggered communications.

Part V: Quantized Communications We solve the problems of cooperative path-following and distributed estimation and control with quantized communication by applying the theory of quantized consensus developed in Part II.

Part VI: Tests with Real Vehicles We apply the methods developed in theory in the previous parts to the control of formations of real vehicles.

Part VII: Discussion We summarize the thesis and provide final comments and avenues for future work.

3 Contributions

The work done in the scope of this thesis led to several contributions and related publications, listed below for each part.

Part II: Mathematical Background We extend some results in standard consensus. In particular, Lemma 1 goes further than Theorem 1 in Xiao and Boyd [2004], and Lemma 2 which is equivalent to Theorem 3 in Hartfiel and Spellmann [1972] is proven with a different method in this thesis. We also give conditions for stability of a quantized consensus algorithm with progressive quantization that extend the conditions found in Li et al. [2011], in that they consider directed networks and allow faster convergence rates. We also extend these stability conditions for the case where the values stored in each agent are affected by some bounded noise. These conditions will be applied in Part V.

- F. F. C. Rego, Y. Pu, A. Alessandretti, A. P. Aguiar, and C. Jones. A consensus algorithm for networks with process noise and quantization error. In Proceedigs of the *53rd Annual Allerton Conference on Communication, Control, and Computing*, 2015. (Rego et al. [2015])

Part III: Distributed Estimation We provide a literature survey on the state of the art in distributed state estimation for linear systems and propose a new distributed design method for a distributed state estimation algorithm that has the potential to perform better than most estimation algorithms in the literature, and requires only the transmission of its estimate to the out-neighbours and the computation of a small multiplications and additions on-line.

- F. F. C. Rego, A. P. Aguiar, A. M. Pascoal, and C. Jones. A design method for distributed Luenberger observers. IEEE, 2017. Accepted for the *56th IEEE Conference on Decision and Control, 2017. CDC 2017*. (Rego et al. [2017])

Part IV: Event-based Communications We propose an algorithm for cooperative path-following with self-triggered communications with guaranteed input to state stability for delays and packet losses. The work in this part is a continuation of the work in Vanni [2007] in that we provide full proofs of stability of the cooperative path-following algorithms and we define formally the filter structure for an arbitrary network.

- F. F. C. Rego, A. P. Aguiar, and A. M. Pascoal. A packet loss compliant logic-based communication algorithm for cooperative path-following control. In Proceedings of the *9th IFAC Conference on Control Applications in Marine Systems 2013*, 2013. (Rego et al. [2013])

Part V: Quantized Communications We provide a method for cooperative path-following with quantized communications (Rego et al. [2015]), and an algorithm for distributed estimation and control with quantized communications, which goes further than in Rego et al. [2016b] since we consider that the state estimate of each agent is used for feedback control of the plant.

- F. F. C. Rego, Y. Pu, A. Alessandretti, A. P. Aguiar, A. M. Pascoal, and C. Jones. Design of a distributed quantized Luenberger filter for bounded noise. In Proceedings of the *2016 American Control Conference (ACC)*, pages 6393–6398, July 2016, doi: 10.1109/ACC.2016.7526675. (Rego et al. [2016b])
- The theorems and lemmas in Rego et al. [2016b] are proven in the technical report Rego et al. [2016a].

Part VI: Tests with Real Vehicles For an introduction to the problem of cooperative navigation and to the hardware setup used in the following tests we provide a report of the tests of a range-based formation control algorithm for underwater vehicles.

We apply the event-triggered cooperative path-following algorithm to the control of a formation of three real autonomous marine vehicles and we employ the distributed estimation algorithm to the cooperative navigation of model cars measuring ranges among them.

- F. F. C. Rego, J. M. Soares, A. Pascoal, A. P. Aguiar, and C. Jones. Flexible triangular formation keeping of marine robotic vehicles using range measurements. In Proceedings of the *19th IFAC World Congress*, 2014.(Rego et al. [2014])

4 Notation

In this section we summarize the notation used throughout the thesis. Given two square matrices of the same dimension X and Y the matrix inequality $X \preceq Y$ means $Y - X$ is positive semidefinite and $X \prec Y$ means $Y - X$ is positive definite. Similarly $X \succeq Y$ means $X - Y$ is positive semidefinite and $X \succ Y$ means $X - Y$ is positive definite. The symbol $\otimes$ stands for the Kronecker product. The symbols $\|\cdot\|$ and $\|\cdot\|_\infty$ represent the $2-$ and $\infty-$norm, respectively of a vector of real numbers. Given a positive definite matrix P we define the ellipsoidal or P-norm of x as $\|x\|_P := x^T P x$, where x is a vector of appropriate dimensions. We also define the matrix induced P-norm of a matrix A as $\|A\|_P := \sup_{\|x\|_P=1} \|Ax\|_P$, where A is a matrix of appropriate dimensions. We define the symmetric square root of a symmetric positive definite matrix P as $P^{\frac{1}{2}} := Q\Lambda^{\frac{1}{2}}Q^T$, where $P = Q\Lambda Q^T$ is the singular value decomposition of P, and its inverse as $P^{-\frac{1}{2}}$. The notation $|\cdot|$ represents the cardinality of a set.

The symbol $\lfloor\cdot\rfloor$ represents the floor operator, or the rounding down to the closest lower integer, $\lceil\cdot\rceil$ represents the ceiling operator, or the rounding up to the closest higher integer, the function $\operatorname{sgn}(\cdot)$ is the sign function, and $\rho(\cdot)$ is the spectral radius of a square matrix. Given a square matrix P, $\lambda_{\max}(P)$ denotes the maximum norm of any eigenvalue of P, $\lambda_{\min}(P)$ the minimum norm of any eigenvalue of P, and $\sigma_{\max}(P)$ its maximum singular value, which is equal to the norm of P, $\|P\|$, induced by the vector $2-$norm. Further, $\sigma_{\min}(P)$ denotes the minimum singular value of P which, if P is nonsingular, is equal to $\|P^{-1}\|^{-1}$. I_M represents an $M \times M$ identity matrix, and $\mathbf{1}$ represents a $N \times 1$ vector with ones in every entry. The vector $\boldsymbol{e}_i$ is a column vector with all entries equal to 0 except at entry i which is 1. For a matrix A we define $A^\dagger$ as the Monroe-Penrose pseudo-inverse that is computed as follows. For a non-negative diagonal matrix Σ we compute its Monroe-Penrose pseudo-inverse $\Sigma^\dagger$ by taking the reciprocal of each non-zero element on the diagonal, leaving the zeros in place. For a generic matrix A, given its singular value decomposition $A = U\Sigma V^\star$ where Σ is a non-negative diagonal matrix, and V and U are unitary matrices, and $V^\star$ is the conjugate transpose of V, the Monroe-Penrose pseudo-inverse is defined as $A^\dagger := V\Sigma^\dagger U^\star$.

When clear from the context, the superscript of a variable, e.g. X^i, refers to the node index of that variable, where $i \in \mathcal{N} := \{1, \ldots, N\}$. In this context where $i \in \{1, \ldots, N\}$, the operator $\operatorname{row}(\cdot)$ is defined as

$$\operatorname{row}\left(X^i\right) := \left[X^1, \ldots, X^N\right],$$

the operator $\operatorname{col}(\cdot)$ as

$$\operatorname{col}\left(X^i\right) := \operatorname{row}\left({X^i}^T\right)^T,$$

and the operator $\operatorname{diag}\left(X^i\right)$ yields a block diagonal matrix whose diagonal elements are $X^1, \ldots, X^N$. Given $|\mathcal{N}|^2$

matrices A^{ij}, $i, j \in \mathcal{N}$, we define the notation

$$\left[A^{ij}\right]_{i,j\in\mathcal{N}} := \begin{bmatrix} A^{11} & A^{12} & \dots & A^{1N} \\ A^{21} & A^{22} & \dots & A^{2N} \\ \vdots & \vdots & \ddots & \vdots \\ A^{N1} & A^{N2} & \dots & A^{NN} \end{bmatrix}.$$

For a stochastic variable the operator $E[\cdot]$ represents its expected value. If $x \in \mathbb{R}^n$ is a stochastic variable, then the notation $x \sim \mathcal{N}(x_0, P)$ indicates that x has a Gaussian probability distribution, with

$$\begin{aligned} E[x] &= x_0, \\ E\left[xx^T\right] &= P, \end{aligned}$$

for a positive definite matrix P.

If $I \subset [0,\infty)$ is an interval, then $\|u\|_I$ denotes the essential supremum norm of a signal $u : [0,\infty) \to \mathbb{R}^n$, that is $\|u\|_I := \operatorname{ess\,sup}_{t\in I} |u(t)|$. For a signal $v : \mathbb{R} \to \mathbb{R}^m$, with $m \geq 1$ we will use the notation $v(t^+) := \lim_{s\to t^+} v(s)$. When time is omitted, we use the notation $v^+ := v(t^+)$. A continuous function $\alpha : [0,\infty) \to [0,\infty)$ is said to belong to class $\mathcal{K}$, or $\alpha \in \mathcal{K}$ if it is strictly increasing and $\alpha(0) = 0$, if $\lim_{r\to\infty} \alpha(r) = \infty$ then α is said to be of class $\mathcal{K}_\infty$. A continuous function $\beta : [0,\infty) \times [0,\infty) \to [0,\infty)$ is said to belong to class $\mathcal{KL}$, or $\beta \in \mathcal{KL}$, if, for each fixed t, the mapping $\beta(r;t)$ belong to class $\mathcal{K}$ with respect to r and, for each fixed r, the mapping $\beta(r;t)$ is decreasing with respect to t and $\beta(r;t) \to 0$ as $t \to \infty$.

Mathematical Background Part II

5 Properties of Nonlinear Continuous-Time Systems

Consider the autonomous continuous-time system

$$\dot{x} = f(t, x), \tag{5.1}$$

where $t \in \mathbb{R}$ is the time, $x \in \mathbb{R}^n$ is the state of the system and f is assumed to be continuous in t and Lipschitz continuous in x. To express stability of an autonomous continuous-time system, the following definition is required.

Definition 1. System (5.1) is said to be *ultimately bounded* (UB) if there exists a function $\beta \in \mathcal{KL}$ and a positive scalar ϵ such that

$$\|x(t)\| \leq \beta(\|x(0)\|, t) + \epsilon. \tag{5.2}$$

Moreover, if $\epsilon = 0$ the system is said to be *asymptotically stable* (AS).

The following theorem states how to determine if a function is ultimately bounded or asymptotically stable by constructing an auxiliary function, referred to as Lyapunov function.

Theorem 1 (Theorem 4.18 of Khalil [1996])**.** Let $V : [0;\infty) \times \mathbb{R} \to \mathbb{R}$ be a continuously differentiable function such that there exist functions $\alpha_1, \alpha_2 \in \mathcal{K}_\infty$, a continuous function W such that $W(x) > 0, \forall \|x\| > 0$, and

$$\alpha_1(\|x\|) \leq V(t, x) \leq \alpha_2(\|x\|), \forall (t, x) \in [0, \infty) \times \mathbb{R}^n, \tag{5.3}$$

$$\frac{\partial V}{\partial t} + \frac{\partial V}{\partial x} f(t, x) \leq W(x), \forall \|x\| > \epsilon, t \in [0, \infty). \tag{5.4}$$

Then the system (5.1) is uniformly bounded.

Consider now the non-autonomous continuous-time system

$$\dot{x} = f(t, x, u), \tag{5.5}$$

where $t \in \mathbb{R}$ is the time, $x \in \mathbb{R}^n$ is the state of the system, $u \in \mathbb{R}^m$ is the input of the system which is assumed to be piecewise continuous and f is assumed to be continuous in t and u and Lipschitz continuous in x. When analyzing continuous time systems of the form (5.5) one important concept that will be used in this Thesis is that of input to state practically stability Khalil [1996].

Definition 2. System (5.5)-(5.9) is said to be *input to state practically stable* (ISpS) if there exist functions $\beta \in \mathscr{K}\mathscr{L}$ and $\sigma \in \mathscr{K}$ and a positive scalar ϵ such that

$$\|x(t)\| \leq \beta(\|x(0)\|, t) + \sigma\left(\|u\|_{[0,t]}\right) + \epsilon. \tag{5.6}$$

Moreover, if $\epsilon = 0$ the system is said to be *input to state stable* (ISS).

The following theorem gives the Lyapunov function based method of determining input to state practical stability of a system.

Theorem 2 (Theorem 4.19 of Khalil [1996])**.** Let $V : [0;\infty) \times \mathbb{R} \to \mathbb{R}$ be a continuously differentiable function such that there exist functions $\alpha_1, \alpha_2 \in \mathscr{K}_\infty$, $\rho \in \mathscr{K}$ a continuous function W such that $W(x) > 0, \forall \|x\| > 0$, and

$$\alpha_1(\|x\|) \leq V(t,x) \leq \alpha_2(\|x\|), \forall (t,x) \in [0,\infty) \times \mathbb{R}^n \times \mathbb{R}^m, \tag{5.7}$$

$$\frac{\partial V}{\partial t} + \frac{\partial V}{\partial x} f(t,x,u) \leq W(x), \forall \|x\| > \rho(\|u\|) + \epsilon, t \in [0,\infty). \tag{5.8}$$

Then the system (5.5) is ISpS. Moreover, if $\epsilon = 0$ then the system is ISS.

Consider now the measurement equation

$$y = h(t,x), \tag{5.9}$$

where $y \in \mathbb{R}^l$ is the output of the system. The following property is useful in order to assess how the input given to a system affects its output.

Definition 3. System (5.5)-(5.9) is said to be *input-output practically stable* (IOpS) or $\mathscr{L}_\infty$ stable if there exist functions $\beta^{\mathscr{O}} \in \mathscr{K}\mathscr{L}$ and a positive scalar $\epsilon^{\mathscr{O}}$ such that

$$\|y(t)\| \leq \beta^{\mathscr{O}}(\|x(0)\|, t) + \sigma^{\mathscr{O}}\left(\|u\|_{[0,t]}\right) + \epsilon^{\mathscr{O}}. \tag{5.10}$$

Moreover, if $\epsilon^{\mathscr{O}} = 0$ the system is said to be *input-output stable* (IOS).

The following theorem states sufficient conditions for IOpS.

Theorem 3 (Theorem 5.4 of Khalil [1996])**.** If the system (5.5) is ISpS and there exists a function $\sigma^h \in \mathscr{K}$ and a positive scalar ϵ^h such that

$$\|y(t)\| \leq \sigma^h(\|x(t)\|) + \epsilon^h, \tag{5.11}$$

then we can say that the system (5.5)-(5.9) is input-output practically stable (IOpS). Moreover, if the system is ISS and $\epsilon^h = 0$ then we can say that the system is IOS.

5.1 Interconnection of Input to State Practically Stable Systems: The Small-Gain Theorem

The concept of input to state stability is particularly useful in the study of interconnected systems, since it expresses the effects of the system in the size of the norm of a signal passing through it. One example is the case of a cascade connection of Figure 5.1. Consider two ISpS systems Σ^1 and Σ^2.

$$\Sigma^1: \quad \dot{x}_1 = f_1(t, x_1, u_1),$$

and

$$\Sigma^2: \quad \dot{x}_2 = f_2(t, x_2, x_1, u_2),$$

which satisfy the ISpS properties

$$\|x_1(t)\| \le \beta^1\left(\|x_1(0)\|, t\right) + \sigma^1\left(\|u_1\|_{[0,t]}\right) + \epsilon_1, \tag{5.12}$$
$$\|x_2(t)\| \le \beta^2\left(\|x_2(0)\|, t\right) + \sigma_2^{x_1}\left(\|x_1\|_{[0,t]}\right) + \sigma^2\left(\|u_2\|_{[0,t]}\right) + \epsilon_2, \tag{5.13}$$

where $\beta^1, \beta^2 \in \mathcal{KL}$ and $\sigma^1, \sigma^2, \sigma_2^{x_1} \in \mathcal{K}$, ϵ_1, ϵ_2 are positive scalars. If we analyze the cascade connection where

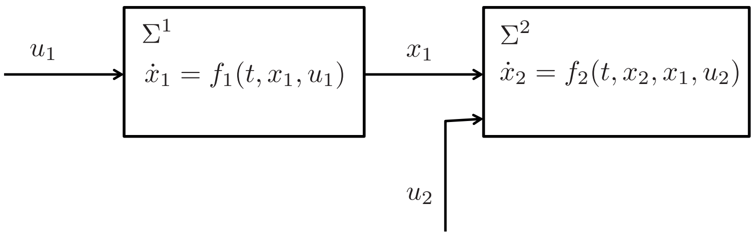

Figure 5.1 – Cascade connection of two systems.

x_1 is an input of Σ^2, as illustrated on Figure 5.1 we can guarantee that the overall system is stable, i.e. the system whose state is $x_{12} := \left[x_1^T \; x_2^T\right]^T$ and the input is $u_{12} := \left[u_1^T \; u_2^T\right]^T$ is ISpS

Theorem 4 (Lemma 4.7 of Khalil [1996]). Given systems Σ^1 and Σ^2 satisfying the ISpS properties (5.12)-(5.13), and suppose the two systems are connected in cascade with x_1 as an input of Σ^2, then the state of the interconnected system is ultimately bounded, that is, there exists functions $\beta^{12} \in \mathcal{KL}$, $\sigma^{12} \in \mathcal{K}$, and a non-negative scalar ϵ_{12} such that

$$\|x_{12}(t)\| \le \beta^{12}\left(\|x_{12}(0)\|, t\right) + \sigma^{12}\left(\|u_{12}\|_{[0,t]}\right) + \epsilon_{12}.$$

Moreover if Σ^1 and Σ^2 are ISS, that is $\epsilon_1 = 0$ and $\epsilon_2 = 0$, then the overall system is ISS, that is, $\epsilon_{12} = 0$.

The property of input to state practical stability is particularly useful in the study of the feedback connection of Figure 5.2. Consider two ISpS systems Σ^2 defined as before satisfying property (5.13) and Σ^1 redefined as

$$\Sigma^1: \quad \dot{x}_1 = f_1(t, x_1, x_2, u_1),$$

which satisfy the ISpS properties

$$\|x_1(t)\| \le \beta^1\left(\|x_1(0)\|, t\right) + \sigma_1^{x_2}\left(\|x_2\|_{[0,t]}\right) + \sigma^1\left(\|u_1\|_{[0,t]}\right) + \epsilon_1, \tag{5.14}$$

where $\sigma_1^{x_2} \in \mathcal{K}$. If we analyze the setup where x_2 is an input of Σ^1, and x_1 is an input of Σ^2, as illustrated on Figure 5.2 we can guarantee that the overall system is stable, i.e. the system whose state is $x_{12} := \left[x_1^T \; x_2^T\right]^T$ and the output is $u_{12} := \left[u_1^T \; u_2^T\right]^T$ is ISpS, if the conditions of the small-gain theorem in Jiang et al. [1994] and Khalil [1996], reproduced here in a slightly different form, are observed.

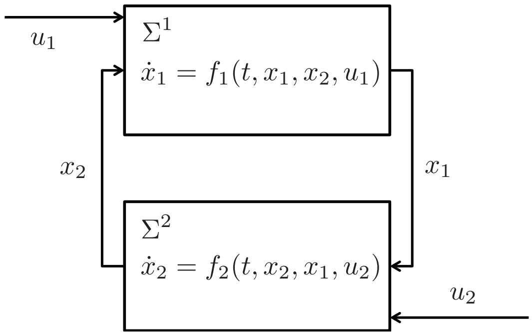

Figure 5.2 – Feedback interconnection of two systems.

Theorem 5 (Small-gain Theorem Jiang et al. [1994])**.** Given systems Σ^1 and Σ^2 satisfying the ISpS properties (5.13) and (5.14), and suppose the two systems are interconnected with x_2 as an input of Σ^1, and x_1 as an input of Σ^2, if

$$\sigma_2^{x_1}\left(\sigma_1^{x_2}(r)\right) < r \quad \forall r > 0,$$

then the state of the interconnected system is ultimately bounded, that is, there exists functions $\beta^{12} \in \mathcal{KL}$, $\sigma^{12} \in \mathcal{K}$, and a non-negative scalar ϵ_{12} such that

$$\|x_{12}(t)\| \le \beta^{12}(\|x_{12}(0)\|, t) + \sigma^{12}\left(\|u_{12}\|_{[0,t]}\right) + \epsilon_{12}.$$

Moreover if Σ^1 and Σ^2 are ISS, that is $\epsilon_1 = 0$ and $\epsilon_2 = 0$, then the overall system is ISS, that is, $\epsilon_{12} = 0$.

6 Ellipsoidal Norm

6.1 Motivation

As defined in Chapter 4, given a positive definite matrix P the ellipsoidal or P-norm of x is defined as $\|x\|_P := x^T P x$, where x is a vector of appropriate dimensions. This chapter describes the properties of the ellipsoidal norm, which can be a useful tool for analysis of linear systems with bounded norm. The ellipsoidal norm is extremely well suited to describe the Lyapunov stability property of linear systems, as well as the effect of noise and disturbances with bounded norm. The usefulness of the ellipsoidal norm comes from expressing Lyapunov functions as norms, which enables us to use the usual properties of a norm such as the triangular inequality.

The ellipsoidal norm is not a new concept and was studied for example in Blondel et al. [2005] for the computation of the joint spectral radius of a set of matrices. It is also used in Du et al. [2016, 2017] for the computation of a Maholanobis distance. However, to the best of the authors' knowledge, its usefulness for the analysis of stable, discrete-time linear systems has not been reported before.

In Section 6.2 we present some properties of the matrix induced ellipsoidal norm which are useful for the analysis of linear systems, and in Section 6.3 we give some illustrative examples that illustrate the usefulness of the ellipsoidal norm in the analysis of linear systems.

6.2 Properties of the ellipsoidal norm

This section gives some useful properties of the matrix induced ellipsoidal norm. The proofs of these properties are given in the next section. As with any induced norm, the matrix induced ellipsoidal norm is sub-multiplicative.

Property P1 (Sub-multiplicative)**.** The matrix induced ellipsoidal norm is sub-multiplicative, i.e. given two matrices A and B of appropriate dimensions, and a positive definite matrix P, we have

$$\|AB\|_P \leq \|A\|_P \|B\|_P.$$

Since for stability and convergence analysis we wish to quantify the rate of decrease of an appropriate norm of the state of a stable system, the next property will be useful.

Property P2 (Norm decreasing property of stable systems)**.** Given a matrix A with $\rho(A) < 1$, there exists a symmetric positive definite matrix P such that $\|A\|_P < 1$. Furthermore, if for a positive definite matrix Q we have $A^T PA - P = -Q$, then $\|A\|_P = \sqrt{1 - \sigma_{\min}\left(Q^{\frac{1}{2}} P^{-\frac{1}{2}}\right)^2} < 1$.

Note that in general one cannot infer that $\|A\| < 1$ if $\rho(A) < 1$, therefore the use of the ellipsoidal norm given in Property P2 might be preferable to the $\mathscr{L}_2$ norm in the analysis of stable LTI systems.

Finally, it will be useful to make the equivalence between the ellipsoidal norm and the infinity norm of a vector explicit, as well as between two ellipsoidal norms of a vector.

Property P3 (Equivalence between the ellipsoidal norm and the infinity norm of a vector)**.** The ellipsoidal norm and the infinity norm of a vector are equivalent, i.e. given a symmetric positive definite matrix P of size $n \times n$, for a vector x of appropriate dimensions we have

$$m(P)\|x\|_\infty \leq \|x\|_P \leq M(P)\|x\|_\infty,$$

with

$$\begin{aligned} m(P) &:= \min_{1 \leq i \leq n} \frac{1}{\left\| P^{-\frac{1}{2}} F_i^T \right\|}, \\ M(P) &:= \max_{1 \leq i \leq 2^n} \|v_i\|_P, \end{aligned}$$

where F_i is the ith row of the matrix $F := [I_n, -I_n]^T$, and v_i is the ith vertex of the hypercube $\mathscr{H} := \{y | \|y\|_\infty \leq 1\} = \{y | Fy \leq \mathbf{1}\}$. Moreover, given two symmetric positive definite matrices P_1 and P_2, we have

$$\begin{aligned} m(P_1 \otimes P_2) &= m(P_1)\, m(P_2)\,, \\ M(P_1 \otimes P_2) &= M(P_1)\, M(P_2)\,, \end{aligned}$$

Notice how, from the definitions of $m(\cdot)$ and $M(\cdot)$, and for the case of the $2-$norm, we retrieve the known results $m(I_N) = 1$ and $M(I_N) = \sqrt{N}$. One can also observe that the number of evaluations of the P-norm for the computation of $M(P)$ is exponential on the dimension of P. Therefore, if the dimensions of P are large, it is preferable to use, instead of $M(P)$, its upper bound

$$M(P) \leq \max_{\|y\| \leq \sqrt{n}} \left\| P^{\frac{1}{2}} y \right\| = \sqrt{n} \left\| P^{\frac{1}{2}} \right\|,$$

where the inequality comes from the definition of $M(\cdot)$ and the fact that $\|v_i\| = \sqrt{n}$ for all $i \in \{1 \leq i \leq 2^n\}$.

Property P4 (Equivalence between two ellipsoidal norms)**.** Given two symmetric positive definite matrices P_1 and P_2 it follows that the P_1-norm and the P_2-norm are equivalent, i.e. for a vector x of appropriate dimensions we have

$$m(P_1, P_2)\, \|x\|_{P_2} \leq \|x\|_{P_1} \leq M(P_1, P_2)\, \|x\|_{P_2},$$

where

$$\begin{aligned} m(P_1, P_2) &:= \sigma_{\min}\left(P_1^{\frac{1}{2}} P_2^{-\frac{1}{2}}\right) > \sqrt{\frac{\sigma_{\min}(P_1)}{\sigma_{\max}(P_2)}}, \\ M(P_1, P_2) &:= \sigma_{\max}\left(P_1^{\frac{1}{2}} P_2^{-\frac{1}{2}}\right) < \sqrt{\frac{\sigma_{\max}(P_1)}{\sigma_{\min}(P_2)}}. \end{aligned}$$

Moreover, given four symmetric positive definite matrices P_1, P_2, P_3 and P_4 of appropriate dimensions we can observe, directly from the properties of the Kronecker product, that

$$m(P_1 \otimes P_2, P_3 \otimes P_4) = m(P_1, P_3)m(P_2, P_4) > \sqrt{\frac{\sigma_{\min}(P_1)\sigma_{\min}(P_2)}{\sigma_{\max}(P_3)\sigma_{\max}(P_4)}},$$
$$M(P_1 \otimes P_2, P_3 \otimes P_4) = M(P_1, P_3)M(P_2, P_4) < \sqrt{\frac{\sigma_{\max}(P_1)\sigma_{\max}(P_2)}{\sigma_{\min}(P_3)\sigma_{\min}(P_4)}},$$

Property P5 (Kronecker product)**.** Given two symmetric positive definite matrices P_1 and P_2 and two matrices A and B of appropriate dimensions, then

$$\|A \otimes B\|_{P_1 \otimes P_2} = \|A\|_{P_1} \|B\|_{P_2}$$

6.3 Application Examples

In this section we describe examples of applications of the elliptical norm, such as the cases of a stable LTI system driven by bounded noise, a system stabilized with an LQR controller and a Luenberger observer. The examples found in this section can be found in Ogata [1995], Franklin and Workman [1998], Hespanha [2009] and Anderson and Moore [1979], however in this section we provide explicit upper bounds on ellipsoidal norms of the states or estimation errors, depending on upper bounds of appropriate norms of the disturbances acting on the system. We will also address the case of LQR stabilized systems when only a quantized measurement of the state is available to the controller.

6.3.1 Stable system with noise

Consider a discrete-time LTI system of the form

$$x_{t+1} = Ax_t + w_t, \tag{6.1}$$

where $x_t \in \mathbb{R}^n$ is the state, $A \in \mathbb{R}^{n\times n}$, and $w_t \in \mathbb{R}^n$ is the process noise, which satisfies, for a symmetric positive definite matrix P_w, $\|w_t\|_{P_w} < 1$. Assume also that the system is stable, that is $\rho(A) < 1$. Therefore we have, from Property P2 that $\|A\|_P < 1$, for some appropriately chosen positive definite matrix P, which may be computed by solving the discrete-time Lyapunov equation $A^T PA - P = -Q$, for some positive definite matrix Q. See Ogata [1995] and Hespanha [2009] for an introduction to Lyapunov stability for discrete-time linear time invariant systems. With this property we can derive the next theorem which is the main result of this section and supports the use of the use of ellipsoidal norm as an analysis tool for discrete-time stable LTI systems.

Theorem 6. Consider the stable LTI system (6.1) with uniformly bounded process noise, i.e. $\|w_t\|_{P_w} < 1$, $\forall t \geq 0$ for some positive definite matrix P_w. Defining $a := \|A\|_P < 1$ where P is an appropriately chosen positive definite matrix, whose existence is guaranteed by Property P2, the norm of the system state is bounded by

$$\|x_t\|_P \leq a^t \|x_0\|_P + \frac{M(P, P_w)}{1-a},$$

with $M(P, P_w)$ given in Property P4.

Proof. From (6.1), the triangular inequality of a norm, and Property P3 we have

$$\begin{aligned}\|x_{t+1}\|_P &\leq a\|x_t\|_P + \|w_t\|_P \\ &\leq a\|x_t\|_P + M(P, P_w).\end{aligned}$$

Applying recursively the previous inequality and using the geometric series property we can conclude that

$$\|x_t\|_P \le a^t \|x_0\|_P + M(P,P_w)\left(\sum_{i=0}^{t-1} a^i\right) = a^t \|x_0\|_P + M(P,P_w)\frac{1-a^t}{1-a} \le a^t \|x_0\|_P + \frac{M(P,P_w)}{1-a}.$$

□

6.3.2 LQR controlled linear system

We now consider the case of a controlled linear system described by

$$x_{t+1} = Ax_t + Bu_t + w_t, \tag{6.2}$$

where $x_t \in \mathbb{R}^n$ is the state, $A \in \mathbb{R}^{n\times n}$ is the state matrix, $u_t \in \mathbb{R}^m$ is the control input, $B \in \mathbb{R}^{n\times m}$ is the input matrix, and $w_t \in \mathbb{R}^n$ is process noise, which satisfies, for a symmetric positive definite matrix P_w, $\|w_t\|_{P_w} < 1$. We assume that the pair (A,B) is stabilizable. In contrast to the previous case we do not assume that $\rho(A) < 1$. We assume linear feedback, i.e. $u_t = Kx_t$. In this case the state dynamics become

$$x_{t+1} = (A + BK)\, x_t + w_t.$$

As in Franklin and Workman [1998], we now show how to design the gain K and, in the same process, how to obtain the ellipsoidal norm of the state x_t with a guaranteed decrease property as in the previous case. Given positive $n \times n$ matrices, Q and R, let P be the unique positive definite solution of the algebraic Riccati equation (ARE)

$$P = Q + A^T PA - A^T PB\left(R + B^T PB\right)^{-1} B^T PA,$$

and compute the controller gain as

$$K = \left(R + B^T PB\right)^{-1} B^T PA.$$

It is well known from LQR theory that this selection of control gain minimizes the cost

$$\sum_{t=0}^{\infty} \left(x_t^T Q x_t + u_t^T R u_t\right),$$

for a system without disturbances when the state is measured directly. Notice from the definition of K that

$$A^T PB\left(R + B^T PB\right)^{-1} B^T PA = A^T PBK = K^T\left(B^T PB + R\right)K.$$

Therefore, the ARE becomes

$$(A - BK)^T P(A - BK) - P + Q + K^T RK = 0,$$

which, combined with the proof of Property P2 results in $a := \|A - BK\|_P = \sqrt{1 - \sigma_{\min}\left(Q_c^{\frac{1}{2}} P^{-\frac{1}{2}}\right)^2}$, where $Q_c := Q + K^T RK$. Following the analysis in the previous subsection we can bound the state as

$$\|x_t\|_P \le a^t \|x_0\|_P + \frac{M(P,P_w)}{1-a}.$$

6.3.3 Luenberger observer

This subsection addresses the stability of a Luenberger observer for an LTI system of the form (6.1) and measurement equation

$$y_t = Cx_t + v_t,$$

where $y_t \in \mathbb{R}^l$ is the measurement at time t, $C \in \mathbb{R}^{l\times n}$ and $v_t \in \mathbb{R}^n$ is the measurement noise, which satisfies, for a symmetric positive definite matrix P_v, $\|v_t\|_{P_v} < 1$. We assume that the pair (A, C) is detectable. The theory behind the discrete-time Luenberger observer is given in Franklin and Workman [1998] and with more detail in Anderson and Moore [1979]. In the Luenberger observer, the state estimate has the dynamics

$$\hat{x}_{t+1} = A\hat{x}_t + L\left(y_t - C\hat{x}_t\right),$$

where $\hat{x}_t \in \mathbb{R}^n$ is the state estimate and $L \in \mathbb{R}^{n\times l}$ is an appropriately chosen observer gain matrix. Defining the estimation error as $e_t = (x_t - \hat{x}_t)$, the estimation error dynamics becomes

$$e_{t+1} = (A - LC)e_t + w_t - Lv_t.$$

To compute the observer gain matrix L we define positive definite matrices V and W of appropriate dimensions and compute the solution Σ to the algebraic Riccati equation

$$\Sigma = W + A\Sigma A^T - A\Sigma C^T\left(V + C\Sigma C^T\right)^{-1} C\Sigma A^T,$$

from which it follows that the observer gain L is given by

$$L = A\Sigma C^T\left(V + C\Sigma C^T\right)^{-1}.$$

This choice of observer gain is known from Kalman filtering theory to asymptotically minimize the mean of the square estimation error for the centralized case, when the measurement noise covariance is V^{-1} and the process noise covariance is W^{-1}.

Following the same computations as for the controller, the above ARE can be re-written as

$$(A - LC)\Sigma(A - LC)^T - \Sigma + W + LVL^T = 0, \tag{6.3}$$

However, to compute $\|A - LC\|_P$ one would prefer a Lyapunov equation in the form

$$(A - LC)^T P(A - LC) - P = -Q.$$

Following the derivations in Olfati-Saber [2009] it follows that

$$A - LC = A - A\Sigma C^T\left(C\Sigma C^T + V\right)^{-1} C.$$

Moreover, defining $\tilde{\Sigma} := \left(\Sigma^{-1} + CV^{-1}C^T\right)^{-1}$, from (6.3) using the Schur complement inverse property [1] we have $\Sigma = A\tilde{\Sigma}A^T + W$.

Defining $P := \Sigma^{-1}\tilde{\Sigma}\Sigma^{-1}$ and $\tilde{W} := W + \Sigma CV^{-1}C^T\Sigma$ we obtain

$$P^{-1} = \Sigma\tilde{\Sigma}^{-1}\Sigma$$

[1] Given four matrices A, B, C, and D of appropriate dimensions, where A and D are positive definite, the Schur complement inverse property consists of the fact that $\left(A - BD^{-1}C\right)^{-1} = A^{-1} + A^{-1}B\left(D - CA^{-1}B\right)^{-1}CA^{-1}$.

$$
\begin{aligned}
&= \Sigma\left(\Sigma^{-1} + CV^{-1}C^T\right)\Sigma \\
&= \Sigma + \Sigma CV^{-1}C^T\Sigma \\
&= A\tilde{\Sigma}A^T + W + \Sigma CV^{-1}C^T\Sigma \\
&= A\tilde{\Sigma}A^T + \tilde{W}.
\end{aligned}
$$

Finally, using P to define the quadratic Lyapunov function yields

$$
\begin{aligned}
&(A-LC)^T P(A-LC) - P = \\
&= \Sigma^{-1}\tilde{\Sigma}\left(A^T PA - \tilde{\Sigma}^{-1}\right)\tilde{\Sigma}\Sigma^{-1} \\
&= -\Sigma^{-1}\left(\tilde{\Sigma} - \tilde{\Sigma}A^T\left(A\tilde{\Sigma}A^T + \tilde{W}\right)A\tilde{\Sigma}\right)\Sigma^{-1} \\
&= -\Sigma^{-1}(\tilde{\Sigma}^{-1} + A^T\tilde{W}^{-1}A)\Sigma^{-1},
\end{aligned}
$$

where in the last equality we used the Schur complement property.

We now define $Q := \Sigma^{-1}\left(\tilde{\Sigma}^{-1} + A^T\tilde{W}^{-1}A\right)\Sigma^{-1}$, which is positive definite since Σ and $\tilde{\Sigma}$ are positive definite. Then, the last equation combined with Property P2 results in $a := \|A-LC\|_P = \sqrt{1-\sigma_{\min}\left(Q^{\frac{1}{2}}P^{-\frac{1}{2}}\right)^2}$. Following the analysis of subsection 6.3.1 we can bound the estimation error as follows

$$
\|e_t\|_P \le a^t\|e_0\|_P + \frac{M(P,P_w) + \|L\|_P M(P,P_v)}{1-a}.
$$

6.3.4 LQR controlled linear system with uniform quantization

We now apply the ellipsoidal norm concept to the case where we wish to stabilize an LTI system, and the controller only has available a quantized version of the state. This case occurs in practice when the state is measured with a finite number of bits. Formally, the quantizer with a step-size Δ is defined by the operator[2]

$$
Q(x) := \operatorname{sgn}(x)\Delta\left\lfloor \frac{\|x\|}{\Delta} + \frac{1}{2}\right\rfloor.
$$

When x is a vector in R^n, $Q(x)$ applies the quantization element-wise. It can be seen that with this definition of $Q(\cdot)$, the quantization error is bounded as $\|x_t - Q(x_t)\|_\infty \le \frac{\Delta}{2}$. Applying an LQR controller to the system (6.2), as in subsection 6.3.2 yields the following dynamics

$$
x_{t+1} = Ax_t + BKQ(x_t) + w_t = (A+BK)x_t + BK\left(Q(x_t) - x_t\right) + w_t.
$$

Taking the ellipsoidal norm of the state we obtain

$$
\begin{aligned}
\|x_{t+1}\|_P &\le a\|x_t\|_P + \|Q(x_t) - x_t\|_{K^TB^TPBK} + M(P,P_w) \\
&\le a\|x_t\|_P + \frac{\Delta}{2}M\left(K^TB^TPBK\right) + M(P,P_w),
\end{aligned}
$$

and from the proof of Theorem 6 we have

$$
\|x_t\|_P \le a^t\|x_0\|_P + \frac{M\left(K^TB^TPBK\right)\Delta/2 + M(P,P_w)}{1-a}.
$$

[2] In this chapter we consider quantization with an infinite quantization interval, that is, we considered that the quantization operates in the same manner everywhere in the domain $\mathbb{R}^n$. A formal definition of the quantizer with a limited quantization interval is given in Section 7.1. In the case of a limited quantization interval, we would need to show that the value to be quantized is within the quantization interval, that is $\|x - Q(x)\|_\infty$, in order to guarantee that the quantization error is bounded. The quantizer is thus defined as

6.3.5 LQR controlled linear system with progressive quantization

In the last subsection we used a constant quantization step-size and we obtained an ultimate bound on the system state which depends on the quantization step-size as $\frac{M\left(K^T B^T PBK\right)\Delta/2+M(P,P_w)}{1-a}$. In order to obtain an ultimate bound which depends only on a and $M(P,P_w)$ we can define a decreasing quantization step-size $\Delta_t = \Delta_0\alpha^t$, where $\Delta_0 > 0$ and $0 < \alpha < 1$. This method is named progressive quantization and is studied in detail, applied to an optimization algorithm, in Pu et al. [2017], and to quantized consensus in Li et al. [2011] and Thanou et al. [2013].

Taking the ellipsoidal norm of the state we obtain

$$\begin{aligned}
\|x_{t+1}\|_P &\le a\|x_t\|_P + \|Q(x_t) - x_t\|_{K^T B^T PBK} + M(P,P_w) \\
&\le a\|x_t\|_P + \frac{\Delta_t}{2} M\left(K^T B^T PBK\right) + M(P,P_w).
\end{aligned}$$

Applying the previous inequality recursively yields

$$\begin{aligned}
\|x_t\|_P &\le a^t\|x_0\|_P + \sum_{i=0}^{t-1}\left(a^i\left(M(P,P_w) + \alpha^{t-1-i}\frac{\Delta_0}{2} M\left(K^T B^T PBK\right)\right)\right) \\
&\le a^t\|x_0\|_P + \alpha^{t-1}\frac{\Delta_0}{2} M\left(K^T B^T PBK\right)\left(\sum_{i=0}^{t-1}\left(\frac{a}{\alpha}\right)^i\right) + \frac{M(P,P_w)}{1-a} \\
&\le a^t\|x_0\|_P + \alpha^t\frac{M\left(K^T B^T PBK\right)\Delta_0}{2(\alpha-a)} + \frac{M(P,P_w)}{1-a},
\end{aligned}$$

where we can see that the ultimate bound is $\frac{M(P,P_w)}{1-a}$.

Besides progressive quantization, other quantization methods have been studied for the stabilization of LTI systems such as logarithmic quantization in Elia and Mitter [2001], Ishii and Başar [2005].

7 Quantized Consensus

7.1 Uniform Quantizer

We now define the meaning of quantization formally. The concept is motivated by the requirement to transmit a message with a limited number of bits and a known precision, given that both the transmitter and the receiver have the same quantizer parameters: mid-value, quantization interval, and number of transmitted bits.

Consider the quantization interval $\left[\bar{x}-\frac{\Lambda}{2}, \bar{x}+\frac{\Lambda}{2}\right]$ of size Λ centered at the mid-value $\bar{x}$. A uniform quantizer with a quantization step-size Δ is given by

$$Q(x) := \begin{cases} \bar{x}-\frac{\Lambda}{2} & \text{if } x \in \left(-\infty, \bar{x}-\frac{\Lambda}{2}\right) \\ \bar{x}+\operatorname{sgn}(x-\bar{x})\Delta\left\lfloor \frac{\|x-\bar{x}\|}{\Delta}+\frac{1}{2}\right\rfloor & \text{if } x \in \left[\bar{x}-\frac{\Lambda}{2}, \bar{x}+\frac{\Lambda}{2}\right] \\ \bar{x}+\frac{\Lambda}{2} & \text{if } x \in \left(\bar{x}+\frac{\Lambda}{2}, \infty\right) \end{cases} . \tag{7.1}$$

The quantizer is illustrated in Figure 7.1.

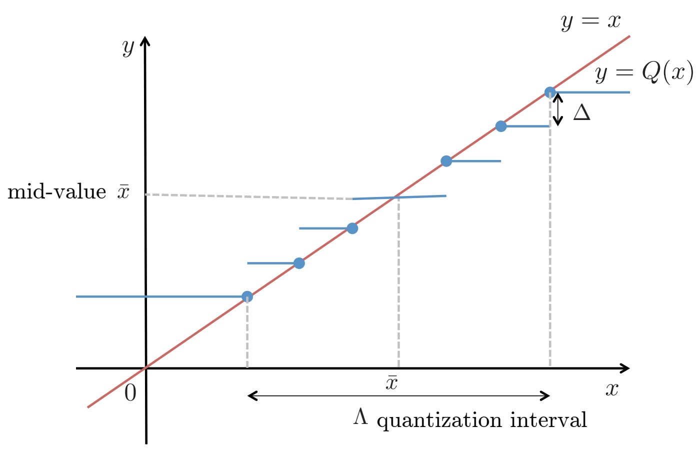

Figure 7.1 – Example of quantizer with $n_b = 3$.

The parameter Δ is determined by the number n_b of bits of the quantizer as $\Delta := \frac{\Lambda}{2^{n_b}-2}$. From (7.1), the quantization error is upper-bounded by

$$\|x - Q(x)\| \leq \frac{\Delta}{2} = \frac{\Lambda}{2^{n_b+1} - 4}. \tag{7.2}$$

For the case where the input of the quantizer and the mid-value are vectors with the same dimension, the quantizer Q is taken element-wise.

7.2 Communication Network

This chapter formulates the concept of a communication network that is at the core of this thesis.

We consider a very general setup consisting of: I) a set of nodes $\mathcal{N}$, with cardinality $N := |\mathcal{N}|$. II) a communication network between nodes $(\mathcal{N}, \mathcal{A})$, where $\mathcal{A} \subseteq \mathcal{N} \times \mathcal{N}$ is the set of node pairs describing the directed connections between these nodes (each standing for a data link), i.e. node i can communicate with node j, in this direction, if and only if $(i, j) \in \mathcal{A}$. The following assumption describes the communication limitations among sensors.

Assumption A1. The nodes are able to communicate according to the network structure defined by $\mathcal{A}$, i.e. a node i is able to send messages to node j if and only if $(i, j) \in \mathcal{A}$.

The concept of communication network is illustrated in Figure 7.2. Let $\mathcal{N}^i$ be the index set of the vehicles that communicate with vehicle i, i.e. $\mathcal{N}^i := \{j : (j, i) \in \mathcal{A}\}$ (the so called neighbouring set of vehicle i or the set of in-neighbors of i, we will use the terms *neighbour* and *in-neighbour* interchangeably throughout this thesis). From Figure 7.2 we can observe that $\mathcal{N}^8 = \{4, 7\}$. We define a directed path as an ordered sequence of nodes such that any pair of consecutive nodes in the sequence is an edge of the graph, i.e. a directed path of length n from node i to node j is a sequence of nodes $i_1, i_2, \ldots, i_n$, where $i_1 = i$, $i_n = j$, and for any $l \in \{1, \ldots, n-1\}$ $(i_l, i_{l+1}) \in \mathcal{A}$.

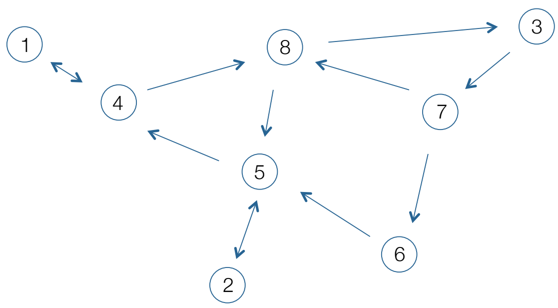

Figure 7.2 – Example of communication network where $\mathcal{N} = \{1, \ldots, 8\}$, $N = 8$ and $\mathcal{A} = \{(1,4),(4,1),(4,8),(8,3),(3,7),(7,8),(8,5),(5,4),(7,6),(6,5),(5,2),(2,5)\}$.

A cycle in a network is a directed path that starts and ends at the same node and that contains no repeated node except for the initial and the final node. In the Network of Figure 7.2 one can find three cycles: $\{4,8,5,4\}$; $\{8,3,7,8\}$ and $\{8,3,7,6,5,4,8\}$. A network is aperiodic if the greatest common divisor of the lengths of its cycles is one. Note that if self-loops are allowed, i.e. if for any $i \in \mathcal{N}$, $(i, i) \in \mathcal{A}$, then the network is automatically aperiodic.

A node of a network is globally reachable if it can be reached from any other node by traversing a directed path. A network is strongly connected if every node is globally reachable. Analysing Figure 7.2 one can conclude that the graph is strongly connected. A graph $(\mathcal{N}, \mathcal{A})$ is weakly connected or just connected if the minimal undirected graph that contains it[1] is strongly connected. For undirected graphs, i.e. if $i \in \mathcal{N}^j$ implies $j \in \mathcal{N}^i$, connected and strongly connected are equivalent concepts.

The adjacency matrix of a graph, denoted $\boldsymbol{A}$, is a square matrix with rows and columns indexed by the nodes such that the i,j-entry of $\boldsymbol{A}$ is 1 if $j \in \mathcal{N}^i$ and zero otherwise. The degree matrix D of a graph $(\mathcal{N},\mathcal{A})$ is a diagonal matrix where the i-entry equals $\|\mathcal{N}^i\|$, the cardinality of the set of in-neighbours of i, $\mathcal{N}^i$. The Laplacian of a graph is defined as $\boldsymbol{L} := \boldsymbol{D} - \boldsymbol{A}$. Thus, every row sum of $\boldsymbol{L}$ equals zero, that is, $\boldsymbol{L}\mathbf{1} = \mathbf{0}$. For the graph of Figure 7.2 the Laplacian is

$$\boldsymbol{L} = \begin{bmatrix} 1 & 0 & 0 & -1 & 0 & 0 & 0 & 0 \\ 0 & 1 & 0 & 0 & -1 & 0 & 0 & 0 \\ 0 & 0 & 1 & 0 & 0 & 0 & 0 & -1 \\ -1 & 0 & 0 & 2 & -1 & 0 & 0 & 0 \\ 0 & -1 & 0 & 0 & 3 & -1 & 0 & -1 \\ 0 & 0 & 0 & 0 & 0 & 1 & -1 & 0 \\ 0 & 0 & -1 & 0 & 0 & 0 & 1 & 0 \\ 0 & 0 & 0 & -1 & 0 & 0 & -1 & 2 \end{bmatrix}.$$

It is well known that if $(\mathcal{N},\mathcal{A})$ is strongly connected, $\boldsymbol{L}$ has a simple eigenvalue at zero with an associated eigenvector $\mathbf{1}$ and the remaining eigenvalues are all positive, see e.g. Godsil and Royle [2013]. We also define for a non-negative square matrix B of size N, where $b^{i,j}$ is the element of B in the ith row and jth column, the graph $G(B) := (\mathcal{N},\mathcal{B})$ where $\mathcal{B} := \{(i,j)|b^{i,j} > 0\}$. A non-negative square matrix B is irreducible if for every pair of indices i and j, there exists a natural number k such that $b_k^{i,j} > 0$, where $b_k^{i,j}$ is the element of B^k in the ith row and jth column. It can be shown, see e.g. Meyer [2000], that B is irreducible if and only if its associated graph $G(B)$ is strongly connected. The period of i is defined as the greatest common divisor of all natural numbers k such that $b_k^{i,i} > 0$. When B is irreducible, it is easily seen that the period of every index is the same and is called the period of B. It is easily shown that the period of B is 1 if and only if its associated graph $G(B)$ is aperiodic, and in that case we say that B is aperiodic. A primitive matrix is a nonnegative square matrix B for which there exists a positive integer k such that all elements of B^k are strictly positive. It can be proved, see e.g. Meyer [2000], that primitive matrices are the same as irreducible aperiodic non-negative matrices.

7.3 Standard Consensus Algorithm

7.3.1 Problem Definition

The problem of consensus can be described coarsely as that of determining what computations should be performed and what messages should be exchanged among multiple agents so that they asymptotically agree on the value(s) of some relevant variable(s). A particular case of the consensus problem is that of distributed averaging, where all the agents should obtain in the end the average of the values stored initially at each agent. Due to their applicability in a wide range of practical problems involving the coordination of multiple systems, from distributed state estimation to flocking or rendez-vous of fleets of autonomous vehicles, consensus algorithms (in particular distributed averaging) are probably the most ubiquitous ones in a distributed setting. In this section we give an introduction to the standard algorithm of distributed averaging. In the process, we also summarize some basic results related to consensus and doubly stochastic matrices. Some of these results can be found in Xiao and Boyd [2004], while others when explicitly mentioned are original.

[1] $(\mathcal{N},\bar{\mathcal{A}})$ is the minimal undirected graph that contains $(\mathcal{N},\mathcal{A})$ if $\bar{\mathcal{A}}$ is the set with the minimum number of elements such that $\mathcal{A} \subseteq \bar{\mathcal{A}}$ and if $(i,j) \in \bar{\mathcal{A}}$, then $(j,i) \in \bar{\mathcal{A}}$.

Consider the network defined in Section 7.2, where each node i in $\mathcal{N}$ is initalized with a variable z_0^i and we wish to compute at each node the average of all nodes $\frac{1}{N}\sum_{i\in\mathcal{N}} z_0^i$. In the standard consensus algorithm, at each iteration l a variable z_l^i is stored at node i which is then transmitted to its out-neighbours as is shown in Figure 7.3.

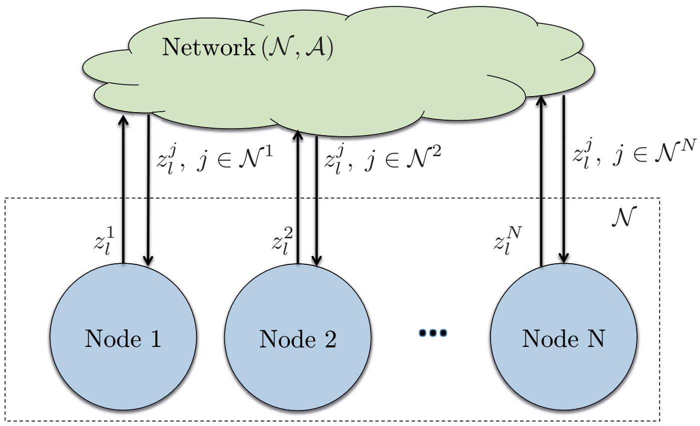

Figure 7.3 – Standard consensus problem consisting of a network $(\mathcal{N}, \mathcal{A})$ and a set of nodes $\mathcal{N}$.

7.3.2 Literature Survey on Consensus

Some of the fundamental results on distributed averaging are given in Xiao and Boyd [2004], where the authors derive general conditions under which distributed linear iterations characterized by appropriately defined weighting matrices will yield distributed averaging consensus over a network. The paper also shows how to compute the optimal weight matrix consistent with a given network so as to obtain the fastest possible convergence factor. In the case of undirected networks, this is shown to be equivalent to a semidefinite optimization program.

In line with the framework adopted in Xiao and Boyd [2004], the work in Mosquera et al. [2010] addresses the case where additive noise perturbs the exchange of information among the agents in a network and proposes a greedy approach to step-size sequence design that minimizes the mean squared error at each iteration. As shown later, the concepts introduced in Mosquera et al. [2010] can be exploited to solve the problem of quantized consensus if one considers the quantization error as communication noise.

Recently, a number of results on the conditions that the topology of a time-varying graph should satisfy in order to obtain distributed consensus have come to the fore. Among such results, the work in Charron-Bost [2013] establishes orientation and connectivity based criteria for an agreement algorithm to achieve asymptotic consensus in the context of time-varying topologies and communication delays. The results are very general and provide a general framework under which the results of other related papers are obtained as special cases of the theorems derived in Charron-Bost [2013]. Also in the context of time-varying topologies, Blondel and Olshevsky [2014] provides a necessary and sufficient condition to achieve consensus using a finite set of consensus matrices, the so-called avoiding sets condition, which is proven to be NP-hard to verify.

7.3.3 Algorithm

Consider that the generic node i at iteration l contains a vector denoted $z_l^i \in \mathbb{R}^n$. A standard consensus algorithm consists of updating the internal vector z_l^i with a weighted sum of the vectors stored in the neighbors, z_l^j, $j \in \mathcal{N}^i$, according to the rule

$$z_{l+1}^{i} = \sum_{j \in \mathcal{N}} \pi^{i,j} z_{l}^{j}, \tag{7.3}$$

where we denote by $\pi^{i,j} \in \mathbb{R}$ the weight that the node i uses to incorporate the information available from node j, with $\pi^{i,j} = 0$ if $(i,j) \notin \mathcal{A}$. We remark that we represent the iteration number of the consensus algorithm as l and not t, which denotes time, since in the context of distributed estimation we consider that there are multiple iterations of the consensus algorithm at each time instant.

The matrix Π whose component (i,j) is equal to $\pi^{i,j}$ is termed a consensus matrix. This matrix is assumed to satisfy the following standard assumptions in consensus design:

Assumption A2. The consensus matrix Π is doubly stochastic [2] and primitive.

Assumption A3. The consensus matrix Π has a positive diagonal, i.e. $\pi^{i,i} > 0$ for all $i \in \mathcal{N}$.

Given Assumption A2, we can define σ_2 as the second largest singular value of Π. The following lemmas, which build on results available in Hartfiel [1971], Hartfiel and Spellmann [1972], Xiao and Boyd [2004], Tifenbach [2011], show the importance of Assumption A2 and clarify under what conditions the assumption is valid.

Lemma 1. Consider the standard consensus algorithm (7.3). Then,

$$\lim_{l \to \infty} z_{l}^{i} = \sum_{j \in \mathcal{N}} \frac{1}{N} z_{0}^{j}, \; \forall i \in \mathcal{N},$$

if and only if Assumption A2 is satisfied and, in this case, if Assumption A3 is satisfied, then $\left\| \Pi - \frac{1}{N} \mathbf{1}\mathbf{1}^{T} \right\| = \sigma_2 < 1$, where σ_2 is the second largest singular value of Π.

Lemma 2. There exists a matrix Π such that Assumptions A2 and A3 are satisfied if and only if the network $(\mathcal{N}, \mathcal{A})$ is strongly connected, and self loops are allowed, as defined in Section 7.2.

The proofs are given in Appendix B.1.

A result similar to that in Lemma 1 is given in Xiao and Boyd [2004]. However, Lemma 1 goes further than Theorem 1 in the reference above, since it guarantees that $\|\Pi - \frac{1}{N}\mathbf{1}\mathbf{1}^{T}\| < 1$ if Assumption A3 is satisfied.

We remark that if the graph is bidirectional, i.e. if $(i,j) \in \mathcal{A}$ implies $(j,i) \in \mathcal{A}$, and if self-loops are allowed, Assumption A2 can be satisfied by designing Π with Metropolis-Hastings local-degree weights, see Xiao and Boyd [2004]. That is, Π satisfies Assumption A2 if

$$\pi^{i,j} = \begin{cases} 0 & \text{if } j \notin \mathcal{N}^{i} \\ \frac{1}{\max\{|\mathcal{N}^{i}|, |\mathcal{N}^{j}|\}} & \text{if } j \in \mathcal{N}^{i} \text{ and } i \neq j \\ \sum_{j \in \mathcal{N}^{i}, j \neq i} \pi^{i,j} & \text{if } i = j \end{cases} .$$

This is not possible if the communication network is directed. However, if self-loops are allowed, which is very often the case in practice, Lemma 2 guarantees that it is possible to build a consensus matrix satisfying Assumption A2 if $(\mathcal{N}, \mathcal{A})$ is strongly connected. The proof of this result, which gives an explicit method to build such a matrix, is given in Section B.1. For the rare cases where self-loops are not always present, it can be seen that, if the communication network is strongly connected, the existence of self-loops in every node is only a sufficient but not necessary condition for the existence of a consensus matrix satisfying Assumption A2. In

[2] A doubly stochastic matrix is a square matrix of nonnegative real numbers, whose rows and columns sum to 1.

fact, one can find networks without any self-loops such that there exist a matrix satisfying Assumption A2. One example is a network with two or more cycles with mutually prime lengths that do not intersect at any node and span the whole network, and a single cycle that also spans the whole network.

7.3.4 Guarantees with a Finite Number of Iterations

We have seen that under Assumptions A2-A3, using the standard consensus algorithm the value stored at each node $z_l^i \in \mathbb{R}^n$ converges to $\sum_{j\in\mathcal{N}} \frac{1}{N} z_0^j$, but we did not quantify the deviation from the average at a given iteration. In what follows we quantify bounds on the deviation $z_l^i - \sum_{j\in\mathcal{N}} \frac{1}{N} z_0^j$ at any given iteration of the standard consensus algorithm.

In order to compute formally the deviation from the average, we first define the variables $z_l := \mathrm{col}\left(z_l^i, i \in \mathcal{N}\right)$, $z_l^{\text{avg}} := (1/N)\left(\mathbf{1}\mathbf{1}^T\right) \otimes I_n z_l$, and $q_l := z_l - z_l^{\text{avg}}$. The consensus step can be written in compact form as

$$z_{l+1} = \Pi \otimes I_n z_l. \tag{7.4}$$

Note that using the property $\frac{1}{N}\mathbf{1}\mathbf{1}^T\Pi = \frac{1}{N}\mathbf{1}\mathbf{1}^T$, from Assumptions A2-A3 and the update (7.4), the vector of averages follows the dynamics $z_{l+1}^{\text{avg}} = z_l^{\text{avg}}$. Combining (7.4) with the fact that $z_{l+1}^{\text{avg}} = z_l^{\text{avg}}$ yields

$$q_{l+1} = \left(\Pi - \frac{1}{N}\mathbf{1}\mathbf{1}^T\right) \otimes I_n q_l, \tag{7.5}$$

and the convergence of the standard consensus algorithm can be established. Since in the rest of the thesis we will work with a quadratic P-norm for some symmetric positive definite matrix P of size $n \times n$, we describe the convergence of the difference between the values in each node and their average in terms of $\|q_l\|_{I_N\otimes P}$, as stated in the following theorem.

Theorem 7 (Convergence of standard consensus)**.** Consider the recursion (7.4). If Assumptions A2-A3 hold, then, for any $l \geq 0$, the values of q_l satisfy

$$\|q_l\|_{I_N\otimes P} \leq \sigma_2^l \|q_0\|_{I_N\otimes P}.$$

7.4 Literature survey on quantized consensus

In what follows we give a brief summary of the state of the art in quantized consensus, as organized by the type of method adopted.

7.4.1 Gossip Quantized Consensus Algorithms

One of the first methods considered for quantized consensus involved the use of gossip algorithms, where at each step one edge or communication link in a network graph is selected at random and the values stored in the nodes at both ends of the edge change according to some rule. In this context, the work in Kashyap et al. [2007] addresses a class of gossip algorithms to achieve consensus on integer numbers and proves probabilistic convergence to consensus of these algorithms. Since the paper deals with consensus of integers, it also deals with the case where the integer numbers represent quantized real numbers. However, a quantization error still exists after convergence, and, since this is a probabilistic method, it is not possible to determine for each agent in the network how close to the average its own state is. More recently, in Basary et al. [2014] it is proven that the use of the Metropolis-Hastings method for edge selection in the gossip algorithm yields faster convergence to consensus than an unbiased edge selection.

In many situations, such as those considered in the present thesis, where a number of nodes can communicate at the same time, the use of gossip algorithms may be slow when compared to algorithms where multiple nodes communicate at the same time, since they use the full capacity of the network. For this reason, we now focus on quantized consensus algorithms where all the network links are active at the same time.

7.4.2 Dithered quantization

One particular method to do quantized distributed averaging consists of performing the standard linear iterations of unquantized distributed averaging as in Xiao and Boyd [2004], while quantizing the communicated values with a probabilistic quantizer, i.e. performing dithered quantization. This approach guarantees that the quantization error is a zero mean additive noise. The work that we summarize next deals with consensus with probabilistic quantization and yields algorithms with guaranteed probabilistic convergence.

The principle of consensus with dithered quantization was first proposed in Aysal et al. [2008] where the authors present a proof of probabilistic convergence of the consensus algorithm. It is also shown in Aysal et al. [2008] that the values of all the agents will converge to the same quantization level and that the expected value of that quantization level is the average of the initial values.

In Yildiz and Scaglione [2008], the authors propose a quantized consensus scheme with the same probabilistic guarantees as in Aysal et al. [2008]; however, in this case the authors consider a communication rate that decays to zero. This is achieved through the design of an optimal predictive coding which uses information of the previously received messages. The authors of Yildiz and Scaglione [2008] also address the design of an optimal Wyner-Zyv decoder, which uses each agent's own state sequence in the decoder.

The work in Kar and Moura [2010] deals with the quantized consensus algorithm with dithered quantization and shows that when the quantizer range is unbounded, consensus is achieved asymptotically to some value, the expected value of which is the average of the initial values. Moreover, it is shown that the quantization step-size can be made arbitrarily small for a smaller variance. The paper also deals with the case of a bounded quantization interval and provides a lower bound on the probability that the difference between the final consensus value and the initial average is smaller than a threshold as a function of the number of quantization levels and the quantization interval size.

A stronger result for consensus with dithered quantization is derived in Fang and Li [2009], where the authors prove that using the dithered quantization scheme proposed in Aysal et al. [2008], and performing a temporal average of the values at each agent, the sequence of averaged values converges to the average of the initial values. This is stronger than proving that the expectation of the limit value is equal to the average of the initial values.

It is important to stress that dithered quantization is probabilistic in nature. For this reason, the results on distributed averaging in this setup are necessarily probabilistic and not deterministic, that is, the values in all nodes converge almost surely to the same value. However, it is impossible to determine with absolute certainty at any moment how distant the computed value of a certain node is with respect to the values on all other nodes. In what follows we present results that deal with deterministic quantization methods.

7.4.3 Deterministic Quantized Consensus with Fixed Quantization Interval

In this context, the first method considered consists of performing linear iterations of a distributed averaging algorithm while the exchanged messages are quantized with a uniform quantizer with a fixed quantization interval. This concept is studied in Frasca et al. [2009], which provides a quantized consensus algorithm where the average of all the agents' states is preserved. The worst case and probabilistic performance of the proposed quantized consensus algorithm is also addressed. The quantization interval is considered to be constant.

In the related work reported in Nedić et al. [2009], the problem of distributed averaging over time-varying topologies with quantized communications is studied, where the quantization method considered is the rounding down of the absolute value, and there is no preservation of the average as in Frasca et al. [2009]. With this method, the values can only converge to within some bound of the initial average which depends on the number of quantization levels.

So far, it has been assumed that the quantization interval is fixed. For this reason, the quantization error does not converge to zero and there will be at each node, after convergence, an ultimate error to the average value of all nodes. To overcome this problem the quantization interval must necessarily decrease. The remaining literature survey on quantized consensus describes the results of work in which the quantization interval decreases or the quantizer is non-uniform, thus guaranteeing that the difference from the average at each node converges to zero.

7.4.4 Adaptive Quantization Interval

When the quantization interval changes at each iteration, based on past data, we say that the quantization interval is adaptive. Adaptive quantization in the context of consensus is studied in Fang and Li [2009], where the authors propose a modification of the classic consensus algorithm in Xiao and Boyd [2004], in order to achieve consensus if the variance of the quantization error converges to zero. They further propose an adaptive quantization scheme that drive the quantization interval to zero, thus satisfying the requirements for convergence.

Similarly, regarding adaptive quantization intervals, Carli et al. [2010] presents two schemes of quantized average consensus. The first is the zoom-in zoom-out method, where the quantization interval shrinks or increases depending on whether a saturation constraint is active or not. The second is a logarithmic quantizer, i.e. the value that is quantized is the logarithm of the state of the agent, which guarantees that the quantization error is proportional to the magnitude of the quantized value. Conditions on the parameters of the logarithmic quantizer that guarantee convergence of the algorithm are also given.

When off-line information of the network topology and of the models of the system and sensors is available, one can be more efficient and just decrease exponentially the quantization interval at a pre-specified rate. This is the principle behind progressive quantization that will be examined next.

7.4.5 Progressive Quantizers

A particular case of quantization with varying quantization intervals is progressive quantization, where the quantization interval decreases exponentially to zero. Progressive quantization is studied in Thanou et al. [2012, 2013], where the authors propose a progressive quantizer that exploits the increasing correlation between the values exchanged by the sensors throughout the iterations of the consensus algorithm by progressively reducing the quantization intervals, and derive conditions on the quantizer parameters to guarantee deterministic convergence to consensus. In particular, Thanou et al. [2013] provides an asymptotic convergence rate of the difference between the value at each node and the average of the values. However, no performance bounds are given.

Performance bounds for consensus with progressive quantization are available in Li et al. [2011], where the authors describe a method of computing the parameters of a progressive quantizer depending on the network topology and the communication rate, such that convergence is guaranteed if the values at each agent always fall inside the quantization interval. This paper also provides conditions that guarantee that in expectation the values at each agent always fall inside the same quantization interval.

In this chapter, we chose a progressive quantization algorithm as in Li et al. [2011], Thanou et al. [2012, 2013], which has the advantage of guaranteed convergence to the average of the initial values. However, in the deterministic case considered in this chapter, as in Li et al. [2011], it is necessary to know a priori an upper bound on the initial deviation of the value in each node from average and which communication topology and consensus matrix will be used.

As a contribution to the field of quantized consensus, in Section 7.5 we give conditions on the quantizer parameters under which the quantized consensus algorithm algorithm converges. The convergence conditions are different from those in Li et al. [2011] in that we consider directed networks, whereas there it is assumed that network is undirected, the decrease rate can be arbitrarily close to the second singular value of the consensus matrix Π, σ_2, and unlike Li et al. [2011] which limits the choice of the consensus matrix to $\Pi = I_N - hL$ where L is the network Laplacian and h is a sufficiently small positive scalar, which limits the minimum achievable σ_2, we only require Π to be doubly stochastic. Morevoer, unlike Li et al. [2011] the stability conditions do not depend on the network degree, $\max_{i\in\mathcal{N}} \left|\mathcal{N}^i\right|$, and on the smallest eigenvalue in norm of the Laplacian of the communication network.

7.5 Quantized Consensus Theory

The main result of this section draws from the convergence properties of a consensus based distributed Luenberger observer and from the convergence in norm of a consensus algorithm that takes into account the fact that the data exchanged during the consensus step are quantized, as described in detail next. Therefore, this section, which contains results from Rego et al. [2015], addresses the convergence analysis of a consensus algorithm where the communications among nodes are subject to quantization error.

The quantized consensus algorithm here derived builds upon the progressive quantization scheme considered in Li et al. [2011], Thanou et al. [2012, 2013]. In what follows we provide performance bounds, i.e. bounds on the norm of the estimation error at each iteration, that tend to zero. Performance bounds of the same kind were also derived in Li et al. [2011]. However, in this section we provide a different bound which is more suitable to the problems of the following chapters of this thesis.

Here, we consider the case where the messages exchanged are quantized, i.e. the messages sent are generated by the quantizer $Q_l^i\left(z_l^i\right)$ of the form (7.1), where the quantizer mid-value depends on the node i and iteration number l, and the quantization interval size depends on the iteration number l. To this end, we define the quantization error $\eta_l^i := Q_t^i\left(z_l^i\right) - z_l^i$ and the variable $\eta_l := \mathrm{col}\left(\eta_l^i, i \in \mathcal{N}\right)$.

Because we consider quantized messages, the desired consensus dynamics take the form

$$z_{l+1}^i := \sum_{j\in\mathcal{N}^i} \pi^{i,j} Q_l^j\left(z_l^j\right) - \left(Q_l^i\left(z_l^i\right) - z_l^i\right). \tag{7.6}$$

The consensus step can then be written in compact form as

$$\begin{aligned} z_{l+1} &= \Pi \otimes I_n Q_l(z_l) - (Q_l(z_l) - z_l) \\ &= \Pi \otimes I_n z_l + (\Pi - I_N) \otimes I_n \eta_l. \end{aligned} \tag{7.7}$$

Following the same arguments of Subsection 7.3.4, it follows that

$$q_{l+1} = \left(\Pi - \frac{1}{N}\mathbf{1}\mathbf{1}^T\right) \otimes I_n q_l + (\Pi - I_N) \otimes I_n \eta_l. \tag{7.8}$$

If the time dependent quantization interval is selected as $\Lambda_l := r\alpha^l$, where r and α are appropriately chosen positive constants, with $0 < \sigma_2 < \alpha < 1$, and the mid-value of the quantizer is recursively chosen to be

$$\bar{z}_l = Q_{l-1}(z_{l-1}), \tag{7.9}$$

the quantization error decreases linearly as $\|z_l - Q(z_l)\|_\infty \leq \frac{r\alpha^l}{2^{n_b+1}-4}$, and we can conclude the main result of this section.

Theorem 8 (Convergence of quantized consensus)**.** Consider the quantizer Q_l given by (7.1) with n_b bits and where $\Lambda_l = r\alpha^l$, with $0 < \sigma_2 < \alpha < 1$. For the recursion (7.7)-(7.9), if Assumptions A2-A3 hold and if the number of bits n_b, the initial quantization interval r, and the initial mid-value $\bar{z}_0$ satisfy

$$s_1 + s_2 \frac{r}{2^{n_b+1} - 4} \leq \frac{r}{2}, \tag{7.10}$$

where

$$s_2 := \frac{2\sqrt{N} M(P)(\alpha+1) + (\alpha - \sigma_2) m(P)}{m(P)\alpha(\alpha - \sigma_2)}, \tag{7.11}$$

and s_1 satisfies

$$s_1 \geq m(P)^{-1} \left(\frac{\alpha+1}{\alpha} \|q_0\|_{I_N \otimes P} + \|\bar{z}_0 - z_0^{\text{avg}}\|_{I_N \otimes P} \right), \tag{7.12}$$

then, for any $l \geq 0$, the values of q_l satisfy

$$\|q_l\|_{I_N \otimes P} \leq \alpha^l \left[\|q_0\|_{I_N \otimes P} + \frac{\sqrt{N} M(P) r}{(\alpha - \alpha_2)(2^{n_b} - 2)} \right]. \tag{7.13}$$

The proof is given in Appendix B.2. It is worth noticing that the assumption in (7.10) can be satisfied by proper design of the quantizer. More specifically, by choosing n_b such that

$$n_b > \log_2(s_2 + 2),$$

and r such that

$$s_1 \leq \left(1 - \frac{s_2}{2^{n_b} - 2}\right) \frac{r}{2}.$$

Notice that s_1 and s_2 depend on the network through σ_2 and the decrease rate α. The parameter s_2 is also proportional to the initial parameters $\|q_0\|_{I_N \otimes P}$ and $\|\bar{z}_0 - z_0^{\text{avg}}\|_{I_N \otimes P}$.

7.6 Quantized Consensus with Noise

We now consider a hypothetical case where we cannot assign an exact value to z_l^i, and instead of (7.6) the quantized consensus iterations are

$$z_{l+1}^i := \sum_{j \in \mathcal{N}^i} \pi^{i,j} Q_l^j \left(z_l^j\right) - \left(Q_l^i \left(z_l^i\right) - z_l^i\right) + v_l^i, \tag{7.14}$$

where $v_l^i \in \mathbb{R}^n$ is a process disturbance. We consider that the process disturbance is bounded with an a-priori known bound. Therefore, the following assumption is needed in the rest of this section:

Assumption A4. The disturbances satisfy

$$\|v_l^i\|_\infty \leq \delta_v + \epsilon_v \alpha_v^l,\ i \in \mathcal{N}, l \in \mathbb{N}_0,$$

for some constants $\epsilon_v, \delta_v \geq 0$, and $1 > \alpha_v \geq 0$, where α_v^l is α_v to the power of l.

This assumption covers the cases of a vanishing process noise when $\delta_v = 0$ and $\epsilon_v > 0$, of a uniformly bounded noise when when $\delta_v > 0$ and $\epsilon_v = 0$, or a combination of the two. These assumptions are suitable for scenarios where we cannot have absolute control over the local variable of interest, on which we desire to perform consensus, but we can assign the value of that local variable of interest with an error or disturbance which is ultimately bounded. One example where these assumptions apply can be seen in Chapter 11.

Defining $v_l := \mathrm{col}(v_l^i)$, the consensus step can be written in a compact form as

$$z_{l+1} = \Pi \otimes I_n z_l + (\Pi - I_N) \otimes I_n \eta_l + v_l. \tag{7.15}$$

Note that using the property $\frac{1}{N}\mathbf{1}\mathbf{1}^T \Pi = \frac{1}{N}\mathbf{1}\mathbf{1}^T$, from Assumptions A2-A3 and the update (7.7), the vector of averages follows the dynamics $z_{l+1}^{\text{avg}} = z_l^{\text{avg}} + \frac{1}{N}\left(\mathbf{1}\mathbf{1}^T\right) \otimes I_n v_l$. Combining (7.7) with the fact that $z_{l+1}^{\text{avg}} = z_l^{\text{avg}} + \frac{1}{N}\left(\mathbf{1}\mathbf{1}^T\right) \otimes I_n v_l$, we can write

$$q_{l+1} = \left(\Pi - \frac{1}{N}\mathbf{1}\mathbf{1}^T\right) \otimes I_n q_l + (\Pi - I_N) \otimes I_n \eta_t + \left(I_N - \frac{1}{N}\mathbf{1}\mathbf{1}^T\right) \otimes I_n v_l. \tag{7.16}$$

If the time dependent quantization interval is selected as $\Lambda_l := r_1 \alpha^l + r_2$, with $0 < \sigma_2 < \alpha < 1$ and $\alpha_v < \alpha$, and the mid-value of the quantizer is recursively chosen to be $\bar{z}_l = Q_l(z_{l-1})$, the convergence of the quantized consensus can be established, as stated in the following theorem.

Theorem 9 (Convergence of quantized consensus)**.** Consider a quantizer Q_l from (7.1) with n_b bits and where $\Lambda_l = r_1 \alpha^l + r_2$, with $0 < \sigma_2 < \alpha < 1$ and $\alpha_v < \alpha$. For the recursion (7.7), if assumptions A2 and A3 hold and if the number of bits n_b, the initial quantizer parameters r_1, and r_2 and the initial mid-value $\bar{z}_0$ satisfy

$$a_1 + a_2 \frac{r_1}{2^{n_b+1} - 4} \leq \frac{r_1}{2}, \quad b_1 + b_2 \frac{r_2}{2^{n_b+1} - 4} \leq \frac{r_2}{2}, \tag{7.17}$$

where a_1, a_2, b_1 and b_2 are defined as

$$a_1 := m(P)^{-1}\left(\frac{(\alpha+1)\|q_0\|_{I_N \otimes P}}{\alpha} + \|\bar{z}_0 - z_0^{\text{avg}}\|_{I_N \otimes P}\right) + \left(\frac{\sqrt{N}M(P)(\alpha+1)}{m(P)\alpha(\alpha - \sigma_2)} + \frac{1}{\alpha}\right)\epsilon_v, \tag{7.18a}$$

$$a_2 := \frac{2\sqrt{N}M(P)(\alpha+1)}{m(P)\alpha(\alpha-\sigma_2)} + \frac{1}{\alpha}, \tag{7.18b}$$

$$b_1 := \left(\frac{2\sqrt{N}M(P)}{m(P)(1-\sigma_2)} + 1\right)\delta_v, \tag{7.18c}$$

$$b_2 := \frac{4\sqrt{N}M(P)}{m(P)(1-\sigma_2)} + 1. \tag{7.18d}$$

then for any $l \geq 0$ the values of q_l satisfy

$$\|q_l\|_{I_N \otimes P} \leq \alpha^l \left[\|q_0\|_{I_N \otimes P} + \frac{\sqrt{N}M(P)}{\alpha - \sigma_2}\left(\frac{r_1}{2^{n_b} - 2} + \epsilon_v\right)\right] + \left(\frac{r_2}{2^{n_b} - 2} + \delta_v\right)\frac{\sqrt{N}M(P)}{1 - \sigma_2}. \tag{7.19}$$

The proof is given in Appendix B.3.

It is worth noticing that the assumption in (7.17) can be satisfied by properly designing the quantizer. More specifically, choosing n_b such that

$$n_b > \log_2(\max(a_2, b_2) + 2),$$

and r_1 and r_2 such that

$$a_1 \le \left(1 - \frac{a_2}{2^{n_b} - 2}\right)\frac{r_1}{2}, \quad b_1 \le \left(1 - \frac{b_2}{2^{n_b} - 2}\right)\frac{r_2}{2}.$$

It is worth noticing that a_1, a_2, b_1 and b_2 depend on the network through σ_2 and on the decrease rate α. The parameter a_2 is also proportional to the initial parameters ϵ_v, $\|q_0\|_{I_N \otimes P}$ and $\|\bar{z}_0 - z_0^{\text{avg}}\|_{I_N \otimes P}$. Finally b_2 is also proportional to the ultimate bound of the noise δ_v.

Distributed Estimation Part III

8 Distributed Estimation Survey

This chapter is a brief literature survey of distributed estimation for discrete-time linear systems. The objective is to review the state of the art in this field and summarize previous work, in order to obtain the proper historical context. We also reproduce here some of the main results given in the literature.

8.1 Motivation

Given a certain system, a number of sensors with computing capabilities, and a communication network between the sensors, i.e. each sensor is a node of the network, the problem of *distributed state estimation* consists of estimating the state of the system at every node. This problem arises mostly in situations where the sensors are physically displaced, it is not possible to recover the state of the system with just one of the sensors and communications are scarce, which prevents the use of centralized approaches. Distributed state estimation has been considered in a wide range of applications where these conditions hold, from network localization to environmental monitoring, surveillance, object tracking, collaborative information processing, and traffic monitoring (see Akyildiz et al. [2002], Xu [2002], Bethke et al. [2007], Smith and Hadaegh [2007], Zavlanos [2008], Ghabcheloo et al. [2009], Bahr et al. [2009], Mesbahi and Egerstedt [2010], Aberer et al. [2010], Prathap et al. [2012], Soares et al. [2013], Rawat et al. [2014], Soares et al. [2015b,a], Dong et al. [2017], Wang and Ren [2017], Zhang et al. [2017] for an introduction to these topics). In what follows we give a survey of the state of the art in distributed estimation, where some of the main theoretical points will be discussed in detail, with emphasis on consensus based estimation and particularly on linear time-invariant systems.

In the literature, one can find many references that give an overview of the field of distributed state estimation which influenced the organization of this chapter. The reader is referred to the book Hall and Llinas [2001] for an early overview of the problem of distributed sensor fusion. The paper Wah and Rong [2003] contains a comparison and a technical summary of some of the most relevant methods of distributed estimation. An overview of many aspects related to data fusion applied to target tracking is given in Zhao et al. [2002], Smith and Singh [2006]. Two surveys of several techniques and problems associated information fusion for sensor networks are given in Makarenko and Durrant-Whyte [2004], Nakamura et al. [2007]. More recently, Mahmoud and Khalid [2013] and Li et al. [2015b] give extensive literature surveys of the state of the art in distributed state estimation and Garin and Schenato [2010] gives an overview of the technical details associated with consensus-based distributed estimation.

8.2 Problem Definition

This section formulates the problem that is at the core of the chapter.

8.2.1 Networked System

In this paper we consider a very general setup composed by: I) a discrete-time dynamical system; II) a set of nodes $\mathcal{N}$ endowed with local sensing and actuation capabilities, with cardinality $N := |\mathcal{N}|$. At each node $i \in \mathcal{N}$, a sensor measures an output y_t^i of the system; III) a communication network between nodes. This setup is shown in Figure 8.1. The discrete-time dynamical system is given by

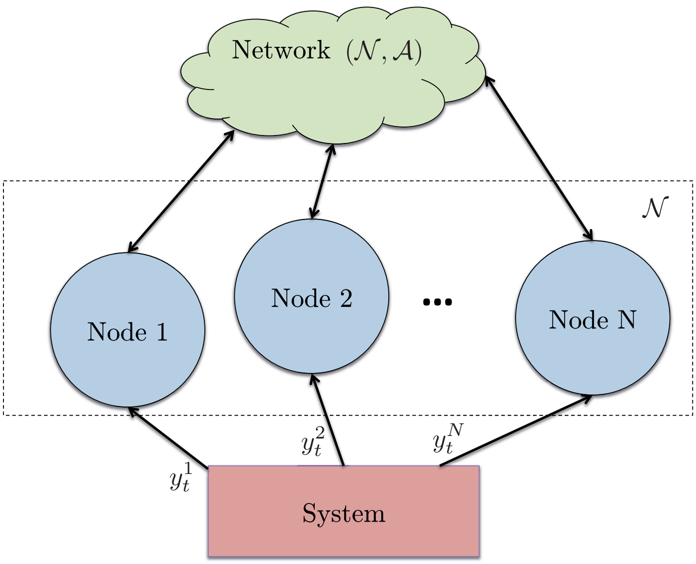

Figure 8.1 – Problem setup.

$$x_{t+1} = Ax_t + w_t, \tag{8.1}$$

where $x_t \in \mathbb{R}^n$ and $w_t \in \mathbb{R}^n$ denote the state vector, and the state noise vector, respectively, at time t, and $A \in \mathbb{R}^{n\times n}$ is the dynamics matrix.

The measurement equation associated with the generic node $i \in \mathcal{N}$ is defined as

$$y_t^i = C^i x_t + v_t^i, \tag{8.2}$$

where $y_t^i \in \mathbb{R}^{m_i}$ and $v_t^i \in \mathbb{R}^{m_i}$ denote the observation vector and the observation noise vector, respectively, considered at time t, and C^i is a matrix of appropriate dimensions.

The following assumptions are made on the detectability of the system and the intensity of the disturbances.

Assumption A5. The system (8.1)-(8.2) is collectively detectable, i.e. the pair (A, C) is detectable, where $C := \text{col}(C^i)$.

Note that we only assume global detectability but not local detectability of the system, i.e. we do not require that the pair (A, C^i) be detectable for any $i \in \mathcal{N}$.

Assumption A6. The matrix A in (8.1) is invertible.

Remark. *As shown in the appendix B of Park and Martins [2016], and in Appendix C.1, Assumption A6 is mild. Even if the matrix A is not invertible we can observe the state of the system by partitioning the system into two subsystems. One of the subsystems satisfies Assumption A6 and the other can be ignored.*

Since in this chapter we aim to guarantee ultimate boundedness of the estimation error at every node, we require the following assumption on the magnitude of the disturbances.

Assumption A7. The $\mathscr{L}_\infty$ norm of the disturbance signals satisfy

$$\|w_t\|_\infty \le \epsilon_w, \qquad \|v_t^i\|_\infty \le \epsilon_{v^i},\ i \in \mathscr{N},$$

for some constants $\epsilon_w > 0$ and $\epsilon_{v^i} > 0$.

In Assumption A7 we chose the $\mathscr{L}_\infty$ norm since it is the norm which we find most suitable in many applications. Equivalently, different norm bounds can also be considered, such as quadratic norms.

Another case is when the disturbances are stochastic instead of deterministic. In the latter case, instead of Assumption A7 we make the following assumption about the measurement and process noise.

Assumption A8. The measurement and process noise satisfy

$$w_t \sim \mathscr{N}(\mathbf{0}, Q), \qquad v_t^i \sim \mathscr{N}\left(\mathbf{0}, R^i\right),\ i \in \mathscr{N},$$

for some positive definite matrices $Q \in \mathbb{R}^{n\times n}$ and $R^i \in \mathbb{R}^{m_i \times m_i}$. Moreover, the process and measurement noise of different sensors are uncorrelated among themselves, that is,

$$E\left[\left(v_t^i\right)^T v_t^j\right] = \mathbf{0},\ i, j \in \mathscr{N}, i \neq j \qquad E\left[w_t \left(v_t^i\right)^T\right] = \mathbf{0},\ i \in \mathscr{N}.$$

For simplicity, we consider that the covariance matrices are fixed in time. However, without adding much more complexity to the stability proofs, we could also assume that the covariance matrices are time varying and uniformly bounded over time. We note that Assumption A8 can be considered as a strong assumption since one normally assumes only that Q is positive semi-definite in order to model dimensions of the system state without any process noise, such as in the case of single integrator. The reason behind this assumption is that it avoids singularities in the Kalman filter algorithm that will be discussed later in this chapter. When Assumption A8 does not hold and the covariance of the process or measurement noise is positive semi-definite, one can take matrices Q or R^i as upper bounds on the covariance of the process or measurement noise, that is, $E\left[\left(v_t^i\right)^T v_t^i\right] \preceq R^i$ and $E\left[w_t^T w_t\right] \preceq Q$, incurring in a small cost on the performance of the estimation methods depending on how tight the bounding is.

We assume that the nodes are synchronized.

Assumption A9. The nodes are synchronized, i.e. the nodes have knowledge of the global time t, and take measurements and communicate at the same rate.

Finally, the nodes are allowed to communicate according to the following assumption.

Assumption A10. At each measurement time the nodes are able to communicate a finite number of times l_f according to the network structure defined by $\mathscr{A}$, i.e. a node i is able to send l_f messages to node j if and only if $(i, j) \in \mathscr{A}$.

8.2.2 Distributed State Estimation Problem

Under Assumptions A5, A6, A7 for the deterministic case or A8 for the stochastic case, A9 and A10 this chapter discusses solutions for the problem of distributed state estimation using distributed observers. In this setup, each node reconstructs locally the state of the global system (8.1), denoted $\hat{x}_t^i$. In the deterministic case, it is required that the estimation error, $x_t - \hat{x}_t^i$, converges to an ultimate bound proportional to the magnitude of the disturbances $\epsilon_w > 0$ and $\epsilon_{v^i}, i \in \mathcal{N}$. In the stochastic case, it is required that the covariance of the estimation error becomes upper bounded after a finite time by a positive definite matrix, proportional to Q and $R^i, i \in \mathcal{N}$.

8.3 Notation

In this chapter we will use the following notation. An estimate of the state will be denoted as $\hat{x}_t$, and the predicted state at time t given $\hat{x}_{t-1}$ is denoted as $\bar{x}_t$. The estimation error is defined as $e_t := \hat{x}_t - x_t$ and the prediction error is defined as $\bar{e}_t := \bar{x}_t - x_t$. Given a local estimate of the state at node i, denoted as $\hat{x}_t^i$, the predicted state at time t given $\hat{x}_{t-1}^i$ is denoted as $\bar{x}_t^i$. Their estimation errors are defined respectively as $e_t^i := \hat{x}_t^i - x_t$ and $\bar{e}_t^i := \bar{x}_t^i - x_t$. In the context with different estimates at each node, e_t is defined as $e_t := \mathrm{col}\left(e_t^i\right)$ and $\bar{e}_t := \mathrm{col}\left(\bar{e}_t^i\right)$.

The estimation error covariance is defined as $P_t := E\left[e_t e_t^T\right]$ and the prediction error covariance as $\bar{P}_t := E\left[\bar{e}_t \bar{e}_t^T\right]$. The information matrix is defined as $\Omega_t := P_t^{-1}$ and the inverse of the prediction error covariance is $\bar{\Omega}_t := \bar{P}_t^{-1}$. In the context of multiple nodes we define $P_t^i := E\left[e^i\left(e^i\right)^T\right]$ and its inverse $\Omega_t^i := \left(P_t^i\right)^{-1}$, $\bar{P}_t^i := E\left[\bar{e}^i\left(\bar{e}^i\right)^T\right]$ and its inverse $\bar{\Omega}_t^i := \left(\bar{P}_t^i\right)^{-1}$. We also define the matrices $W := Q^{-1}$, $V = R^{-1}$, $V^i := \left(R^i\right)^{-1}$, $S := C^T V C$, and $S^i := \left(C^i\right)^T V^i C^i$, and the vectors $s_t := C^T V y_t$ and $s_t^i := \left(C^i\right)^T V^i y_t$.

8.4 Covered Topics

In this chapter we will cover key topics related to distributed state estimation, with a particular focus on linear time invariant systems. We will give next a general overview of the topics that we address.

8.4.1 Known Correlations

One approach that potentially requires only one communication after each measurement is to solve the problem of distributed state estimation through a recursive solution, after taking a measurement and communicating with the neighbors, of a minimum variance estimation problem, given the prediction from the previous step, the current measurement, and the estimates from the neighboring sensors.

This approach was first considered in Bar-Shalom [1981] and is therefore often referred to as the Bar-Shalom fusion method. Similar methods were studied subsequently in the papers Kim [1994], Li and Wang [2000], Li and Zhang [2001b,a], Li et al. [2002, 2003], Zhang et al. [2003], Li [2003], and Alriksson and Rantzer [2006] among others. This approach requires that each node maintain the covariance matrix of the estimation error of all nodes and the cross-covariance matrix between all the nodes of the network.

If the system is linear and time-invariant, then these matrices can be computed off-line. However, if the matrices do not converge to fixed values, one can only compute the matrices for a finite number of steps. If we require the estimator to run for a long period, one must consider other methods of distributed state estimation. Moreover, if the sensor model is time varying and only available locally at the sensor node, then this method is not feasible and other methods are required such as the ones we will discuss next.

8.4.2 Exchange of Measurements

Another method of performing distributed state estimation is by only exchanging the measurements, or some transformation of the measurements, among the nodes. This principle has been widely studied in the literature, e.g. in Rao and Durrant-Whyte [1991], Manyika [1993], Mutambara [1998], Durrant-Whyte [2000], Alriksson and Rantzer [2006].

The advantage of this method is that since the measurements are usually uncorrelated, to perform sensor fusion each node only needs to know the covariance of its current estimate and the covariance of the measurement noise of the neighbouring sensors, and there is no need of pre-computing off-line the covariance matrices or exchanging covariance matrices.

On the downside, this method only guarantees that the estimation error is bounded if for each node the system is observable with its own measurement and the measurement of the neighbours, which is a stronger assumption than being observable given the measurements of all nodes in the network. We will discuss this issue in detail later in this chapter.

8.4.3 Distributed Solvers for Linear Systems

Noting that, for linear systems, the solution of the centralized state estimation problem, consisting of estimating the state of the system given the measurements of all the sensors, amounts to solving a linear system of equations, one method of performing distributed state estimation consists of using specialized algorithms to solve the same linear system in a distributed fashion.

This method has been discussed recently in the papers Khan and Moura [2008], Pasqualetti et al. [2010]. In this chapter we will briefly explain formally the techniques of distributed state estimation through distributed solvers for linear systems and discuss some of the state of the art. As a drawback, distributed solvers for linear systems usually require many communications (exchange of messages) after each measurement.

8.4.4 Unknown Correlations

If one has restrictions of bandwidth, an alternative method to maintaining uncorrelated filters is to use approaches to the problem of fusing two estimates that do not rely on the knowledge of cross-correlation of the estimation error among different nodes.

One such method is covariance intersection, where each node fuses its own estimate with the estimates of the neighbours and computes an overestimation of the state estimation covariance with no knowledge of the cross-covariance. This fusion method consists of computing the fused information vector, the inverse covariance matrix times the estimate, as a convex combination of the information vectors of the neighbour set and the fused inverse covariance as a convex combination of the inverse covariances of the neighbours. The method guarantees that the computed covariance is always greater than the actual covariance of the estimate. Thus, one can guarantee that if this upper bound of the estimation error covariance is ultimately bounded, then the actual covariance is also ultimately bounded.

This method came to the fore early during the development of the field of distributed state estimation in the works reported in Uhlmann [1996], Julier and Uhlmann [1997, 2001]. In the context of consensus based estimation, covariance intersection was extended in Battistelli et al. [2015], Battistelli and Chisci [2016] to consider multiple sensors and guarantee deterministic convergence of the estimates. Despite not being considered originally as extensions of covariance intersection and only as applications of consensus to distributed estimation, similar methods had been studied previously in Casbeer and Beard [2009], Cattivelli and Sayed [2010]. An application of this technique to cooperative localization can be seen in Carrillo-Arce et al. [2013].

Besides covariance intersection, one can find in the literature other methods of data fusion such as the largest ellipsoid method Benaskeur [2002], the covariance union method for estimation with spurious measurements Uhlmann [2003], and the ellipsoidal intersection Sijs and van den Bosch [2015]. We will review these methods in a subsequent section of this chapter.

8.4.5 Consensus-Based Methods

Another method of distributed estimation involves distributing to every sensor information from all the sensors through a distributed averaging, or consensus algorithm. This method assumes that multiple messages are exchanged between the sensors between two instants of time t and $t+1$.

One of the earliest works in consensus-based distributed estimation is Olfati-Saber [2005], where the author proposes the use of continuous time consensus filters to recover the centralized Kalman filter at each sensor.

This paper has been at the origin of a flurry of activity on consensus-based distributed estimators, as in Mosquera and Jayaweera [2008], Kamgarpour and Tomlin [2008], Olfati-Saber [2009], Olfati-Saber and Jalalkamali [2012]. More recently, the work in Battistelli and Chisci [2014], Battistelli et al. [2015], Battistelli and Chisci [2016] also considers the case of many iterations of a consensus algorithm, by taking instead of the consensus matrix Π its power Π^{l_f}.

If, instead of basing the design of the distributed observers on the centralized Kalman filter, we base the design on a centralized Luenberger observer, we obtain the distributed Luenberger observer that is used in Chapter 12, which also has the property of a fixed gain matrix and therefore of known convergence rate. If designed through LQR it approaches its optimality properties as $l_f \to \infty$.

8.4.6 Distributed Linear Time-Invariant (LTI) Observers

In addition to the above mentioned methods, there has been a flurry of activity in the development of other methods that rely on the exchange of estimates with deterministic, instead of stochastic, convergence guarantees. Among the many references on distributed estimation, in the discrete-time setting, many are based on Kalman filtering such as Khan and Moura [2007, 2008], Long et al. [2012]. These methods require that the estimation error covariances computed locally be exchanged among nodes, which increases the amount of data needed to communicate. The issue of bandwidth efficiency is of paramount importance in practical applications, since lower bandwidth translates into lower energy consumption and therefore increased operational autonomy. Moreover, since in these methods the estimates have time-varying dynamics, it is difficult to obtain convergence rates beforehand for the estimation errors.

The above two issues, the need to exchange covariances and the difficulty in computing guaranteed error convergence rates, do not occur for distributed Luenberger observers, also named distributed linear time-invariant (LTI) observers, or distributed fixed gain observers, where the dynamics of the estimation errors are linear and time-invariant, unlike in Kalman filtering where the observer gains are typically time-varying. Distributed Luenberger observers have been the object of many recent studies, see Hashemipour et al. [1988], Khan et al. [2010], Matei and Baras [2012], Orihuela et al. [2013], Khan and Jadbabaie [2011], Ugrinovskii [2011], Viegas et al. [2012], Ugrinovskii [2013], Das and Moura [2013a,c,b], Doostmohammadian and Khan [2013], Li and Sanfelice [2014], Das and Moura [2015], Park and Martins [2016], Mitra and Sundaram [2016]. In a later section we will describe in detail some of these methods and reproduce the proofs of the convergence guarantees of some of the methods in the literature.

8.4.7 Nonlinear Methods

If the system that one is observing is inherently non-linear, then one should use methods suitable for distributed state estimation of nonlinear systems, such as moving horizon estimation Farina et al. [2012], extended Kalman filtering Lee and West [2010, 2013] or particle filtering, as in Manuel and Bishop [2014].

In moving horizon estimation, one computes on line the estimate which fits best a finite number of past measurements. Extended Kalman Filtering computes at each step the linearization of the nonlinear system at the current estimates and computes a linear Kalman filter update based on the measurement. Particle filtering computes the trajectory of several samples and attributes a probability to each sample given the measurements at each sensor, then the estimated state is a weighted average of the samples. We will later give a survey of methods of distributed estimation for nonlinear systems.

8.4.8 Related problems

Finally, we note that there are many problems related to distributed state estimation that have been the focus of much activity. This chapter would not be complete if such topics were not covered. Among those problems we cite network localization Barooah [2007], Barooah et al. [2010], Todescato et al. [2015], distributed detection Tenney and Sandell [1981], Chair and Varshney [1986], Tsitsiklis [1993], Viswanathan and Varshney [1997], Blum et al. [1997], Willett et al. [2000], Chamberland and Veeravalli [2003], static estimation Borkar and Varaiya [1982], Xiao and Boyd [2004], Speranzon et al. [2008], Kibangou [2010] and field estimation Delouille et al. [2004], Cortes [2009]. The problem of network localization consists of estimating at each sensor their own position based only on relative measurements to neighbours. Distributed detection is the problem of deciding at each node if a certain hypothesis is true, given that at each node a sensor takes a measurement and communicates with neighbour nodes. Static estimation is the problem of estimating a certain vector fixed in time given that there are different sensors taking different measurements of that vector. Finally, field estimation is the problem of determining the value of a field at each node which takes a measurement of the field at a particular location which is correlated with the measurements of the neighbour nodes depending on the distance among the locations of the two nodes. In the last section of this chapter we will give an overview of these problems related to distributed estimation.

8.4.9 Structure

In summary, the following topics related to distributed state estimation will be covered in each subsection.

- *Section 8.5: Kalman Filtering* - Description of the classical theory of centralized Kalman filtering and proof of deterministic convergence.
- *Section 8.7: Known Correlations* - Considering the distributed state estimation problem as a sequence of different minimum variance estimators and maintaining at every node the covariance and cross-covariance matrices of all nodes.
- *Section 8.8: Exchange of Measurements* - Methods that rely on the assumption that only the measurements, or some transformation of the measurements are exchanged among nodes.
- *Section 8.9: Distributed Solvers for Linear Systems or Matrix Inversion* - Transforming the global state estimation problem into that of solving a linear system or a matrix inversion problem and using specialized algorithms to solve it in a distributed fashion.
- *Section 8.10: Unknown Correlations* - Methods with guaranteed boundedness of the estimation errors or

its covariance but do not require the computation of cross-covariances among different state estimates. The emphasis is on the covariance intersection method.

- *Section 8.11: Consensus-Based Methods* - Methods of distributed estimation that are based on consensus.
- *Section 8.12: Distributed Linear Time-Invariant (LTI) Observers* - Techniques of distributed state estimation with convergence guarantees of the estimation error which are time-invariant.
- *Section 8.14: Nonlinear Methods* - Methods suitable for distributed state estimation of nonlinear systems, such as moving horizon estimation, extended Kalman filtering or particle filtering.
- *Section 8.15: Related Problems* - Other problems related to distributed state estimation: Network localization, distributed detection, static estimation and field estimation.
- *Section 8.16: Overview* - A summary of the conclusions comparing the different methods discussed in this chapter. 8.16

8.5 Kalman Filtering

Before proceeding to the theory of distributed estimation one must first start with the basics of Kalman filtering, and yet before with its basic building block, the Best Linear Unbiased Estimation (BLUE). We borrow from Verhaegen and Verdult [2007] to describe the concepts of BLUE and Kalman Filtering.

8.5.1 Best Linear Unbiased Estimation

The problem of BLUE consists of reconstructing, with minimum variance, a deterministic variable with noisy measurements. That is, we want to estimate a deterministic variable $x \in \mathbb{R}^n$, denoted $\hat{x}$, given the measurements expressed as

$$y = Fx + \epsilon$$

where $\epsilon \sim \mathcal{N}(\mathbf{0}, P)$ is a random signal with $P > 0$, and $F \in \mathbb{R}^{n\times m}$, with $m \geq n$, is full rank. The following lemma establishes the solution to the BLUE problem.

Lemma 3 (Theorem 4.2 in Verhaegen and Verdult [2007]; Lemma 2.2.4 and Theorem 3.4.1 in Kailath et al. [2000]; Sections 4k and 5a in Rao [1973])**.** The estimate

$$\hat{x} = (F^T P^{-1} F)^{-1} F^T P^{-1} y$$

is the only estimate of x of the form $\hat{x} = My$ such that $E[\bar{x}] = x$, and where for any other estimate $\bar{x}$ of the same form the estimation error covariance satisfies $E\left[(\hat{x}-x)(\hat{x}-x)^T\right] = (F^T P^{-1} F)^{-1} \preceq E\left[(\bar{x}-x)(\bar{x}-x)^T\right]$.

The estimate $\hat{x} = (F^T P^{-1} F)^{-1} F^T P^{-1} y$ is termed the Best Linear Unbiased Estimator (BLUE).

8.5.2 Kalman Filtering

One of the standard methods in state estimation for linear systems is Kalman filtering, where the covariance of the state estimation error is computed at each time and the observer gain is computed based on this covariance. The Kalman filter can be derived by applying the concept of BLUE to the problem of centralized state estimation in the case of stochastic noise, i.e. the problem of estimating the state of a discrete-time linear system of the form (8.1) with measurements of the form

$$y_t = Cx_t + v_t,$$

with $C \in \mathbb{R}^{m\times n}$ and $v_t \sim \mathcal{N}(\mathbf{0}, R)$, with R positive definite.

As a first step we wish to predict the state at time $t+1$ given a prior estimate of x_t, $\hat{x}_t$, with estimation error $e_t := \hat{x}_t - x_t$ satisfying $e_t \sim \mathcal{N}(\mathbf{0}, P_t)$. The only possible linear unbiased estimator of x_{t+1} is

$$\bar{x}_{t+1} = A\hat{x}_t, \tag{8.3}$$

and the prediction error $\bar{e}_{t+1} := \bar{x}_{t+1} - x_{t+1}$ satisfies, $\bar{e}_{t+1} \sim \mathcal{N}(\mathbf{0}, \bar{P}_{t+1})$, where the covariance of the predicted state is derived as

$$\bar{P}_{t+1} := AP_tA^T + Q. \tag{8.4}$$

Then, given a predicted state $\bar{x}_t \sim \mathcal{N}(x_t, \bar{P}_t)$ and the measurement at time t, y_t, one wants to compute a BLUE of x_t. This can be achieved directly from Lemma 3 noting that stacking y_t and $\bar{x}_t$ we obtain

$$\begin{bmatrix} y_t \\ \bar{x}_t \end{bmatrix} = \begin{bmatrix} C \\ I_n \end{bmatrix} x_t + \begin{bmatrix} v_t \\ \bar{e}_t \end{bmatrix},$$

with

$$\begin{bmatrix} v_t \\ \bar{e}_t \end{bmatrix} \sim \mathcal{N}\left(\mathbf{0}, \begin{bmatrix} R & \mathbf{0} \\ \mathbf{0} & \bar{P}_t \end{bmatrix}\right).$$

Therefore, we can apply Lemma 3 with

$$y := \begin{bmatrix} y_t \\ \bar{x}_t \end{bmatrix}, \quad F := \begin{bmatrix} C \\ I_n \end{bmatrix}, \quad P := \begin{bmatrix} R & \mathbf{0} \\ \mathbf{0} & \bar{P}_t \end{bmatrix}.$$

The BLUE is thus

$$\begin{aligned} \hat{x}_t &= \left(C^TR^{-1}C + \bar{P}_t^{-1}\right)^{-1}\left(C^TR^{-1}y_t + \bar{P}_t^{-1}\bar{x}_t\right) \\ &= \left(S + \bar{P}_t^{-1}\right)^{-1}\left(s_t + \bar{P}_t^{-1}\bar{x}_t\right) \\ &= \bar{x}_t + \left(S + \bar{P}_t^{-1}\right)^{-1} C^TR^{-1}(y_t - C\bar{x}_t), \end{aligned} \tag{8.5}$$

and the estimation error $e_t := \hat{x}_t - x_t$ satisfies $e_t \sim \mathcal{N}(\mathbf{0}, P_t)$ with

$$P_{t+1} := \left(S + \left(AP_tA^T + Q\right)^{-1}\right)^{-1}. \tag{8.6}$$

This minimum variance estimator of the state is termed the Kalman filter, and is arguably the most successful kind of state estimator to date. It can be shown that if the pair (A, C) is observable, then the estimation error converges and remains close to a neighbourhood of the origin.

We will now demonstrate, borrowing the results of Battistelli and Chisci [2014], the convergence properties of the estimation error of the Kalman filter, considering Assumption A6, i.e. that A is invertible. Although convergence of the Kalman filter follows from its optimal properties and the stability of the Luenberger observer, Theorems 10 and 11 containing explicit bounds on the estimation error covariances or deterministic bounds on the estimation error, are new to the best of this author's knowledge. The proofs of the theorems are given in Appendix C.2.

For the stochastic case, i.e. when $w_t \sim \mathcal{N}(\mathbf{0}, Q)$ and $v_t \sim \mathcal{N}(\mathbf{0}, R)$ one can show that the Kalman filter estimate covariance is bounded above after a fixed time, i.e. for $t \geq t_0 \geq 1$, $P_t \preceq \mathring{P}$ for some positive definite matrix $\mathring{P}$. This result is given in the following theorem.

Theorem 10. Given the Kalman filter (8.5)-(8.6), if the pair (A, C) is observable, A is invertible, and the disturbances w_t, v_t and initial estimation error e_0 satisfy for positive definite matrices Q, R and P_0 of appropriate dimensions

$$w_t \sim \mathcal{N}(\mathbf{0}, Q), \quad v_t \sim \mathcal{N}(\mathbf{0}, R), \quad e_0 \sim \mathcal{N}(\mathbf{0}, P_0),$$

we obtain upper and

$$\breve{P} \preceq E[e_t^T e_t] := P_t \preceq \mathring{P}, \quad \forall t \geq 0,$$

where $\mathring{P}$ and $\breve{P}$ are positive definite matrices. Moreover, we obtain for $t \geq 1$,

$$P_t^{-1} \preceq \breve{\Omega} := W + S, \tag{8.7}$$

and for $t \geq n$,

$$P_t^{-1} \succeq \mathring{\Omega} := \sum_{i=0}^{n-1} \breve{\beta} \left(A^{-i}\right)^T S A^{-i}, \tag{8.8}$$

where $\breve{\beta}$ is a positive scalar variable such that $\left(A\Omega^{-1}A^T + Q\right)^{-1} \succeq \breve{\beta} A^{-T} \Omega A^{-1}$ for any $\Omega \preceq \breve{\Omega}$, whose existence is guaranteed by Lemma 20.

For the deterministic case, i.e. when $\|w_t\|_\infty \leq \epsilon_w$ and $\|v_t\|_\infty \leq \epsilon_v$ for some positive constants $\epsilon_w, \epsilon_v > 0$, we will show that the estimation error is ultimately bounded. To establish the deterministic convergence of the Kalman filter we first note that the estimation error dynamics are given by

$$\bar{e}_{t+1} = Ae_t - w_t, \tag{8.9}$$

and

$$\begin{aligned} e_t &= \bar{e}_t - \left(S + \bar{\Omega}_t\right)^{-1} C^T V \left(C\bar{e}_t - v_t\right) \\ &= \left(I_n - \left(S + \bar{\Omega}_t\right)^{-1} S\right) \bar{e}_t + P_t C^T V v_t \\ &= \left(S + \bar{\Omega}_t\right)^{-1} \bar{\Omega}_t \bar{e}_t + P_t C^T R^{-1} v_t \\ &= P_t \bar{\Omega}_t \bar{e}_t + P_t C^T V v_t. \end{aligned} \tag{8.10}$$

Combining (8.9) and (8.10) yields

$$e_{t+1} = P_{t+1}\bar{\Omega}_{t+1} A e_t + P_{t+1}\left(C^T V v_{t+1} - \bar{\Omega}_t w_t\right) = P_{t+1}\bar{\Omega}_{t+1} A e_t + P_{t+1}\varepsilon_t, \tag{8.11}$$

with $\varepsilon_t := C^T R^{-1} v_{t+1} - \bar{\Omega}_t w_t$. We can now derive the result on deterministic ultimate boundedness of the estimation error.

Theorem 11. Given the Kalman filter (8.5)-(8.6), if the pair (A, C) is observable, A is invertible, and the disturbances w_t, v_t satisfy, for positive constants ϵ_w and ϵ_v,

$$\|w_t\|_\infty \leq \epsilon_w, \quad \|v_t\|_\infty \leq \epsilon_v,$$

we obtain

$$\limsup_{t\to\infty} \|e_t\| \leq \delta,$$

where given a positive scalar $1 > \theta > 0$

$$\delta := \sqrt{\frac{\sigma_{\max}(\breve{\Omega})}{\sigma^3_{\min}(\mathring{\Omega})}} \max\left(\frac{2\|A\|}{\theta\sigma_{\min}\left(A^T\breve{\Omega}^{-1}A+Q\right)\sigma_{\min}\left(\mathring{\Omega}\right)}, \frac{1}{\sqrt{1-\mathring{\beta}-\theta}}\right)\epsilon_M,$$

$$\epsilon_M := \|C^T R^{-1}\|\sqrt{m}\epsilon_v + \frac{1}{\sigma_{min}\left(A^T\breve{\Omega}^{-1}A+Q\right)}\sqrt{n}\epsilon_w,$$

$$\mathring{\beta} := \frac{1}{1+\frac{\sigma_{\max}\left(A^TQ^{-1}A\right)}{\sigma_{\min}\left(\mathring{\Omega}\right)}}.$$

To avoid cumbersome notation, for the remainder of this chapter we will prove convergence of the estimation error, for some of the observer algorithms, only in the noiseless case, that is, when $w_t = 0$ and v_t^i for all $i \in \mathcal{N}$, $t \geq 0$. However, using the analysis in the proofs of Theorems 10 and 11 one could also conclude that the estimation errors are ultimately bounded if Assumption A7 holds or that the covariance matrix of the estimation error is bounded after a finite time if Assumption A8 holds.

8.6 Generic Formulation for Distributed Estimation Algorithms

Many of the methods described in this chapter share the same formulation. The difference among them lie on the computation procedure for some design parameters. The method with known cross-correlations from Section 8.7 and the covariance intersection method of Subsection 8.10.1 can be written in the form

$$\bar{x}_{t+1}^i = \left(\sum_{j\in\mathcal{N}^i} D_t^{ij}\bar{x}_t^j\right) + F_t^i y_t^i, \tag{8.12}$$

where $D_t^{ij} \in \mathbb{R}^{n\times n}$ and $F_t^i \in \mathbb{R}^{n\times m_i}$ are selected such that $\left(\sum_{j\in\mathcal{N}^i} D_t^{ij}\right) + F_t^i C^i = A$. The difference between the two methods is how to select the parameters D_t^{ij} and F_t^i.

As mentioned previously, there are some disadvantages of having time varying parameters, D_t^{ij} and F_t^i, namely the computation of the matrices is an extra burden in real-time and the convergence rate of the estimation error is unknown beforehand. These issues are not present in the distributed linear time invariant methods of Section 8.12. The method in Subsection 8.12.2 has form 8.12 for all the nodes except one, where the dimension of the observer state is increased but the dynamics remain linear.

8.7 Known Correlations

When each node can only communicate once with one neighbour after each measurement, one can apply the theory of BLUE to the problem of distributed estimation. This method consists of computing recursively the BLUE given the prediction from the previous step, the current measurement, and the estimates from the neighboring sensors. We will see that this method assumes that each node knows all the covariances of the estimates in all nodes, and the cross-correlations among estimates of all nodes. Therefore, with this method, the computations may be heavy if the number of nodes is high.

In detail, the method works as follows. Assume that we begin with an estimate $\bar{x}_t^i$ with a Gaussian distribution and the following characteristics:

$$E\left[\bar{x}_t^i - x_t\right] = 0, \tag{8.13}$$

$$E\left[\left(\bar{x}_t^i - x_t\right)\left(\bar{x}_t^j - x_t\right)^T\right] := \bar{P}_t^{ij}. \tag{8.14}$$

We define the global covariance matrix as $\bar{P}_t := \left[\bar{P}_t^{ij}\right]_{ij\in\mathcal{N}}$ and the vector $\bar{x}_t := \mathrm{col}\left(\bar{x}_t^i\right)$. The following theorem states how to compute the BLUE of the state at the next time $\bar{x}_{t+1}^i$ given the local measurement y_t^i and the estimates of the neighbours $\bar{x}_t^j$, $j \in \mathcal{N}^i$, as well as the global covariance matrix $P_{t+1} := E\left[\bar{e}_{t+1}\bar{e}_{t+1}^T\right]$, where $\bar{e}_t := \mathrm{col}(\bar{e}_t^i)$ with $\bar{e}_t^i := \bar{x}_t^i - x_t$.

Theorem 12. Consider the matrices $\eta_i \in \mathbb{R}^{|\mathcal{N}^i|n\times Nn}$, defined by $\eta_i := \mathrm{row}\left(\boldsymbol{e}_j, j \in \mathcal{N}^i\right) \otimes I_n$, where vector $\boldsymbol{e}_i$ is a column vector with all entries equal to 0 except at entry i which is 1, $\mathbf{1}_i \in \mathbb{R}^{|\mathcal{N}^i|\times n}$ defined by $\mathbf{1}_i := \mathbf{1} \otimes I_n$, and $\Gamma_{ij} \in \mathbb{R}^{|\mathcal{N}^i|n\times n}$ defined by $\Gamma_{ij} := \eta_i\left(\boldsymbol{e}_j \otimes I_n\right)$.

Define $\tilde{\Omega}_t^i := \mathbf{1}_i^T\left(\eta_i\bar{P}_t\eta_i^T\right)^\dagger\mathbf{1}_i$ and $\Omega_t^i := \tilde{\Omega}_t^i + S^i$, where $\left(\eta_i\bar{P}_t\eta_i^T\right)^\dagger$ is the Monroe-Penrose pseudo-inverse of $\eta_i\bar{P}_t\eta_i^T$[1] defined in Chapter 4.

Given the estimates $\bar{x}_t^i$, $i \in \mathcal{N}$, satisfying (8.13) and the global covariance matrix $\bar{P}_t := \left[\bar{P}_t^{ij}\right]_{ij\in\mathcal{N}}$, defining the correction terms $s_t^i := \left(C^i\right)^T V^i y_t^i$ and $S^i := \left(C^i\right)^T V^i C^i$, the BLUE of the state at time $t+1$ at node i given the local measurement y_t^i and the estimates of the neighbours $\bar{x}_t^j$, $j \in \mathcal{N}^i$ is given by

$$\bar{x}_{t+1}^i = A\left(\Omega_t^i\right)^{-1}\left(\sum_{j\in\mathcal{N}^i}\mathbf{1}_i^T\left(\eta_i\bar{P}_t\eta_i^T\right)^\dagger\Gamma_{ij}\bar{x}_t^j + s_t^i\right), \tag{8.15}$$

and the global covariance matrix is given by

$$\bar{P}_{t+1} = T_t\bar{P}_tT_t^T + \mathrm{diag}\left(AP_t^iS^iP_t^iA^T\right) + \left(\mathbf{1}_N\mathbf{1}_N^T\right)\otimes Q, \tag{8.16}$$

where T_t is defined as $T_t := \left[T_t^{ij}\right]$

$$T_t^{ij} := \begin{cases} AP_t^i\mathbf{1}_i^T\left(\eta_i\bar{P}_t\eta_i^T\right)^\dagger\Gamma_{ij}, & j \in \mathcal{N}^i \\ 0, & j \notin \mathcal{N}^i \end{cases}$$

One may observe that since the size of $\bar{P}_t$ is $nN \times nN$, the computations can be very costly to compute on-line if the number of nodes is high. However, if the system is linear and time-invariant, then the sequence of global covariance matrices P_t can be computed off-line. Thus, the main problem with this method is that if the matrices do not converge to fixed values, one can only compute the matrices for a finite number of steps. In this case, this method cannot be used if one requires that the estimator run for an unbounded period of time. Moreover, if the sensor model, i.e. C^i is only available locally at the sensor node i, then this method is not feasible, and other methods are required such as the ones we will discuss next. It should be noted that this is the only method discussed in this chapter that assumes that only one message is received from the neighbours between two discrete-time instants t and $t+1$ and that is optimal in the stochastic sense, in that the covariance of each estimation error is minimized.

To the best of the author's knowledge this method, exactly in this form, is not described in the literature. However, the general idea is present in many publications. In one of the first works in distributed state estimation, Bar-Shalom [1981], this method is developed for fully connected networks. For this reason, this method is

[1] which is equivalent to $\left(\eta_i\bar{P}_t\eta_i^T\right)^{-1}$ if $\eta_i\bar{P}_t\eta_i^T$ is full rank

sometimes referred to as the Bar-Shalom method, which is revisited in Kim [1994].

In the series of papers Li and Wang [2000], Li and Zhang [2001b,a], Li et al. [2002, 2003], Zhang et al. [2003] and Li [2003], the problem of BLUE distributed parameter estimation is addressed. This is a particular case of distributed state estimation when the system is static and there is no process noise. The last paper of this series, Li [2003], deals with the problem of distributed state estimation with BLUE estimates of linear dynamic systems for the case of two sensors.

Another similar work is Alriksson and Rantzer [2006], where the estimate fusion among neighbours is done with averaging, with optimal weights minimizing an upper bound of the estimation error covariance after a finite time. In this work optimal estimator covariances, i.e. the covariances of the BLUE estimator, are computed off-line, with a recursive process. The estimator is time invariant using only the converged covariances. However, conditions for convergence of the covariance matrices are not provided.

8.8 Exchange of Measurements

An alternative method which does not require pre-computing off-line the global covariance matrix is obtained by only exchanging the measurements, among the nodes, that is, every node performs the Kalman Filter computations by taking its own measurements, and the measurements of the neighbours, $y_t^j,\ j \in \mathcal{N}^i$. The prediction equations are the same as in the standard Kalman filter. The predicted state is $\bar{x}_{t+1}^i = A\hat{x}_t^i$ and the covariance of the prediction is $\bar{P}_t^i = AP_t^iA^T + Q$.

The update equations can be seen as a particular case of the update equation of the standard Kalman filter, where one has multiple measurements with uncorrelated measurement noise. The update equations amount to computing a BLUE of x_t, given the predicted state $\bar{x}_t^i \sim \mathcal{N}(x_t, \bar{P}_t^i)$ and the measurements of the neighbours at time t, $y_t^j,\ j \in \mathcal{N}^i$. Expressing the neighbour set as $\mathcal{N}^i := \{i_1, \ldots, i_{|\mathcal{N}^i|}\}$ we obtain by stacking $y_t^j,\ j \in \mathcal{N}^i$, and $\bar{x}_t^i$ the following equation:

$$\begin{bmatrix} y_t^{i_1} \\ \vdots \\ y_t^{i_{|\mathcal{N}^i|}} \\ \bar{x}_t^i \end{bmatrix} = \begin{bmatrix} C^{i_1} \\ \vdots \\ C^{i_{|\mathcal{N}^i|}} \\ I_n \end{bmatrix} x_t + \begin{bmatrix} v_t^{i_1} \\ \vdots \\ v_t^{i_{|\mathcal{N}^i|}} \\ \bar{e}_t \end{bmatrix},$$

with

$$\begin{bmatrix} v_t^{i_1} \\ \vdots \\ v_t^{i_{|\mathcal{N}^i|}} \\ \bar{e}_t \end{bmatrix} \sim \mathcal{N}\left(\mathbf{0}, \begin{bmatrix} R^{i_1} & & \mathbf{0} & \\ & \ddots & & \\ & & R^{i_{|\mathcal{N}^i|}} & \\ \mathbf{0} & & & \bar{P}_t^i \end{bmatrix}\right).$$

From the above equations, the BLUE can be obtained by applying Lemma 3 with

$$y := \begin{bmatrix} y_t^{i_1} \\ \vdots \\ y_t^{i_{|\mathcal{N}^i|}} \\ \bar{x}_t^i \end{bmatrix}, \quad F := \begin{bmatrix} C^{i_1} \\ \vdots \\ C^{i_{|\mathcal{N}^i|}} \\ I_n \end{bmatrix}, \quad P := \begin{bmatrix} R^{i_1} & & \mathbf{0} & \\ & \ddots & & \\ & & R^{i_{|\mathcal{N}^i|}} & \\ \mathbf{0} & & & \bar{P}_t^i \end{bmatrix},$$

which yields

$$\hat{x}_t^i = \left(\sum_{j\in\mathcal{N}^i} S^j + \bar{\Omega}_t^i\right)^{-1} \left(\sum_{j\in\mathcal{N}^i} s_t^j + \bar{\Omega}_t^i \bar{x}_t^i\right)$$
$$= \bar{x}_t^i + \left(\sum_{j\in\mathcal{N}^i} S^j + \bar{\Omega}_t^i\right)^{-1} \left(C^i\right)^T V^i \sum_{j\in\mathcal{N}^i} \left(y_t^j - C^j \bar{x}_t^i\right). \tag{8.17}$$

The estimation error $e_t^i := \hat{x}_t^i - x_t$ satisfies $e_t^i \sim \mathcal{N}\left(\mathbf{0}, P_t^i\right)$, with

$$P_{t+1}^i := \left(\sum_{j\in\mathcal{N}^i} S^j + \left(AP_t^i A^T + Q\right)^{-1}\right)^{-1}. \tag{8.18}$$

The method described in this subsection is optimal in the stochastic case, given the information received by the sensors. However, with this method each agent does not receive information from sensors other than the neighbours and it can be seen from the analysis of the standard Kalman filter, that this method only guarantees that the estimation error is bounded if for each node the system is observable with its own measurement and the measurement of the neighbours, i.e. if the pair $(A, \mathrm{col}\left(C^j, j \in \mathcal{N}^i\right))$ is observable for every node $i \in \mathcal{N}$, which is a stronger assumption than being observable given the measurements of all nodes in the network.

This method has been widely studied in the literature during the past three decades, e.g. in Rao and Durrant-Whyte [1991], Manyika [1993], Mutambara [1998], Durrant-Whyte [2000], Kamgarpour and Tomlin [2008] where the method is named the decentralized information filter, or the decentralized Kalman filter. More recently, in Olfati-Saber [2009], this method is termed Kalman-consensus information filter. To overcome the limitation of the requirement of local observability, some papers combine both exchange of measurements and exchange of estimates such as Alriksson and Rantzer [2006], Battistelli et al. [2015].

8.9 Distributed Solvers for Linear Systems or Matrix Inversion

One possible method of distributed state estimation is the use of distributed solvers for linear systems. These algorithms consider a set-up where there are multiple computing nodes and a general communication network among the nodes. The objective is to compute at each node a vector c that is the solution of the linear system $b = Ac$, where A is a matrix of appropriate dimensions known to all nodes and $b = \mathrm{col}(b^i)$, where vector b^i is only known to node i. This should be achieved while taking into consideration that each node is only able to communicate with its neighbours in the communication graph. The transformation of the distributed state estimation problem, described in Section 8.2, as the problem of solving a linear system in a distributed manner is described in Pasqualetti et al. [2010]. Here, we describe a slightly different transformation than what is given in Pasqualetti et al. [2010]. Starting with an estimate of the state at time $t-1$, $\hat{x}_{t-1}$, with an error covariance of P_{t-1} we can obtain the predicted state at time t as $\bar{x}_t$ and its error covariance $\bar{P}_t := AP_t A^T + Q$. Defining the following matrices

$$U_t := \begin{bmatrix} \bar{e}_t \\ v_t^1 \\ \vdots \\ v_t^N \end{bmatrix},\ Y_t := \begin{bmatrix} \bar{x}_t \\ y_t^1 \\ \vdots \\ y_t^N \end{bmatrix},\ O_t := \begin{bmatrix} I_n \\ C^1 \\ \vdots \\ C^N \end{bmatrix},$$

we obtain

$$Y_t = O_t x_0 + U_t,$$

where $\bar{e}_t := \bar{x}_t - x_t$ and the covariance of U_t is known. Notice that the BLUE estimate of x_t, $\hat{x}_t$, can be computed with the knowledge of Y_t, O_t by solving a linear system, as seen in Lemma 3. However, in the problem of distributed estimation each node does not have knowledge of the full matrix Y_t and only has available y_t^i and $\bar{x}_t$, where i is the node index. Therefore, a distributed solver for linear systems is required to compute the BLUE estimate of x_t given Y_t. The characteristics of this method depends on which distributed solver one uses, and whether the solver is terminated before convergence or not. If the solver computes accurately the solution of the linear system of equations this method is equivalent to a centralized Kalman filter. However, it should be noted that potentially a large number of iterations are required between two discrete-time instants, or some particular type of communication network is needed.

For this purpose, in Pasqualetti et al. [2010] a distributed solver for a linear system for half duplex mediums (only one node can broadcast a message at each iteration), full networks (every node can communicate with every other node) and which requires $N+1$ iterations is proposed. The application of the Jacobi algorithm on distributed solvers for linear systems to the problem of network localization, that is to estimate the location of sensors measuring only the position difference to other nodes, a particular case of distributed estimation, is widely discussed in Barooah [2007], Barooah et al. [2010].

A different perspective on distributed estimation, which makes use of distributed matrix inversion algorithms, is given in Khan and Moura [2008]. Here, the objective is to obtain a distributed algorithm that approximates the classical centralized Kalman filter. To guarantee that the computations are scalable with the number of nodes, in the paper each node only estimates the parts of the state that contribute to that node's measurement, and not the full state. The paper also assumes that initially every node only has knowledge of its local observation matrix C^i and does not know the observation matrix of any other node. Therefore, to compute the covariance matrix at each step, one requires distributed matrix inversion algorithms. For this purpose, the authors of the paper propose the distributed iterate collapse inversion (DICI) algorithm, for covariance inversion, which assumes that the inverted covariance matrix can be approximated as a L-banded matrix. This approximation is shown to be mild, given the sparseness of the dynamics and observation matrices.

8.10 Unknown Correlations

In this section we consider a setup where each node runs one filter and transmits to the neighbours the estimate and the computed covariance. The objective is to perform data fusion of the received estimates without knowing the cross-covariance between the estimates and computing an upper bound of the covariance of the estimate. A solution to this problem is proposed in Uhlmann [1996] with the covariance intersection method, which will be described here.

Other methods of data fusion with unknown correlation which are less present in the literature include the largest ellipsoid Benaskeur [2002] method and the covariance union method Uhlmann [2003].

8.10.1 Covariance Intersection

Covariance intersection Uhlmann [1996], Julier and Uhlmann [1997, 2001] was one of the earliest distributed state estimation methods. Given its simplicity and theoretical support, it has become a popular method of fusing correlated estimates.

The paper by Battistelli et al. [2015] contains strong theoretical guarantees on the stability of the distributed consensus based Kalman filter, which is the application of covariance intersection to the problem of distributed state estimation, requiring only global and not local observability and only one communication at each step. In that paper, the authors summarize the different consensus-based approximations of a Kalman filter in a distributed setting, which apply the concept of covariance intersection: consensus on information, consensus on measurements, and a hybrid version.

The method works as follows. Suppose that at time t we have at each node $i \in \mathcal{N}$ the predicted state $\bar{x}_t^i$, and the computed estimation error covariance P_t^i, satisfy $E\left[\bar{x}_t^i - x_t\right] = \mathbf{0}$ and $E\left[\left(\bar{x}_t^i - x_t\right)\left(\bar{x}_t^i - x_t\right)^T\right] \preceq \bar{P}_t^i$. The pair $\bar{x}_t^i$, $\bar{P}_t^i$ satisfying these properties is referred to as a consistent estimate. We assume that the filters are possibly correlated, that is, it might happen that $E\left[\left(\bar{x}_t^i - x_t\right)\left(\bar{x}_t^j - x_t\right)^T\right] \neq \mathbf{0}$ for $j \neq i$. Define the information matrix $\bar{\Omega}_t^i := \left(\bar{P}_t^i\right)^{-1}$, and the correction terms $s_t^i := \left(C^i\right)^T V^i y_t^i$ and $S^i := \left(C^i\right)^T V^i C^i$, where V^i is some positive definite matrix which, if under Assumption A8 holds, it is defined as $V^i := \left(R^i\right)^{-1}$. Also, consider the consensus coefficients $\pi^{i,j} \geq 0$ where $i, j \in \mathcal{N}$ and $\pi^{i,j} = 0$ if $j \notin \mathcal{N}^i$, $\pi^{i,j} > 0$ if $j \in \mathcal{N}^i$ and $\sum_{j \in \mathcal{N}} \pi^{i,j} = 1$. The fusion method is described by the equations

$$\hat{x}_t^i = P_t^i \left(\sum_{j \in \mathcal{N}} \pi^{i,j} \bar{\Omega}_t^j \bar{x}_t^j + s_t^i \right), \tag{8.19}$$

$$\Omega_t^i = \sum_{j \in \mathcal{N}} \pi^{i,j} \bar{\Omega}_t^j + S^i. \tag{8.20}$$

The fused estimated covariance is recovered as $P_t^i = \left(\Omega_t^i\right)^{-1}$. It is straightforward to show that $E\left[\hat{x}_t^i - x_t\right] = \mathbf{0}$, and therefore to guarantee consistency one must show that $P_t^i \succeq E\left[\left(\hat{x}_t^i - x_t\right)\left(\hat{x}_t^i - x_t\right)^T \middle| \bar{x}_t^j, y_t^i, j \in \mathcal{N}^i\right]$.

The consistency of this method is shown in Julier and Uhlmann [2001]. For a geometric interpretation based on sigma contours the reader is referred to Uhlmann [1996]. Sigma contours are level sets of the quadratic function defined by the estimate and its covariance, which represent areas with a defined probability of containing the true state. The covariance intersection method is shown to yield an estimate whose sigma contours contain the intersection of the sigma contours of the estimates to be fused, hence its name.

The prediction equations are the same as in the standard Kalman filter, that is,

$$\hat{x}_{t+1}^i = A \bar{x}_t^i, \tag{8.21}$$

and

$$\bar{\Omega}_{t+1}^i = W - WA\left(\Omega_t^i + A^T W A\right)^{-1} A^T W, \tag{8.22}$$

where W is some positive definite matrix which, if under Assumption A8 holds, it is defined as $W := Q^{-1}$. In the stochastic setting, the paper by Battistelli and Chisci [2016] shows that the information matrices for every node are lower bounded given global observability, showing that the estimation error covariances remain bounded and proving the usefulness of this method.

In the deterministic setting, the work in Battistelli et al. [2015] gives a stability proof of the distributed Kalman filter given only global observability which we will summarize here. Some of the technical details of the Theorems in Battistelli and Chisci [2016] are given in Battistelli and Chisci [2014]. The main result is the following.

Theorem 13 (Lemma 2 of Battistelli et al. [2015])**.** Let assumptions A6-A7 hold, and assume that the system (8.1)-(8.2) is collectively observable, i.e. the pair (A, C) is observable, where $C := \mathrm{col}(C^i)$. Then, given the distributed consensus-based Kalman filter defined by equations (8.19)-(8.22), the estimation error $e_t^i := \hat{x}_t^i - x_t$ at each node is ultimately bounded, i.e. there exists a positive scalar $\epsilon > 0$ such that for all $i \in \mathcal{N}$

$$\limsup_{t \to \infty} \|e_t^i\| \leq \epsilon.$$

The abbreviated proof is given in Appendix C.2, which makes use of Lemmas 20 and 21, also contained in Appendix C.2.

Remark. *In Theorem we used the assumption that the system is collectivelly observable instead of detectable as in Assumption A5. However, if the system is not collectivelly observable and Assumption A5 holds, it can be shown that the estimation error is ultimatelly bounded in the same fashion of Appendix C.1, by performing an observability decomposition of the system and showing that the estimation errors associated to the unobservable subspace are naturally stable, and that Theorem 13 shows that the estimation errors associated with the observable subspace are stable.*

As stated in Theorem 13, given collective observability, this method guarantees ultimate boundedness of the estimation error. Moreover, in the stochastic case we obtain an upper bound on estimation error covariance, which is bounded by above. As disadvantages, this method is not optimal in the stochastic case, and requires the transmission of covariances or the computation of a large number of covariance matrices.

This method was studied in a number of research papers. In Battistelli and Chisci [2016] an extension of this method to the case of nonlinear systems is given through an adaptation of the extended Kalman filter. A similar method, named the diffusion Kalman filter, was studied in Cattivelli and Sayed [2010] which offered a proof of stochastic convergence of the method that requires local observability. A survey of different fusion rules which yield stable observers is given in Sijs and van den Bosch [2015], which derives a stability condition guaranteeing that the estimates are consistent. Another fusion method, the ellipsoidal intersection, which satisfies the stability condition is proposed and analyzed. The application of covariance intersection to the problem of distributed state estimation is also analyzed in Casbeer and Beard [2009] in the perspective of information filtering. The concept of covariance intersection was applied to the problem of cooperative localization in Carrillo-Arce et al. [2013].

8.10.2 Other Fusion Methods with Unknown Correlations

The covariance intersection method gives a conservative over-approximation of the fused estimate covariance. The largest ellipsoid method Benaskeur [2002] computes the largest ellipsoid that is included in the level sets of the quadratic functions determined by the covariances of the estimates to be fused. This is less a conservative method than covariance intersection, but does not guarantee consistency.

To fuse with spurious estimates, i.e. when one or more estimates are not accurate in terms of expected value and covariance, in Uhlmann [2003] the Covariance Union (CU) method is developed. This method consists of computing a conservative estimate that is consistent with both estimates, instead of being consistent with the fusion of the estimates. In Uhlmann [2003] inconsistency between estimates is detected through the Maholanobis Distance between expected values.

8.11 Consensus-Based Methods

We now review other estimation methods that are based on consensus. We first describe the method of Olfati-Saber [2005], the application of a consensus algorithm to the distributed Kalman filtering problem. We then describe a distributed consensus-based Luenberger observer, which will be used in Chapter 12 to address the problem of distributed estimation and control with quantized communications. Both of these methods have the disadvantage, in comparison with other methods in this chapter, that multiple iterations of a consensus algorithm are required between every two discrete-time instants t and $t+1$.

8.11.1 Consensus-based Distributed Kalman Filter

A seminal work in distributed Kalman filtering is Olfati-Saber [2005]. The key technique used involves writing the Kalman filter equations in information form, i.e. in terms of the inverse of the covariance matrix, termed the information matrix. The latter is then computed by averaging local information matrices and the global measurement is computed as the averaging of linear transformations of the local measurements.

The main idea of Olfati-Saber [2005] is the following. If one can compute averages, e.g. through distributed averaging, the centralized Kalman filter can be recovered as follows. The prediction equations remain identical to the standard Kalman filter.

$$\begin{aligned}\bar{x}_{t+1} &= A\hat{x}_t,\\ \bar{P}_{t+1} &= AP_tA^T + Q.\end{aligned}$$

The update equations can be recovered by using distributed averaging to compute the following values:

$$\begin{aligned}S^{\text{avg}} &= \frac{1}{N}\sum_{i\in\mathcal{N}} S^i,\\ s_t^{\text{avg}} &= \frac{1}{N}\sum_{i\in\mathcal{N}} s_t^i.\end{aligned}$$

Using the update equations we obtain

$$\begin{aligned}\hat{x}_t &= \left(NS^{\text{avg}} + \bar{P}_t^{-1}\right)^{-1}\left(s_t^{\text{avg}} + \bar{P}_t^{-1}\bar{x}_t\right),\\ P_{t+1} &= \left(NS^{\text{avg}} + \left(AP_tA^T + Q\right)^{-1}\right)^{-1}.\end{aligned}$$

In Olfati-Saber [2005], it is assumed that the nodes communicate continuously and therefore continuous time consensus filters are proposed to compute the averages. In a similar work, Kamgarpour and Tomlin [2008], discrete-time communications are assumed and the averages are computed through dynamic discrete-time consensus filters. For an historical perspective, this method was already considered, for the case of fully connected networks in the paper by Hashemipour et al. [1988].

We now examine the case where the consensus algorithm used to compute $\tilde{y}_t$ is the standard consensus algorithm in Section 7.3 of Chapter 7 with a limited number of iterations l_f, that is we assign $z^i_{t,0} = s^i_t$, and perform l_f iterations of the form

$$z^i_{t,l+1} = \sum_{j\in\mathcal{N}^i} \pi^{i,j} z^j_{t,l},$$

and we approximate $\tilde{y}_t$ at node i by $\tilde{y}^i_t := z^i_{t,l_f}$. In this case we estimate s_t at node i as

$$\hat{s}^i_t = s_t + Nq^i_t,$$

where $q^i_t := z^i_{t,l_f} - \frac{1}{N}\sum_{j\in\mathcal{N}} z^j_{t,0}$. Defining $q_{t,0} := \operatorname{col}\left(z^i_{t,0}\right) - \mathbf{1}\frac{1}{N}\sum_{j\in\mathcal{N}} z^j_{t,0}$ yields

$$q_{t,0} = \left(I_N - \frac{1}{N}\mathbf{1}\mathbf{1}^T\right)\otimes I_n \operatorname{col}\left(S^i\right)x_t.$$

From Theorem 7 we have that

$$q_t = \left(\Pi - \frac{1}{N}\mathbf{1}\mathbf{1}^T\right)^{l_f}\otimes I_N q_{t,0} = \left(\Pi - \frac{1}{N}\mathbf{1}\mathbf{1}^T\right)^{l_f}\otimes I_n \operatorname{col}\left(S^i\right)x_t.$$

Repeating the analysis of the Kalman filter in Section 8.5, we obtain

$$e^i_{t+1} = P_{t+1}\bar{\Omega}_{t+1}Ae^i_t + P_{t+1}\epsilon_t + P_{t+1}q^i_t,$$

and the global estimation error $e_t := \mathrm{col}\left(e^i_t\right)$ is

$$e_t = I_N \otimes \left(P_{t+1}\bar{\Omega}_{t+1}A\right)e_t + I_N \otimes P_{t+1}\epsilon_t + N\left(\Pi - \frac{1}{N}\mathbf{1}\mathbf{1}^T\right)^{l_f} \otimes P_{t+1}\,\mathrm{col}\left(S^i\right)x_t.$$

Since the estimation error dynamics depends on x_t, as can be seen in the last equation, if the system is unstable then the estimation error is also unstable, and therefore, rigorously, we cannot consider that the distributed estimation problem is solved with this algorithm. However, if the number of consensus iterations l_f is large then the interconnection between x_t and e_t becomes week, and we can only observe the instability effect if the algorithm runs for a long time, and the algorithm has a similar performance to the centralized Kalman filter.

A further development in the distributed Kalman filter appears in Olfati-Saber [2009], where it is shown how to compute the optimal gain matrix of a linear observer given that at each time an agent communicates with a limited set of neighbours. However, it is also shown that the computation of this optimal gain requires data from the neighbours of the neighbours, which requires two communication cycles. In addition, the work in Olfati-Saber [2009] gives a simplified, more tractable, version of the distributed Kalman filter with stability guarantees, but which requires local observability, i.e. the state of the system can be observed by each sensor individually. The work in Olfati-Saber and Jalalkamali [2012] builds on the results in Olfati-Saber [2009] to tackle the problem of simultaneous state estimation and tracking.

More recently, the work in Battistelli and Chisci [2014], Battistelli et al. [2015], Battistelli and Chisci [2016] also considers the case of many iterations of a consensus algorithm, by taking instead of the consensus matrix Π its power Π^{l_f}. As was seen in Subsection 8.10.1 this consensus-based distributed estimation algorithm has stability guarantees for the estimation error, unlike Olfati-Saber [2005] when using the standard consensus algorithm.

8.11.2 Consensus-based Luenberger Observer

A central concept in this chapter is that of state estimation using a Luenberger observer. We first consider the hypothetical centralized case where all the nodes have access to all of the outputs, or equivalently, to the vector $y_t := \mathrm{col}(y^i_t)$, and the objective is to estimate the state of the system x_t with a bounded error. Let L be a gain matrix of appropriate dimensions such that $\rho(A - LC) < 1$, which can always be found since (A, C) is detectable. Further let $\hat{x}_t \in \mathbb{R}^n$ denote a state estimate of x_t. The centralized Luenberger observer algorithm is described by

$$\hat{x}_{t+1} = A\hat{x}_t + L\left(y_t - C\hat{x}_t\right).$$

It follows easily from the above that the estimation error $e_t := \hat{x}_t - x_t$ satisfies the dynamics

$$e_{t+1} = (A - LC)\,e_t + w_t + L\mathrm{col}(v^i_t).$$

Since $\rho(A - LC) < 1$, in the deterministic case where Assumption A7 holds, one can observe from its dynamics that the estimation error e_t is ultimately bounded. Similarly in the stochastic case when Assumption A8 holds, since $\rho(A - LC) < 1$ the covariance of the estimation error $P_t := E[e_t e_t^T]$ is ultimately bounded.

The above centralized version of the Luenberger observer can be re-written in distributed form as follows. Consider $L^i \in \mathbb{R}^{n\times m_i}$ such that $L := \frac{1}{N}\mathrm{row}(L^i)$. Then, the estimates $\hat{x}_{t+1}$ provided by the Luenberger observer can be reformulated as the average $\hat{x}_{t+1} := \frac{1}{N}\sum_{i\in\mathcal{N}} z^i_{t+1}$ of the local variables z^i_{t+1} defined by

$$z^i_{t+1} := A\hat{x}_t + L^i\left(y^i_t - C^i\hat{x}_t\right). \tag{8.23}$$

Due to the limited communication resources, it is in general not possible to compute the average perfectly, and one must compute an approximation of the average. One possible method of computing an approximation of the average is the consensus algorithm in Section 7.3 of Chapter 7.

We now consider the application of the consensus algorithm (7.3) to the problem of distributed state estimation. One would like to compute the the real average value $\frac{1}{N}\sum_{j\in\mathcal{N}} z^j_t$, with z^i_t defined in 8.23. However, in general, due to bandwidth limitations, it is only possible to perform a finite number of iterations, denoted here as l_f, of the consensus algorithm (7.3).

Since in the proposed approach consensus is unattainable, each agent keeps an internal value $\hat{x}^i_t$, which may be different from node to node. Therefore, one wants an approximation of the average of the following local variables

$$z^i_{t,0} := A\hat{x}^i_{t-1} + L^i\left(y^i_{t-1} - C^i\hat{x}^i_{t-1}\right), \tag{8.24}$$

i.e. one wishes to compute an approximation of $\frac{1}{N}\sum_{j\in\mathcal{N}} z^j_{t,0}$. This approximation is computed with l_f iterations of the consensus algorithm (7.3), which in the present case takes the following form:

$$z^i_{t,l+1} = \sum_{j\in\mathcal{N}} \pi^{i,j} z^j_{t,l},$$

Finally, the state estimate is computed as $\hat{x}^i_t := z^i_{t,l_f}$.

Defining the estimation error of node i as $e^i_t := \hat{x}^i_t - x_t$, the consensus error as $q^i_t := \hat{x}^i_t - \frac{1}{N}\sum_{j\in\mathcal{N}} z^j_{t,0}$, and the average error as $e^{avg}_t := \frac{1}{N}\sum_{j\in\mathcal{N}}\hat{x}^j_t - x_t$, one can observe that the estimation error satisfies the dynamics

$$e^i_{t+1} = (A - LC)\,e^{avg}_t - q^i_{t+1} + \frac{1}{N}\sum_{j\in\mathcal{N}}\left(A - L^iC^i\right)q^j_t + w_t + L\,\mathrm{col}(v^i_t). \tag{8.25}$$

Notice that if the consensus algorithm approaches perfect averaging, i.e. if $\hat{x}^i_t \approx \frac{1}{N}\sum_{j\in\mathcal{N}} z^j_{t,0}$, either because of a large number of performed iterations l_f or because the network is highly connected, the estimation error dynamics coincides with the hypothetical centralized Luenberger case, since for all $i\in\mathcal{N}$ we obtain $e^i_t \approx e^{avg}_t$ and $q^i_t \approx 0$. Therefore, the performance of the consensus algorithm must be taken into account in the analysis of the estimation error dynamics. The following theorem provides a lower limit on the number of iterations of the consensus algorithm, such that stability of the estimation errors is guaranteed.

Theorem 14. Let assumptions A5-A7 hold. Then, given the distributed Luenberger observer defined by equations (8.19)-(8.22), assuming that the number of consensus iterations satisfies

$$\sigma_2^{l_f} > \frac{1 - \|A - LC\|_{P_1}}{\max\left(\left\|A - L^iC^i\right\|_{P_1}\right)\max\left(1, \frac{\|A-L^iC^i\|_{P_1}}{\|A-LC\|_{P_1}}\right)},$$

where P_1 is a positive definite matrix such that $\|A - LC\|_{P_1} < 1$, the estimation error $e^i_t := \hat{x}^i_t - x_t$ at each node is ultimately bounded, i.e. there exists a positive scalar $\epsilon > 0$ such that for all $i\in\mathcal{N}$

$$\limsup_{t\to\infty} \|e^i_t\| \le \epsilon.$$

We have seen in Theorem 14 that stability is guaranteed with a known convergence rate for l_f sufficiently large. Moreover, in the stochastic case, for a very large number of consensus iterations, i.e. as l_f goes to infinity, the covariance of the estimation errors as t goes to infinity are the same as the covariance of the estimation error of the centralized Kalman filter.

8.12 Distributed Linear Time-Invariant (LTI) Observers

We now review time-invariant estimation methods that involve exchange of state estimates among nodes. We must mention that most methods mentioned above involve, in one form or another, transmitting the covariance of the estimation error at each node, or the off-line computation and storage of a potentially large number of matrices. Moreover, since the assumed covariances are, in general, time-varying, it is difficult to obtain convergence rates of the estimation error beforehand, which is important to know if the observer is used in connection with another system. In order to avoid communicating covariances among nodes, to save bandwidth, and to obtain convergence rates of the estimation error, one is naturally led to the use of distributed LTI observers, or distributed Luenberger observers, which will be studied in depth in this section.

8.12.1 Connectivity-Based Norm Decrease

The concept of distributed Luenberger observer is developed in Khan et al. [2010], which studies the network tracking capacity of this type of observers, i.e. distributed estimators with fixed innovation gain, which communicate only once between agents between measurements. Given a set of sensors connected via a communication network, the network tracking capacity is the maximum vector induced 2-norm of the dynamics matrix of an observed system such that it is possible to compute a fixed gain matrix for a distributed observer with guaranteed ultimate boundedness of the estimation error. The authors study observers which depend only on one parameter to obtain an analytical lower bound on the network tracking capacity, and show that this lower bound is always greater than one for strongly connected communication graphs.

The main idea of the paper Khan et al. [2010] will be summarized next. The scalar gain estimator proposed in Khan et al. [2010] has the following form

$$\hat{x}^i_{t+1} = A\hat{x}^i_t - \alpha A\left(\left(\sum_{j\in\mathcal{N}^i}\left(\hat{x}^i_t - \hat{x}^j_t\right)\right) - \left(C^i\right)^T (y^i_t - C^i\hat{x}^i_t)\right).$$

Defining the matrices A_e, G and D_C:

$$\begin{aligned}
A_e &:= (I_N \otimes A)(I_{nN} - \alpha G),\\
G &:= L \otimes I_N + D_C,\\
D_C &:= \begin{bmatrix} \left(C^1\right)^T C^1 & & \mathbf{0} \\ & \ddots & \\ \mathbf{0} & & \left(C^N\right)^T C^N \end{bmatrix},
\end{aligned}$$

and the time-varying vectors e_t, u_t and g_t

$$\begin{aligned}
e_t &:= \left[e^i_t\right]_{i\in\mathcal{N}},\\
u_t &:= g_t - 1_N \otimes w_t,
\end{aligned}$$

$$g_t := (I_N \otimes A)B \begin{bmatrix} \left(C^1\right)^T v_t^1 \\ \vdots \\ \left(C^N\right)^T v_t^N \end{bmatrix},$$

the estimation error dynamics are described by

$$e_{t+1} = A_e e_t + u_t.$$

Given the above defined matrices, the design process consists of choosing α as

$$\alpha = \operatorname{argmin}_\mu \|I_{nN} - \mu G\| = \frac{2}{\lambda_{\max}(G) + \lambda_{\min}(G)},$$

from which it can be shown that stability is guaranteed if $\|P\| < 1$, that is, if

$$\|A\| < \frac{1}{\|I_{nN} - \alpha G\|} = \frac{\lambda_{\max}(G) + \lambda_{\min}(G)}{\lambda_{\max}(G) - \lambda_{\min}(G)}.$$

Following the framework of Khan et al. [2010], the authors in Das and Moura [2013a,c,b, 2015] describe variations of the distributed Kalman filter algorithms, with consensus on pseudo-innovations, and analyze their stability. One of the main assumptions in these papers is that the 2-norm of the matrix A in (8.1), $\|A\|$, is smaller than or equal to some value. As seen in the previous analysis in Khan et al. [2010] this bound is $\|A\| < \frac{\lambda_{\max}(G)+\lambda_{\min}(G)}{\lambda_{\max}(G)-\lambda_{\min}(G)}$, which is closely related to the connectivity of the communication network. As a positive aspect of this design, we note that the design of the observer is very simple requiring only an eigenvalue decomposition and the transmission to every agent of a scalar value.

8.12.2 Stabilizing the Estimation Errors from a Single Node

The work in Park and Martins [2016] gives a method to design stable distributed LTI observers with very mild assumptions, which are weaker than strong connectivity of the network. Specifically, it is only required that all source components, strongly connected subsets of the network with no incoming edges from the rest of the network, be collectively observable. Since in that paper it is proposed that the gains of all the observers except one are chosen randomly, it is apparent that this method may not be competitive in terms of performance, as measured by the convergence rate and ultimate estimation error bound.

The method proposed in Park and Martins [2016] can be summarized as follows. Suppose, without loss of generality, that we stabilize the observers through node 1, then the observers take the following form for nodes $i \in \mathcal{N} \backslash 1$

$$\hat{x}_{t+1}^i = A \sum_{j \in \mathcal{N}^i} \pi^{i,j} \hat{x}_t^j + L^i (y_t^i - C^i \hat{x}_t^i),$$

where $L^i \in \mathbb{R}^{n \times m_i}$, $i \in \mathcal{N}$ is referred to as the local observer gain. For node $i = 1$ they are described by

$$\hat{x}_{t+1}^1 = A \sum_{j \in \mathcal{N}^1} \pi^{1,j} \hat{x}_t^j + L^1 (y_t^1 - C^1 \hat{x}_t^1) + u_t.$$

The estimation error dynamics can then be expressed as

$$e_{t+1} = A_F e_t + \bar{B}^1 u_t + \mu_t,$$

where $A_F = \Pi \otimes A + \sum_{i=1}^N \bar{B}^i L^i \bar{C}^i$, $\bar{B}^i = \boldsymbol{e}_i \otimes I_n$, $\bar{C}^i = \boldsymbol{e}_i^T \otimes C^i$, and $\mu_t := 1 \otimes I_n w_t + \sum_{i=1}^N \bar{B}^i L^i v_t^i$. From node 1 we can measure the estimation error e_t^1 through the innovation $\bar{y}_t = y_t^1 - C^1 \hat{x}_t^1 = -\bar{C}^1 e_t + v_t^1$. In Park and Martins

[2016], it is proposed that the observer gains L^i be chosen at random from realizations of uniform distributions. It is shown that for almost all choices of L^i the triple $(A_F, \bar{B}^1, -\bar{C}^1)$ is observable and controllable under collective observability. Therefore we can choose, through LQR, eigenvalue assignment or any other method, $u_t = K\hat{e}_t$, with $K \in \mathbb{R}^{n\times Nn}$, such that $A_F + \bar{B}^1 K$ has all eigenvalues inside the unit circle.

To compute $\hat{e}_t$ on node 1 we design an observer of e_t of the following form:

$$\hat{e}_{t+1} = A_F\hat{e}_t + L^e(y_t^1 - C^1\hat{x}_t^1 + \bar{C}^1\hat{e}_t),$$

with L^e such that $A_F + L^e\bar{C}^1$ has all eigenvalues inside the unit circle. Combining the observer of e_t and the dynamics of e_t it follows from the separation principle of linear systems that since $\rho\left(A_F + \bar{B}^1 K\right) < 1$ and $\rho\left(A_F + L^e\bar{C}^1\right) < 1$ the observer is stable. As stated previously, this method has a potentially slow convergence rate. However, we note that the design procedure is simple, and can be done in just one node, all the others are completely independent and do not require any knowledge of the system model.

8.12.3 Observability Decomposition

Another paper that deals with the general case of collectively observable systems is Mitra and Sundaram [2016], which gives a method to design stable distributed LTI observers. The method consists of decomposing the state for each sensor into observable and unobservable subspaces. This decomposition is done sequentially, i.e. sensor 2 only decomposes the unobservable sub-state of sensor 1 and so forth. Then each sensor estimates only its observable sub-state and diffuses, with a consensus law, its estimated sub-state. This design method ensures that convergence occurs sequentially, in that since the observable sub-state of node i, if it exists, depends on the observable sub-states of nodes up to $i-1$, the convergence of the estimation error at i depends on the convergence of the estimation errors up to that node.

The method proposed in Mitra and Sundaram [2016] consists of performing a state transformation

$$\xi_t := \mathscr{T}^T x_t,$$

where the unitary matrix $\mathscr{T} \in \mathbb{R}^{n\times n}$ is referred to as the transformation map. With this transformation, considering without loss of generality that the set of sensors with associated observable sub-states is $\mathscr{N}^o = \{1,\dots,N^o\} \subseteq \mathscr{N}$, the state dynamics and measurement equations become

$$\begin{aligned}\xi_{t+1} &= \bar{A}\xi_t + \mathscr{T}^T w_t,\\ y_t^i &= \bar{C}^i\xi_t + v_t^i,\end{aligned}$$

where $\bar{C}^i := C^i\mathscr{T}$ takes the form for $i \in \mathscr{N}^o$

$$\bar{C}^i = \begin{bmatrix} C^{i1\mathscr{O}} & C^{i2\mathscr{O}} & \dots & C^{i(i-1)\mathscr{O}} & C^{i\mathscr{O}} & \mathbf{0}\end{bmatrix},$$

where $C^{ij\mathscr{O}}$ and $C^{i\mathscr{O}}$ for $i, j \in \mathscr{N}^o$ are local measurement matrices of appropriate size, and with

$$\bar{A} := \mathscr{T}^T A\mathscr{T} = \begin{bmatrix} A_{1\mathscr{O}} & & & & \mathbf{0} \\ A_{21} & A_{2\mathscr{O}} & & & \\ \vdots & \vdots & \ddots & & \\ A_{N^o1} & A_{N^o2} & \dots & A_{N^o\mathscr{O}} & \\ A_1 & A_2 & \dots & A_{N^o} & A_{\mathscr{U}\mathscr{O}} \end{bmatrix},$$

where A_{ij}, $A_{i\mathscr{O}}$, A_i and $A_{\mathscr{U}\mathscr{O}}$ are local matrices of appropriate size, $(A_{i\mathscr{O}}, C^{i\mathscr{O}})$ is observable and $\rho(A_{\mathscr{U}\mathscr{O}}) < 1$. The analysis in Mitra and Sundaram [2016] guarantees that the transformation $\mathcal{T}$ exists for collectively observable systems. As mentioned before, this transformation $\mathcal{T}$ can be obtained sequentially using standard methods of computing the observability staircase form of a system. Obtaining the observability staircase form of system (8.1) for sensor 1 we decompose the state of the system in observable and unobservable modes. Then for sensor 2 we only decompose the unobservable modes of sensor 1 and so forth.

This transformation is designed such that the state can be partitioned in multiple sub-states as

$$\xi_t = \begin{bmatrix} \xi^{(1)} \\ \vdots \\ \xi^{(N^o)} \\ \xi^{\mathcal{UO}} \end{bmatrix},$$

where the measurement equations become

$$y_t^i = C^{i\mathcal{O}} \xi_t^{(i)} + \sum_{j=1}^{i-1} C^{ij\mathcal{O}} \xi_t^{(j)} + v_t^i.$$

Moreover, the dynamics of the sub-states $\xi_t^{(i)}$, $i \in \mathcal{N}$ take the form

$$\xi_{t+1}^{(i)} = A_{i\mathcal{O}} \xi_t^{(i)} + \sum_{j=1}^{i-1} A_{ij} \xi_t^{(j)} + \left(\mathcal{T}^{(i)}\right)^T w_t,$$

where $\mathcal{T}^{(i)}$ is the column of $\mathcal{T}$ associated with $\xi_t^{(i)}$. The dynamics of the unobservable sub-state $\xi_t^{\mathcal{UO}}$ are

$$\xi_{t+1}^{\mathcal{UO}} = A_{\mathcal{UO}} \xi_t^{\mathcal{UO}} + \sum_{j=1}^{N} A_j \xi_t^{(j)} + \left(\mathcal{T}^{\mathcal{UO}}\right)^T w_t,$$

where $\mathcal{T}^{\mathcal{UO}}$ is the column of $\mathcal{T}$ associated with $\xi_t^{\mathcal{UO}}$. It is shown in Mitra and Sundaram [2016] that collective observability ensures that the transformation map $\mathcal{T}$ exists.

The distributed observer can be designed as follows. For the nodes $i \in \mathcal{N}$ such that $i \notin \mathcal{N}^o$ the measurements are discarded and the observers are simply

$$\hat{x}_{t+1}^i = A \sum_{j \in \mathcal{N}^i} \pi^{i,j} \hat{x}_t^j.$$

We choose observer gains L^i such that $\rho(A_{i\mathcal{O}} - L^i C^{i\mathcal{O}}) < 1$, which exist since the pairs $(A_{i\mathcal{O}}, C^{i\mathcal{O}})$ are observable. Then, at each node $i \in \mathcal{N}$ we estimate the sub-states $\xi_t^{(j)}$ for $j \in \mathcal{N}$ as $\hat{\xi}_t^{(j)i}$ and the unobservable sub-state $\xi_t^{\mathcal{UO}}$ as $\hat{\xi}_t^{\mathcal{UO}i}$ with the following observers. For i, the observer is

$$\hat{\xi}_{t+1}^{(i)i} = A_{i\mathcal{O}} \hat{\xi}_t^{(i)i} + \sum_{j=1}^{i-1} A_{ij} \hat{\xi}_t^{(j)i} + L^i \left(y_t^i - \left(C^{i\mathcal{O}} \hat{\xi}_t^{(i)i} + \sum_{j=1}^{i-1} C^{ij\mathcal{O}} \hat{\xi}_t^{(j)i} \right) \right).$$

For $j \neq i$, the observer takes the form

$$\hat{\xi}_{t+1}^{(j)i} = A_{j\mathcal{O}} \sum_{l \in \mathcal{N}^i} \pi^{i,l} \hat{\xi}_t^{(j)l} + \sum_{l=1}^{j-1} A_{jl} \hat{\xi}_t^{(l)i}.$$

Finally, for the unobservable sub-state the observer is

$$\hat{\xi}^{\mathscr{U}\mathscr{O}i}_{t+1} = A_{\mathscr{U}\mathscr{O}}\hat{\xi}^{\mathscr{U}\mathscr{O}i}_{t} + \sum_{j=1}^{N} A_j \hat{\xi}^{(j)i}_{t}.$$

It is also shown in Mitra and Sundaram [2016] that this design yields stable observers. However, it must be noted that the design must be done in a centralized fashion and some measurements taken by some sensors (the sensors not in $\mathscr{N}^o$) might be ignored, which can diminish the performance of the algorithm or slow the convergence rate. Also, since the convergence of the estimation errors occurs sequentially, the performance and convergence rate depends on the topology of the network and how the sensors are ordered.

8.13 Other Methods

In most of the methods discussed above, the observers take the form

$$\hat{x}^i_{t+1} = A \sum_{j\in\mathscr{N}} \pi^{i,j} \hat{x}^j_t - L^i (y^i_t - C^i \hat{x}^i_t). \tag{8.26}$$

There has also been a vast number of works that propose design methods of the observer gains L^i through the solution of some optimization problem such as H_2 or H_∞ filtering, e.g. Ugrinovskii [2011], Orihuela et al. [2013], Ugrinovskii [2013]. A similar methodology was used in Viegas et al. [2012] for the H_2 filtering design of a continuous-time distributed observer for the problem of cooperative localization of AUVs.

Observers of the form (8.26) were studied by several authors. The paper Mosquera and Jayaweera [2008] studies the convergence properties of a distributed Kalman filter of the form (8.26) with time-varying gains L^i and fixed consensus weights. In Matei and Baras [2012], a distributed Luenberger observer of the form (8.26) with time-varying observer gains and consensus weights which guarantee a certain level of performance with respect to a quadratic cost is presented. Finally, the paper Doostmohammadian and Khan [2013] analyzes the design of observers of the form (8.26) based on the results of structured systems, taking into account the structure of the matrix A in (8.1), the measurement matrices, and the communication graph.

When multiple iterations of the consensus algorithm are allowed between measurements, in Khan and Jadbabaie [2011] the authors show that it is possible to design distributed estimators with fixed innovation gain, which are stable if enough iterations of the consensus algorithm are performed. Namely, if the number of iterations are greater or equal to the primitivity index of the consensus matrix.

Finally, for the case of continuous-time linear systems, in Li and Sanfelice [2014] an optimization based design method for a continuous-time Luenberger observer is proposed.

8.14 Nonlinear Methods

Until this point we have assumed that the observed system is linear. There are many cases, however, where this assumption is too restrictive, when the system exhibits nonlinear behaviours. In these cases one should use methods suitable for distributed state estimation of nonlinear systems.

One of the most popular methods of state estimation is the Extended Kalman Filter (EKF). This method consists of doing the prediction by solving an ODE with the nonlinear dynamics of the system, and computing the updated estimate and the covariances based on the linearization of the system about the predicted state. The extension of this method to the distributed case is studied in Lee and West [2010], Long et al. [2012], where the authors propose distributed extended Kalman filters based on generalizations of the distributed Kalman filter found in Olfati-Saber [2005].

Another method of nonlinear state estimation is Moving Horizon Estimation (MHE). In MHE, one computes on-line the estimates of the past and present states which best fit a finite number H of past measurements, named the horizon length. In this method we assign a certain cost to the deviation of each state from its prediction taking into account the previous estimated state, another cost to the deviation from the estimated state at a particular time and the measurement at that time, and another cost function to the deviation from the estimated state at $t-H$, and its estimate in the previous time step. The extension of this method to a distributed setting is given in Farina et al. [2012], is based on the results from linear systems in Farina et al. [2010]. In the method proposed, the nodes exchange and perform averaging of estimates of time $t-H$, where H is the horizon length. The weight matrix defining the deviation cost of the estimate at $t-H$, or terminal cost, is also exchanged among nodes and computed in a distributed fashion.

Finally, there is also the method of particle filtering, which consists of computing the trajectory of several samples of a probability density function, and attributing a probability to each sample given the measurement taken. The assumed probability density function is then computed as a weighted sum of kernel functions centered at the samples. Distributed particle filtering methods can be found in Lee and West [2013] and Manuel and Bishop [2014]. The methods work by having the nodes exchange samples and fusing the probability density functions defined by the samples, until consensus is reached.

8.15 Related Problems

There are many problems which fall within the scope of distributed state estimation and can be seen as a particular case. For each of these problems, different methods have been developed for their solution. We will discuss in this section a subset of those problems: network localization, distributed detection, distributed static estimation, and distributed field estimation.

8.15.1 Network Localization

The problem of network localization consists of having each node localizing itself, i.e. estimating its own position, based on the difference between its position and that of the neighbours. Computing the global BLUE estimate based on the available measurements, the network localization problem can be cast as the problem of solving a linear system. In Barooah [2007] and Barooah et al. [2010] it is shown that, for the linear system of equations that needs to be solved, the Jacobi method for solving linear systems of equations can be implemented in a distributed fashion. This fact and its implications are extensively studied in Barooah et al. [2010]. Another method for network localization is given in Todescato et al. [2015] where the communications among agents are assumed asynchronous and the method is inspired in gradient-based optimization.

8.15.2 Distributed Detection

Distributed detection consists of testing one or more hypothesis given that each node makes a measurement which depends on each of the hypothesis being valid or not. This problem is similar to distributed state estimation where the state is discrete and can assume only two values, true or false. Distributed detection was one of the first problems related to distributed estimation to be studied. Since then, it has been the subject of many research articles, e.g. Tenney and Sandell [1981], Chair and Varshney [1986], Tsitsiklis [1993], Viswanathan and Varshney [1997], Blum et al. [1997], Willett et al. [2000], Chamberland and Veeravalli [2003].

8.15.3 Distributed Static Estimation

If one wants to estimate in a distributed fashion static parameters, then the problem of distributed static estimation arises. This is a particular case of distributed state estimation when the matrix A in (8.1) is equivalent to the identity and the process noise is zero. The problem has been the subject of much research for many decades now. In Borkar and Varaiya [1982] the problem of static estimation with multiple sensors is studied in a stochastic framework. More recently, in Xiao and Boyd [2004], distributed static estimation is formulated as a consensus problem and a solution based on distributed averaging is presented. The paper Speranzon et al. [2008] studies the problem of distributed state estimation of a time varying signal instead of a static parameter, i.e. when there is process noise. Finally, in Kibangou [2010] a method of distributed static estimation is proposed that considers network delays and unknown communication channel properties.

8.15.4 Distributed Field Estimation

Distributed field estimation is the problem of estimating a field based on measurements of sensors placed at different locations, while communicating according to a communication network. This problem was studied in Delouille et al. [2004] for multiple static sensors and in Cortes [2009] multiple mobile sensors, using the Kriging method.

8.16 Overview

In Table 8.1 we summarize the main characteristics of the methods discussed in this chapter. We compare the known correlations method of Section 8.7, the method with exchange of measurements of Section 8.8, the method of covariance intersection method of Subsection 8.10.1, the consensus-based distributed Kalman filter of Subsection 8.11.1, the consensus-based distributed Luenberger observer of Subsection 8.11.2, the connectivity-based norm decrease method of Subsection 8.12.1, the method of stabilizing the estimation errors from a single node of Subsection 8.12.2 and the observability decomposition method of Subsection 8.12.3 in terms of the assumptions required for stability, or ultimate boundedness, in the deterministic setting, the optimality of the scheme in the stochastic case, that is, if the estimation errors have the minimum possible covariance, the type of data exchanged, the communication rate, that is, the amount of times data is exchanged with the neighbours between two discrete-time instants t and $t+1$, the on-line computations that must be done between two discrete-time instants and the off-line computations required.

In terms of the assumptions required for stability, collective detectability is the most general assumption, and is the only assumption in many methods. In the consensus-based Kalman filter with the standard consensus algorithm of Section 7.3 of Chapter 7 there are no stability guarantees if $\rho(A) > 1$, however if l_f is large, the instability effects might only be noticed when the magnitude of the system state becomes very large.

In the stochastic case, the only optimal scheme given the state estimates of the neighbours is the known correlations method. The consensus-based methods only recover optimality when the number of consensus iterations tend to infinity. The distributed linear, time-invariant methods that are discussed in this chapter are not optimal.

With the exception of the method of exchange of measurements, the type of data exchanged is usually a state estimate, or a variable of equal size. The covariance intersection scheme also requires the transmission of information matrices. With the method that only relies on measurements exchange we can only guarantee stability if we have local detectability, i.e. if the pairs $\left(A, \operatorname{col}\left(C^j, j \in \mathcal{N}^i\right)\right)$ are detectable for all $i \in \mathcal{N}$, since each sensor does not receive information from other sensors other than the neighbours.

Method	Assump. for stability	Optimality	Type of data com.	Com. rate	On-line comp.	Off-line comp.
Known Correlations	Collective detectability	Yes	$\hat{x}_t^i \in \mathbb{R}^n$	Once between two DT instants	Each node inverts of N matrices of size greater than n	Init. with PD matrices
Exchange of Meas.	Local detectability	Yes, given only the meas. from neighbours	$y_t^i \in \mathbb{R}^{m_i}$	Once between two DT instants	Standard KF comp.	Init. with PD matrices
Covariance Intersection	Collective detectability	No	$\hat{x}_t^i \in \mathbb{R}^n$ $\bar{\Omega}_t^i \in \mathbb{R}^{n \times n}$	Once between two DT instants	Equivalent to Standard KF comp.	Init. with PD matrices
Consensus-Based Dist. Kalman Filter	$\rho(A) < 1$	Yes, when $l_f \to \infty$	$z_{l,t}^i \in \mathbb{R}^n$	l_f iterations between two DT instants	Standard KF comp.	Init. with PD matrices, and Init. of consensus algorithm
Consensus-Based Luenberger Observer	Collective detectability and sufficiently large l_f	Yes, when $t \to \infty$ and $l_f \to \infty$	$z_{l,t}^i \in \mathbb{R}^n$	l_f iterations between two DT instants	Mult. and additions of the order of n^2	Solving an ARE of size n, and Init. of consensus algorithm
Connec.-Based Norm Decrease	Sufficiently small $\|A\|$	No	$\hat{x}_t^i \in \mathbb{R}^n$	Once between two DT instants	Mult. and additions of the order of n^2	Eigenvalue decomp. of a matrix of size Nn
Stab. the Est. Errors from a Single Node	Collective detectability	No, and might converge slowly	$\hat{x}^i \in \mathbb{R}^n$	Once between two DT instants	Mult. and additions of the order of n^2	Solving an ARE of size Nn
Observ. Decomp.	Collective detectability	No	$\hat{x}^i \in \mathbb{R}^n$	Once between two DT instants	Mult. and additions of the order of n^2	Solving N AREs of dim. smaller than n

Table 8.1 – Comparison between different distributed estimation methods. The cells colored in green correspond to the best methods for a particular characteristic, in red the most disadvantageous methods and in yellow methods with intermediate characteristics.

Regarding the communication rates there are multiple communications between two discrete-time instants t and $t+1$ on the consensus based methods, and just one communication between two instants for all the other methods.

In terms of on-line computations, the linear time-invariant methods, including the consensus-based Luenberger observer, are the most efficient, requiring a number of multiplications in the order of n^2 and a number of sums in the order of n. The worst method in terms of on-line computations is the method with known correlations, since between each two time instants we need to compute all the covariances and cross-covariances of the estimation errors, which involve inverting N matrices of size $n|\mathcal{N}^i| \times n|\mathcal{N}^i|$. All the other methods perform computations equivalent to the standard Kalman filter computations, involving the inversion of an $n \times n$ matrix.

Finally, regarding off-line computations, most methods, except the linear time-invariant methods, just require the initialization with positive definite matrices. In the case of consensus-based methods, we require also the initialization. With the linear time-invariant methods we simplify the on-line computations by increasing the complexity of the off-line computations, which usually involve the computation of the solution of algebraic Riccatti equations, except in the connectivity-based norm decrease method, which requires the computation of the eigenvalues of an $Nn \times Nn$ matrix.

From the analysis above it is apparent that some methods are more adequate for certain situations. When on-line computations are very fast compared to the sampling rate of the system and communications expensive, the known correlations method of Section 8.7 is a better choice. When the nodes have little computational power, communications are expensive, and there is an off-line design phase where a central computer has information about all the nodes, the distributed Luenberger observers such as the ones in Section 8.12.2 or 8.12.3 fare better. When computations are expensive and communications are relatively inexpensive when compared to the required performance, the consensus-based Luenberger observer of Section 8.11.2 is better. When off-line computations are infeasible and on-line computations and communications are relatively expensive, the covariance intersection method of Section 8.10.1 is more adequate.

9 A New Design Method for a Distributed Luenberger Observer

9.1 Introduction

This section addresses the problem of designing distributed observers for discrete linear time-invariant (LTI) systems with distributed sensor nodes subjected to bounded measurement noise. A solution is proposed in terms of a distributed LTI Luenberger observer that departs from common linear time-varying solutions rooted in consensus-based distributed estimation techniques. The solution does not require the exchange of covariance matrices. It is shown, under the conditions of collective observability, strong connectivity of the sensor communication network, and invertibility of the matrix A in (8.1) that the resulting observer yields ultimate boundedness of the estimation error. A design example is given where the asymptotic performance of the proposed observer is shown to be similar to that obtained using a time-varying distributed Kalman filtering approach.

As with any distributed Luenberger observers seen in Chapter 8 the proposed method is more advantageous than the other described methods in terms of required communications or required on-line computations. Comparing with other distributed Luenberger observer methods seen in Chapter 8, the method in this chapter can be more advantageous in that the off-line design process can be performed in a distributed fashion with a finite number of iterations, and its performance is potentially better in some cases as illustrated in simulations of a particular case.

9.2 Algorithm

In what follows, to simplify the notation, we will omit the time index t. For this purpose, for a time-varying vector x_t, when omitting the time index t we will use the notation x^+ to refer to x_{t+1}.

Consider the consensus coefficients $\pi^{i,j} \geq 0$, where $i, j \in \mathcal{N}$ and $\pi^{i,j} = 0$ if $j \notin \mathcal{N}^i$, $\pi^{i,j} > 0$ if $j \in \mathcal{N}^i$ and $\sum_{j \in \mathcal{N}} \pi^{i,j} = 1$, and the consensus matrix Π whose ijth element is $\pi^{i,j}$ and which is primitive, i.e. there exists an integer $k > 0$ such that Π^k is strictly positive. As was mentioned in Section 7.2, if the network $(\mathcal{N}, \mathcal{A})$ is strongly connected and aperiodic this condition is satisfied. Note that since we only require Π to be stochastic and not doubly stochastic, for an arbitrary network each node of the network $i \in \mathcal{N}$ can compute its local consensus coefficients knowing the number of in-neighbours $\mathcal{N}^i$ for example as

$$\pi^{i,j} = \begin{cases} \frac{1}{|\mathcal{N}^i|}, & \text{if } j \in \mathcal{N}^i \\ 0, & \text{otherwise} \end{cases} .$$

The algorithm proposed in this section has the following form:

$$\hat{x}^{i+} = A\left(\Omega^i\right)^{-1}\left(\sum_{j\in\mathcal{N}} \pi^{i,j}\bar{\Omega}^j\hat{x}^j + \left(C^i\right)^T\left(R^i\right)^{-1}y^i\right), \tag{9.1}$$

where Ω^i, and $\bar{\Omega}^i$ are appropriately chosen positive definite matrices of size $n\times n$, n is the size of the state x, and R^i is a positive definite matrix of size $m^i\times m^i$, where m^i is the size of the measurement vector y^i.

This observer algorithm is similar to the distributed Kalman filter with consensus on information given in Battistelli et al. [2015]. However, in the present we consider that the matrices Ω^i and $\bar{\Omega}^i$ are fixed in time.

The main problem that we address in this chapter is how to compute the matrices Ω^i and $\bar{\Omega}^i$. The design method is described in the next subsection.

9.3 Design

The design proceeds is as follows. We first choose the parameter $0<\tilde{\beta}<1$ and define the matrix

$$\tilde{\Omega}^i := \sum_{\tau=0}^{\bar{k}-1}\tilde{\beta}^\tau\left(A^{-\tau}\right)^T\left(\sum_{j\in\mathcal{N}}\pi_\tau^{i,j}S^j\right)A^{-\tau}, \tag{9.2}$$

where $S^i := \left(C^i\right)^T\left(R^i\right)^{-1}C^i$, $\pi_\tau^{i,j}$ is the element i,j of matrix Π^τ, $\bar{k} := k+n$ where k is the primitivity index of Π, i.e. the lowest integer such that Π^k is strictly positive, and n is the dimension of the state. It can be seen, from the collective observability property and the fact that Π^k is strictly positive, that $\tilde{\Omega}^i$ is positive definite

Given the above we may compute the matrix $\bar{\Omega}^i$ as

$$\bar{\Omega}^i := \tilde{\beta}\left(A^{-1}\right)^T\tilde{\Omega}^iA^{-1}. \tag{9.3}$$

Finally Ω^i is computed as

$$\Omega^i := S^i + \sum_{j\in\mathcal{N}}\pi^{i,j}\bar{\Omega}^j. \tag{9.4}$$

The motivation for this choice of matrices Ω^i and $\bar{\Omega}^i$ is given in the proof of stability presented in the next subsection.

From equations (9.2), (9.3) and (9.4) one can observe that the design can be done in a distributed fashion in $\bar{k}$ steps. Since the observer is linear, each node is only required to store its own state estimate, and perform a finite number of multiplications and sums at each time of the order of nm_i, where n is the dimension of the state and m_i is the size of the measurement at sensor i.

In contrast with the design method of this chapter, the methods in Mitra and Sundaram [2016], Park and Martins [2016] and Khan et al. [2010] require the observers to be designed beforehand in a centralized fashion. Similarly to the method proposed in this paper, since those methods yield linear observers, they just require a finite number of operations at every step of the order of nm_i. In Park and Martins [2016], one of the observers is also required to store and perform computations with an augmented state of the order of N, the number of sensors. It should also be noted that the method in Battistelli et al. [2015] does not require an a priori design of the observers. However, it requires a matrix inversion at every time.

9.4 Main Theorem

Before proceeding to the main result of this chapter the following result is in order.

Lemma 4. Consider the matrices $\tilde{\Omega}^i$, and Ω^i computed as in (9.4) and (9.2) respectively. Given assumptions A6-A7, and assuming that the system (8.1)-(8.2) is collectively observable, we obtain

$$\Omega^i \succ \tilde{\Omega}^i.$$

Proof. Using the fact that the system is collectively observable and $\pi_{\bar{k}}^{i,j} > 0$ for all $i, j \in \mathcal{N}$, we have that $\tilde{\beta}^{\bar{k}} \left(A^{-\bar{k}}\right)^T \left(\sum_{j\in\mathcal{N}} \pi_{\bar{k}}^{i,j} S^j\right) A^{-\bar{k}}$ is positive definite. It then follows that

$$\begin{aligned}
\Omega^i &= S^i + \sum_{j\in\mathcal{N}} \pi^{i,j} \bar{\Omega}^j \\
&= S^i + \sum_{\tau=1}^{\bar{k}} \tilde{\beta}^{\tau} \left(A^{-\tau}\right)^T \left(\sum_{j\in\mathcal{N}} \pi_{\tau}^{i,j} S^j\right) A^{-\tau} \\
&= \tilde{\Omega}^i + \tilde{\beta}^{\bar{k}} \left(A^{-\bar{k}}\right)^T \left(\sum_{j\in\mathcal{N}} \pi_{\bar{k}}^{i,j} S^j\right) A^{-\bar{k}} \\
&\succ \tilde{\Omega}^i,
\end{aligned}$$

□

We now present the main result of this chapter.

Theorem 15. Consider the distributed LTI observer (9.1), with matrices Ω^i, and $\bar{\Omega}^i$ computed as in (9.3)-(9.4). Given assumptions A6-A7, and assuming that the system (8.1)-(8.2) is collectively observable, the estimation errors $\hat{x}^i - x, i \in \mathcal{N}$ are ultimately bounded with ultimate bounds on $\|\hat{x}^i - x\|, i \in \mathcal{N}$ proportional to the bounds on the magnitude of the noise $\epsilon_w > 0$ and $\epsilon_{v^i}, i \in \mathcal{N}$.

Proof. We first consider the noiseless case

$$\begin{aligned}
x^+ &= Ax, \\
y^i &= C^i x.
\end{aligned}$$

Defining the estimation error as $\eta^i := \hat{x}^i - x$ it follows from (9.1) that

$$\begin{aligned}
\eta^{i+} &= A\left(\Omega^i\right)^{-1} \left(\sum_{j\in\mathcal{N}} \pi^{i,j} \bar{\Omega}^j \hat{x}^j + S^i x - \Omega^i x\right) \\
&= A\left(\Omega^i\right)^{-1} \left(\sum_{j\in\mathcal{N}} \pi^{i,j} \bar{\Omega}^j \eta^j\right),
\end{aligned}$$

where the last equality is obtained using (9.4), and the fact that Π is stochastic.

Define the local cost function $\mathcal{L}^i := \left(\eta^i\right)^T \bar{\Omega}^i \eta^i$. Using (9.3)-(9.4), Lemma 2 of Battistelli and Chisci [2014], the fact that $\Omega^i \succ \tilde{\Omega}^i$ (from Lemma 4) and that A is invertible, it follows that

$$\mathcal{L}^{i+} = \left(\sum_{j\in\mathcal{N}} \pi^{i,j} \bar{\Omega}^j \eta^j\right)^T \left(\Omega^i\right)^{-1} A^T \bar{\Omega}^i A \left(\Omega^i\right)^{-1} \left(\sum_{j\in\mathcal{N}} \pi^{i,j} \bar{\Omega}^j \eta^j\right)$$

$$
\begin{aligned}
&= \tilde{\beta}\left(\sum_{j\in\mathcal{N}} \pi^{i,j}\bar{\Omega}^j\eta^j\right)^T \left(\Omega^i\right)^{-1}\tilde{\Omega}^i\left(\Omega^i\right)^{-1}\left(\sum_{j\in\mathcal{N}} \pi^{i,j}\bar{\Omega}^j\eta^j\right)\\
&\le \tilde{\beta}\left(\sum_{j\in\mathcal{N}} \pi^{i,j}\bar{\Omega}^j\eta^j\right)^T \left(\Omega^i\right)^{-1}\Omega^i\left(\Omega^i\right)^{-1}\left(\sum_{j\in\mathcal{N}} \pi^{i,j}\bar{\Omega}^j\eta^j\right)\\
&\le \tilde{\beta}\left(\sum_{j\in\mathcal{N}} \pi^{i,j}\bar{\Omega}^j\eta^j\right)^T \left(\sum_{j\in\mathcal{N}} \pi^{i,j}\bar{\Omega}^j\right)^{-1}\left(\sum_{j\in\mathcal{N}} \pi^{i,j}\bar{\Omega}^j\eta^j\right)\\
&\le \tilde{\beta}\sum_{j\in\mathcal{N}} \pi^{i,j}\eta^{jT}\bar{\Omega}^j\eta^j = \tilde{\beta}\sum_{j\in\mathcal{N}} \pi^{i,j}\mathcal{L}^j.
\end{aligned}
$$

In vector form, defining $\mathcal{L} := \mathrm{col}\left(\mathcal{L}^i\right)$ yields

$$\mathcal{L}^+ \le \tilde{\beta}\Pi\mathcal{L},$$

where the inequality is interpreted element-wise.

Since Π is stochastic, 1 is an eigenvalue and we can find its left eigenvalue $\boldsymbol{p}$ which satisfies $\boldsymbol{p}^T\Pi = \boldsymbol{p}^T$. Finally, defining the Lyapunov function $\mathcal{V} := \boldsymbol{p}^T\mathcal{L}$ we can compute

$$\mathcal{V}^+ = \boldsymbol{p}^T\mathcal{L}^+ \le \tilde{\beta}\boldsymbol{p}^T\Pi\mathcal{L} = \tilde{\beta}\boldsymbol{p}^T\mathcal{L} = \tilde{\beta}\mathcal{V}.$$

Since the Lyapunov function decreases at each step, we have that the estimation errors for the noiseless case converge to zero. Therefore, from Assumption A7 and classical results on LTI systems (e.g. Theorem 9.6 of Hespanha [2009]), since the error dynamics are linear time-invariant, one can compute an ultimate bound on the estimation error - using the solution to a generic non-homogeneous discrete-time linear time invariant system (given in Section 6.5 of Hespanha [2009] or in Theorem 6) - that is proportional to ϵ_w and ϵ_{v^i}, and the Theorem follows. □

Remark. *In Theorem 15 we used the assumption that the system is collectively observable instead of detectable as in Assumption A5. However, as was mentioned in the remark of Section 8.10.1, if the system is not collectively observable and Assumption A5 holds, it can be shown that the estimation error is ultimately bounded using the same method of Appendix C.1, that is, by performing an observability decomposition of the system and showing that the estimation errors associated to the unobservable subspace are naturally stable, and that Theorem 15 shows that the estimation errors associated with the observable subspace are stable.*

9.5 Computation

To make clear the distributed nature of the design process and the low on-line computational requirements, we now summarize the computational details of the proposed distributed Luenberger observer and its design. The design algorithm is described as follows.

Data: $\bar{\beta}$, S^i, A and $\pi^{i,j},\ j \in \mathcal{N}^i$
Result: $\bar{\Omega}^i$ and Ω^i
$\tilde{\Omega}^i = S^i$
$l = 0$
while $l < \bar{k}$ **do**
  Receive $\tilde{\Omega}^j,\ j \in \mathcal{N}^i$ from in-neighbours
  $\tilde{\Omega}^i = \bar{\beta}\left(A^{-1}\right)^T \left(\sum_{j\in\mathcal{N}^i} \pi^{i,j}\tilde{\Omega}^j\right) A^{-1}$
  Send $\tilde{\Omega}^i$ to out-neighbours
  $l = l + 1$
end
$\bar{\Omega}^i := \tilde{\beta}\left(A^{-1}\right)^T \tilde{\Omega}^i A^{-1}$
$\Omega^i := S^i + \sum_{j\in\mathcal{N}} \pi^{i,j}\bar{\Omega}^j$

Algorithm 1: Design algorithm.

The on-line computations are simply described by the following algorithm.

Data: $\pi^{i,j} A\left(\Omega^i\right)^{-1}\bar{\Omega}^j$, $A\left(\Omega^i\right)^{-1}\left(C^i\right)^T\left(R^i\right)^{-1}$, y^i, $\hat{x}^i$ and $\hat{x}^j,\ j \in \mathcal{N}^i$
Result: $\hat{x}^{i+}$
$\hat{x}^{i+} = \sum_{j\in\mathcal{N}} \pi^{i,j} A\left(\Omega^i\right)^{-1}\bar{\Omega}^j\hat{x}^j + A\left(\Omega^i\right)^{-1}\left(C^i\right)^T\left(R^i\right)^{-1} y^i$

Algorithm 2: On-line computations.

Notice that the matrices $\pi^{i,j} A\left(\Omega^i\right)^{-1}\bar{\Omega}^j$ and $A\left(\Omega^i\right)^{-1}\left(C^i\right)^T\left(R^i\right)^{-1}$ for $i \in \mathcal{N}$ and $j \in \mathcal{N}^i$ can be precomputed off-line, and therefore the on-line computations consist of $\left|\mathcal{N}^i\right| n^2 + nm_i$ multiplications and $n\left(\left|\mathcal{N}^i\right| n + m_i - 1\right)$ sums.

9.6 Illustrative Example

In this section we illustrate the performance of the algorithm proposed in this chapter through a design exercise. We also compare its performance against that obtained with other methods available in the literature. Namely, the scalar gain observer method of Khan et al. [2010] (an algorithm that requires a bound on the $\mathcal{L}_2$ norm of A), the distributed Kalman filter algorithm with consensus on information (and not on measurements) in Battistelli et al. [2015], and the method in Park and Martins [2016].

In order to assess the performance of the distributed algorithms, we will consider a distributed system of the form (8.1)-(8.2) with collective but not local observability where the eigenvalues of A can be assigned. We will consider a network of 11 nodes. The dynamical system considered has matrix A defined as $A := \lambda\,\mathrm{diag}\left(A^i\right)$, where A^i is a random unitary matrix and λ will be defined later. This matrix represents a setting where we have a set of heterogeneous systems with decoupled dynamics, all having the same eigenvalues.

Let $\boldsymbol{e}_i$ be a row vector with 1 at position i and zero at every other position. With this notation, the observation matrices are defined as

$$C^i := \begin{bmatrix} (\boldsymbol{e}_i - \boldsymbol{e}_{i+1})^T \\ (\boldsymbol{e}_{i-1} - \boldsymbol{e}_i)^T \end{bmatrix} \otimes I_2,$$

except at $i = 1$, where we replace $i-1$ by N, and at $i = N$, where we define $C^N := \boldsymbol{e}_N^T \otimes I_2$. This set of observation matrices translates to a setting where the heterogeneous systems with decoupled dynamics mentioned above have coupling in the measurements. It can be observed that with this choice of A and C matrices we have collective observability but not local observability at each node, thus requiring the use of distributed observers to reconstruct the state.

The process and measurement noises are generated randomly with a Gaussian distribution. With this method of stochastic noise generation one cannot determine beforehand the noise bounds; however, at each realization the noise is bounded and we have that the estimation errors are ultimately bounded for stable observers. The covariances chosen for the noises were $Q = I_{2N}$ for process noise and $R^i = 10^{-2} I_{m_i}$ for measurement noise. The initial state is also randomly generated with a Gaussian distribution with covariance $P_0 = 10^2 I_{2N}$. The matrix R^i in (9.1) was set equal to the covariance of the measurement v^i. The communication network considered was an undirected circular network, i.e. the neighbor set at each node is defined as $\mathcal{N}^i := \{i-1, i+1\}$ except at node $i = 1$ where it is $\mathcal{N}^i := \{N, 2\}$, and at node $i = N$ where it is $\mathcal{N}^i := \{N-1, 1\}$.

In what follows we will compare the different algorithms in terms of the norm of the global estimation, i.e. $\| \operatorname{col}(\hat{x}^i - x) \|$. To remove the randomness effect of a single simulation run, we perform 50 runs and plot the average values.

In the algorithm proposed in this chapter, stability is guaranteed for any choice of the parameter $\tilde{\beta}$ satisfying $1 > \tilde{\beta} > 0$. To assess the effect of the choice of $\tilde{\beta}$ we plot in Figure 9.1 the norm of the estimation error for different values of $\tilde{\beta}$, when $\lambda = 1.05$.

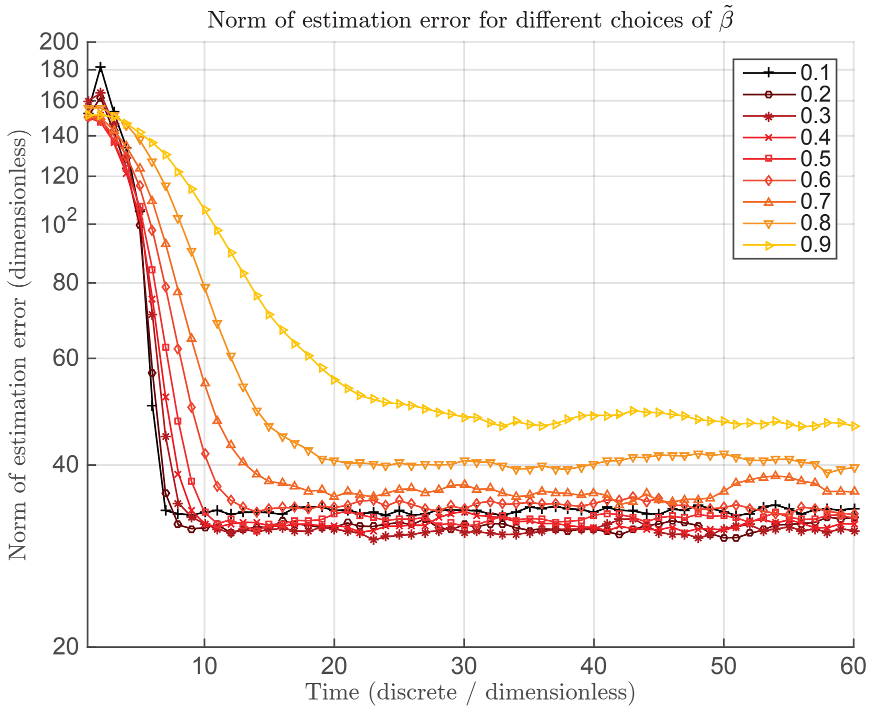

Figure 9.1 – Norm of estimation error for different choices of $\tilde{\beta}$.

We can observe from Figure 9.1 that, for this case, the best asymptotic performance is achieved for a value of $\tilde{\beta} = 0.3$ and this is the parameter choice that will be used in the following simulations. In the following plots we will present the results of the scalar gain observer in Khan et al. [2010] in red, the distributed Kalman filter in Battistelli et al. [2015] in green, the method in Park and Martins [2016] in blue, the method in Mitra and

Sundaram [2016] in cyan, and the algorithm of this chapter in magenta. For reference we also plot the norm of the stacked state vector $\|\mathbf{1} \otimes I_{2N} x\| = \sqrt{N}\|x\|$ in black. The results for $\lambda = 0.9$ are shown in Figure 9.2 and the results for $\lambda = 1.05$ are shown in Figure 9.4.

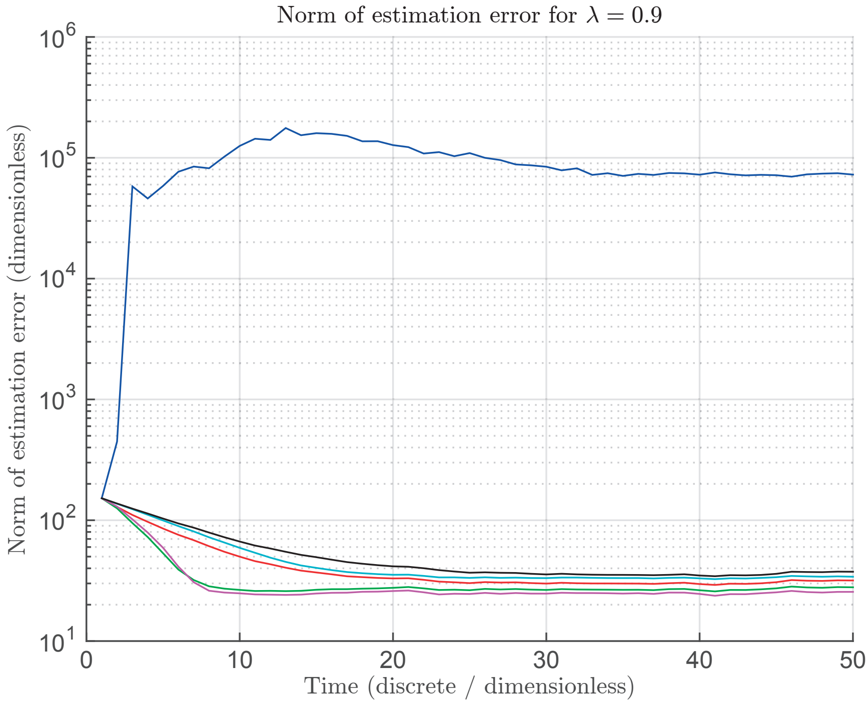

Figure 9.2 – Norms of global estimation errors for $\lambda = 0.9$. The results for the scalar gain observer in Khan et al. [2010] are in red, for the distributed Kalman filter in Battistelli et al. [2015] in green, for the method in Park and Martins [2016] is in blue, for the method in Mitra and Sundaram [2016] in cyan, for the algorithm of this chapter is in magenta, and for the norm of the stacked state vector is in black.

From Figure 9.2 one can observe that all estimators are stable. However, the observer in Park and Martins [2016] has worse convergence rates and worse asymptotic errors than that of the stacked state norm. This is not surprising since the observer gains in all of the nodes except one are assigned randomly. We can also notice that the asymptotic bound of the estimation error of the observer proposed in this chapter is slightly lower than the ultimate bound observed for the method in Battistelli et al. [2015], and is lower than the other methods that are being compared.

Figure 9.4 shows that, since the norm of the state transition matrix is greater than the bound required for stability in Khan et al. [2010], the method in the latter paper yields an unstable observer, although with an increase rate lower than that of the stacked state. Also, as expected, the observer designed with the method in Park and Martins [2016] is stable, but has a very high asymptotic estimation error when compared to the other stable methods. The method in this chapter converges faster and achieves a smaller ultimate error than the method in Mitra and Sundaram [2016]. Finally, it must be stressed that the asymptotic performance and the convergence rate of the method proposed in this chapter is comparable to those achieved by the method in Battistelli et al. [2015]. Recall, also, that in Battistelli et al. [2015] there is exchange of the covariance matrices.

9.7 Conclusion

In this chapter we provided the design method of an LTI observer with guaranteed stability, which departs from common linear time-varying solutions rooted in consensus-based distributed estimation techniques, and does not require exchange of covariance matrices. It was shown, under the conditions of collective observability,

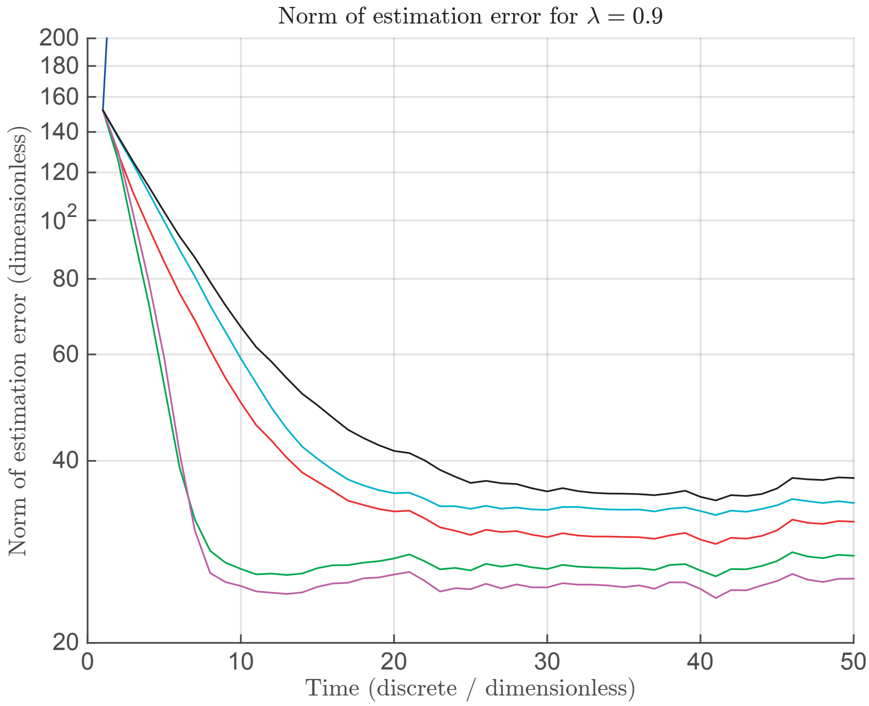

Figure 9.3 – Close-up of Figure 9.2.

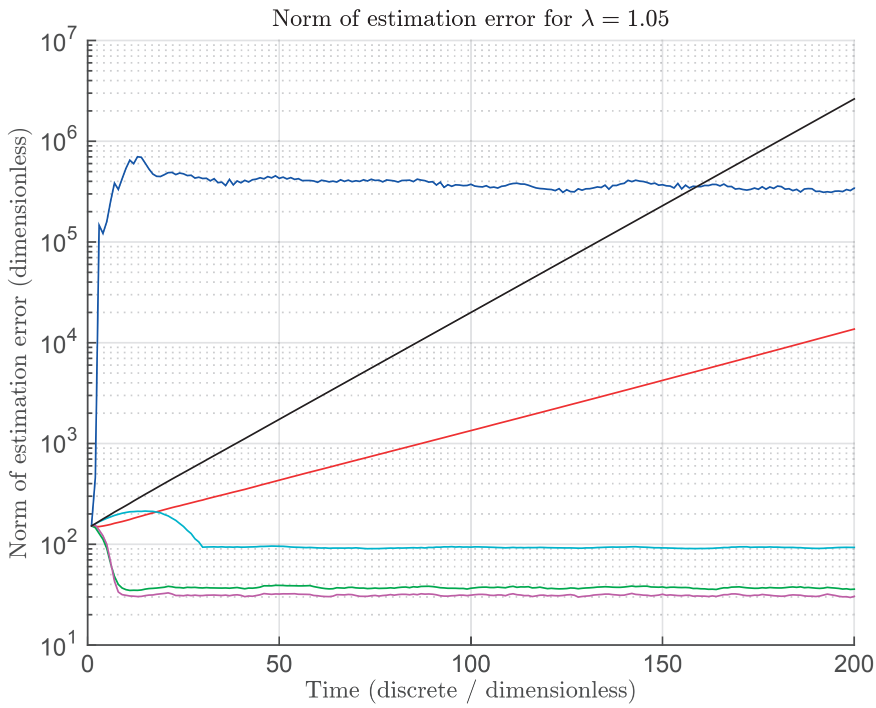

Figure 9.4 – Norms of global estimation errors for $\lambda = 1.05$.

strong connectivity of the sensor communication network, and invertibility of A that the resulting observer yields ultimate boundedness of the estimation error. From the simulation results of an illustrative example we show that the asymptotic performance of the proposed observer is shown to be similar to that of Battistelli et al. [2015].

Continuing the table of Section 8.16, the method proposed in this chapter has the following characteristics. We

Method	**Assump. for stability**	**Optimality**	**Type of data com.**	**Com. rate**	**On-line comp.**	**Off-line comp.**
New Dist. Luen. Obs.	Collective detectability	No	$\hat{x}^i \in \mathbb{R}^n$	Once between two DT instants	Mult. and additions of the order of n^2	Distributed algorithm with $\bar{k}$ iterations

can observe that the proposed method of this chapter is equivalent to the other distributed Luenberger observers seen in Chapter 8 in terms of required communications or required on-line computations and therefore fares better than the other described method in those aspects. The advantage with regard to the other distributed Luenberger observer methods of the method in this chapter is that the off-line design process can be performed in a distributed fashion with a finite number of iterations, whereas the other methods require a centralized design process with knowledge of information from all the nodes. Also, although the method is not optimal in the stochastic case, compared to the other distributed Luenberger observers, the performance in terms of the asymptotic norm of the estimation errors is potentially better as illustrated in the simulations of a particular case.

A number of topics warrant future research. Namely, optimizing the selection of parameter $\tilde{\beta}$, designing plug and play procedures for adding and removing sensors and, because we have a-priori known convergence rates, one can explore the use of progressive quantizers to exchange messages as in the case of Chapter 12.

Event-based Communications Part IV

10 Cooperative Path-Following with Logic-based Communications

10.1 Introduction

As was mentioned in the introduction of this thesis, in the field of cooperative motion control, a wide range of applications require the solution of the problem of cooperative path following (CPF). The problem of CPF consists of, given N autonomous vehicles and different spatial paths assigned to them, deriving control laws to drive and maintain the vehicles on their paths with desired speed profiles, holding a specified formation pattern.

A common strategy to solve the CPF problem consists of decoupling the CPF problem in i) a path-following (PF) problem, where the goal is to derive closed loop control laws to drive each vehicle to and follow its assigned path while tracking a path-dependent speed profile and ii) a multiple vehicle coordination problem, where the objective is to adjust the speed of each vehicle so as to achieve the desired formation pattern. The PF problem has been extensively addressed in the literature, see for example Dagci et al. [2003], Soetanto et al. [2003], Skjetne et al. [2004] and Plaskonka [2012].

The coordination problem, however, requires further study to address the limitations of the communication network between vehicles. These limitations are particularly stringent in underwater applications due to the communications medium. However, in the literature some of these issues have been addressed using graph theory to model the communication network and Lyapunov-based techniques to cope with intermittent communication failures and switching topologies; see for example Moreau [2005], Ihle et al. [2006], Ghabcheloo et al. [2006] and Ghabcheloo et al. [2009].

This chapter extends the CPF framework discussed in Ghabcheloo et al. [2006, 2009] to take into account that communication between vehicles occur at discrete instants, instead of continuously. In this respect the results of this chapter go further than in Ghabcheloo et al. [2006, 2009], where communication failures and switching topologies were considered, but communications take place continuously. The goal of this chapter is also to minimize the frequency of information exchange between vehicles. For this purpose, we borrow ideas from Yook et al. [2002] and Xu and Hespanha [2006] which consider distributed control systems, where the controller for each system uses the states of its own system and estimates of the states of the systems it communicates with. The communication strategy considered there assumes that each system has an internal estimator of its own state, synchronized with its neighbors. This setup allows each system to determine the estimation error of its neighbours by taking the difference between the actual and the estimated state. The communication logic consists of only transmitting information when the estimation error exceeds a certain threshold. With this method communication occurs asynchronously at discrete instants of time.

The general idea of event-triggered control, where a task such as broadcasting a variable or applying a control input only when a certain condition is satisfied has been the subject of many works such as Tabuada [2007], Aström [2008], Lunze and Lehmann [2010], Jetto and Orsini [2011] and Donkers and Heemels [2012] for single systems and Mazo and Tabuada [2011], De Persis and Wirth [2011], Wang and Lemmon [2011] and Wang et al. [2012] for multiple agents. In the context of control of multiple agents it is important that each agent is able to compute its own triggering condition, which leads to the field of self-triggered control, see e.g. Yook et al. [2002], Velasco et al. [2003], Xu and Hespanha [2006], Wang and Lemmon [2009], Mazo et al. [2010], Anta and Tabuada [2010], Shanbin and Bugong [2011] and Battistelli et al. [2012].

The works of Dimarogonas and Johansson [2009], Dimarogonas et al. [2012], Seyboth et al. [2013] and Fan et al. [2013] use the principle of self-triggered communications on consensus of single or double integrators. In Dimarogonas and Johansson [2009], Dimarogonas et al. [2012] a control law for continuous-time consensus with event-based communications is given, where it is considered that the estimates of the neighbouring states are piecewise constant and only change at communication times. The paper Dimarogonas et al. [2012] proposes multiple communication triggering conditions (CTC) with different characteristics. One of the proposed CTCs can only be computed centrally, another can be computed distributively with information from the neighbours, and the last one is completely distributed and only requires local information. The work in Seyboth et al. [2013] proposes a time-varying CTC that can be computed distributively, and also addresses consensus of double integrators. The work in Fan et al. [2013] provides a consensus algorithm where the agents read the states of the neighbours at communication times rather than sending their own states, and provides a communication protocol to compute the communication times guaranteeing stability of the scheme.

The application of event-triggered communications to the problem of consensus of linear or nonlinear multi-agent systems is analyzed in Guo et al. [2014], Garcia et al. [2014], Viel et al. [2016] and Almeida et al. [2017]. In Guo et al. [2014], a consensus control law of continuous-time systems with self-triggered communications is proposed where the triggering conditions is evaluated periodically. The work in Garcia et al. [2014] provides an algorithm with guaranteed convergence to consensus, where the state estimates do not take into account the control input, and therefore each agent only needs to estimate the states of the neighbours. Alternatively, Viel et al. [2016] proposes an estimator taking into account estimates of the states of all the agents. Here, convergence to consensus is guaranteed by using unsynchronized estimates of the neighbours for control, and less accurate estimates synchronized among neighbours, to provide an upper bound of the estimation error of the more accurate estimate. Finally, Almeida et al. [2017] extends the work in Seyboth et al. [2013] for LTI systems and directed networks.

Regarding more complex system models, the work in Viel et al. [2017] extends the work in Viel et al. [2016] for Euler-Lagrange systems, and Jain et al. [2017] applies some principles in Seyboth et al. [2013] to the problem of cooperative path following with self-triggered control. However, the evaluation of triggering condition requires continuous communications with the neighbours. In the work of this chapter, we use the same principles in Seyboth et al. [2013] and Jain et al. [2017] on the problem of coordinated path-following yielding a control algorithm with self-triggered communications.

This work is a continuation of the work in Vanni [2007] and Vanni et al. [2008] in that we provide full proofs of stability of the cooperative path-following algorithms that consider the interconnection between the coordination controller and the path-following controller when it exists, and we design an algorithm where that interconnection does not exist. Moreover, in the stability proofs we consider explicitly the delays and provide an upper bound on the delay such that the closed-loop system is stable. Also, unlike Vanni [2007] we define formally the filter structure for an arbitrary network.

10.2 Coordinated path-following control system architecture

This chapter proposes a CPF control architecture for a group of N decoupled agents, $\Sigma_i, i \in \mathcal{N}$ modeled by general systems of the form

$$\Sigma_i : \quad \dot{x}_i = \mathscr{F}_i\left(x_i, u_i, w_i\right), \tag{10.1a}$$
$$y_i = \mathscr{H}_i\left(x_i, u_i, v_i\right), \tag{10.1b}$$
$$z_i = \mathscr{J}_i\left(x_i\right), \tag{10.1c}$$

where $x_i \in \mathbb{R}^{n_i}$ denotes the state of agent i, $u_i \in \mathbb{R}^{m_i}$ its control input, $y_i \in \mathbb{R}^{p_i}$ its measured noisy output, w_i an input disturbance, and v_i measurement noise. The output $z_i \in \mathbb{R}^{q_i}$ is a signal that we require to reach and follow a desired feasible path $z_{d_i} : \mathbb{R} \to \mathbb{R}^{q_i}$ parametrized by $\gamma_i \in \mathbb{R}$. The following notation is required:

$$\boldsymbol{z_{d_i}}(\gamma_i) := \begin{bmatrix} z_{d_i}(\gamma_i) \\ \frac{\partial z_{d_i}}{\partial \gamma_i}(\gamma_i) \\ \vdots \\ \frac{\partial^k z_{d_i}}{\partial \gamma_i^k}(\gamma_i) \end{bmatrix}, \quad \boldsymbol{v_r}(\gamma_i) := \begin{bmatrix} v_r(\gamma_i) \\ \frac{\partial v_r}{\partial \gamma_i}(\gamma_i) \\ \vdots \\ \frac{\partial^l v_r}{\partial \gamma_i^l}(\gamma_i) \end{bmatrix}, \quad \boldsymbol{\gamma}_i := \begin{bmatrix} \gamma_i \\ \dot{\gamma}_i \\ \vdots \\ \gamma_i^{(n)} \end{bmatrix}.$$

The generalized path $\boldsymbol{z_{d_i}}$ is a vector that contains the desired path z_{d_i} and its partial derivatives with respect to γ_i up to some order k, the generalized speed profile $\boldsymbol{v_r}$ is a vector that contains the reference speed v_r and its partial derivatives with respect to γ_i up to some order l and the generalized path variable $\boldsymbol{\gamma}_i$ is a vector that contains the path-following variable γ_i and its time derivatives up to some order n.

In this chapter we introduce a new architecture for the coordinated path-following control system (CPFCS). The CPFCS consists of a control system for each agent which communicates with a set of neighbours. The innovation in this chapter consists of introducing a communication system which considers asynchronous communications between agents.

The objective of CPFCS is to drive the output of each agent z_i to converge to and remain inside a tube centered around the desired path $z_{d_i}(\gamma_i)$, while ensuring that its rate of progression $\dot{\gamma}_i$ also converges to and remains inside a tube centered around the desired speed profile $v_r(\gamma_i)$. Additionally, CPFCS must also guarantee that the path variables $\gamma_i, i \in \mathcal{N}$, are synchronized, that is, all the coordination errors $\gamma_i - \gamma_j,\ i, j \in \mathcal{N}$ converge to and remain inside a ball around the origin. The path variables γ_i may also be called parameterizing variables, path-following variables or, given their role in the coordination of agents, coordination states.

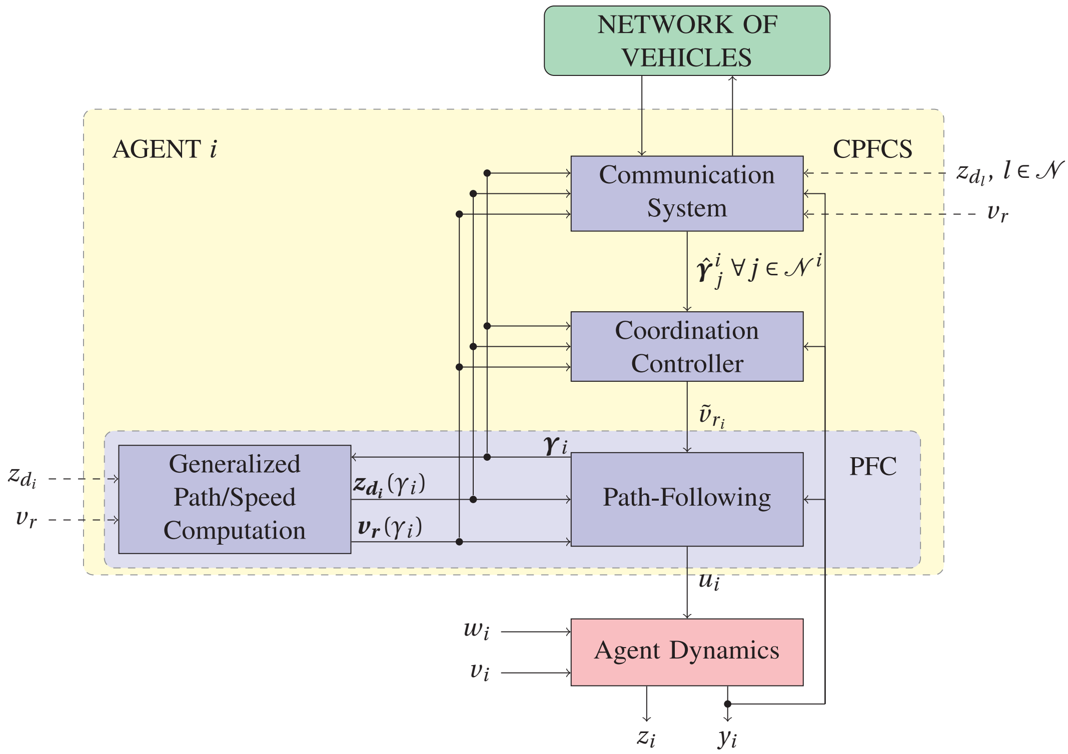

Figure 10.1 – Coordinated path-following control system (CPFCS) architecture with logic-based communication system.

The architecture for a general CPFCS proposed in this chapter is shown in Figure 10.1. The CPFCS architecture consists of three interconnected subsystems for each agent:

Path-following controller (PFC, see Figure 10.1) - This is a dynamical system whose inputs are a spatial path z_{d_i}, a desired speed profile v_r that is common to all agents, and the agent's output y_i. Its output is the agent's input, computed so as to make it follow the path at the assigned speed, asymptotically. In preparation for its connection with the coordination controller, this system produces also a generalized path $\boldsymbol{z}_{\boldsymbol{d}_i}$, a generalized speed profile $\boldsymbol{v}_{\boldsymbol{r}}$ and a generalized path variable $\boldsymbol{\gamma}_i$. Furthermore, it accepts corrective speed action from the coordination controller via the signal $\tilde{v}_{r_i}$. This corrective action is aimed at making the vehicles synchronize along the paths. Notice that the dynamics of the parameterizing variable γ_i are defined internally at this stage and play the role of an extra design knob to tune the performance of the path-following control law.

Coordination controller - This is a dynamical system whose inputs are the measured noisy output y_i, the desired generalized path $\boldsymbol{z}_{\boldsymbol{d}_i}$ and speed profile $\boldsymbol{v}_{\boldsymbol{r}}(\gamma_i)$, the generalized path variable $\boldsymbol{\gamma}_i$, and estimates of the generalized coordination states $\boldsymbol{\gamma}_j; j \in \mathcal{N}^i$, where $\mathcal{N}^i$ is defined as the set of neighbours of agent ith. Its output is the correction speed signal $\tilde{v}_{r_i}$, which is used to synchronize agent i with its neighbours.

Logic-based communication system - This is a logic-based dynamical system that makes the interface with the network system through which the agents output y_i, the generalized desired path $\boldsymbol{z}_{\boldsymbol{d}_i}$, the generalized speed profile $\boldsymbol{v}_{\boldsymbol{r}}$, and the generalized path variable $\boldsymbol{\gamma}_i$ can be communicated to the neighbour agents. Its output is an estimate $\hat{\boldsymbol{\gamma}}_j$ of the generalized coordination states of the neighbouring agents $\boldsymbol{\gamma}_j, j \in \mathcal{N}^i$. This communication system has knowledge of the spatial paths z_{d_l}, $l \in \mathcal{N}$, and the desired speed profile v_r

In order to assess what are the necessary conditions for the CPFCS to achieve its goals, the objectives must be precisely defined in the form of the CPF problem. In Ghabcheloo et al. [2009], the CPF problem was defined and conditions were derived so that the path-following and coordination controllers solve the CPF problem. In Section 10.3 we will derive the conditions for the CPFCS to solve robustly the CPF problem, considering bounded estimation errors of the path variables. In the same Section we introduce the communication problem, that amounts to guaranteeing that the estimation error is bounded with asynchronous communication between agents. In Section 10.4 we will give an example of a CPFCS design which solve the CPF problem for a class of autonomous marine vehicles.

10.3 Problem statement

The purpose of the path-following and coordination controllers is to solve robustly the CPF problem, assuming that each agent estimates the coordination state of its neighbours with bounded estimation error.

In this section we will review the concepts of a path-following controller and a coordination controller present in Ghabcheloo et al. [2009], while also considering estimation errors of the neighbours' path-variables. As in Ghabcheloo et al. [2009] we will apply the small gain theorem to derive conditions under which the interconnection between the path-following controller and the coordination controller is stable.

10.3.1 Path-following controller

As stated in Skjetne et al. [2004], a path following controller can be considered to have two assignments, the geometric task and the dynamic task. The geometric task consists of driving the agent output z_i to a desired path z_{d_i} parametrized by a continuous scalar variable, the path-following variable γ_i. The dynamic task consists of forcing the path-following variables γ_i to a certain dynamic behaviour. More specifically, the dynamic task considered in this section is a speed assignment where we require the parameterizing variables to have a desired speed $v_r(\gamma_i)$, assumed to be globally Lipschitz in γ_i.

For the sake of clarity and rigor, in what follows we give a formal definition of the output path-following problem. This is instrumental in understanding the conditions that a path-following controller must satisfy in order to perform successfully the geometric and dynamic tasks.

Since a path-following controller acts as a feedback controller for the agent Σ_i, its output is the agent control input u_i and admits as input the agent's output y_i. Also, it requires a reference of the desired path and speed profile, therefore it admits as input the generalized desired path $\boldsymbol{z_{d_i}}$ and speed reference $\boldsymbol{v_r}$. Finally, the path-following controller also admits a correction speed signal from the coordination controller $\tilde{v}_{r_i}$. Before proceeding with the definition of the path-following problem, we have to define the class of admissible speed profiles $\mathcal{V}_r$ which is the set of continuously differentiable functions in $\mathbb{R}$ and for a function $v_r \in \mathcal{V}_r$, the class of admissible paths $\mathcal{Z}_{d_i}(v_r)$ which is the set of continuously differentiable functions $z_{d_i} : \mathbb{R} \to \mathbb{R}^n$, such that there exists a function $u_i^* : \mathbb{R}^{n_i} \times \mathbb{R} \to \mathbb{R}^{m_i}$ such that for any $\gamma \in \mathbb{R}$ and $x_i^* \in \mathbb{R}^{n_i}$ satisfying $z_{d_i}(\gamma) = \mathscr{J}_i\left(x_i^*\right)$ we have

$$\frac{\partial z_{d_i}}{\partial \gamma}(\gamma)\, v_r(\gamma) = \frac{\partial \mathscr{J}_i}{\partial x_i}\left(x_i^*\right) \mathscr{F}_i\left(x_i^*, u_i^*(x_i^*, \gamma), 0\right).$$

Definition 4 (Path-following problem)**.** Consider a set of n agents $\Sigma_i, i \in \mathcal{N}$ with dynamics (10.1) and let $\mathcal{Z}_{d_i}$ and $\mathcal{V}_r$ be the classes of admissible paths and speed profiles, respectively. We say that a given set of controllers given by $\Sigma_i^{pf}, i \in \mathcal{N}$

$$\Sigma_i^{pf}: \qquad \dot{x}_i^{pf} = \mathscr{F}_i^{pf}\left(x_i^{pf}, y_i, \boldsymbol{z_{d_i}}, \boldsymbol{v_r}(\gamma_i), \tilde{v}_{r_i}\right), \tag{10.2a}$$

$$u_i = \mathcal{H}_i^{pf}\left(x_i^{pf}, y_i, \boldsymbol{z_{d_i}}, \boldsymbol{v_r}(\gamma_i), \tilde{v}_{r_i}\right), \tag{10.2b}$$

solves robustly the *output path-following problem* if for every prescribed speed profile $v_r \in \mathcal{V}_r$ and path $z_{d_i} \in \mathcal{Z}_{d_i}(v_r)$, there exist functions $\sigma_w^e, \sigma_v^e, \sigma_{\tilde{v}_r}^e, \sigma^e \in \mathcal{K}_\infty, \beta^e \in \mathcal{KL}$, a non-negative scalar μ and a signal error $\boldsymbol{e}$ such that for each initial condition $\boldsymbol{x^0} := \text{col}\left(x_i(0), x_i^{pf}(0)\right)$ and bounded signals $w := \text{col}(w_i)$, $v := \text{col}(v_i)$ and $\tilde{v}_r = \text{col}\left(\tilde{v}_{r_i}\right)$, all the states of the closed-loop system (10.1)-(10.2), $i \in \mathcal{N}$ with the exception of $\gamma_i(t)$ are bounded, the path-following errors

$$e_i(t) := z_i(t) - z_{d_i}(\gamma_i(t)), \forall i \in \mathcal{N},$$

and speed errors

$$e_{\dot{\gamma}_i}(t) := \dot{\gamma}_i(t) - v_r(\gamma_i), \forall i \in \mathcal{N},$$

satisfy the detectability condition

$$\|e_i(t)\| + \|e_{\dot{\gamma}_i}(t)\| \leq \sigma^e\left(\|\boldsymbol{e}\|_{[0,t]}\right), \forall i \in \mathcal{N}, \tag{10.3}$$

and $\boldsymbol{e}$ is input-to-output practically stable (IOpS) with respect to w, v, and $\tilde{v}_r$, that is,

$$\|\boldsymbol{e}(t)\| \leq \beta^e\left(\left\|\boldsymbol{x^0}\right\|, t\right) + \sigma_w^e\left(\|w\|_{[0,t]}\right) + \sigma_v^e\left(\|v\|_{[0,t]}\right) + \sigma_{\tilde{v}_r}^e\left(\|\tilde{v}_r\|_{[0,t]}\right) + \mu. \tag{10.4}$$

Remark. *Note that one can define the error signal* $\boldsymbol{e}$ *as*

$$\boldsymbol{e} := \text{col}\left(\begin{bmatrix} e_i \\ e_{\dot{\gamma}_i} \end{bmatrix}\right).$$

However, the definition of the CPF problem allows for other definitions of the error signal such as the one in Lemma 5.

In simple terms, the geometric task amounts to impose a (small) bound on the path-following errors e_i and the dynamic task consists in forcing a bound on the speed errors $e_{\dot{\gamma}_i}$. From the detectability condition (10.3), both tasks are satisfied if we can bound the signal error $\boldsymbol{e}$. The IOpS condition (10.4) implies that if the process noise w, the measurement noise v and the input from the coordination controller $\tilde{v}_r$ are bounded, then we can compute a bound on $\boldsymbol{e}$ assymptotically, independently from the initial conditions of the agents $x_i(0)$ and the path-following controllers $x_i^{pf}(0)$, here represented by $\boldsymbol{x^0}$.

10.3.2 Coordination controller

Besides meeting the requirements of path-following, that is, making each agent follow a desired path z_{d_i} at some required speed v_r, we also require coordination of the entire group of agents so as to achieve a desired formation pattern compatible with the paths adopted. We say that two agents are coordinated, are synchronized or have reached agreement if and only if $\gamma_i - \gamma_j = 0, \forall i, j \in \mathcal{N}$. Since nullifying the coordination errors $\gamma_i - \gamma_j$ is a very strict requirement, we require instead that the coordination errors became bounded by a small number after some settling time. To be more precise regarding the necessary characteristics of coordination controller for coordinating the agents, we now define the coordination control problem.

Since the coordination controller acts on the path-following controller Σ_i^{pf}, its output is the correction speed signal $\tilde{v}_{r_i}$ and admits as input the path-following variable γ_i, included in x_i^{pf}, and the sensors output y_i from Σ_i. Also, the coordination controller requires a reference of the desired path and speed profile, therefore it admits as input the generalized desired path $\boldsymbol{z_{d_i}}$ and speed reference $\boldsymbol{v_r}$. Finally, the communication system has the role of providing the the coordination controller with the value of the path-following variables of the neighbours $\gamma_j,\ j \in \mathcal{N}^i$. Since we aim to save the number of communications the output of the communication system is instead estimates of the generalized path-following variables $\hat{\boldsymbol{\gamma}}_j,\ j \in \mathcal{N}^i$, and we define the estimation error as $\tilde{\boldsymbol{\gamma}}_j^i := \hat{\boldsymbol{\gamma}}_j^i - \boldsymbol{\gamma}_j$.

Definition 5 (Coordination control problem)**.** Consider a set of N agents $\Sigma_i,\ i \in \mathcal{N}$ with dynamics (10.1), equipped with path-following controllers $\Sigma_i^{pf},\ i \in \mathcal{N}$ with dynamics given by (10.2), and the speed profile $v_r \in \mathcal{V}_r$ and paths $z_{d_i} \in \mathcal{Z}_{d_i}(v_r),\ i \in \mathcal{N}$. Assume that $\boldsymbol{\gamma}_i$ and $\hat{\boldsymbol{\gamma}}_j,\ \forall j \in \mathcal{N}_i$ are available to agent i and define the estimation error as $\tilde{\boldsymbol{\gamma}}_j^i := \hat{\boldsymbol{\gamma}}_j^i - \boldsymbol{\gamma}_j$.

$$\Sigma_i^{cc}: \quad \dot{x}_i^{cc} = \mathcal{F}_i^{cc}\left(x_i^{cc}, y_i, \boldsymbol{z_{d_i}}, \boldsymbol{v_r}(\gamma_i), \boldsymbol{\gamma}_i, \mathrm{col}\left(\hat{\boldsymbol{\gamma}}_j^i, j \in \mathcal{N}^i\right)\right), \tag{10.5a}$$

$$\tilde{v}_{r_i} = \mathcal{H}_i^{cc}\left(x_i^{cc}, y_i, \boldsymbol{z_{d_i}}, \boldsymbol{v_r}(\gamma_i), \boldsymbol{\gamma}_i, \mathrm{col}\left(\hat{\boldsymbol{\gamma}}_j^i, j \in \mathcal{N}^i\right)\right), \tag{10.5b}$$

solves robustly the *coordination control problem* if there exist functions $\beta^\xi \in \mathcal{KL}$, $\sigma^\xi, \sigma_v^\xi, \sigma_w^\xi, \sigma_\gamma^\xi, \sigma_e^\xi \in \mathcal{K}_\infty$ and a coordination error signal ξ that satisfies the detectability property

$$\max_{i \in \mathcal{N}; j \in \mathcal{N}^i} \|\gamma_i(t) - \gamma_j(t)\| \le \sigma^\xi\left(\|\xi\|_{[0,t]}\right), \tag{10.6}$$

and the evolution of the coordination error signal $\boldsymbol{\xi} := \left[\xi^T,\ \mathrm{col}\left(x_i^{cc}\right)^T,\ \tilde{v}_r\right]^T$ satisfies, for each initial condition $\boldsymbol{x_\xi^0} := \mathrm{col}\left(\left[x_i(0)^T,\ x_i^{pf}(0)^T,\ x_i^{cc}(0)^T\right]^T\right)$,

$$\|\boldsymbol{\xi}(t)\| \le \beta^\xi\left(\left\|\boldsymbol{x_\xi^0}\right\|, t\right) + \sigma_v^\xi\left(\|v\|_{[0,t]}\right) + \sigma_w^\xi\left(\|w\|_{[0,t]}\right) + \sigma_\gamma^\xi\left(\|\tilde{\boldsymbol{\gamma}}\|_{[0,t]}\right) + \sigma_e^\xi\left(\|\boldsymbol{e}\|_{[0,t]}\right), \tag{10.7}$$

where $v := \mathrm{col}(v_i)$, $w := \mathrm{col}(w_i)$, $\tilde{\boldsymbol{\gamma}} := \mathrm{col}\left(\tilde{\boldsymbol{\gamma}}_i^j, i \in \mathcal{N}, j \in \mathcal{N}^i\right)$.

In plain terms, our approach to coordination amounts to imposing an upper bound on the coordination errors $\|\gamma_i(t) - \gamma_j(t)\|, \forall i \in \mathcal{N}; j \in \mathcal{N}^i$. From the detectability property (10.6), we can bound the coordination errors if we can bound the coordination error signal ξ. The IOpS condition (10.7) implies that if the measurement noise v, the process noise w, and the estimation errors $\tilde{\boldsymbol{\gamma}}$ are bounded, then, after some settling time, we can compute a bound on ξ, independently from the initial condition of the agents $x_i(0)$, the path-following controllers $x_i^{pf}(0)$ and the coordination controllers $x_i^{cc}(0)$ here represented by $\boldsymbol{x_\xi^0}$. The bound on ξ depends on the the bounds on the measurement noises, process disturbances, and the estimation error. The impact of those bounds on the controller performance, given by $\sigma_v^\xi\left(\|v\|_{[0,t]}\right)$, $\sigma_w^\xi\left(\|w\|_{[0,t]}\right)$ and $\sigma_\gamma^\xi\left(\|\tilde{\boldsymbol{\gamma}}\|_{[0,t]}\right)$, are expected to be small when compared to the precision required for coordination control. This was found to be the case in the experiments of Chapter 14.

10.3.3 Coordinated path-following

It is important to note, however, that the coordination control problem and the path-following problem are not independent because, if both problems are solved, the dynamics of ξ and $\boldsymbol{e}$ are interconnected. Noting that the vector $\boldsymbol{\xi}$ contains $\tilde{v}_r$ this interconnection can be seen in Equations 10.4 and 10.7 of Definitions 5 and 4, and is illustrated in Figure 10.2. Therefore, to make sure the interconnection between the path-following and coordination controllers solves the geometric and dynamic tasks and approaches coordination at the same time it is not sufficient that the path-following and coordination problems be solved independently. The CPF problem defined next, if solved, guarantees that all mentioned objectives (dynamic and geometric tasks and coordination)

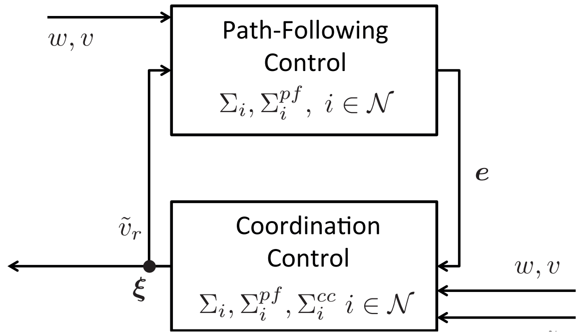

Figure 10.2 – Feedback interconnection of the path-following control system and the coordination control system.

are achieved by the interconnection, for bounded process and measurement noise.

Definition 6 (Coordinated path-following problem)**.** Consider the closed-loop system Σ^{cl} composed by n agents of the form (10.1) and the path-following controller and coordination controller defined by (10.2) and (10.5) respectively. We say that Σ^{cl} solves robustly the *CPF problem* if for every agent $i \in \mathcal{N}$, every prescribed speed profile $v_r \in \mathcal{V}_r$ and path $z_{d_i} \in \mathcal{Z}_{d_i}(v_r)$, there exist functions $\sigma^{\bar{e}}, \sigma_w^{\bar{e}}, \sigma_v^{\bar{e}} \in \mathcal{K}_\infty$, $\beta^{\bar{e}} \in \mathcal{KL}$, a positive scalar $\mu^{\bar{e}}$, and a error signal $\bar{\boldsymbol{e}}$ such that for each initial condition $\boldsymbol{x_e^0} := \mathrm{col}\left(\left[x_i(0)^T,\ x_i^{pf}(0)^T,\ x_i^{cc}(0)^T\right]^T\right)$ and bounded disturbance signals $w := \mathrm{col}(w_i)$ and $v := \mathrm{col}(v_i)$, the path-following errors, speed errors, and coordination errors satisfy the detectability condition

$$\max_{i\in\mathcal{N}}\left(\|e_i\| + \|e_{\dot{\gamma}_i}\| + \max_{j\in\mathcal{N}^i}\|\gamma_i - \gamma_j\|\right) \le \sigma^{\bar{e}}\left(\|\bar{\boldsymbol{e}}\|_{[0,t]}\right), \tag{10.8}$$

and $\bar{\boldsymbol{e}}$ is IOpS with respect to w and v, that is,

$$\|\bar{\boldsymbol{e}}(t)\| \le \beta^{\bar{e}}\left(\left\|\boldsymbol{x_e^0}\right\|, t\right) + \sigma_w^{\bar{e}}\left(\|w\|_{[0,t]}\right) + \sigma_v^{\bar{e}}\left(\|v\|_{[0,t]}\right) + \mu^{\bar{e}}. \tag{10.9}$$

Remark. *Note that one can define the error signal* $\bar{\boldsymbol{e}}$ *as*

$$\bar{\boldsymbol{e}} := \mathrm{col}\left(\begin{bmatrix} e_i \\ e_{\dot{\gamma}_i} \\ \mathrm{col}\left(\gamma_i - \gamma_j, j \in \mathcal{N}^i\right)\end{bmatrix}\right).$$

However, the definition of the CPF problem allows for other definitions of the error signal such as the one in Lemma 7.

The geometric and dynamic tasks are satisfied and coordination is achieved if e_i, $e_{\dot{\gamma}_i}$ and $\gamma_i - \gamma_j, j \in \mathcal{N}^i$ are bounded. The detectability condition (10.8) guarantees that if the error signal $\bar{\boldsymbol{e}}$ is bounded then e_i, $e_{\dot{\gamma}_i}$ and $\gamma_i - \gamma_j, j \in \mathcal{N}_i$ are bounded. Finally, the IOpS condition (10.9) guarantees that if v and w are bounded, then $\bar{\boldsymbol{e}}$ becomes bounded after some settling time. Therefore, if the CPF problem is solved robustly, for bounded measurement and process noise (v and w respectively), the closed loop system Σ^{cl} satisfies the geometric and dynamic tasks and achieves coordination.

The following theorem gives conditions under which a closed loop system Σ^{cl} solves the CPF problem, assuming it consists of the interconnection of the path-following and coordination controllers which solve the path-following and coordination problems, respectively.

Theorem 16. Suppose that in the closed-loop system Σ^{cl} each path-following controller Σ_i^{pf} and coordinated controller Σ_i^{cc} solve robustly the output path-following and coordination problem, respectively, that is, inequalities (10.3)-(10.4), (10.6)-(10.7) hold. Suppose further that $\tilde{\boldsymbol{\gamma}}$ is bounded and there exists $r_0 \geq 0$ such that

$$\sigma_{\tilde{v}_r}^{e} \circ \sigma_{e}^{\xi}(r) < r, \qquad \forall r > r_0. \tag{10.10}$$

Then, the closed-loop system Σ^{cl} solves robustly the CPF problem.

Proof. From (10.4) and (10.7) we conclude that the path-following and coordinated controllers can be viewed as two interconnected IOpS systems with outputs $\boldsymbol{e}$ and $\tilde{v}_r := \mathrm{col}\left(\tilde{v}_{r_i}\right)$, respectively. A straightforward application of the small-gain theorem, Theorem 5, and Theorem 3, implies that if (10.10) holds then the connection is IOpS. We can then conclude (10.9) since $\tilde{\boldsymbol{\gamma}}$ is bounded. Inequality (10.8) follows using the detectability conditions (10.3) and (10.6). □

This theorem states that the closed-loop system Σ^{cl} solves robustly the CPF problem if the estimation errors are bounded, all the path-following controllers and coordination controllers solve robustly the path-following and coordination problems, and inequality (10.10) holds, i.e. the interconnection between the path-following controller and the coordination controller is stable.

10.3.4 Logic-based communication system

In order to consider bandwidth limitations, to save the number of communications, instead of sending continuously the generalized path-following variables $\boldsymbol{\gamma}_i$, $i \in \mathcal{N}$, to the out-neighbours, they are exchanged through communication systems that send messages at discrete instants of time asynchronously using some logic, the communication triggering condition (CTC). Since the coordination controller assumes as input the generalized path-following variables of the neighbours in continuous time, the communication system estimates the generalized path-following variables, as $\hat{\boldsymbol{\gamma}}_i$, based on the data received. To guarantee that the coordination control error is smaller than some upper bound, we still need to guarantee that the communication system produces estimations of the neighbours path variables with a bounded estimation error $\tilde{\boldsymbol{\gamma}}_i := \hat{\boldsymbol{\gamma}}_i - \boldsymbol{\gamma}_i$. Therefore, the main innovation introduced in this chapter is a logic based communication system which has as its main goal keeping the estimation errors $\tilde{\boldsymbol{\gamma}}_i$ bounded.

Inspired by the communication logic proposed in Xu and Hespanha [2006], each communication subsystem is composed by a bank of estimators of the neighbours' generalized path-following variables $\hat{\boldsymbol{\gamma}}_j^i$, $j \in \mathcal{N}^i$ and a communication logic. The estimators run open-loop most of the time but are sometimes reset (not necessarily periodically) to correct their state when measurements are received through the network. The communication logic is responsible for determining for each agent $i \in \mathcal{N}$ how well the out-neighbour agents can predict, as $\hat{\boldsymbol{\gamma}}_i^j$, $j \in \mathcal{N}^i$, the value of its local generalized coordination state $\boldsymbol{\gamma}_i$ and decide when it should communicate the actual measured value to its out-neighbours so as to guarantee that $\left\|\tilde{\boldsymbol{\gamma}}_j^i(t)\right\| \leq \epsilon,\ \forall j \in \mathcal{N}^i, \forall t \geq 0$, for some positive scalar $\epsilon > 0$.

In this section, we formulate the general problem of coordinated path-following with self-triggered communications using the same principles in Seyboth et al. [2013] and Jain et al. [2017]. It is important to note that unlike Jain et al. [2017] where the control input is self-triggered but requires continuous communications, the communications in the work of this chapter are assumed to be self-triggered. To be more precise regarding the necessary characteristics of a communication system for keeping the estimation errors bounded we need a formal definition of the communication problem.

Definition 7 (Communication problem)**.** Consider the closed-loop system Σ^{cl}, composed of n agents of the form

(10.1) and the path-following controller and coordination controller defined by (10.2) and (10.5) respectively, the formation speed assignments $v_r \in \mathcal{V}_r$, and corresponding paths $z_{d_i} \in \mathcal{Z}_{d_i}(v_r)$. Assume that $\boldsymbol{z_{d_i}}$, $\boldsymbol{v_r}(\gamma_i)$, $\boldsymbol{\gamma}_i$, $\boldsymbol{\gamma}_i$, y_i, x_i^{pf}, x_i^{cc} are continuously available to agent i and $\boldsymbol{z_{d_j}}$, $\boldsymbol{v_r}(\gamma_j)$, $\boldsymbol{\gamma}_j$, y_j, x_j^{pf}, x_j^{cc}; $\forall j \in \mathcal{N}^i$ are available asynchronously through the network system. Let $t_k^{[i]}, k \geq 0$ indicate the instants of data transmission, which occur when a communication triggering condition (CTC) is satisfied. We say that a given set of logic based impulse dynamical systems $\Sigma_i^{lbc}; i \in \mathcal{N}$ defined as

For $t \neq t_k^{[j]}, \forall j \in \mathcal{N}^i \cup \{i\}, k \geq 0$

$$\Sigma_i^{lbc}: \quad \dot{x}_i^{lbc} = \mathscr{F}_i^{lbc}\left(x_i^{lbc}\right), \tag{10.11a}$$

$$\hat{\boldsymbol{\gamma}}_j^i = \mathscr{H}_{ij}^{lbc}\left(x_i^{lbc}\right), \; j \in \mathcal{N}^i, \tag{10.11b}$$

If $\exists j \in \mathcal{N}^i \cup \{i\}$ such that $t = t_k^{[j]}, k \geq 0$

$$x_i^{lbc}\left(t^+\right) = \mathscr{J}_{ji}^{lbc}\left(x_i^{lbc}, y_j, x_j^{pf}, x_j^{cc}, x_j^{lbc}, \boldsymbol{z_{d_j}}, \boldsymbol{v_r}(\gamma_j), \boldsymbol{\gamma}_j\right), \tag{10.12}$$

where $x(t^+) := \lim_{s \to t^+} x(s)$, and the CTC triggering communications at times $t_k^{[i]}$ when the condition

$$\mathscr{C}_i^{lbc}\left(x_i^{lbc}, y_i, x_i^{pf}, x_i^{cc}, x_i^{lbc}, \boldsymbol{z_{d_i}}, \boldsymbol{v_r}(\gamma_i), \boldsymbol{\gamma}_i\right) = 0 \tag{10.13}$$

is satisfied, solve robustly the *communication problem* if for every $i \in \mathcal{N}$

$$\left\|\tilde{\boldsymbol{\gamma}}_j^i(t)\right\| \leq \epsilon, \qquad \forall j \in \mathcal{N}^i, \forall t \geq 0 \tag{10.14}$$

for some scalar $\epsilon > 0$ where $\tilde{\boldsymbol{\gamma}}_j^i := \hat{\boldsymbol{\gamma}}_j^i - \boldsymbol{\gamma}_j$.

In the definition above, information is sent from agent i at instants $t_k^{[i]}$ and x_i^{lbc} is updated instantaneously. Accordingly, at instants $t_k^{[j]}, j \in \mathcal{N}^i$ information is received by agent i from its neighbour j. At this point, for the sake of generality, we purposely avoid discussing the mechanism for generation of communication times $t_k^{[i]}$. This will be done later in this chapter. Here we consider that the information sent can contain elements of x_i^{pf}, x_i^{cc}, x_i^{lbc}, y_i and $\boldsymbol{\gamma}_i$. While no data is sent or received the communication system only uses internal information to compute the path variables estimates. To estimate the coordination states, the communication system relies on the assigned path z_{d_i}, and on the required speed v_r for each agent $i \in \mathcal{N}$.

The particular strategy to solve the communication problem that we apply in this chapter is, as proposed in Xu and Hespanha [2006], to consider that the estimators for each of the neighbours are independent among themselves, and that each agent contains estimators of its own variable synchronized with its out-neighbours with the purpose of computing the estimation errors in the out-neighbours. That is Σ_i^{lbc} is composed by the systems Σ_{ij}^{lbc} $j \in \mathcal{N}^i$ defined by

$$\Sigma_{ij}^{lbc}: \quad \dot{x}_{ij}^{lbc} = F_{ij}^{lbc}\left(x_{ij}^{lbc}\right),$$

$$\hat{\boldsymbol{\gamma}}_j^i = H_{ij}^{lbc}\left(x_{ij}^{lbc}\right),$$

and by synchronized copies of the estimates Σ_{ji}^{lbc} $i \in \mathcal{N}^j$ contained in the agents j such that $i \in \mathcal{N}^j$, i.e. the out-neighbours, which give as output the estimates $\hat{\boldsymbol{\gamma}}_i^j$ in the out-neighbours. Therefore the state of the communication system is of the form

$$x_i^{lbc} = \begin{bmatrix} \mathrm{col}\left(x_{ji}^{lbc},\ i \in \mathcal{N}^j\right) \\ \mathrm{col}\left(x_{ij}^{lbc},\ j \in \mathcal{N}^i\right) \end{bmatrix}.$$

Given that agent i has access to the estimates $\hat{\boldsymbol{\gamma}}_i^j := H_{ji}^{lbc}\left(x_{ji}^{lbc}\right)$, $i \in \mathcal{N}^l$, agent i can compute the estimation errors $\tilde{\boldsymbol{\gamma}}_i^j$ in its out-neighbours. Therefore a communication is triggered by agent i at the times $t_k^{[i]}$ when the condition $\left\|\tilde{\boldsymbol{\gamma}}_i^j\left(t_k^{[i]}\right)\right\| = \epsilon$ is satisfied for some $j \in \mathcal{N}$ such that $i \in \mathcal{N}^j$. If at some time $t = t_k^{[i]}$ $\left\|\tilde{\boldsymbol{\gamma}}_i^j(t)\right\| = \epsilon$ then on agent i and j the state x_{ji}^{lbc} is updated with some rule of the form

$$x_{ji}^{lbc}\left(t^+\right) = J_{ji}^{lbc}\left(x_{ji}^{lbc}, y_j, x_j^{pf}, x_j^{cc}, x_j^{lbc}, \boldsymbol{z}_{\boldsymbol{d}_j}, \boldsymbol{v}_{\boldsymbol{r}}(\gamma_j), \boldsymbol{\gamma}_j\right),$$

satisfying

$$\hat{\boldsymbol{\gamma}}_j^i(t^+) = H_{ij}^{lbc}\left(J_{ji}^{lbc}\left(x_{ji}^{lbc}, y_j, x_j^{pf}, x_j^{cc}, x_j^{lbc}, \boldsymbol{z}_{\boldsymbol{d}_j}, \boldsymbol{v}_{\boldsymbol{r}}(\gamma_j), \boldsymbol{\gamma}_j\right)\right) = \boldsymbol{\gamma}_j(t).$$

By ensuring that on agent i and j the state x_{ji}^{lbc} is updated at the same time with the same rule, we can guarantee that the estimates are kept synchronized. Moreover, since whenever $\left\|\tilde{\boldsymbol{\gamma}}_i^j(t)\right\| = \epsilon$ we have $\left\|\tilde{\boldsymbol{\gamma}}_i^j\left(t^+\right)\right\| = 0$ the condition (10.14) is satisfied and the communication problem is solved.

We now state the main result of this section.

Theorem 17. Consider the overall closed loop system Σ^{ocl} composed by n agents of the form (10.1) and the CPFCS defined by (10.2), (10.5) and (10.11)-(10.12). Suppose that each PF controller Σ_i^{pf} and coordinated controller Σ_i^{cc} solve robustly the output path-following and coordination problem, respectively, that is, inequalities (10.3)-(10.4), (10.6)-(10.7) hold. Suppose further that the logic-based communication satisfies (10.14) $\forall i \in \mathcal{N}$ and there exists $r_0 \geq 0$ such that inequality (10.10) holds. Then, the closed-loop system Σ^{cl} solves robustly the CPF problem.

Proof. Since the logic-based communication system satisfies (10.14) $\forall i \in \mathcal{N}$, $\tilde{\boldsymbol{\gamma}}$ is bounded. Therefore all the assumptions of Theorem 16 hold. □

The comunication problem of Definition 7 is a general formulation for non-delayed communications without packet losses. However, on Subsection 10.4.4, and on Section 10.6 we propose communication systems that can cope with packet losses and delays that depart from the formulation of Definition 7. To be robust to packet losses we will require that the communication systems send a reply whenever they receive a message to the sender of that same message. Therefore in the remainder of this chapter we assume that the communication network is undirected, that is if $i \in \mathcal{N}^j$ then $j \in \mathcal{N}^i$.

It should also be noted that in Definition 7 we allow for the estimates of the generalized path-following variable of agent i, $\boldsymbol{\gamma}_i$, on its out-neighbours, $\hat{\gamma}_i^j$, $i \in \mathcal{N}^j$, to be different between each other, that is it is admissible that for some $j \neq l$ such that $i \in \mathcal{N}^j \cup \mathcal{N}^l$ $\hat{\gamma}_i^j \neq \hat{\gamma}_i^j$. However, in the communication system of the ideal communications case of Subsection 10.4.4 all estimates of the path-following variable of an agent are equal, that is for every two agents j and l such that $i \in \mathcal{N}^j \cup \mathcal{N}^l$, we have $\hat{\boldsymbol{\gamma}}_i^j = \hat{\boldsymbol{\gamma}}_i^l$. Only on Section 10.6 we propose a scheme with different estimates for different agents.

10.4 Controller Design

In this section, to illustrate how we can apply the framework described in the previous section, we consider the case of CPF of autonomous marine vehicles maneuvering in 2D.

10.4.1 Vehicle model

In this subsection we describe the mathematical model of a class of autonomous marine vehicles used for motion control design. We can consider this mathematical model as the agent dynamics.

We write the kinematic equations of motion of a vehicle moving in the horizontal plane by using a global inertial coordinate frame $\{\mathcal{U}\}$ and a body-fixed coordinate frame $\{\mathcal{B}\}$, with origin at the vehicle's center of mass, yielding

$$\dot{x} = u\cos(\psi) - v\sin(\psi), \tag{10.16a}$$
$$\dot{y} = u\sin(\psi) + v\cos(\psi), \tag{10.16b}$$
$$\dot{\psi} = r, \tag{10.16c}$$

where u and v are body-fixed frame components of the vehicle's velocity, x and y are the inertial Cartesian coordinates of its center of mass, and ψ defines its orientation (heading angle). The kinematic equations (10.16b)-(10.16c) can be written in compact form by defining $\boldsymbol{p} := [x,\ y]^T$ and $\boldsymbol{v} := [u,\ v]^T$, leading to

$$\begin{aligned} \dot{\boldsymbol{p}} &= R\boldsymbol{v}, \\ \dot{\psi} &= r, \end{aligned}$$

where R is the orthonormal transformation matrix from $\{\mathcal{B}\}$ to $\{\mathcal{U}\}$, i.e.

$$R = \begin{bmatrix} \cos(\psi) & -\sin(\psi) \\ \sin(\psi) & \cos(\psi) \end{bmatrix}.$$

In the presence of a constant and irrotational ocean current, $\boldsymbol{v}$ is the sum of the vehicle's velocity with respect to the water $\boldsymbol{v}_w := [u_w,\ v_w]^T$ and the water current velocity $\boldsymbol{v}_c := [u_c,\ v_c]^T$, both expressed in the body-fixed reference frame, i.e.

$$\boldsymbol{v} := \begin{bmatrix} u \\ v \end{bmatrix} = \boldsymbol{v}_w + \boldsymbol{v}_c = \begin{bmatrix} u_w + u_c \\ v_w + v_c \end{bmatrix}.$$

10.4.2 Path-following controller

The path-following controller considered in this section is described in Vanni [2007]. To solve the problem of driving a vehicle along a desired path, the key idea exploited is to make the vehicle approach a virtual target that moves along the path. Let $\boldsymbol{p}_d(\gamma)$ be the position of the target, and $v_r(\gamma)$ its desired rate of progression. We decompose the motion-control problem into an inner-loop dynamic task, which consists of making the vehicle's surge velocity u and heading rate r track desired references u_d and r_d, respectively, and an outer-loop kinematic task on the speed and heading rate references $\boldsymbol{u}_d := [u_d,\ r_d]^T$ and the evolution of the path parameter γ, which *i)* regulates the evolution of the virtual target $\boldsymbol{p}_d(\gamma)$ and *ii)* assigns the reference speed $\boldsymbol{u}_d := [u_d,\ r_d]^T$ so as to achieve convergence to the path.

In what follows we assume that the inner-loop controller satisfies the following stability assumption:

Assumption A11. Let $\tilde{u} := u - u_d$ and $\tilde{r} := r - r_d$ be the speed and heading rate tracking errors, v_w be the sway velocity, and let $\boldsymbol{x}_{il}^0$ the initial condition of the state of the inner-loop system. There exist functions $\beta^{\tilde{r}}, \beta^{\tilde{u}}, \beta^{v} \in \mathcal{KL}$ and positive constants $\epsilon_{\tilde{r}}$, $\epsilon_{\tilde{u}}$, ϵ_v such that

$$\|\tilde{r}(t)\| \leq \beta^{\tilde{r}}\left(\|\boldsymbol{x}_{il}^0\|, t\right) + \epsilon_{\tilde{r}}, \qquad \|\tilde{u}(t)\| \leq \beta^{\tilde{u}}\left(\|\boldsymbol{x}_{il}^0\|, t\right) + \epsilon_{\tilde{u}}, \qquad \|v_w(t)\| \leq \beta^{v}\left(\|\boldsymbol{x}_{il}^0\|, t\right) + \epsilon_v.$$

We also assume that each vehicle contains an observer for the lateral water current velocity v_c which satisfies the following assumption:

Assumption A12. Let $\tilde{v}_c := v_c - \hat{v}_c$ be the estimation error and $\boldsymbol{x}_{v_c}^0$ be the initial condition of the state of the lateral water current velocity estimator. There exists a function $\beta^{v_c} \in \mathcal{KL}$ and a positive constant ϵ_{v_c} such that

$$\|\tilde{v}_c(t)\| \leq \beta^{v_c}\left(\|\boldsymbol{x}_{v_c}^0\|, t\right) + \epsilon_{v_c}.$$

Given the above mentioned assumptions the kinematics of the vehicle can be described as

$$\begin{aligned} \dot{\boldsymbol{p}} &= R\begin{bmatrix} u_d + \tilde{u} \\ \hat{v}_c + \tilde{v}_c + v_w \end{bmatrix}, \\ \dot{\psi} &= r_d + \tilde{r}. \end{aligned}$$

The path-following problem for the outer loop can be formulated in this context as follows:

Definition 8 (Path-following problem)**.** Consider the vehicle whose motion is described by (10.16), and let $\boldsymbol{p}_d(\gamma) \in \mathbb{R}^2$ be a desired path parametrized by a continuous variable $\gamma \in \mathbb{R}$ and $v_r(\gamma) \in \mathbb{R}$ a desired speed assignment. Suppose that $\boldsymbol{p}_d(\gamma)$ is sufficiently smooth and its derivatives with respect to γ are bounded. Solving robustly the *path-following problem* of Definition 4 amounts to deriving control laws, subject to Assumptions A11 and A12, for $\boldsymbol{u}_d$ and $\dot{\gamma}$, such that the position error $\|\boldsymbol{p}(t) - \boldsymbol{p}_d(\gamma(t))\|$ and the speed error $\|\dot{\gamma}(t) - v_r(\gamma(t))\|$ converge to a small neighbourhood of the origin as $t \to \infty$.

Notice that the speed v_r is not an actual vehicle speed: it expresses the desired rate at which parameter γ changes.

Define the position error $\boldsymbol{e}$ as the difference between the positions of the vehicle and the virtual target expressed in the body frame $\{\mathcal{B}\}$,

$$\boldsymbol{e} := R^T\left(\boldsymbol{p} - \boldsymbol{p}_d\right).$$

Its dynamics are described by

$$\dot{\boldsymbol{e}} = -S(r)\boldsymbol{e} + \begin{bmatrix} u_d + \tilde{u} \\ v_c + v_w \end{bmatrix} - R^T\frac{\partial \boldsymbol{p}_d}{\partial \gamma}\dot{\gamma}, \qquad S(r) = \begin{bmatrix} 0 & -r \\ r & 0 \end{bmatrix}, \tag{10.17}$$

where we used the fact that $\dot{R} = RS(r)$.

To make the desired speed $\boldsymbol{u}_d := [u_d,\ r_d]^T$ appear in the position error dynamics we introduce a constant design vector $\boldsymbol{\delta} := [\delta,\ 0]^T$, $\delta < 0$. From (10.17), simple computations show that the position error dynamics are then given by

$$\dot{\boldsymbol{e}} = -S(r)(\boldsymbol{e}-\boldsymbol{\delta}) + \Delta \boldsymbol{u}_d - R^T \frac{\partial \boldsymbol{p}_d}{\partial \gamma}\dot{\gamma} - \begin{bmatrix} 0 \\ \delta \tilde{r} \end{bmatrix} + \begin{bmatrix} \tilde{u} \\ v_w + v_c \end{bmatrix}, \tag{10.18}$$

where $\Delta := \begin{bmatrix} 1 & 0 \\ 0 & -\delta \end{bmatrix}$. Defining the virtual target speed error

$$\omega := \dot{\gamma} - (v_r + \tilde{v}_r), \tag{10.19}$$

where $\tilde{v}_r$ is piecewise continuous, and computing its time derivative where it is defined yields $\dot{\omega} = \ddot{\gamma} - \dot{v}_r(\gamma) - \dot{\tilde{v}}_r = \ddot{\gamma} - \frac{\partial v_r}{\partial \gamma}(\gamma)\dot{\gamma} - \dot{\tilde{v}}_r$. By explicitly controlling $\ddot{\gamma}$ when $\dot{\tilde{v}}_r$ is defined we introduce an additional control variable. Moreover at the instants t_k where $\dot{\tilde{v}}_r$ is not defined, if we assign $\dot{\gamma}\left(t_k^+\right) = \dot{\gamma}(t_k) - \tilde{v}_r(t_k) + \tilde{v}_r\left(t_k^+\right)$, we have $\omega(t_k) = \omega\left(t_k^+\right)$, and therefore ω is continuous.

Lemma 5 (Path-following controller)**.** Consider the vehicle model described by (10.16), in closed-loop with the output feedback control law composed by an inner loop that satisfies Assumption A11, a lateral current estimator which satisfies Assumption A12, and, when $\dot{\tilde{v}}_r$ is defined, the outer loop given by

$$\ddot{\gamma} = -k_\omega \omega + \dot{v}_r + \dot{\tilde{v}}_r + \frac{1}{c_\omega}(\boldsymbol{e}-\boldsymbol{\delta})^T R^T \frac{\partial \boldsymbol{p}_d}{\partial \gamma}(\gamma), \tag{10.20}$$

$$\boldsymbol{u}_d = \Delta^{-1}\left(-K_k(\boldsymbol{e}-\boldsymbol{\delta}) - \begin{bmatrix} 0 \\ \hat{v}_c \end{bmatrix} + R^T \frac{\partial \boldsymbol{p}_d}{\partial \gamma}(\gamma)(v_r + \tilde{v}_r)\right), \tag{10.21}$$

where $K_k := \operatorname{diag}\left(k_x, k_y\right)$, and the design parameters k_x, k_y, k_ω and c_ω satisfy $k_x, k_y, k_\omega, c_\omega > 0$.

At the instants t_k where $\dot{\tilde{v}}_r$ is not defined we assign

$$\dot{\gamma}\left(t_k^+\right) = \dot{\gamma}(t_k) - \tilde{v}_r(t_k) + \tilde{v}_r\left(t_k^+\right). \tag{10.22}$$

Then, the error vector

$$\eta_e := \begin{bmatrix} \boldsymbol{e}-\boldsymbol{\delta} \\ \sqrt{c_\omega}\,\omega \end{bmatrix},$$

is ultimately bounded (UB), that is, there exist functions $\beta^e, \beta^e_{il}, \beta^e_{obs} \in \mathcal{KL}$ and a positive constant ε_e such that

$$\|\eta_e\| \le \beta^e\left(\|\eta_e(0)\|, t\right) + \beta^e_{il}\left(\|\boldsymbol{x}^0_{il}\|, t\right) + \beta^e_{obs}\left(\|\boldsymbol{x}^0_{v_c}\|, t\right) + \varepsilon_e. \tag{10.23}$$

Therefore, the control laws (10.20-10.21) solve robustly the path-following problem.

Proof. See Appendix. □

With this strategy the evolution of the position of the virtual target $\boldsymbol{p}_d$ depends on the position error $\boldsymbol{e}-\boldsymbol{\delta}$ in that if the vehicle is ahead/behind the desired position the virtual target moves faster/slower.

Remark. *The concept of stabilizing the error $\boldsymbol{e}-\boldsymbol{\delta}$ instead of directly stabilizing the path-following error $\boldsymbol{e}$ stems from the fact that taking the control Lyapunov function candidate $V = \frac{1}{2}\boldsymbol{e}^T\boldsymbol{e}$, considering the disturbance* *free case where* $\tilde{u} = v_c = v_w = 0$*, the time derivative of* V*, from* (10.17)*, yields*

$$\dot{V} = u_d \boldsymbol{b}\boldsymbol{e} - \dot{\gamma} \frac{\partial \boldsymbol{p}_d}{\partial \gamma}^T R\boldsymbol{e},$$

where $\boldsymbol{b} := [1, 0]$*, and when* $\boldsymbol{b}\boldsymbol{e} = 0$*,* u_d *has no influence on* $\dot{V}$ *and therefore it is impossible to define a function* $u_d(\boldsymbol{e}, \gamma, \dot{\gamma})$ *such that* $\dot{V} < 0$ *for all* $\boldsymbol{e}$*,* γ*,* $\dot{\gamma}$ *such that* $V > 0$*. Therefore* V *cannot be a Lyapunov function. In contrast, defining the Lyapunov function candidate* $V = \frac{1}{2}(\boldsymbol{e} - \boldsymbol{\delta})^T(\boldsymbol{e} - \boldsymbol{\delta})$ *and, in the disturbance free case, taking its time derivative yields, from* (10.18)*,*

$$\dot{V} = (\boldsymbol{e} - \boldsymbol{\delta})^T \Delta \boldsymbol{u}_d - \dot{\gamma} \frac{\partial \boldsymbol{p}_d}{\partial \gamma}^T R(\boldsymbol{e} - \boldsymbol{\delta}),$$

and we can observe that simply by taking, for some positive scalar k

$$\boldsymbol{u}_d = \Delta^{-1}\left(-k(\boldsymbol{e} - \boldsymbol{\delta}) + R^T \frac{\partial \boldsymbol{p}_d}{\partial \gamma} \dot{\gamma}\right),$$

we obtain, whenever $V > 0$*, that is when* $\|\boldsymbol{e} - \boldsymbol{\delta}\| > 0$*,* $\dot{V} = -k\|\boldsymbol{e} - \boldsymbol{\delta}\|^2 < 0$*, and therefore* V *is a Lyapunov function.*

This strategy for trajectory tracking or path-following of nonholonomic vehicles can be traced back to the work of Aguiar and Hespanha [2007], which borrows concepts from Skjetne et al. [2004]. This method was applied to the problem of cooperative path-following in Ghabcheloo et al. [2006] and in Vanni et al. [2008]. More recently this method was considered as an auxiliary control law for a model predictive control algorithm for path-following of an underactuated vehicle in Alessandretti et al. [2013] and its application to the control of multiple vehicles is given in Aguiar et al. [2017]

In the literature we can find other strategies for the control of underactuated vehicles such as controlling the vehicle's heading to stabilize the cross-track error, as in Samson and Ait-Abderrahim [1991], Micaelli and Samson [1993], Encarnação and Pascoal [2000], Lapierre et al. [2003] and Astolfi et al. [2004], and the line of sight method in Healey and Lienard [1993], Fossen and Pettersen [2014] and Flåten and Brekke [2017].

10.4.3 Coordination controller

In this subsection we develop the coordination controller, which follows closely the methods developed in Ghabcheloo et al. [2009]. To this effect we first recall some key concepts from algebraic graph theory.

Consider now the coordination control problem with a communication topology defined by a graph $(\mathcal{N}, \mathcal{A})$. We assume that the graph is undirected, that is, the communication links are bidirectional, if $i \in \mathcal{N}^j$ then $j \in \mathcal{N}^i$.

Remark. *The assumption of an undirected graph will be important in this chapter for the case where packet losses exist and we require that the vehicles send an acknowledgment message to their in-neighbours acknowledging that a data message was received. If we assume that there are no packet losses, this assumption could be relaxed without much effort.*

Using a Lyapunov-based design and the backstepping technique, we propose a decentralized feedback law for $\tilde{v}_{r_i}$ as a function of the information obtained from the neighbouring agents. Following Ghabcheloo et al. [2009], we introduce the coordination or synchronization error vector

$$\xi := \Gamma\gamma, \qquad \Gamma := I_N - \frac{1}{N}\mathbf{1}\mathbf{1}^T,$$

where $\gamma := \mathrm{col}(\gamma_i)$. From (10.19), the dynamics of the coordination subsystem can be written in vector form as

$$\dot{\gamma} = \bar{v}_r + \tilde{v}_r + \bar{\omega},$$

where $\bar{v}_r := \mathrm{col}(v_r(\gamma_i))$, $\bar{\omega} := \mathrm{col}(\omega_i)$, and $\tilde{v}_r := \mathrm{col}(\tilde{v}_{r_i})$. Consider the control Lyapunov function $V := \frac{1}{2}\xi^T\xi$. Computing its time-derivative yields

$$\dot{V} = \xi^T\Gamma(\bar{v}_r + \tilde{v}_r + \bar{\omega}).$$

To make ξ ISS with respect to input $\bar{\omega}$, a natural choice would be $\tilde{v}_r = -k\boldsymbol{L}\xi = -k\boldsymbol{L}\Gamma\gamma = -k\boldsymbol{L}\gamma$, where $\boldsymbol{L}$ is the Laplacian of the graph $(\mathcal{N}, \mathcal{A})$ and k is a positive scalar, or equivalently, $\tilde{v}_{r_i} = -k\sum_{j\in\mathcal{N}^i}(\gamma_i - \gamma_j)$ (the so-called neighbouring rule). To reduce the communication rate using a logic based dynamical system, we will lift the assumption that each agent receives information from its neighbourhoods continuously. We assume instead that it relies on the estimates $\hat{\gamma}_j^i$, $j \in \mathcal{N}^i$. Therefore, defining the estimation error $\tilde{\gamma}_j^i := \hat{\gamma}_j^i - \gamma_j$, the coordination control law becomes

$$\tilde{v}_{r_i} = -k\sum_{j\in\mathcal{N}^i}\left(\gamma_i - \hat{\gamma}_j^i\right) = -k\sum_{j\in\mathcal{N}^i}(\gamma_i - \gamma_j) + k\sum_{j\in\mathcal{N}^i}\tilde{\gamma}_j^i, \tag{10.24}$$

or, in vector form, $\tilde{v}_r = -k\boldsymbol{L}\xi + k\bar{\gamma}$, where $\bar{\gamma} := \mathrm{col}\left(\sum_{j\in\mathcal{N}^i}\tilde{\gamma}_j^i\right)$. Defining $\tilde{\gamma} := \mathrm{col}\left(\tilde{\gamma}_j^i, i \in \mathcal{N}, j \in \mathcal{N}^i\right)$ and $d^* := \max_{i\in\mathcal{N}}\left(|\mathcal{N}^i|\right)$ we have $\|\bar{\gamma}\| \leq d^*\|\tilde{\gamma}\|$. Note that unlike Almeida et al. [2017], in this work we do not require that the average of the coordination variables $\frac{1}{N}\sum_{i\in\mathcal{N}}$ remains constant, and therefore it is not necessary the use of an average preserving coordination law as $\tilde{v}_{r_i} = -k\sum_{j\in\mathcal{N}^i}\left(\hat{\gamma}_i^j - \hat{\gamma}_j^i\right)$ proposed in Almeida et al. [2017], and we can adopt the control law $\tilde{v}_{r_i} = -k\sum_{j\in\mathcal{N}^i}\left(\gamma_i - \hat{\gamma}_j^i\right)$, which does not introduce the estimation error associated with $\hat{\gamma}_i^j$. The time derivative of V becomes

$$\dot{V} = -k\xi^T\boldsymbol{L}\xi + \xi^T\Gamma\left(v_r + \bar{\omega} + k\bar{\gamma}\right).$$

In this case, the term $-k\xi^T\boldsymbol{L}\xi$ is negative definite provided that the graph that models the constraints imposed by the communication topology among the agents is connected, see e.g. Godsil and Royle [2013]. We can then conclude the following result.

Lemma 6 (Coordination)**.** If $(\mathcal{N}, \mathcal{A})$ is connected then ξ is ISS with respect to the inputs $\bar{\omega}$ and $\tilde{\gamma}$, for k satisfying $k > l/\sigma_2$, where σ_2 is the second lowest singular value of $\boldsymbol{L}$ and l is the Lipschitz constant of v_r, that is, there exist functions $\sigma_{\tilde{\gamma}}^{\xi}, \sigma_{\omega}^{\xi} \in \mathcal{K}_\infty$ and $\beta^{\xi} \in \mathcal{KL}$ such that

$$\|\xi\| \leq \beta^{\xi}\left(\|\xi(0)\|, t\right) + \sigma_{\omega}^{\xi}\left(\|\bar{\omega}\|_{[0,t]}\right) + \sigma_{\tilde{\gamma}}^{\xi}\left(\|\tilde{\gamma}\|_{[0,t]}\right).$$

Proof. See Appendix. □

We are now ready to state the main result of this section.

Lemma 7 (CPF)**.** Consider the closed-loop system Σ_{CL} composed by n agents of the form (10.16) with inner loops satisfying Assumption A11 and the path-following controller and coordination controller defined by (10.20)-(10.21) and (10.24) respectively. If $(\mathcal{N}, \mathcal{A})$ is connected then, for $k > \frac{l}{\sigma_2}$, the error vector

$$\eta_{e\xi\omega} := \begin{bmatrix} \boldsymbol{e}_\delta \\ \bar{\omega} \\ \xi \end{bmatrix},$$

is ISpS with respect to the input $\tilde{\gamma} := \mathrm{col}\left(\tilde{\gamma}^i_j, i \in \mathcal{N}, j \in \mathcal{N}^i\right)$, that is, there exist functions $\sigma^{e\xi\omega}_{\tilde{\gamma}} \in \mathcal{K}_\infty$ and $\beta^{e\xi\omega}, \beta^{e\xi\omega}_{il}, \beta^{e\xi\omega}_{obs} \in \mathcal{KL}$ and a positive constant $\varepsilon_{e\xi\omega}$ such that

$$\|\eta_{e\xi\omega}\| \leq \beta^{e\xi\omega}\left(\|\eta_{e\xi\omega}(0)\|, t\right) + \beta^{e\xi\omega}_{il}\left(\|\boldsymbol{x}^0_{il}\|, t\right) + \beta^{e\xi\omega}_{obs}\left(\|\boldsymbol{x}^0_{v_c}\|, t\right) + \sigma^{e\xi\omega}_{\tilde{\gamma}}\left(\|\tilde{\gamma}\|_{[0,t]}\right) + \varepsilon_{e\xi\omega}.$$

Therefore, Σ_{CL} solves robustly the CPF problem.

Proof. See Appendix. □

10.4.4 Logic-based communication system

In this subsection we present the logic-based communication system, which builds on the methods developed in Xu and Hespanha [2006] and Yook et al. [2002]. We will start with the case where the communication links are ideal, that is, there are no delays or packet losses. We then move on to the case where there are bounded communication delays. Finally, we will describe a communication system that is robust to limited packet losses.

Ideal communication links

The logic-based communication system structure for a node i, with neighbours j_1 to $j_{|\mathcal{N}^i|}$ belonging to $\mathcal{N}^i$, is illustrated in Figure 10.3. The communication system is composed by observers of the path-following variables of the neighbours j_1 to $j_{|\mathcal{N}^i|}$, $\hat{\gamma}_{j_1}$ to $\hat{\gamma}_{j_{|\mathcal{N}^i|}}$, which are reset when a data message is received by the respective neighbour, and, to compute the communication triggering condition, an observer of the own path-following variable, $\hat{\gamma}_i$, which only uses data that are sent to the neighbours. The emitter compares the observed path-following variable $\hat{\gamma}_i$ to the real γ_i and if the norm of the difference reaches the value ε a data message is sent to the neighbours containing the present γ_i.

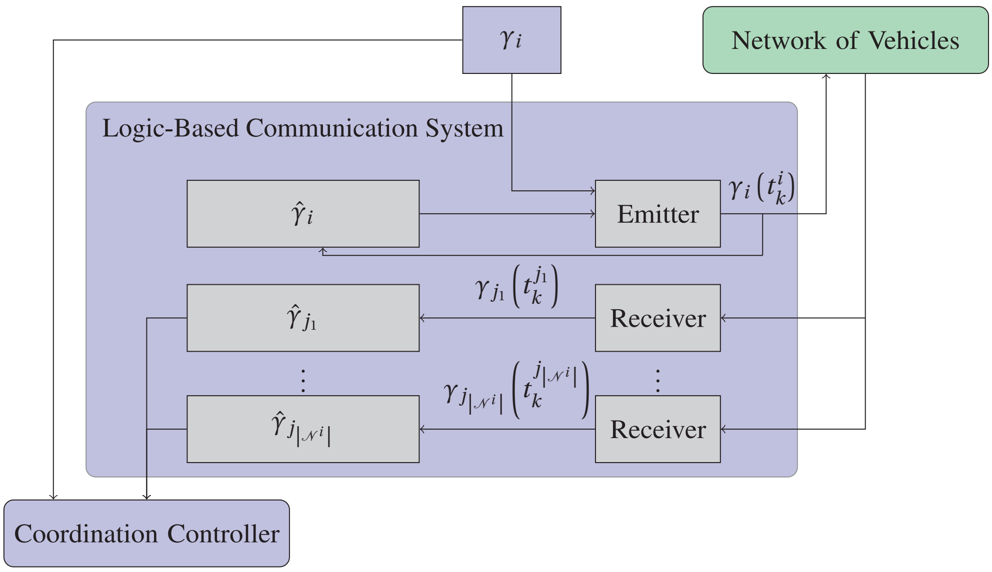

Figure 10.3 – Logic-Based Communications System for ideal communication links

Let t^i_k, $k > 0$ denote the instants of time at which agent i transmits information to the neighbours. Following the procedure described in Section 10.3 and taking account the dynamic equations of the coordination subsystem, we propose for each agent i the following logic-based communication system:

-For $t_k^i < t < t_{k+1}^i$,

$$\dot{\hat{\gamma}}_i(t) = v_r\left(\hat{\gamma}_i\right).$$

-For $t = t_k^i$

$$\hat{\gamma}_i\left(t_k^{i+}\right) = \gamma_i\left(t_k^i\right).$$

Since the communication links are ideal we consider in this case that there are copies of $\hat{\gamma}_i$ in all the neighbours of i, $\mathcal{N}^i$ and in i.

We note that if we define $T_r(\gamma) := \int_0^\gamma \frac{1}{v_r(\sigma)} \mathrm{d}\sigma$ and its inverse as $\Gamma_r(t)$, i.e. $T_r\left(\Gamma_r(t)\right) := t$, we have for $t_k^i < t < t_{k+1}^i$, $\hat{\gamma}_i(t) = \Gamma_r\left(t - t_k^i + T_r\left(\gamma_i\left(t_k^i\right)\right)\right)$. The estimator can thus be described as

$$\hat{\gamma}_i(t) = \Gamma_r\left(t - t_r^i(t) + T_r\left(\gamma_i\left(t_r^i(t)\right)\right)\right), \tag{10.25}$$

where $t_r^i(t) := \max_{k \in \mathbb{N}, t_k^i < t} t_k^i$. When v_r is constant the above expression simplifies to

$$\hat{\gamma}_i(t) = \gamma_i\left(t_r^i(t)\right) + \left(t - t_r^i(t)\right) v_r.$$

The choice of the estimator (10.25) is motivated by the fact that if, for some $t_\omega > 0$, $\bar{\omega}(t) = \mathbf{0}$ and $\xi(t) = \mathbf{0}$ for $t > t_\omega$, if $\hat{\gamma}_i(t_\omega) - \gamma_i(t_\omega) = 0$ we would have $\hat{\gamma}_i(t) - \gamma_i(t) = 0$ for $t > t_\omega$. The estimators (10.25) were also considered due to their simplicity. However, it would be also possible to chose more complex reproductions of the corresponding dynamic models, see Vanni et al. [2008].

To solve robustly the communication problem (see Definition 7) we introduce the *communication triggering condition* (CTC) $\|\tilde{\gamma}_i\| \geq \varepsilon$ where $\varepsilon > 0$, where $\tilde{\gamma}_i := \hat{\gamma}_i - \gamma_i$. Agent i transmits to j a data message with γ_i at time t_k^i when the CTC is satisfied.

Note that the post reset value of $\tilde{\gamma}_i$ is $\tilde{\gamma}_i\left(t_k^i\right) = 0$. Consequently, $\tilde{\gamma}_i \in \{\tilde{\gamma}_i^j \in \mathbb{R} : \tilde{\gamma}_i \leq \varepsilon\}$ and, hence, (10.14) holds, and from Lemma 7 we have that in the ideal communications case the overall closed-loop system together with the logic-based communication system is input to state practically stable, i.e. the path-following, speed and coordination errors converge to a neighbourhood of zero, and the size of this neighbourhood depends on the size of perturbations, which in this thesis are considered to be ultimately bounded by $\epsilon_{\tilde{r}}$, $\epsilon_{\tilde{u}}$ and ϵ_v.

Delayed information

We now consider the case where the communication channels have bounded, time-varying and non-homogeneous delays. Consider the following situation: agent i sends data at time t_k^i, and agent j receives it at time $t_k^i + \tau_k^{ij}$. We assume that

$$\tau_k^{ij} \leq \bar{\tau}, \qquad \forall i, j, k$$

where the constant $\bar{\tau} > 0$ is known a priori. The main idea is to keep estimators always synchronized, therefore both the emitter and the receiver only update the estimators at some time, with the same information, at $t_k^i + \bar{\tau}$.

Suppose that at time t_k^i agent i transmits a data message, which contains the following data: $\{t_k^i, \gamma_l\}$. Then, the estimators $\hat{\gamma}_i$ in agent i and its neighbours $\mathcal{N}^i$ cannot be immediately updated. This is because we must guarantee that the value of the state estimate $\hat{\gamma}_i$ can be computed in all agents in $\mathcal{N}^i$. To this end, both estimates can only be updated at time $t = t_k^i + \bar{\tau}$. Upon receiving t_k^i, the coordination state estimate $\hat{\gamma}_l^{ij}$ running in agent j should be updated at time $t = t_k^i + \bar{\tau}$ to

$$\hat{\gamma}_i\left(\left(t_k^i + \bar{\tau}\right)^+\right) = \Gamma_r\left(\bar{\tau} - t_k^i + T_r\left(\gamma_i\left(t_k^i\right)\right)\right),$$

In the case where v_r is constant, this simplifies to $\hat{\gamma}_i\left(\left(t_k^i + \bar{\tau}\right)^+\right) = \gamma_i\left(t_k^i\right) + \bar{\tau}\, v_r$. With the above procedure, we guarantee that the estimators are always synchronized. The estimator can thus be described as in (10.25) where $t_r^i(t)$ is redefined as $t_r^i(t) := \max_{k\in\mathbb{N}, t_k^i + \bar{\tau} < t} t_k^i$. Therefore, one can consider the ideal case mentioned previously as a particular instance of the delayed communications case with $\bar{\tau} = 0$.

Notice that in general $\tilde{\gamma}_i\left(t_k^i + \bar{\tau}\right)$ will not be zero because $\bar{\omega}_i$ and ξ may not be zero in the interval $\left[t_k^i, t_k^i + \bar{\tau}\right)$. We can therefore only guarantee that this technique is valid if $\bar{\tau}$ is sufficiently small so as to guarantee that $\tilde{\gamma}_i$ satisfies $\tilde{\gamma}_i\left(\left(t_k^i + \bar{\tau}\right)^+\right) < \varepsilon$. The stability guarantees for the delayed case will be stated in Theorem 18.

Communication losses

We now address the case when the data messages are not always received, i.e. there are packet losses. To make the communication system robust to limited communication losses we require each agent to send an acknowledgment message upon receiving a data message. The agent which sent the data message only updates his estimators $2\bar{\tau}$ time units after the data message has been sent in case the acknowledgment message was received, otherwise another data message is sent. This guarantees that the receiving agent receives a data message at some point after the CTC is satisfied.

The communication system structure, for this case with communication losses, for a node i, with neighbours j_1 to $j_{|\mathcal{N}^i|}$ belonging to $\mathcal{N}^i$, is illustrated in Figure 10.4. The structure is similar to the one in Figure 10.3, with the difference being that, since we wish to allow different data messages to be sent to different agents, we have different estimates of the path-following variable γ_i synchronized with the neighbours j_1 to $j_{|\mathcal{N}^i|}$, $\breve{\gamma}_i^{j_1}$ to $\breve{\gamma}_i^{j_{|\mathcal{N}^i|}}$, respectively.

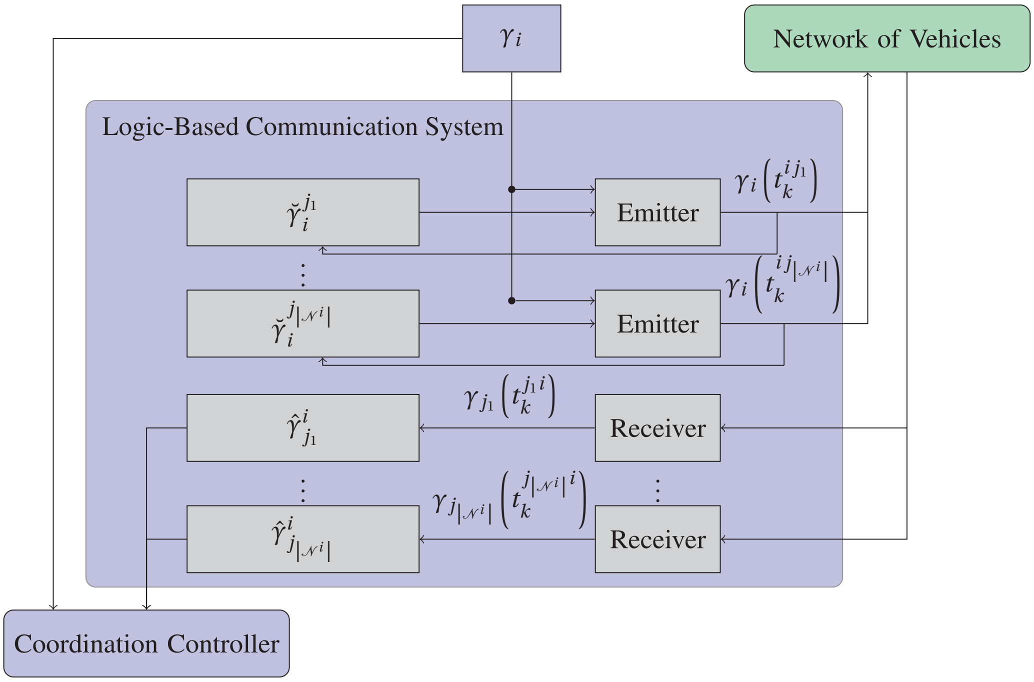

Figure 10.4 – Logic-Based Communications System for the case with packet losses

Consider the case when at time t_k^{ij} agent i transmits to agent j a data message, which contains the following data: $\{t_k^{ij}, \gamma_i\}$. Upon receiving the data message and sending an acknowledgment message, the coordination state estimate $\hat{\gamma}_i^j$ running in agent j should be updated at time $t = t_k^{ij} + 2\bar{\tau}$ to

$$\hat{\gamma}_i^j\left(\left(t_k^i + 2\bar{\tau}\right)^+\right) = \Gamma_r\left(2\bar{\tau} - t_k^i + T_r\left(\gamma_i\left(t_k^i\right)\right)\right).$$

If the acknowledgment message was received by agent i, then the coordination state estimate $\breve{\gamma}_i^j$ running in agent i should be also update at the same time as $\hat{\gamma}_i^j(t_k^{ij} + 2\bar{\tau}) = \hat{\gamma}_i^j(t_k^{ij} + 2\bar{\tau})$, otherwise another data message is sent at $t_{k+1}^{ij} = t_k^{ij} + 2\bar{\tau}$. Note that if agent i did not receive the acknowledgment message, then there is a brief period when the estimators are desynchronized, that is $\breve{\gamma}_l^{ij} \neq \hat{\gamma}_l^{ji}$, however the synchronization is recovered after the acknowledgment message of a later data message is received.

The estimator can be represented formally as

$$\hat{\gamma}_i^j(t) = \Gamma_r\left(t - t_r^{ij}(t) + T_r\left(\gamma_i\left(t_r^{ij}(t)\right)\right)\right), \tag{10.26}$$

where $t_r^{ij}(t) := \max_{k\in\mathbb{N}, t_k^{ij}+2\bar{\tau}<t, \beta_k^{ij}=1} t_k^{ij}$, where β_k^{ij} is 1 if the data message sent by agent i to agent j at time t_k^{ij} is received by agent j.

Equivalently, we can represent the estimator running on agent i synchronized with agent j, $\breve{\gamma}_i^j$ as in

$$\breve{\gamma}_i^j(t) = \Gamma_r\left(t - t_{rb}^{ij}(t) + T_r\left(\gamma_i\left(t_{rb}^{ij}(t)\right)\right)\right), \tag{10.27}$$

where $t_{rb}^{ij}(t) := \max_{k\in\mathbb{N}, t_k^{ij}+2\bar{\tau}<t, \alpha_k^{ij}=1} t_k^{ij}$, where α_k^{ij} is 1 if the data message sent by agent i to agent j at time t_k^{ij} is received by agent j and agent i receives its acknowledgment message.

If we can guarantee that for at least a finite number $N_{\max}$ of consecutive data messages sent one acknowledgment message is received, then if $\bar{\tau}$ is sufficiently small so as to guarantee that $\tilde{\gamma}_i^j$ satisfies $\tilde{\gamma}_i^j\left(\left(t_k^{ij} + 2\bar{\tau}\right)^+\right) < \varepsilon$, we can guarantee that the estimation error is bounded, hence, (10.14) holds.

The emitter communication protocol for the case of delayed information and communication losses are described in the following.

Data: $\Gamma_r(\cdot)$, $T_r(\cdot)$, $\bar{\tau}$ and ε
while *true* **do**
  if $\left\|\tilde{\gamma}_i^j\right\| = \varepsilon$ **then**
    while *no acknowledgment message was received* **do**
      Send a data message containing the current time t_k^{ij} and $\gamma_i\left(t_k^{ij}\right)$;
      Wait until $t_k^{ij} + 2\bar{\tau}$;
    end
    Update $\check{\gamma}_i^j\left(t_k^{ij} + 2\bar{\tau}\right) := \Gamma_r\left(2\bar{\tau} - t_k^{ij} + T_r\left(\gamma_i\left(t_k^{ij}\right)\right)\right)$
  end
end

Algorithm 3: Algorithm for the emitter at agent i to agent j

The receiver communication protocol is the following.

Data: $\Gamma_r(\cdot)$, $T_r(\cdot)$, $\bar{\tau}$ and ε
while *true* **do**
  if *a data message is received containing* t_k^{ij} *and* $\gamma_i(t_k^{ij})$ **then**
    Send an acknowledgment message, acknowledging that a data message was received ;
    Wait until $t_k^{ij} + 2\bar{\tau}$;
    Update $\hat{\gamma}_i^j\left(t_k^{ij} + 2\bar{\tau}\right) := \Gamma_r\left(2\bar{\tau} - t_k^{ij} + T_r\left(\gamma_i\left(t_k^{ij}\right)\right)\right)$
  end
end

Algorithm 4: Algorithm for the receiver at agent j from agent i

We can now state the main result of this chapter.

Theorem 18. Consider the overall closed-loop system Σ_{OCL} consisting of N agents of the form (10.16), equipped with inner loop controllers satisfying Assumption A11, the proposed CPF controller under the assumptions of Lemma 7, with $k > l/\sigma_2$, and the proposed logic-based communication system in the presence of delayed information and communication losses. If it is guaranteed that for a finite number $N_{\max}$ consecutive data messages sent by an agent one acknowledgment message is received, then for sufficiently small time delays $\bar{\tau}$ and sufficiently small values of $\|\xi(0)\|$, $\max_{i\in\mathcal{N}}\|\eta_{e_i}(0)\|$, $\max_{i\in\mathcal{N}}\left\|\boldsymbol{x}_{il_i}^0\right\|$, $\max_{i\in\mathcal{N}}\left\|\boldsymbol{x}_{v_{ci}}^0\right\|$ and ε_e, the overall closed-loop system solves the CPF problem.

In particular, we can compute functions $\beta_{e\omega}^{\tilde{\gamma}}, \beta_{\xi}^{\tilde{\gamma}}, \beta_{il}^{\tilde{\gamma}}, \beta_{obs}^{\tilde{\gamma}} \in \mathcal{KL}$, $\alpha^{e\xi\omega}, \alpha^{\bar{\varepsilon}} \in \mathcal{K}$ and continuous functions $\tilde{\alpha}^{\varepsilon}(N_{\max}\bar{\tau}) : [0,c) \to [1,\infty)$ and $\tilde{\alpha}^{\xi}, \tilde{\alpha}^{\omega} : [0,c) \to [0,\infty)$, for some positive constant c with $\tilde{\alpha}^{\varepsilon}(0) = 1$ and $\alpha^{\xi}(0) = \alpha^{\omega}(0) = 0$, such that

$$\max_{i\in\mathcal{N}, j\in\mathcal{N}^i}\left\|\tilde{\gamma}_i^j(t)\right\| \le \tilde{\alpha}^{\xi}(N_{\max}\bar{\tau})\beta^{\xi}(\|\xi(0)\|, t) + \tilde{\alpha}^{\omega}(N_{\max}\bar{\tau})\left(\beta_{e\omega}^{\tilde{\gamma}}\left(\max_{i\in\mathcal{N}}\|\eta_{e_i}(0)\|, t\right) + \beta_{il}^{\tilde{\gamma}}\left(\max_{i\in\mathcal{N}}\|\boldsymbol{x}_{il_i}^0\|, t\right)\right)$$
$$+ \tilde{\alpha}^{\omega}(N_{\max}\bar{\tau})\left(\beta_{obs}^{\tilde{\gamma}}\left(\max_{i\in\mathcal{N}}\|\boldsymbol{x}_{v_{ci}}^0\|, t\right) + \frac{1}{\sqrt{c_\omega}}\varepsilon_e\right) + \tilde{\alpha}^{\varepsilon}(N_{\max}\bar{\tau})\varepsilon, \tag{10.28}$$

where $\beta^{\xi} \in \mathcal{KL}$ is defined on the proof of Lemma 6.

Before proving Theorem 18 the following lemmas are required.

Lemma 8. Consider the overall closed-loop system Σ_{OCL} of Theorem 18, and the proposed logic-based communication system in the presence of delayed information and packet losses. For any time t_k^{ij} when the messages sent from agent i to j are received by j, if the post-reset value satisfy $\left\|\tilde{\gamma}_i^j\left(\left(t_k^{ij}+2\bar{\tau}\right)^+\right)\right\| < \varepsilon$, then, for sufficiently small $\bar{\tau}$,

$$\left\|\tilde{\gamma}_i^j(t)\right\| \leq \alpha^{\varepsilon}(N_{\max}\bar{\tau})\varepsilon + \alpha^{\xi}(N_{\max}\bar{\tau})\|\xi\|_{[t-2N_{\max}\bar{\tau},t]} + \alpha^{\omega}(N_{\max}\bar{\tau})\|\omega_i\|_{[t-2N_{\max}\bar{\tau},t]}, \forall t \geq 0, i \in \mathcal{N}, j \in \mathcal{N}^i \quad (10.29)$$

for continuous functions $\alpha^{\varepsilon}(N_{\max}\bar{\tau}) : [0,b) \to [1,\infty)$ and $\alpha^{\xi}, \alpha^{\omega} : [0,b) \to [0,\infty)$, for some positive constant b with $\alpha^{\varepsilon}(0) = 1$ and $\alpha^{\xi}(0) = \alpha^{\omega}(0) = 0$.

Proof. See Appendix. □

Lemma 9. Consider the overall closed-loop system Σ_{OCL} of Theorem 18, and the proposed logic-based communication system in the presence of delayed information and packet losses. If for any time t_k^{ij} when the messages sent from agent i to j are received by j, the post-reset value satisfy $\left\|\tilde{\gamma}_i^j\left(\left(t_k^{ij}+2\bar{\tau}\right)^+\right)\right\| < \varepsilon$, for sufficiently small $\bar{\tau}$ and $N_{\max}$ we have that (10.28) is satisfied.

Proof. See Appendix. □

Lemma 10. Consider the overall closed-loop system Σ_{OCL} of Theorem 18, and the proposed logic-based communication system in the presence of delayed information and packet losses. For sufficiently small $\bar{\tau}$ and $N_{\max}$, or sufficiently small values of $\|\eta_{e\xi\omega}(0)\|$, $\|\boldsymbol{x}_{il}^0\|$, $\|\boldsymbol{x}_{v_c}^0\|$ and $\|\varepsilon_{e\xi\omega}\|$, if $\tilde{\gamma}_i^j(t)$ satisfies (10.29), then $\left\|\tilde{\gamma}_i^j\left(\left(t_k^{ij}+2\bar{\tau}\right)^+\right)\right\| < \varepsilon$ follows for any time t_k^{ij} when the data messages sent from agent i are received by j.

Proof. See Appendix. □

Proof of Theorem 18. Suppose that for some time t_k^{ij} when a data message sent from agent i to j is received by j, all the previous data messages sent from any agent $o \in \mathcal{N}$ that are received by some agent $p \in \mathcal{N}^o$, sent at a time $t_{\tilde{k}}^{op} \leq t_k^{ij}$, the post-reset values satisfy $\left\|\tilde{\gamma}_o^p\left(\left(t_{\tilde{k}}^{op}+2\bar{\tau}\right)^+\right)\right\| < \varepsilon$. This holds true if t_k^{ij} is the time when the first data message in the fleet that is received by another agent, is sent.

If $\bar{\tau}$ and $N_{\max}$ are sufficiently small such that they satisfy the conditions of Lemmas 8, 9 and 10, we are under the conditions of Lemma 10, and therefore we have

$$\left\|\tilde{\gamma}_i^j\left(\left(t_k^{ij}+2\bar{\tau}\right)^+\right)\right\| \leq \tilde{\varepsilon},$$

where $\tilde{\varepsilon}$ depends on $\|\xi(0)\|$, $\max_{i\in\mathcal{N}}\|\eta_{e_i}(0)\|$, $\max_{i\in\mathcal{N}}\|\boldsymbol{x}_{il_i}^0\|$, $\max_{i\in\mathcal{N}}\|\boldsymbol{x}_{v_{ci}}^0\|$, ε_e and ε but not on time, and we can apply Lemma 10 for the next received data message.

Noting that, from Lemma 8, one can observe that, when $\dot{\tilde{\gamma}}_i^j(t)$ is defined, $\max_{i\in\mathcal{N},j\in\mathcal{N}^i}\left\|\dot{\tilde{\gamma}}_i^j(t)_i^j(t)\right\| \leq v_{\dot{\tilde{\gamma}}}$, where $v_{\dot{\tilde{\gamma}}}$ depends on $\|\xi(0)\|$, $\max_{i\in\mathcal{N}}\|\eta_{e_i}(0)\|$, $\max_{i\in\mathcal{N}}\|\boldsymbol{x}_{il_i}^0\|$, $\max_{i\in\mathcal{N}}\|\boldsymbol{x}_{v_{ci}}^0\|$, ε_e and ε but not on time.

Therefore, the triggering condition $\left\|\tilde{\gamma}_i^j(t)\right\| = \varepsilon$ can only occur N times within $\frac{\varepsilon-\tilde{\varepsilon}}{v_{\dot{\tilde{\gamma}}}}$ time units. Repeating the same reasoning every time a data message is received by any agent, the theorem holds by recursion. □

Theorem 18 provides stability guarantees in the case with delays and packet losses. The following corollaries of Theorem 18 provide stability guarantees for the cases with only communication delays and with ideal communication links.

Corollary 1 (Delayed Information)**.** Consider the overall closed-loop system Σ_{OCL} of Theorem 18, and the proposed logic-based communication system in the presence of delayed information. For sufficiently small time delays $\bar{\tau}$ and sufficiently small values of $\|\xi(0)\|$, $\max_{i\in\mathcal{N}} \|\eta_{e_i}(0)\|$, $\max_{i\in\mathcal{N}} \left\|\boldsymbol{x}^0_{il_i}\right\|$, $\max_{i\in\mathcal{N}} \left\|\boldsymbol{x}^0_{v_{ci}}\right\|$ and ε_e, the overall closed-loop system solves the CPF problem.

Proof. Since the delayed communication case can be viewed as a particular instance of the communication losses case with $N_{\max} = 1$ and $\bar{\tau}$ halved, Theorem 18 provides a proof of stability of the overall system for all the case with only communication delays. □

Corollary 2 (Ideal Communications)**.** The overall closed-loop system Σ_{OCL} of Theorem 18, and the proposed logic-based communication system with ideal communication links, i.e. there are no delays or communication losses, solves the CPF problem.

Proof. Since the ideal communications case can be viewed as a particular case of the delayed communications one where $\bar{\tau} = 0$, Corollary 1 provides a proof of stability of the overall system for the case with ideal communication links. Moreover, one can observe from Theorem 18 that the boundedness assumptions on $\|\xi(0)\|$, $\max_{i\in\mathcal{N}} \|\eta_{e_i}(0)\|$, $\max_{i\in\mathcal{N}} \left\|\boldsymbol{x}^0_{il_i}\right\|$, $\max_{i\in\mathcal{N}} \left\|\boldsymbol{x}^0_{v_{ci}}\right\|$ and ε_e are not required anymore since $\alpha^{\xi}(0) = \alpha^{\omega}(0) = 0$. □

10.5 Alternative Design

In the case where the vehicles are equipped with heading controllers, rather than yaw rate controllers and we require that the reference surge speed u_d be continuous, as is often the case in practice, we require some adjustments of the path-following controller. With the proposed path-following controller introduced in this section there exists an interconnection between the coordination and the path-following errors and therefore we require a different stability proof methodology. This interconnection between the path-following controller and the coordination controller was also studied in Ghabcheloo et al. [2007] for the path-following control algorithm in Soetanto et al. [2003], which provides conditions such that the overall interconnected system is stable.

This interconnection was not present in the control laws of Section 10.4. This is because, since we require the reference surge speed u_d to be continuous, we must not have discontinuities in $\dot{\gamma}$ as in (10.22), and we remove the term $\dot{\hat{v}}_r$ from the control law of input $\ddot{\gamma}$, since it is not defined when a message is recieved. As will be seen in Subsection 10.5.2, unlike the previous version with these changes one cannot guarantee that the coordination controller speed error $\bar{\omega}$ is independent of ξ and therefore we have the interconnection illustrated in Figure 10.5, where $\boldsymbol{e}_{\delta} := \mathrm{col}\left(\boldsymbol{e}^i - \boldsymbol{\delta}\right)$ and $\boldsymbol{e}^i$ is the path following error of agent i.

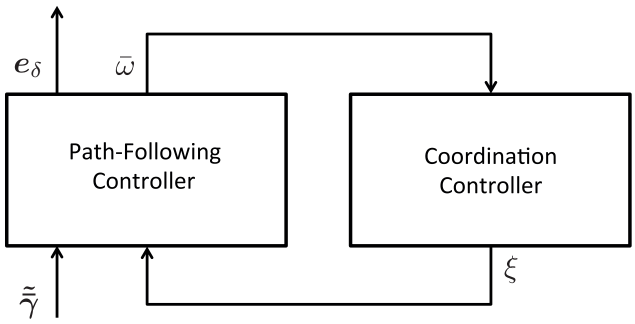

Figure 10.5 – Diagram of the interconnection between the coordination controller and the path-following controller in the alternative design.

10.5.1 Path-following controller

In this section we consider that the vehicles are equipped with inner-loop controllers designed to track heading angle and surge speed commands. We therefore assume that the following holds

Assumption A13. Let $\tilde{u} := u - u_d$ and $\tilde{\psi} := \psi - \psi_d$ be the surge speed and heading errors, respectively and let $\boldsymbol{x}_{il}^0$ be the initial condition of the state of the inner-loop system. There exist functions $\beta^{\tilde{u}}, \beta^{v} \in \mathcal{KL}$ and positive constants $\epsilon_{\tilde{u}}, \epsilon_{\tilde{\psi}}, \epsilon_v$ such that

$$\|\tilde{\psi}(t)\| \le \epsilon_{\tilde{\psi}} \quad \|\tilde{u}(t)\| \le \beta^{\tilde{u}}\left(\|\boldsymbol{x}_{il}^0\|, t\right) + \epsilon_{\tilde{u}} \quad \|v_w(t)\| \le \beta^{v}\left(\|\boldsymbol{x}_{il}^0\|, t\right) + \epsilon_v,$$

where $\frac{\pi}{2} > \epsilon_{\tilde{\psi}}$.

The assumption that the heading error is bounded from the beginning, and does not have a transient phase as the speed, stems from the fact that since it is assumed that the heading is measured directly, one can assign the initial desired heading $\psi_d(0)$ to be equal to the initial measured heading $\psi(0)$ and therefore we have initially $\tilde{\psi}(0) = 0$, thus eliminating the transient phase.

Define the position error $\boldsymbol{e}$ as the difference between the positions of the vehicle and of the virtual target expressed in the reference heading coordinates $\{\mathcal{B}_d\}$, where R_d is the orthonormal transformation matrix from $\{\mathcal{B}_d\}$ to $\{\mathcal{U}\}$, that is,

$$\boldsymbol{e} := R_d^T(\boldsymbol{p} - \boldsymbol{p}_d).$$

The dynamics of $\boldsymbol{e}$ are described by

$$\dot{\boldsymbol{e}} = -S\left(\dot{\psi}_d\right)\boldsymbol{e} + \tilde{R}\begin{bmatrix} u_d + \tilde{u} \\ v_c + v_w \end{bmatrix} - R_d^T \frac{\partial \boldsymbol{p}_d}{\partial \gamma}\dot{\gamma}, \qquad S\left(\dot{\psi}_d\right) = \begin{bmatrix} 0 & -\dot{\psi}_d \\ \dot{\psi}_d & 0 \end{bmatrix}, \tag{10.30}$$

where $\tilde{R}$ is the orthonormal transformation matrix from $\{\mathcal{B}\}$ to $\{\mathcal{B}_d\}$, i.e.

$$\tilde{R} = \begin{bmatrix} \cos\left(\tilde{\psi}\right) & -\sin\left(\tilde{\psi}\right) \\ \sin\left(\tilde{\psi}\right) & \cos\left(\tilde{\psi}\right) \end{bmatrix},$$

and we used the fact that $\dot{R}_d = S\left(\dot{\psi}_d\right)$ and $R_d^T = \tilde{R}R^T$.

To make the desired speed $\boldsymbol{u}_d := [u_d,\, \dot{\psi}_d]^T$ appear in the position error dynamics we introduce a constant design vector $\boldsymbol{\delta} := [\delta,\, 0]^T$, $\delta < 0$. Following from (10.30), simple computations show that the position error dynamics are then given by

$$\dot{\boldsymbol{e}} = -S\left(\dot{\psi}_d\right)(\boldsymbol{e}-\boldsymbol{\delta}) + \Delta \boldsymbol{u}_d + \tilde{R}\begin{bmatrix} \tilde{u} \\ v_w + v_c \end{bmatrix} - R_d^T \frac{\partial \boldsymbol{p}_d}{\partial \gamma}\dot{\gamma}, \tag{10.31}$$

where $\Delta := \begin{bmatrix} \cos\left(\tilde{\psi}\right) & 0 \\ \sin\left(\tilde{\psi}\right) & -\delta \end{bmatrix}$, which is invertible, since from Assumption A13 $\|\tilde{\psi}\| < \frac{\pi}{2}$.

Defining the virtual target speed error

$$e_{\dot{\gamma}} := \dot{\gamma} - (v_r + \tilde{v}_r), \tag{10.32}$$

and computing its time derivative yields $\dot{e}_{\dot{\gamma}} = \ddot{\gamma} - \dot{v}_r(\gamma) = \ddot{\gamma} - \frac{\partial v_r}{\partial \gamma}(\gamma)\dot{\gamma}$.

Lemma 11. Consider the vehicle model described by the kinematics (10.16), with finite values of

$$\sup_{\gamma\in\mathbb{R}} \left\| \frac{\partial \boldsymbol{p}_d}{\partial \gamma}(\gamma) \right\| \quad \text{and} \quad \sup_{\gamma\in\mathbb{R}} \left\| \frac{\partial \boldsymbol{p}_d}{\partial \gamma}(\gamma)\, v_r(\gamma) \right\|,$$

in closed-loop with the output feedback control law composed by an inner loop that satisfies Assumption A13, a lateral current estimator which satisfies Assumption A12, and the outer loop given by

$$\ddot{\gamma} = -k_\omega(\dot{\gamma} - v_r - \tilde{v}_r) + \dot{v}_r + \frac{1}{c_\omega}(\boldsymbol{e}-\boldsymbol{\delta})^T R_d^T \frac{\partial \boldsymbol{p}_d(\gamma)}{\partial \gamma}, \tag{10.33}$$

$$\boldsymbol{u}_d = \Delta^{-1}\left(-K_k(\boldsymbol{e}-\boldsymbol{\delta}) - \tilde{R}\begin{bmatrix} 0 \\ \hat{v}_c \end{bmatrix} + R_d^T \frac{\partial \boldsymbol{p}_d}{\partial \gamma}(v_r + \tilde{v}_r)\right), \tag{10.34}$$

where $K_k := \mathrm{diag}(k_x, k_y)$, and the design parameters k_x, k_y, k_ω and $c_\omega > 0$ satisfy $k_x, k_y, k_\omega, c_\omega > 0$.

Then, defining the error vector

$$\eta_e := \begin{bmatrix} \boldsymbol{e}-\boldsymbol{\delta} \\ \sqrt{c_\omega}\,\omega \end{bmatrix},$$

is IOpS with respect to $\tilde{v}_r$, that is, there exist functions $\sigma^e_{\tilde{v}_r} \in \mathcal{K}_\infty$ and $\beta^e \in \mathcal{KL}$ and a positive constant ε_e then

$$\|\eta_e\| \le \beta^e\left(\|\eta_e(0)\|, t\right) + \beta^e_{il}\left(\|\boldsymbol{x}^0_{il}\|, t\right) + \beta^e_{obs}\left(\|\boldsymbol{x}^0_{v_c}\|, t\right) + \sigma^e_{\tilde{v}_r}\left(\|\tilde{v}_r\|_{[0,t]}\right) + \varepsilon_e. \tag{10.35}$$

Moreover, $\sigma^e_{\tilde{v}_r}$ and ε_e can be defined as

$$\sigma^e_{\tilde{v}_r}(s) := \frac{\max\left(\sqrt{c_\omega}k_\omega, \sup_{\gamma\in\mathbb{R}}\left\|\frac{\partial \boldsymbol{p}_d(\gamma)}{\partial \gamma}\right\|\right)}{\min(k_x, k_y, k_\omega)\theta_e} s, \tag{10.36}$$

and

$$\varepsilon_e := \frac{\sqrt{\epsilon^2_{\tilde{u}} + (\epsilon_v + \epsilon_{v_c})^2}}{\min(k_x, k_y, k_\omega)\theta_e}, \tag{10.37}$$

with $0 < \theta_e < 1$. Thus, the control laws (10.33-10.34) solve robustly the path-following problem.

Proof. See Appendix. □

10.5.2 Coordination controller

Following Ghabcheloo et al. [2009], we introduce the error vector

$$\xi := \Gamma\gamma, \qquad \Gamma := I_N - \frac{1}{N}\mathbf{1}\mathbf{1}^T,$$

where $\gamma := \mathrm{col}(\gamma_i)$. We also define the coordination controller speed error

$$\omega_i := e_{\dot{\gamma}_i} - \tilde{v}_{r_{d_i}}, \tag{10.38}$$

where $\tilde{v}_{r_{d_i}}$ is the desired correction speed signal assuming that measurements of the coordination states $\gamma_j; \forall j \in \mathcal{N}^i$ are available continuously. With ω_i defined as above, the dynamics of the coordination subsystem can be written in vector form as

$$\dot{\gamma} = \bar{v}_r + \tilde{v}_{r_d} + \bar{\omega}, \tag{10.39}$$

where $\bar{v}_r := \mathrm{col}(v_r(\gamma_i))$, $\bar{\omega} := \mathrm{col}(\omega_i)$, and $\tilde{v}_{r_d} := \mathrm{col}\left(\tilde{v}_{r_{d_i}}, i \in \mathcal{N}\right)$. Consider the control Lyapunov function $V := \frac{1}{2}\xi^T\xi$. Computing its time-derivative yields

$$\dot{V} = \xi^T\Gamma(\bar{v}_r + \tilde{v}_r + \bar{\omega}).$$

To make ξ ISS with respect to input $\bar{\omega}$, a natural choice would be $\tilde{v}_{r_d} = -k\boldsymbol{L}\xi = -k\boldsymbol{L}\Gamma\gamma = -k\boldsymbol{L}\gamma$, where k is a positive scalar, or equivalently, $\tilde{v}_{r_{d_i}} = -k\sum_{j\in\mathcal{N}^i}(\gamma_i - \gamma_j)$ (the so-called neighbouring rule). The time derivative of V becomes

$$\dot{V} = -k\xi^T\boldsymbol{L}\xi + \xi^T\Gamma(\bar{v}_r + \bar{\omega}).$$

In this case, the term $-k\xi^T\boldsymbol{L}\xi$ is negative definite provided that the Graph that models the constraints imposed by the communication topology among the agents is connected. We can then conclude the following result.

Lemma 12. If $(\mathcal{N}, \mathcal{A})$ is connected then ξ is ISS with respect to the input $\bar{\omega}$ for k satisfying $k > l/\sigma_2$, where σ_2 is the second lowest singular value of L and l is the Lipschitz constant of v_r, that is, there exist functions $\sigma_\omega^\xi \in \mathcal{K}_\infty$ and $\beta^\xi \in \mathcal{KL}$ such that

$$\|\xi\| \le \beta^\xi(\|\xi(0)\|, t) + \sigma_\omega^\xi(\|\bar{\omega}\|_{[0,t]}).$$

Moreover, σ_ω^ξ can be defined as

$$\sigma_\omega^\xi(s) := \frac{1}{(k\sigma_2 - l)\theta_\xi} s,$$

with $1 > \theta_\xi > 0$.

Proof. See Appendix. □

To reduce the communication rate using a logic based dynamical system, we will lift the assumption that each agent receives information from its neighbourhoods continuously. We assume instead that it relies on estimates. Therefore, the coordination control law becomes

$$\tilde{v}_{r_i} = -k\sum_{j\in\mathcal{N}^i}(\gamma_i - \hat{\gamma}_j^i) = \tilde{v}_{r_{d_i}} + k\sum_{j\in\mathcal{N}^i}\tilde{\gamma}_j^i, \tag{10.40}$$

or in vector form,

$$\tilde{v}_r = \tilde{v}_{r_d} + k\bar{\gamma},$$

where $\bar{\gamma} := \mathrm{col}\left(\sum_{j\in\mathcal{N}^i} \tilde{\gamma}^i_j\right)$.

In order to prove that the coordination control problem is solved with the proposed controllers we need to obtain a result similar to lemma (11) using the Lyapunov function $V = \frac{1}{2}\left(\|\boldsymbol{e}_\delta\|^2 + c_\omega\|\bar{\omega}\|^2\right)$, where $\boldsymbol{e}_\delta := \mathrm{col}\left(\boldsymbol{e}^i - \boldsymbol{\delta}\right)$ and $\boldsymbol{e}^i$ is the path-following error of agent i, with $\bar{\omega}$ instead of $e_{\dot{\gamma}}$.

Lemma 13. Consider the vehicle model described by (10.16), with finite values of $\sup_{\gamma\in\mathbb{R},i\in\mathcal{N}}\left\|\frac{\partial \boldsymbol{p}_{d_i}(\gamma)}{\partial\gamma}\right\|$ and $\sup_{\gamma\in\mathbb{R},i\in\mathcal{N}}\left\|\frac{\partial \boldsymbol{p}_{d_i}(\gamma)}{\partial\gamma}v_r(\gamma)\right\|$, in closed-loop with the output feedback control law composed by an inner loop that satisfies Assumption A13, a lateral current estimator which satisfies Assumption A12, and the outer loop given by (10.33-10.34). Then, if k is chosen satisfying $k < \frac{\min(k_x,k_y,k_\omega)}{\sigma_N}$, where σ_N is the largest singular value of L, the error vector

$$\eta_\omega := \left[\boldsymbol{e}_\delta,\ \sqrt{c_\omega}\bar{\omega}\right]^T,$$

is ISpS with respect to ξ and $\tilde{\gamma}$, that is, there exist functions $\sigma^\omega_\xi, \sigma^\omega_{\tilde{\gamma}} \in \mathcal{K}_\infty$ and $\beta^\omega \in \mathcal{KL}$ and a positive constant ε_ω such that

$$\|\eta_\omega\| \le \beta^\omega(\|\eta_\omega(0)\|, t) + \beta^\omega_{il}\left(\left\|\mathrm{col}\left(\boldsymbol{x}^0_{il_i}\right)\right\|, t\right) + \beta^\omega_{obs}\left(\left\|\mathrm{col}\left(\boldsymbol{x}^0_{v_{c_i}}\right)\right\|, t\right) + \sigma^\omega_\xi(\|\xi\|_{[0,t]}) + \sigma^\omega_{\tilde{\gamma}}(\|\tilde{\gamma}\|_{[0,t]}) + \varepsilon_\omega. \quad (10.41)$$

Moreover, σ^ω_ξ can be defined as

$$\sigma^\omega_\xi(s) := \frac{\sqrt{c_\omega}k\sigma_N(l + k\sigma_N)}{\{\min(k_x, k_y, k_\omega) - k\sigma_N\}\theta_\omega}s, \quad (10.42)$$

with $0 < \theta_\omega < 1$.

Proof. See Appendix. □

We are now ready to state the main result of this section.

Theorem 19. Consider the closed-loop system Σ_{CL} composed by N agents of the form (10.16) with inner loops satisfying Assumption A13 and the path-following controller and coordination controller defined by (10.33)-(10.34) and (10.40) respectively. If the network $(\mathcal{N},\mathcal{A})$ is connected then, choosing k satisfying

$$\frac{l}{2} < k < \frac{k_k}{\sigma_N}, \quad (10.43)$$

where $k_k := \min(k_x, k_y, k_\omega)$, and c_ω satisfying

$$c_\omega < \left(\frac{(k\sigma_2 - \sqrt{N}\sigma_N)(k_k - k\sigma_N)}{k\sigma_N(l + k\sigma_N)}\right)^2, \quad (10.44)$$

then there exists a vector $\eta_{e\xi\omega}$ such that $\boldsymbol{e}_\delta$, $e_{\dot{\gamma}}$, ξ and $\bar{\omega}$ are detectable through $\eta_{e\xi\omega}$, and $\eta_{e\xi\omega}$ is ISpS with respect to the input $\tilde{\gamma} := \mathrm{col}\left(\tilde{\gamma}^i_j, i\in\mathcal{N}, j\in\mathcal{N}^i\right)$, that is, there exist functions $\sigma^{e\xi\omega}, \sigma^{e\xi\omega}_{\tilde{\gamma}} \in \mathcal{K}_\infty$ and $\beta^{e\xi\omega} \in \mathcal{KL}$ and a positive constant $\varepsilon_{e\xi\omega}$ such that

$$\|\boldsymbol{e}_\delta\| + \|e_{\dot{\gamma}}\| + \|\xi\| + \|\bar{\omega}\| \le \sigma^{e\xi\omega}(\|\eta_{e\xi\omega}\|_{[0,t]}), \quad (10.45)$$

and

$$\|\eta_{e\xi\omega}\| \le \beta^{e\xi\omega}(\|\eta_{e\xi\omega}(0)\|, t) + \sigma^{e\xi\omega}_{\tilde{\gamma}}(\|\tilde{\gamma}\|_{[0,t]}) + \varepsilon_{e\xi\omega}.$$

Therefore, Σ_{CL} solves robustly the CPF problem.

Proof. The proof of the above result is based on lemmas 13 and 12, together with the small-gain theorem in Jiang et al. [1994].

Inequality (10.43) follows directly from the hypothesis of Lemmas 13 and 12.

From the small gain theorem we have that Σ_{CL} is ISpS if and only if $\sigma^{\xi}_{\omega} \circ \sigma^{\omega}_{\xi}(s) < s$, that is, if for some $1 > \theta_\omega > 0$ and $1 > \theta_\xi > 0$ we have

$$\frac{1}{(k\sigma_2 - \sqrt{N}\sigma_N)\theta_\xi} \frac{\sqrt{c_\omega}k\sigma_N(l + k\sigma_N)}{(k_k - k\sigma_N)\theta_\omega} < 1, \tag{10.46}$$

which holds if (10.44) is satisfied □

10.6 Alternative Logic-based communication system

This subsection describes an alternative logic-based communication system that takes into account, in the dynamics of its filters, the action of the coordination controller, potentially increasing the period between communications. This filter dynamics requires a more complex communication system structure and communication protocols, since the filter requires local estimates of the path-following variables of multiple agents. We will discuss the cases where 1) the communications are ideal with no packet losses or delays 2) the communications are delayed and 3) the communications are delayed and are subject to packet losses.

1) *Ideal communication links:* Let $t^{[ij]}_k$, $k > 0$ denote the instants of time at which agent i transmits data to j or j transmits data to i, and let $\beta^{ij}_k \in \{i, j\}$ denote the agent which sent data at $t^{[ij]}_k$. Following the procedure described in Subsection 10.3 and taking account the dynamic equations of the coordination subsystem, we propose for each agent i the following logic-based communication system:

-For $t^{[ij]}_k \le t < t^{[ij]}_{k+1}$

$$\dot{\hat{\gamma}}^{ij}_l = v_r\left(\hat{\gamma}^{ij}_l\right) + \hat{\tilde{v}}^{ij}_{r_l}, \tag{10.47a}$$

$$\hat{\tilde{v}}^{ij}_{r_l} := -k_l \sum_{m \in \mathcal{N}^l \cap \mathcal{L}_{ij}} \left(\hat{\gamma}^{ij}_l - \hat{\gamma}^{ij}_m\right), \qquad l \in \mathcal{L}_{ij} \tag{10.47b}$$

-For $t = t^{[ij]}_k$

$$\hat{\gamma}^{ij}_l\left(t^{[ij]+}_k\right) = \hat{\gamma}^{\beta^{ij}_k}_l, \tag{10.48}$$

where $\hat{\gamma}^i_j$ is defined as

$$\hat{\gamma}^i_j := \begin{cases} \gamma_i & \text{if } j = i \\ \hat{\gamma}^{i\alpha_{ij}}_j & \text{otherwise} \end{cases}, \tag{10.49}$$

with $\alpha_{ij} \in \mathcal{N}^i$, $\alpha_{ij} = j$ if $j \in \mathcal{N}_i$ and $\mathcal{L}_{ij} \supseteq \{i, j\}$, where α_{ij} represents a neighbour of i that is closest to j and $\mathcal{L}_{ij}$ represents the set of path-following variables that estimated in the link ij. We will consider

$\mathscr{L}_{ij} = \mathscr{N}$. However, other choices such as $\mathscr{L}_{ij} = \{i, j\}$ could also be considered, in which case we would have $\hat{\bar{v}}^{ij}_{r_i} = -k\left(\hat{\gamma}^{ij}_i - \hat{\gamma}^{ij}_j\right)$ and $\hat{\bar{v}}^{ij}_{r_j} = -k\left(\hat{\gamma}^{ij}_j - \hat{\gamma}^{ij}_i\right)$. To simplify the estimators, we have chosen (10.47) instead of choosing a more complex reproduction of the corresponding dynamic models, which would imply the communication of more variables among the agents, increasing the required bandwidth, without much foreseeable improvement in performance. From the logic-based communication system we obtain the estimates of the neighbours' path-following variables as $\hat{\gamma}^i_j := \hat{\gamma}^{ij}_j$, $j \in \mathscr{N}^i$.

To solve robustly the communication problem (see Definition 7) we introduce the communication threshold $\epsilon > 0$ and $\tilde{\gamma}^j_i := \hat{\gamma}^j_i - \gamma_i$ and use the following logic: agent i transmits to j a message composed by $\left[\hat{\gamma}^i_l\right]_{l\in\mathscr{L}_{ij}}$ at time $t^{[ij]}_k$ when $\lim_{t\to t^{[ij]}_k} \left\|\tilde{\gamma}^j_i(t)\right\| \geq \epsilon$. Since the message was sent by agent i we define the index $\beta^{ij}_k = i$, otherwise $\beta^{ij}_k = j$.

Note that the post reset value of $\tilde{\gamma}^j_i$ is $\tilde{\gamma}^j_i\left(t^{[ij]}_k\right) = 0$ Consequently, $\tilde{\gamma}^j_i \in \left\{\tilde{\gamma}^j_i \in \mathbb{R} : \left\|\tilde{\gamma}^j_i\right\| \leq \epsilon\right\}$ and, hence, (10.14) holds.

However, we did not consider the cases when $\lim_{t\to t^{[ij]}_k} \left\|\tilde{\gamma}^j_i(t)\right\| \geq \epsilon$ and $\lim_{t\to t^{[ij]}_k} \left\|\tilde{\gamma}^i_j(t)\right\| \geq \epsilon$, that is, when both agents send messages at the same time. To handle such cases we consider that each communication link has a primary and a secondary agent. Considering without loss of generality that i is a primary agent on link ij, then $\hat{\gamma}^{ij}_l$ and $\hat{\gamma}^{ji}_l$, $l \in \mathscr{L}_{ij}$ are updated as

$$\hat{\gamma}^{ij}_l\left(t^{[ij]+}_k\right) = \hat{\gamma}^{ji}_l\left(t^{[ij]+}_k\right) = \begin{cases} \hat{\gamma}^j_l & \text{if } \alpha_{jl} \neq i \\ \hat{\gamma}^i_l & \text{if } \alpha_{jl} = i \end{cases}, \tag{10.50}$$

With this method, the post reset values of $\tilde{\gamma}^j_i$ and $\tilde{\gamma}^i_j$ are equal to zero and therefore (10.14) holds also in this case.

2) *Delayed information:* We now consider the case where the communication channels have bounded, time-varying and non-homogeneous delays. Consider the following situation: agent i sends data to j at time $t^{[ij]}_k$, and agent j receives it at time $t^{[ij]}_k + \tau^{ij}_k$. We assume that

$$\tau^{ij}_k \leq \bar{\tau}, \qquad \forall i \in \mathscr{N}, \forall j \in \mathscr{N}^i, \forall k : \beta^{ij}_k = i, \tag{10.51}$$

where $\bar{\tau} > 0$ is known a priori. Suppose that at time $t^{[ij]}_k$ agent i transmits to agent j a message, which contains the following data: $\left\{t^{[ij]}_k, \mathrm{col}\left(\hat{\gamma}^i_l\left(t^{[ij]}_k\right), l \in \mathscr{L}_{ij}\right)\right\}$. Then, the internal estimator $\left[\hat{\gamma}^{ij}_l\right]_{l\in\mathscr{L}_{ij}}$ cannot be immediately updated. This is because we must guarantee that the value of the state estimate $\hat{\gamma}^{ij}_l$ will always remain equal to the corresponding state estimate running in agent j, $\hat{\gamma}^{ji}_l$. To this end, both estimates can only be updated at time $t = t^{[ij]}_k + \bar{\tau}$. Upon receiving $t^{[ij]}_k$, the coordination state estimate $\hat{\gamma}^{[ij]}_l$ running in agent j should be updated at time $t = t^{[ij]}_k + \bar{\tau}$ to

$$\hat{\gamma}^{ij}_l\left(t^{[ij]}_k + \bar{\tau}\right) = \hat{\gamma}^i_l\left(t^{[ij]}_k\right) + \bar{\tau}\, v_r\left(\hat{\gamma}^i_l\left(t^{[ij]}_k\right)\right). \tag{10.52}$$

With the above procedure, we guarantee that the estimators are always synchronized. Notice that in general $\tilde{\gamma}^{ij}_i\left(t^{[ij]}_k + \bar{\tau}\right)$ will not be zero because v_r may not be constant and $\bar{\omega}_i$ and $\tilde{v}_{r_{d_i}}$ may not be zero in the interval $\left[t^{[ij]}_k, t^{[ij]}_k + \bar{\tau}\right)$. The estimation error $\tilde{\gamma}^j_i$ viewed by agent j will be

$$\lim_{t\to t^{[ij]}_k + \bar{\tau}} \tilde{\gamma}^j_i(t) = \epsilon + \int_{t^{[ij]}_k}^{t^{[ij]}_k + \bar{\tau}} \dot{\tilde{\gamma}}^j_i(\sigma)\mathrm{d}\sigma, \tag{10.53}$$

which is bounded assuming that the time delay is bounded, hence, (10.14) holds. Equation (10.53) only holds if $\bar{\tau}$ is sufficiently small and ϵ is selected to be sufficiently small so as to guarantee that the post-reset value of $\tilde{\gamma}_i^j$ satisfies $\left\|\tilde{\gamma}_i^j\right\| < \epsilon$.

We also have to consider the case where, on link ij an agent tries to send a message while the other agent has already sent one message during the $\bar{\tau}$ previous time units. For each link we consider a primary and a secondary agent, as was done before. Considering without loss of generality that i is a primary agent on link ij, then the message sent by agent j is ignored and if $\lim_{t \to t_k^{[ij]}+\bar{\tau}} \left\|\tilde{\gamma}_j^i(t)\right\| \geq \epsilon$ holds, then another message is sent by agent j at time $t_{k+1}^{[ij]} = t_k^{[ij]} + \bar{\tau}$.

The estimation error $\tilde{\gamma}_j^i\left(t_{k+1}^{[ij]} + \bar{\tau}\right)$ is bounded assuming that the time delay is bounded, therefore, (10.14) holds. We can guarantee that this technique is valid if $\bar{\tau}$ is sufficiently small and ϵ is selected to be sufficiently small so as to guarantee that $\tilde{\gamma}_j^i$ satisfies $\left\|\tilde{\gamma}_j^i\left(t_k^{[ij]} + \bar{\tau}\right)\right\| < \epsilon$.

3) *Communication losses:*

To make the communication system robust to limited communication losses we require each agent to send a reply upon receiving a message. The agent which sent the message only updates his estimators $2\bar{\tau}$ time units after the message was sent if the reply was received, otherwise another message is sent.

Consider the case that at time $t_k^{[ij]}$ agent i transmits to agent j a message, which contains the following data: $\left\{t_k^{[ij]}, \mathrm{col}\left(\hat{\gamma}_l^i\left(t_k^{[ij]}\right), l \in \mathscr{L}_{ij}\right)\right\}$. Upon receiving the message and sending a reply, the coordination state estimates $\hat{\gamma}_l^{[ji]}$ running in agent j should be updated at time $t = t_k^{[ij]} + 2\bar{\tau}$ to

$$\hat{\gamma}_l^{ji}\left(t_k^{[ij]} + 2\bar{\tau}\right) = \hat{\gamma}_l^i\left(t_k^{[ij]}\right) + 2\bar{\tau}\, v_r\left(\hat{\gamma}_l^i\left(t_k^{[ij]}\right)\right). \tag{10.54}$$

If the reply was received by agent i then the coordination state estimates $\hat{\gamma}_l^{[ij]}$ running in agent i should be also updated at the same time as $\hat{\gamma}_l^{ij}\left(t_k^{[ij]} + 2\bar{\tau}\right) = \hat{\gamma}_l^{ji}\left(t_k^{[ij]} + 2\bar{\tau}\right)$ otherwise a reply is sent at $t_{k+1}^{[ij]} = t_k^{[ij]} + 2\bar{\tau}$. Note that if agent i did not receive the reply, then there is a brief period when the estimators are desynchronized, that is $\hat{\gamma}_l^{ij} \neq \hat{\gamma}_l^{ji}$, however the equality is replaced after the reply of the next message is received.

We now have to consider the case of conflicting messages. If on link ij an agent tries to send a message while the other agent has already sent one message during the $2\bar{\tau}$ previous time units, we consider, for each link, a primary and a secondary agent. Considering, without loss of generality, that i is a primary agent on link ij, then the message sent by agent j is ignored and, if $\lim_{t \to t_k^{[ij]}+2\bar{\tau}} \left\|\tilde{\gamma}_j^i(t)\right\| \geq \epsilon$ holds, then another message is sent by agent j at time $t_{k+1}^{[ij]} = t_k^{[ij]} + 2\bar{\tau}$.

If we can guarantee that for two consecutive messages sent one reply is received then, if $\bar{\tau}$ is sufficiently small and ϵ is selected to be sufficiently small so as to guarantee that $\tilde{\gamma}_i^j$ satisfies $\left\|\tilde{\gamma}_i^j\left(t_k^{[ij]} + 2\bar{\tau}\right)\right\| < \epsilon$, then the estimation error is bounded, hence, (10.14) holds.

The communication logic for the case with delayed information and communication losses is illustrated in Figure 10.6.

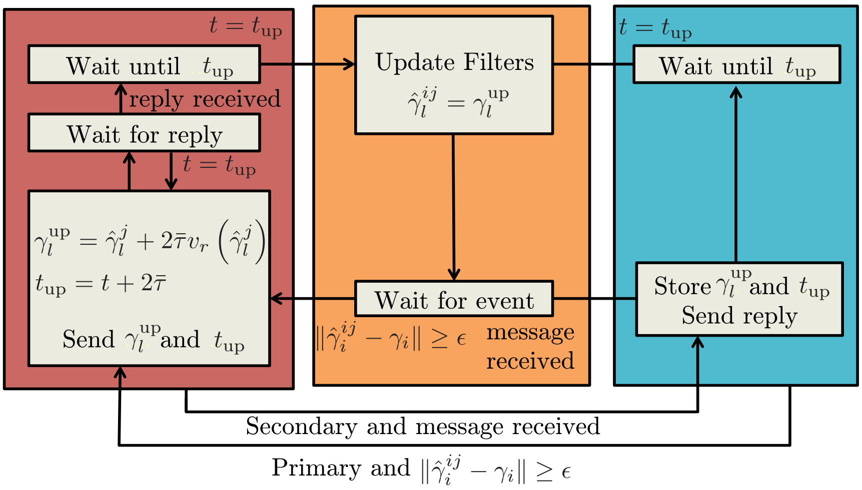

Figure 10.6 – Communication logic diagram.

10.7 Simulation

To assess the performance of the designed CPFCS in simulation, with the alternative design of Section 10.5 and the alternative communication system of Section 10.6 we used a Simulink model of the MEDUSA autonomous marine vehicle with the inner loop controller for heading and speed described in Ribeiro [2011].

We consider a lateral water current observer with the law $\dot{\hat{v}}_c = k_{v_c}\left\{[0\ 1]\, R^T \dot{\boldsymbol{p}} - \hat{v}_c\right\}$.

10.7.1 Test Case

Test set-up

The formation considered consists of three agents, that is $\mathcal{N} = \{1,2,3\}$, where agent 1 communicates with 2, agent 2 communicates with agents 1 and 3, and therefore agent 3 only communicates with agent 2. Agent 2 is a primary agent on both links, 12 and 23. In this case there is no freedom on the selection of α_{ij}. We have in agent 1 $\hat{\gamma}_2^1 := \hat{\gamma}_2^{12}$, $\hat{\gamma}_3^1 := \hat{\gamma}_3^{12}$, in agent 2 $\hat{\gamma}_1^2 := \hat{\gamma}_1^{21}$, $\hat{\gamma}_3^2 := \hat{\gamma}_3^{23}$, and in agent 3 $\hat{\gamma}_1^3 := \hat{\gamma}_1^{32}$, $\hat{\gamma}_2^3 := \hat{\gamma}_2^{32}$. The three vehicles are required to maintain a side-by-side formation with $10m$ between the vehicles. The formation will follow straight trajectories at a speed of $0.5m/s$ with a U-turn upon reaching $x = 160m$. In order to assess the full potential of this control architecture an engine failure of agent 1 is simulated at $t = 500s$ with a recovery at $t = 600s$. In this simulation, a current of $v_c = [-0.05, -0.05\,]^T$ was considered. The network was simulated with delays of 0.1 seconds and 20% of packet losses.

Parameters

Table (10.1) contains the parameter values used in the simulations. Parameters δ, k_x, k_y and k_ω are needed by the path following controller (10.20)-(10.21), k is used by the coordination controller (10.24). The parameter ϵ refers to the CTC.

Parameters	Value
δ	-1.5 (m)
k_k	0.3 (s^{-1})
k_ω	5 (s^{-1})
k	0.1 (s^{-1})
c_ω	0.1 (s^2)
ϵ	0.5

Table 10.1 – Simulation parameters.

10.7.2 Results

The simulated trajectories of the three vehicles can be seen in Figure 10.7 where it is visible that the trajectory is accurately tracked in the conditions of the test.

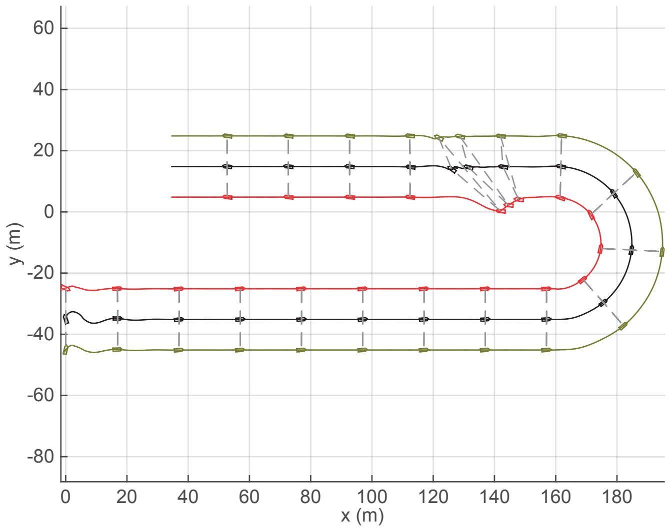

Figure 10.7 – Trajectories of the vehicles.

The communication instants during engine failure can be seen in Figure 10.8. In Figure 10.8 the blue + markers represent sent messages and the red + markers represent replies to received messages. It can be observed that agent 1 communicates heavily with agent 2, agent 2 communicates moderately with agents 1 and 3, and agent 3 receives messages from agent 2 and sends few messages. The reason behind those "frequencies" of communication between vehicles will be explained next.

The estimated coordination states computed by each communication logic block during engine failure are shown in Figures 10.9 to 10.12.

Since the path-following variable kinematics are designed to reduce the path-following errors, that is, to keep the desired position close to the real agent position, γ_1 goes to a stop a few seconds after engine failure. Since the expected path-following variable kinematics of the filters in the communication logic block do not account for the path-following error, the estimation errors of γ_1 become greater than in normal conditions, explaining the heavy need of communication. The path-following variable kinematics of agent 2 imposes a strong deceleration due to the effect of agent 1, therefore there is a slight oscillatory behaviour which degrades the filter performance,

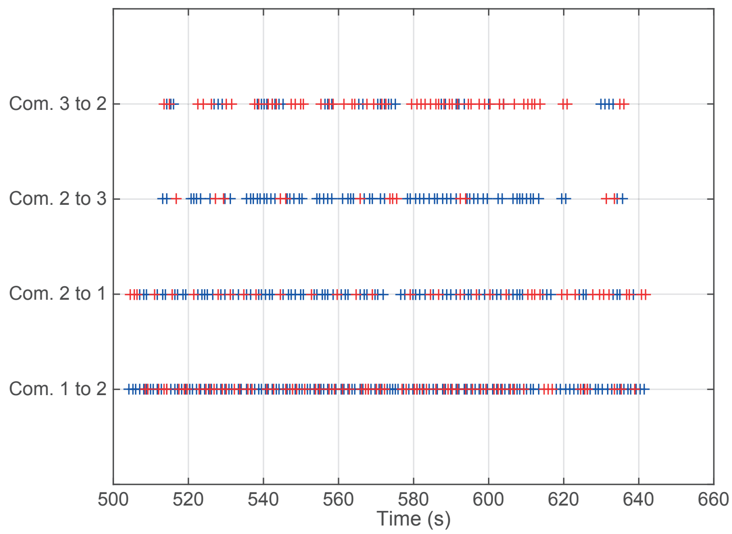

Figure 10.8 – Communication instants.

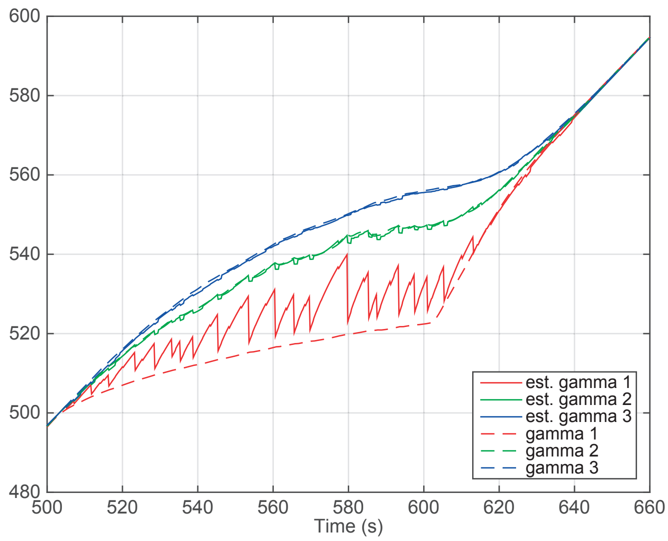

Figure 10.9 – Communication system output on agent 1 synchronized with agent 2.

and therefore there is a small need of communication. Agent 3 is only affected by agent 2 and therefore the decelerations imposed by the path-following variable kinematics are relatively weak, then the path-following has no difficulty in follow $p_d(\gamma)$ and therefore there is little need for updating the filters for γ_3. From Figures 10.7, and 10.9 to 10.12 it can be observed that coordination is achieved while each agent follows its assigned path.

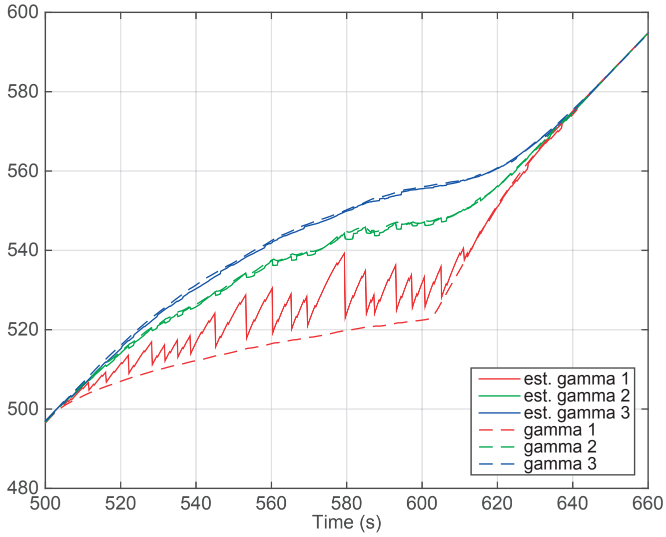

Figure 10.10 – Communication system output on agent 2 synchronized with agent 1.

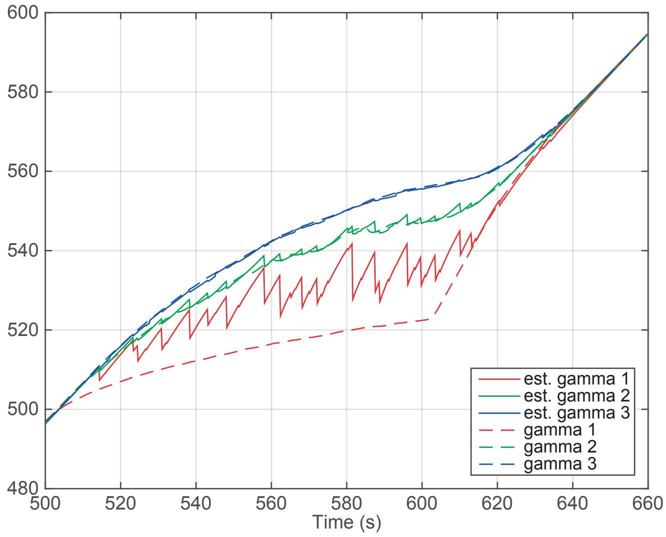

Figure 10.11 – Communication system output on agent 2 synchronized with agent 3.

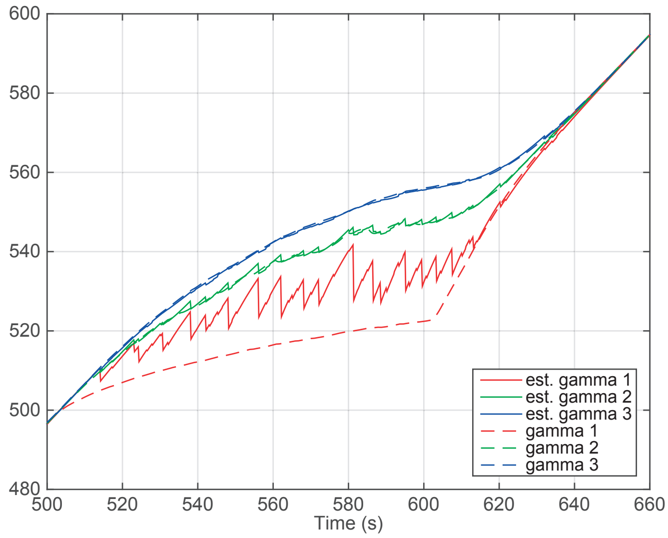

Figure 10.12 – Communication system output on agent 3 synchronized with agent 2.

Quantized Communications Part V

11 Cooperative Path-Following with Quantized Communications

11.1 Motivation and problem description

In this chapter we aim to solve the CPF problem introduced in Chapter 10 while considering bandwidth limitations. The problem of CPF is defined as the problem of given multiple autonomous vehicles and different spatial paths assigned to them, deriving control laws to drive and maintain the vehicles on their paths with desired speed profiles, while holding a specified formation pattern. We have seen in Chapter 10 that a form of solution is a coordination controller which amounts roughly to performing a continuous-time consensus algorithm on the path-following variables, with the dynamics of the vehicles in the loop. To solve the CPF problem while considering bandwidth limitations, in this chapter we apply the quantized consensus algorithm of Section 7.6, and its theoretical guarantees. That is, we consider that each vehicle is a node in a communication network and that each vehicle communicates messages with a finite number of bits with a set of neighbours. Details on the consensus algorithm are given in Subsection 11.2.1. Specifically, in this chapter we consider the problem of cooperative path-following of a network of single integrators driven by process noise, i.e. where the dynamics of each agent are of the form

$$\dot{p} = u + \omega, \tag{11.1}$$

where $p \in \mathbb{R}^m$ is the agent's state $u \in \mathbb{R}^m$ is the agent's input and $\omega \in \mathbb{R}^m$ is the process noise which is bounded by $\|\omega\| \le \epsilon_\omega$.

We now assign to each agent a desired path, a continuously differentiable function $p_d : \mathbb{R} \to \mathbb{R}^m$ and a path-following variable γ that parameterizes the path. The objective is to derive control laws for u and $\ddot{\gamma}$ to steer the state of each agent p to its assigned path $p_d(\gamma)$ and the time derivative of the path-following variable $\dot{\gamma}$ to its assigned value v_r. Since we are considering multiple agents we can make explicit the agent's index on the path-following variable as γ^i, $i \in \mathcal{N}$, and we will omit the agent's index when it is clear from the context that we are referring to a generic agent.

We also want the formation to be coordinated, i.e. we desire that the bound $\|\gamma^i - \gamma^j\|$ for $i \neq j$ converge to zero (or at least to a small value). Defining, $\Gamma := \mathrm{col}\left(\gamma^i, i \in \mathcal{N}\right)$ the above is the same as the convergence of $\left\|\left(I_N - \frac{1}{N}\mathbf{1}\mathbf{1}^T\right)\Gamma\right\|$ to zero (or a small value). In order to enforce consensus we introduce a desired velocity $v_d(t)$ which is a perturbation of v_r where $\|v_d(t) - v_r\|$ is bounded for a bounded deviation from average of the path-following variables $\left\|\left(I_N - \frac{1}{N}\mathbf{1}\mathbf{1}^T\right)\Gamma\right\|$. Therefore we want to drive $\dot{\gamma}$ to $v_d(t)$ and we design $v_d(t)$ to achieve consensus.

In summary, defining the path-following error as $\xi := p - p_d(\gamma)$ and the velocity error as $\eta := \dot{\gamma} - v_d$, the objective of the path-following controller is then to make the agent's error vector defined as $z := [\xi^T \; \eta]^T$ converge to a small neighbourhood of zero. The objective of the consensus algorithm is to ultimately bound the consensus error $\left\| \left(I_N - \frac{1}{N}\mathbf{1}\mathbf{1}^T\right)\Gamma \right\|$. Moreover we also want the deviation from the reference velocity $\|v_d(t) - v_r\|$ to be ultimately bounded.

11.2 Algorithm description

The coordinated path following algorithm considered in this chapter is depicted in Figure 11.1. It is composed of the following three components:

- A *consensus law* which provides the desired path-following variable at the next communication time,
- A *desired velocity generator* which provides the reference velocity to the path-following controller,
- A *path-following control law* which provides the control input u and the second derivative of the path-following variable $\ddot{\gamma}$.

We will now describe each main component in detail.

11.2.1 Consensus

In this application we consider that the agents communicate at discrete instants of time $t_k := k\Delta t$ where $k \in \mathbb{N}$ and Δt is the time between communications. To achieve coordination we set a desired path-following variable at each communication instant according to the quantized consensus algorithm

$$\gamma^{d,i}_{k+1} = \sum_{j \in \mathcal{N}^i} \pi^{i,j} Q^j_k\left(\gamma^j(t_k)\right) - \left(Q^i_k\left(\gamma^i(t_k)\right) - \gamma^i(t_k)\right) + v_r \Delta t, \tag{11.2}$$

where the mid-value of the quantizer $Q^i_{k+1}(\cdot)$ is set as $\bar{\gamma}^{d,i}_{k+1} = Q^i_k\left(\gamma^i(t_k)\right) + v_r\Delta t$ and its interval length is set as $\Lambda_k = r_1\alpha^k + r_2$, for an appropriate decrease rate α and parameters r_1 and r_2 selected under the conditions of Theorem 8. Therefore we want that the values of path-following variables evolve according to $\gamma^i_{k+1} = \gamma^{d,i}_{k+1} + w^i_k$ where the disturbance w^i_k satisfies assumption A4. It can be observed that the introduction of the reference velocity on the algorithm does not change the properties of the algorithm and Theorem 8 still applies.

11.2.2 Desired velocity

Given the desired path following variable at time t_{k+1} we can define the desired velocity for the time segment $t_k < t \le t_{k+1}$ as

$$v_d(t) = \begin{cases} v_r + 2v^c_k \frac{t - t_k}{\Delta t}, & t_k \le t \le t_k + \frac{\Delta_t}{2} \\ v_r + 2v^c_k \frac{t_{k+1} - t}{\Delta t}, & t_k + \frac{\Delta_t}{2} \le t \le t_{k+1} \end{cases}, \tag{11.3}$$

where the impulse perturbation velocity v^c_k is defined as

$$v^c_k := 2\left(\frac{\gamma^d_{k+1} - \gamma(t_k)}{\Delta t} - v_r\right). \tag{11.4}$$

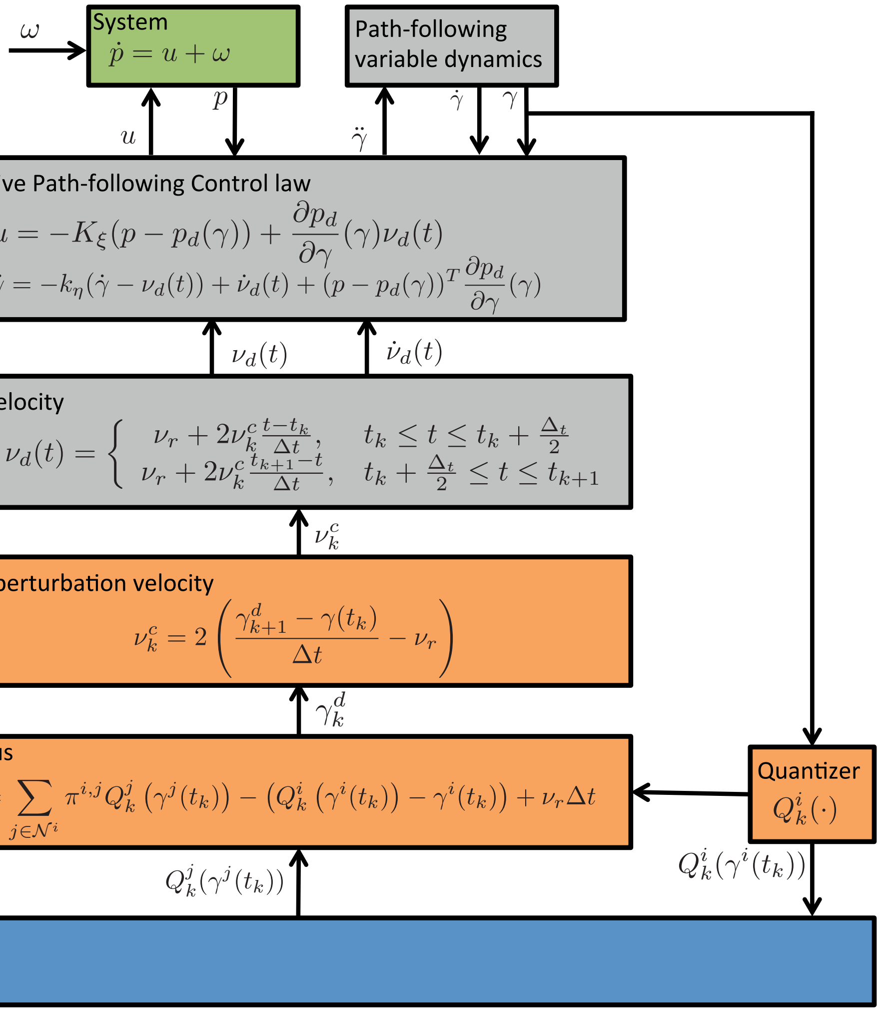

Figure 11.1 – Diagram of the coordinated path-following algorithm. Blocks in gray correspond to continuous-time systems and blocks in orange correspond to discrete-time systems.

Given this desired velocity, recalling that $\eta := \dot{\gamma} - \nu_d$, we can observe that the values of the path-following variable at the communication instants evolve as follows

$$\begin{aligned}\gamma(t_{k+1}) &= \gamma(t_k) + \int_{t_k}^{t_{k+1}} \dot{\gamma}\, dt = \gamma(t_k) + \int_{t_k}^{t_{k+1}} \nu_d(t)\, dt + \int_{t_k}^{t_{k+1}} \eta(t)\, dt \\ &= \gamma_{k+1}^d + \int_{t_k}^{t_{k+1}} \eta(t)\, dt.\end{aligned}$$

Therefore the values of the path-following variable at the communication instants evolve according to $\gamma(t_{k+1}) = \gamma_{k+1}^d + w_k$ where w_k is $w_k := \int_{t_k}^{t_{k+1}} \eta(t)\, dt$.

11.2.3 Path-following controller

We now consider a path-following scheme as described in Vanni et al. [2008] for the case of single integrators. The path-following control law is the following

$$\ddot{\gamma} = -k_\eta \eta + \dot{\nu}_d + \xi^T \frac{\partial p_d}{\partial \gamma}, \tag{11.5}$$

$$u = -K_\xi \xi + \frac{\partial p_d}{\partial \gamma} v_d, \tag{11.6}$$

where $K_\xi := I_m k_\xi$ with $k_\xi > 0$ and $k_\eta > 0$. Since this is a path-following control law, there exist a feedback from the path following error $p - p_d(\gamma)$ to the the dynamics of the path-following variable γ. Compared to trajectory tracking where the path is parameterized by time, as in $p_d(t)$, this method provides a faster convergence of the vehicles to their assigned paths, since the path-following variable dynamics drives $p_d(\gamma)$ closer to the agent's position p. It should be noted that the derivative of the desired velocity $\dot{v}_d$ is not defined at all points. To overcome this problem we must replace $\dot{v}_d$ on the control law for $\ddot{\gamma}$ with some signal which is defined everywhere and is equal to $\dot{v}_d$ where it is defined.

11.3 Design and theoretical guarantees

The path-following control law drives the agent's error vector z to an ultimate bound proportional to ϵ_ω as stated by the following theorem.

Theorem 20. Given the system (11.1), where the process noise is bounded by $\|\omega\| \le \epsilon_\omega$, and the path-following control law (11.5), the norm of the agent's error vector $\|z(t)\|$ satisfies, for all θ such that $0 < \theta < 1$,

$$\|z(t)\| \le \|z(0)\| e^{-(1-\theta)k_m t} + \frac{\epsilon_\omega}{\theta k_m}, \tag{11.7}$$

where $k_m := \min\left(k_\xi, k_\eta\right)$.

From Theorem 20, we can bound $\|w_k\|$ as follows

$$\begin{aligned} \|w_k\| &\le \int_{t_k}^{t_{k+1}} \|\eta(t)\| dt \le \int_{t_k}^{t_{k+1}} \|z(0)\| e^{-(1-\theta)k_m t} + \frac{\epsilon_\omega}{\theta k_m} dt \\ &= \frac{\|z(0)\|}{(1-\theta)k_m}\left(1 - e^{-(1-\theta)k_m \Delta t}\right) e^{-(1-\theta)k_m \Delta t k} + \frac{\epsilon_\omega \Delta t}{\theta k_m}. \end{aligned}$$

The proof is given in Appendix E.1. With this bound we can observe that Assumption A4 is satisfied with $\delta_v := \frac{\epsilon_\omega \Delta t}{\theta k_m}$, $\epsilon_v := \max_{i\in\mathcal{N}} \frac{\|z^i(0)\|}{(1-\theta)k_m}\left(1 - e^{-(1-\theta)k_m\Delta t}\right)$ and $k_v := e^{-(1-\theta)k_m\Delta t}$. Therefore we can apply Theorem 8 to derive lower bound conditions for the number of bits n_b and the quantizer parameters α, r_1 and r_2. Since we can apply Theorem 8 we can also establish ultimate bounds on the consensus error $\left\|\left(I_N - \frac{1}{N}\mathbf{1}\mathbf{1}^T\right)\Gamma\right\|$ using continuity arguments. Moreover, since the consensus error is ultimately bounded we can also establish ultimate bounds on the impulse perturbation velocity v_k^c and therefore ultimately bound the deviation to the reference velocity $\|v_d(t) - v_r\|$.

11.4 Simulation Results

As an example we consider a fleet of six two dimensional vehicles with single integrator dynamics performing a lawnmower mission. The desired shape of the fleet is composed by equilateral triangles and the agents communicate each second with their immediate neighbours only. We consider a coordinated path-following controller with gains $k_\xi = 0.08$ and $k_\eta = 2$, and the process noise is bounded with $\epsilon_\omega = 0.2$. This selection of gains yields a fast convergence of the path-following errors and a slow convergence of the coordination errors. The slow convergence of CC allows for a lower number of transmitted bits.

The parameters ϵ_v, k_v and δ_v, from Assumption A4 were adjusted manually to provide a tight bound on the process noise $\|v_k^i\|$. It was found that the conditions of Theorem 9 are satisfied if six bits are transmitted each second, and in this example, to obtain a reasonably small initial quantization interval, we used eight bits per second.

The trajectories of the agents are represented in the Figure 11.2, where it can be observed that the positions of the agents converge to the desired paths. We can also observe that, as expected, the formation acquires the desired shape, since the path-following variables approach consensus.

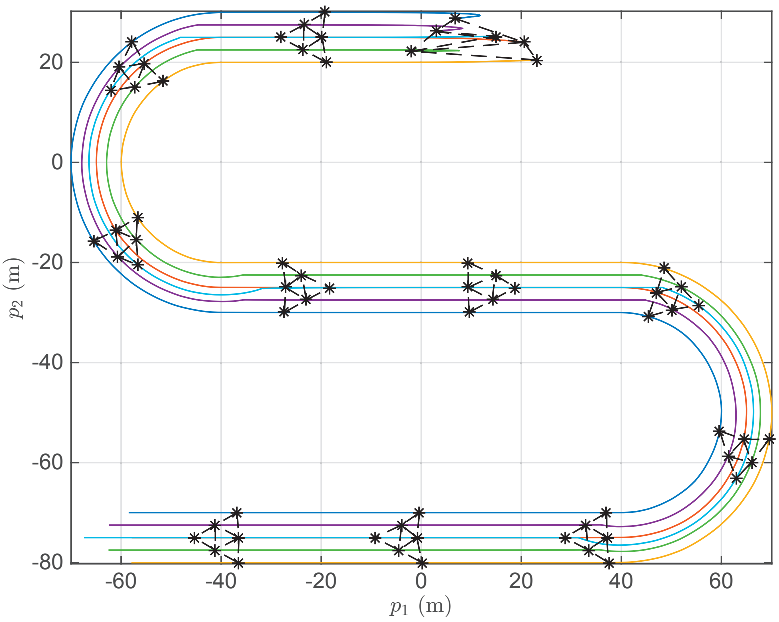

Figure 11.2 – Trajectories of the vehicles. The black markers represent the agents position every 75 seconds and the black dashed lines represent communication links.

The quantization level transmitted by each agent, $Q_k^i\left(\gamma^i(t_k)\right)(2^{n_b}-2)/\Lambda_k$, is shown in Figure 11.3. It can be observed that, for this case, the theoretical guarantees are quite conservative and we could use a much lower number of transmitted bits, since only 16 of the 255 quantization levels were used.

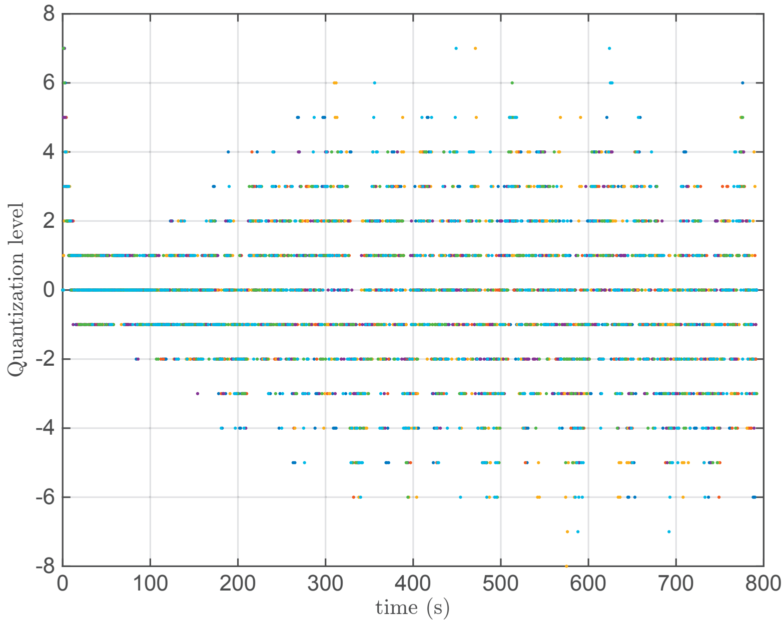

Figure 11.3 – Quantization levels.

The evolution of the difference of the path-following variables to their average, i.e. of $\gamma^i - (1/N)\sum_{j\in\mathcal{N}}\gamma^j$, can be observed in Figure 11.4, the derivative of the path-following variables $\dot{\gamma}^i$, is shown in Figure 11.5, and we can observe the norms of the path-following error $\|p^i - p_d^i(\gamma^i)\|$ in Figure 11.6.

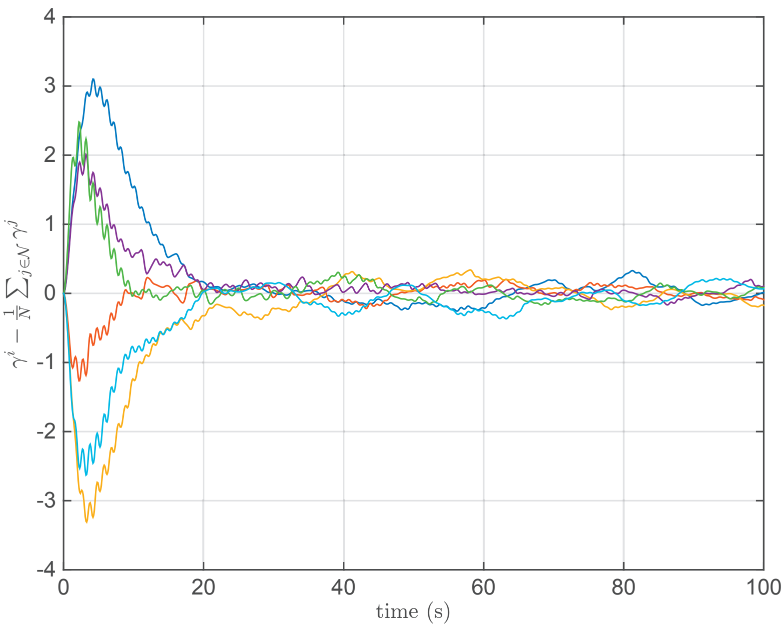

Figure 11.4 – Evolution of the difference of the path-following variables to their average $\gamma^i - (1/N)\sum_{j\in\mathcal{N}}\gamma^j$.

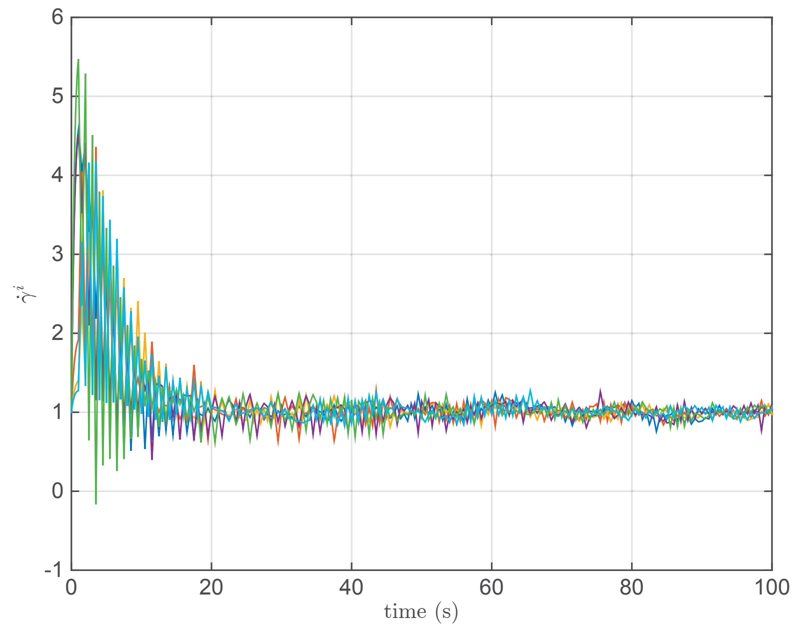

Figure 11.5 – Time derivative of path-following variables $\dot{\gamma}^i$.

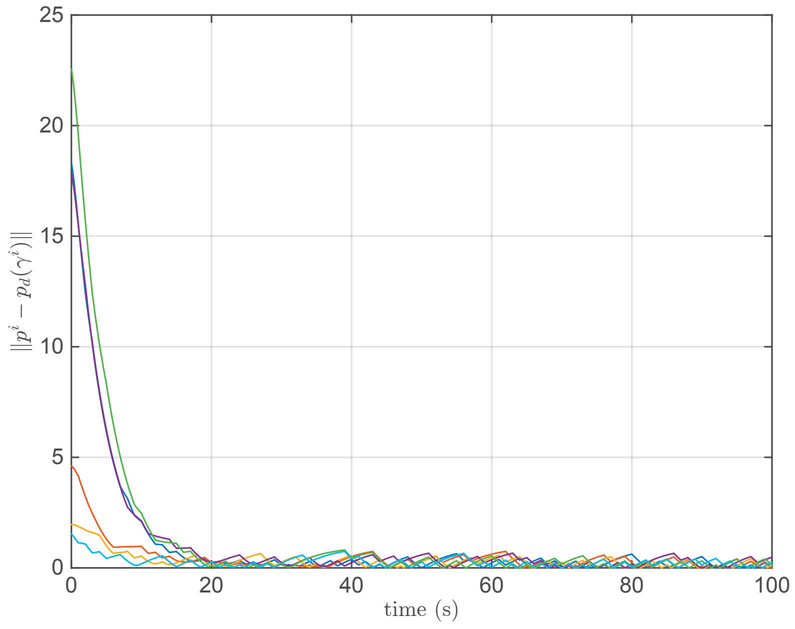

Figure 11.6 – Evolution of the norm of the path-following error $\|p^i - p_d^i(\gamma^i)\|$.

From Figures 11.4, 11.5 and 11.6 we can observe that all the quantities that we wanted to regulate, i.e. the deviation of the path-following variables from the average, the deviation of the time derivative of path-following variables to the reference velocity (one in this case), and the norm of the path-following error, decrease from their initial values until they reach an ultimate bound and remain within that bound, as was expected from the theoretical analysis.

The lower bound on the number of bits required for stability is a conservative over-approximation as indicated by Figure 11.3. In fact, it was observed in simulations that $n_b = 2$ also yields a stable system albeit with degraded performance. Figure 11.7 shows the evolution of the norm of the difference to average of the path-following variables, i.e. of $\|\mathrm{col}(\gamma^i - (1/N)\sum_{j\in\mathcal{N}}\gamma^j)\|$, averaged among 5 different simulation runs, for different number of transmitted bits between 2 and 9, with the same parameters of the previous simulations. We can observe from

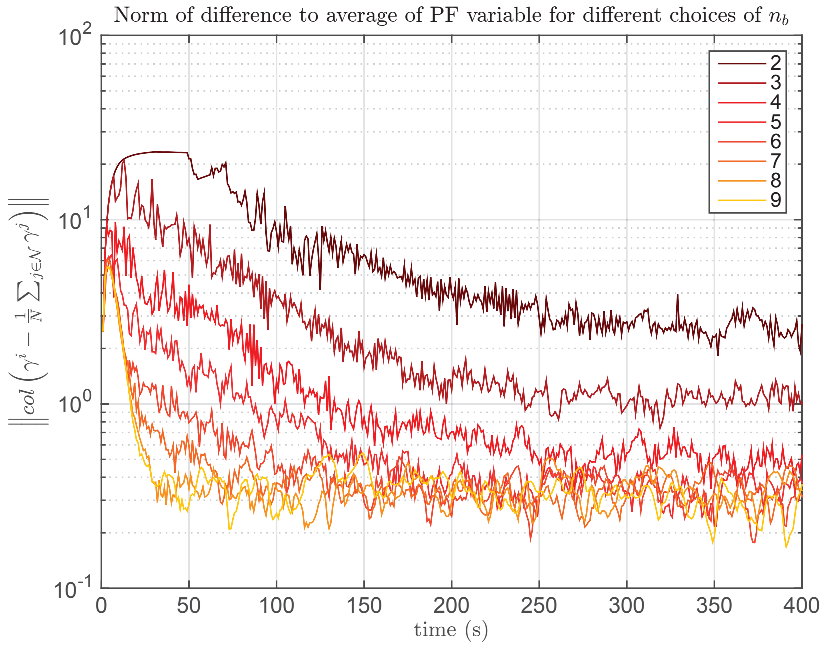

Figure 11.7 – Effect of number of bits on coordination error.

Figure 11.7 that with 5 transmitted bits we obtain approximately the same asymptotic performance as with 8 bits with a smaller convergence rate. It was observed that above 8 bits there is no significant difference in terms of asymptotic performance or convergence rate.

12 Quantized Distributed Estimation

12.1 Introduction

The topic of distributed estimation has been the subject of intensive research, as the literature survey in Li et al. [2015b] shows. Representative examples include the work on distributed estimation in Olfati-Saber [2005], Battistelli and Chisci [2014] and Park and Martins [2016], where the authors proposed distributed state estimators, and proved their stability.

Guaranteeing that a decentralized estimator (observer) satisfies an ISS property in the presence of bandwidth limitations, that is, when only a limited amount of data are exchanged among multiple distributed systems or agents per unit of time, is still an open topic of research. This issue is of paramount importance in practical applications, since lower bandwidth translates into lower energy consumption and, consequently, into increased operational autonomy. Stringent bandwidth limitations occur naturally in the case of underwater applications, due to the nature of the communications medium. These constraints must therefore be taken explicitly into account in the design of distributed estimators and controllers for networked marine vehicles Bahr et al. [2009], Soares et al. [2013], Rego et al. [2014]. In general, to address explicitly bandwidth limitations, it may be expedient to consider that the messages exchanged among agents in a network are quantized, i.e. are encoded with a finite number of bits.

One of the most common distributed algorithms is consensus, where all the network nodes agree on a single value, usually the average of values initially contained in the nodes. Consensus is often used as a mean to apply certain algorithms, designed originally for a single computer, in a distributed setting, as for example the case of Kalman filtering Battistelli et al. [2015]. The problem of distributed averaging with quantized exchanged data has been addressed in many works, see for example Aysal et al. [2008], Frasca et al. [2009], Nedić et al. [2009], Carli et al. [2010] and the references therein. Recently, results have come to the fore that guarantee convergence to the initial average, and not convergence of the expected value, using progressive quantization Li et al. [2011], Thanou et al. [2012, 2013], Pu et al. [2015]. These results motivate the application of consensus with progressive quantization to the problem of distributed estimation in order to guarantee convergence of the estimation error in the absence of disturbances.

One of the main motivations for state estimation is to stabilize or enhance the performance of systems through state feedback when the state is not available directly but can be estimated using a dynamic observer. However, in Chapters 8 and 9 the problem of distributed state estimation of systems was addressed without considering state feedback. In the context of distributed estimation, when the state estimates are used for state feedback, it is not possible to compute precisely the effects of the control input in the dynamics. This is due to the fact that the nodes may have different state estimates and therefore the control action applied by each node is not available to the other nodes. Thus, the separation principle, that states that the design of the controller has no impact on the estimation error dynamics, does not apply in this context, making the design of distributed state estimators more challenging.

Motivated by the above considerations, in this chapter we address the problem of distributed state estimation for linear systems with linear state feedback subjected to process and measurement noise, under the constraints of quantized and rate-limited network data transmission. We propose a linear distributed consensus-based Luenberger observer, where the consensus algorithm is implemented with progressive quantization as in Thanou et al. [2013], and derive a set of conditions on the design parameters of the quantizer that guarantee ultimate boundedness of the estimation error. The latter is shown to depend on the $\mathscr{L}_\infty$ norm of the noise signals and the number of bits transmitted. We further show that the maximum possible estimation convergence rate depends on the number of iterations of the consensus algorithm and can be made arbitrarily close to that obtained with a centralized estimator by increasing the number of iterations. Moreover, the proposed method requires global, and not local observability, i.e. the system state can be reconstructed if information from all the sensors is available but may not be reconstructed with just any individual sensor. A numerical example illustrates the performance of the proposed algorithm.

The design of the estimation algorithm that we propose is straightforward in that the parameters of the algorithm must only satisfy a certain number of inequality conditions. However, the initial design of the algorithm must be done centrally, using global information. This is because some of the design parameters are necessarily the same for all nodes in a network (e.g. the quantization interval parameters and the number of transmitted bits) and the design of parameters satisfying the stability conditions require information about the global communication graph as well as the models of the observed system and of every sensor. The key contributions of the chapter are threefold:

- We propose a distributed linear state estimation algorithm for linear state feedback systems that takes into account limited data-rate communications among agents.
- We provide conditions on the design parameters of the algorithm to guarantee ultimate boundedness of the estimation error.
- Given that the above mentioned conditions are satisfied, we derive explicit bounds on the estimation error norm and on the norm of the state of the system.

12.2 Literature Survey

In what follows we review briefly the contributions of some papers that are relevant to our work.

In J.-J. Xiao et al. [2006], Sun et al. [2007], Li and Fang [2007] and Msechu et al. [2008] the distributed estimation setup considered is one where multiple sensors take quantized measurements of a system, and send their measurements, to a fusion center, i.e. a computer running a centralized estimation algorithm. The papers by J.-J. Xiao et al. [2006] and Li and Fang [2007] address the problem of parameter estimation, i.e. the problem of estimating a time-invariant parameter given multiple noisy measurements. The work in J.-J. Xiao et al. [2006] addresses the problem of minimizing the transmission power consumption while ensuring a given performance for the state estimation algorithms. In Li and Fang [2007], a decentralized estimation method is proposed that makes use of adaptive quantization, and where only one bit of information is exchanged at each epoch. In contrast with the two previously mentioned works, Sun et al. [2007] and Msechu et al. [2008] deal with the general problem of distributed state estimation, i.e. the problem of estimating the state of a discrete-time dynamic system given measurements from multiple sensors. The paper by Sun et al. [2007] proposes a decentralized Kalman filter that takes into consideration the trade-off between number of quantization levels of the sent data and the state estimation performance. Finally, Msechu et al. [2008] proposes a method of scheduling optimally which measurement is sent to the fusion center at each time. It should be noted that the methods proposed in J.-J. Xiao et al. [2006], Sun et al. [2007], Li and Fang [2007] and Msechu et al. [2008] are different from the setup we consider in this thesis in that they require that all agents can communicate with a fusion center, and therefore it is only applicable for very specific topologies of the communication network.

The work in Li et al. [2015a] proposes a distributed Kalman filter with quantized communications between agents, which is gossip based, i.e. uses a gossip algorithm instead of a consensus algorithm for information fusion. In the gossip algorithm, for each node a neighbour is selected at random and the state of the observer, estimated state and covariance, is swapped with that neighbour. The above paper also proves weak convergence (in distribution) of the proposed observers. Since the method considered is gossip-based, it is considerably slower than consensus based algorithms in certain cases, e.g. when the number of neighbours of each agents is considerably larger than one, and therefore it may not be suitable for the set-up considered in this chapter.

To the best of our knowledge, there are no publications that propose consensus-based algorithms to solve the general problem of distributed state estimation considered in this chapter, while taking into account bandwidth limitations. Also, it is important to stress that the papers mentioned above address stochastic convergence of the estimation error, and not deterministic convergence as we aim to guarantee in this chapter. Moreover, since the guarantees are not deterministic, they do not provide methods to compute ultimate bounds of the estimation error, or upper bounds on the convergence rates. To the best of our knowledge, there are also no publications on the design of distributed observers that guarantee input to state stability with respect to measurement and process noise, with quantized communications among agents, i.e. taking into account bandwidth limitations, which is the aim of this chapter. As a contribution to overcome these limitations, we borrow the theory of quantized consensus, which we will review in the next section, to provide input to state stability guarantees for a consensus-based distributed state estimation algorithm.

12.3 Problem Statement

This section formulates the problem that is at the core of the chapter. We first introduce the setup that originates the problem we aim to solve, and the necessary assumptions, in Section 12.3.1. In Section 12.3.2 we describe formally the main problem of this chapter.

12.3.1 Networked System

We consider a very general setup consisting of: I) a discrete-time dynamical system; II) a set of nodes $\mathcal{N}$ endowed with local sensing and actuation capabilities, with cardinality $N = |\mathcal{N}|$. At each node $i \in \mathcal{N}$ and instant t, a sensor measures an output y_t^i of the system and an actuator acts upon the system through a local control input u_t^i; III) a communication network between nodes $(\mathcal{N}, \mathcal{A})$, where $\mathcal{A} \subseteq \mathcal{N} \times \mathcal{N}$ is the set of node pairs describing the directed connections between these nodes, i.e. node i can communicate with node j if and only if $(i, j) \in \mathcal{A}$. This setup is shown in Figure 12.1.

We assume that the discrete-time dynamical system is given by

$$x_{t+1} = Ax_t + \sum_{i \in \mathcal{N}} B^i u_t^i + w_t \tag{12.1}$$

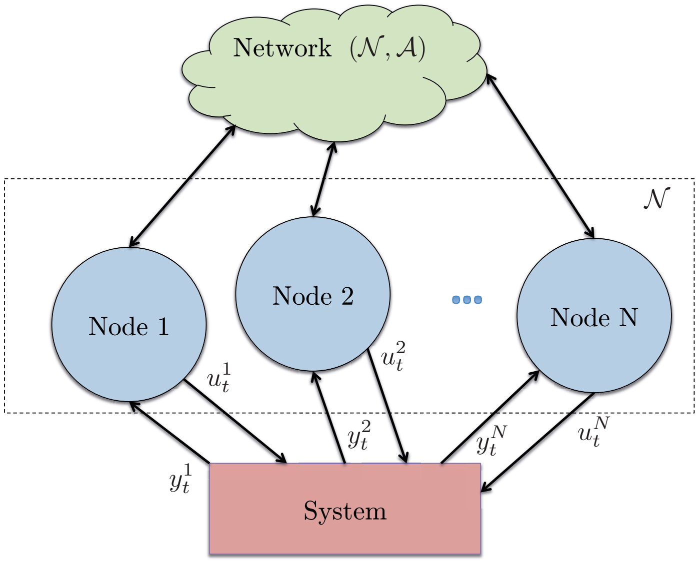

Figure 12.1 – Problem setup consisting of a discrete-time linear dynamical system, sensor and control nodes that take measurements from the system and act upon it, and a communication network that allows the nodes to communicate among themselves.

where $x_t \in \mathbb{R}^n$, $u_t^i \in \mathbb{R}^{l_i}$ and $w_t \in \mathbb{R}^n$ denote the complete state vector, the local control inputs, and the state noise vector, respectively, at time t, $A \in \mathbb{R}^{n \times n}$ is the dynamics matrix and B^i are local input matrices of appropriate dimensions.

The measurement equation associated with the generic node $i \in \mathcal{N}$ is defined as

$$y_t^i = C^i x_t + v_t^i, \tag{12.2}$$

where $y_t^i \in \mathbb{R}^{m_i}$ and $v_t^i \in \mathbb{R}^{m_i}$ denote the observation vector and the observation noise vector, respectively, considered at time t, and C^i is a matrix of appropriate dimensions.

The following assumptions are made on the detectability and stabilizability of the system and the intensity of the disturbances.

Assumption A14. The system (12.1)-(12.2) is collectively detectable, i.e. the pair (A, C) is detectable where $C := \mathrm{col}(C^i)$.

Assumption A15. The system (12.1) is collectively stabilizable, i.e. the pair (A, B) is stabilizable where $B := \mathrm{row}(B^i)$.

Assumption A16. The $\mathcal{L}_\infty$ norm of the disturbance signals satisfy

$$\|w_t\|_\infty \le \epsilon_w, \qquad \|v_t^i\|_\infty \le \epsilon_{v^i}, \; i \in \mathcal{N},$$

for some constants $\epsilon_w > 0$ and $\epsilon_{v^i} > 0$.

Note that we only assume global detectability but not necessarily local detectability of the system, i.e. we do not require that the pair (A, C^i) be detectable for any $i \in \mathcal{N}$. Concerning Assumption A16, different norm bounds can also be considered, such as quadratic norms, as will be seen later in the chapter.

12.3.2 Problem Statement

Given the system and the network described in Subsection 12.3.1, the main problem solved in this chapter is described next.

Assume, in (12.1)-(12.2), that the disturbances w_t and v_t^i are uniformly bounded over time and consider that at each time t the nodes are allowed to communicate quantized messages with a fixed number of bits n_b, according to the network structure defined by $(\mathcal{N}, \mathcal{A})$, for a finite number of times l_f between every two discrete instants of time t and $t+1$. The problem of *distributed state estimation and control with quantized communications* consists of reconstructing at each node the state of the global system (12.1) and simultaneously driving the state of the system to the origin, with the estimation error and the state converging to an ultimate bound proportional to the magnitude of the disturbances.

Stated mathematically, the objective is to compute at each node $i \in \mathcal{N}$ and at each discrete time t a state estimate $\hat{x}_t^i$ and a control input u_t^i such that, for every initial condition, there exists a time T such that for $t \geq T$, $\|\hat{x}_t^i - x_t\| \leq b_1$ and $\|x_t\| \leq b_2$, with b_1 and b_2 proportional to $\epsilon_{v^j}, j \in \mathcal{N}$ and ϵ_w defined in Assumption A16.

12.4 Proposed Estimation and Control System

This section describes the main concepts required for the solution of the problem formulated in 12.3 and outlines the control system proposed in this chapter. We refer to the general set-up introduced before, see Fig. 12.1.

12.4.1 Linear State Feedback

One of the objectives of this chapter is to provide a stabilizing control algorithm for system (12.1), i.e. we wish to stear the state x_t of the system to a small neighbourhood of the origin. For this purpose, we now define the linear control law adopted. Suppose that each node can measure the complete state x_t perfectly (this assumption will be lifted later). Then, local gain matrices $K^i \in \mathbb{R}^{l_i \times n}$ can be defined such that with the global gain matrix $K := \text{row}(K^i)$ we have $\rho(A+BK) < 1$. This is possible because the system is collectively stabilizable and we can set the ith local control input as $u_t^i := K^i x_t$. In this case, the dynamics of the closed loop system are described by

$$x_{t+1} = (A+BK)\, x_t + w_t.$$

Since $\rho(A+BK) < 1$ and since the process disturbance w_t is bounded, it follows that the state x_t is ultimately bounded.

Because in the set-up adopted in this chapter the nodes do not have access to the full state, an observer is required, as described next.

12.4.2 Luenberger Observer

A central concept in this chapter is that of state estimation using a Luenberger observer. We start by considering the case of an hypothetical centralized observer that has access to all of the outputs, that is, to the vector $y_t := \text{col}(y_t^i)$, and the objective is to estimate the state of the system x_t with a bounded error. Let L be a gain matrix of appropriate dimensions such that $\rho(A-LC) < 1$, which can always be found since (A, C) is detectable. Further let $\hat{x}_t \in \mathbb{R}^n$ denote a state estimate of x_t. Under the assumption of a linear state feedback law $u_t^i := K^i \hat{x}_t, i \in \mathcal{N}$, the centralized Luenberger observer algorithm is described by

$$\hat{x}_{t+1} = (A+BK)\hat{x}_t + L\big(y_t - C\hat{x}_t\big),$$

with $K := \mathrm{col}(K^i)$.

It follows easily from the above that the estimation error $e_t := \hat{x}_t - x_t$ satisfies the dynamics

$$e_{t+1} = (A - LC)\, e_t + w_t + L\mathrm{col}(v_t^i).$$

Since $\rho(A - LC) < 1$, and since the measurement and process disturbances v_t^i and w_t are bounded, it follows that the estimation error e_t is ultimately bounded.

The convergence of the estimation error e_t will be expressed quantitatively in the remainder of this chapter through a P_1-norm, $\|e_t\|_{P_1}$, such that $\tilde{\beta} := \|A - LC\|_{P_1} < 1$, which is in general different than the $\mathscr{L}_2$ norm, i.e. $P_1 \neq I_n$[1]. This norm can be found applying directly Property P2 of the P-norm defined before.

The above centralized version of the Luenberger observer can be formally re-written in distributed form as follows. Consider $L^i \in \mathbb{R}^{n \times m_i}$ such that $L := \frac{1}{N}\mathrm{row}(L^i)$. Assuming that all nodes have identical state estimates at time $t-1$, given by $\hat{x}_{t-1}$, the estimates $\hat{x}_t$ provided by the Luenberger observer can be reformulated as the average $\hat{x}_t := \frac{1}{N}\sum_{i \in \mathscr{N}} z_t^i$ of the local variables z_t^i defined by

$$z_t^i := (A + BK)\hat{x}_{t-1} + L^i\left(y_{t-1}^i - C^i\hat{x}_{t-1}\right). \tag{12.3}$$

Due to the limited bandwidth and the topology of the communication network, it is in general not possible to compute the average $\frac{1}{N}\sum_{i \in \mathscr{N}} z_t^i$ perfectly at every node, and one must compute an approximation of that average, which may be different at each node. One possible method of computing an approximation of the average is the consensus algorithm given in the following subsection. This method also guarantees that the estimates remain approximately equal in all agents, which is an assumption of (12.3).

We will discuss the technical details of the distributed Luenberger observer in Subsection 12.4.3.

12.4.3 Distributed Luenberger Observer

In order that all nodes collect in a useful manner information from the measurements of all the nodes at every discrete-time instant, we follow the reasoning in the last part of subsection 12.4.2, where each node computes the average value $\frac{1}{N}\sum_{j \in \mathscr{N}} z_t^j$, with z_t^i defined in 12.3. With the purpose of computing the average, and to ensure that the state estimates contained in all the nodes remain close to each other as required in 12.3 where it is assumed that the estimates are the same in all nodes, we consider the application of the consensus algorithm (7.3) to the problem of distributed state estimation. However, in general, due to bandwidth limitations, it is only possible to perform a finite number of iterations, denoted here as l_f, of the consensus algorithm (7.3), between two consecutive discrete-time iterations. Since it is only possible to perform between two consecutive discrete-time instants a finite number of consensus iterations, each agent keeps an internal value $\hat{x}_t^i$, which may be different from node to node. Therefore, one wants an approximation of the average of the following local variables

$$z_{t,0}^i := (A + BK)\hat{x}_{t-1}^i + L^i\left(y_{t-1}^i - C^i\hat{x}_{t-1}^i\right), \tag{12.4}$$

i.e. one wants to compute an approximation of $\frac{1}{N}\sum_{j \in \mathscr{N}} z_{t,0}^j$. This approximation is computed with l_f iterations of the consensus algorithm (7.3), which in the present case takes the following form:

$$z_{t,l+1}^i = \sum_{j \in \mathscr{N}} \pi^{i,j} z_{t,l}^j, \tag{12.5}$$

[1]However, if (A, C) is observable then it is possible to compute an observer gain matrix L such that $\tilde{\beta} < 1$ with $P_1 = I_n$, i.e. $\|A - LC\| = \tilde{\beta} < 1$, through eigenvalue assignment. This is achieved by assigning n different real eigenvalues to $A - LC$ with $\tilde{\beta} < 1$ as its greatest eigenvalue in absolute value.

Finally, the state estimate is computed as $\hat{x}_t^i := z_{t,l_f}^i$.

Since at each node we have an independent estimate of the state $\hat{x}_t^i, i \in \mathcal{N}$ we apply at each node a control input $u_t^i = K^i \hat{x}_t^i$, which is not available at the other nodes $j \neq i$.

Defining the estimation error of node i as $e_t^i := \hat{x}_t^i - x_t$, the consensus error as $q_t^i := \hat{x}_t^i - \frac{1}{N}\sum_{j\in\mathcal{N}} z_{t,0}^j$, and the average error as $e_t^{avg} := \frac{1}{N}\sum_{j\in\mathcal{N}} \hat{x}_t^j - x_t$, one can observe that the estimation error satisfies the dynamics

$$e_{t+1}^i = (A - LC)\, e_t^{avg} + q_t^i + w_t + L\,\mathrm{col}(v_t^i) + \sum_{j\in\mathcal{N}} B^j K^j (e_t^i - e_t^j).$$

One can observe that if the consensus algorithm approaches perfect averaging, i.e. if $\hat{x}_t^i \approx \frac{1}{N}\sum_{j\in\mathcal{N}} z_{t,0}^j$, either because of a large number of performed iterations l_f or because the network is highly connected, the estimation error dynamics coincides with the hypothetical centralized Luenberger case, since for all $i \in \mathcal{N}$ we obtain $e_t^i \approx e_t^{avg}$ and $q_t^i \approx 0$. Therefore, the performance of the consensus algorithm must be taken into account in the analysis of the estimation error dynamics.

One can also observe that the control feedback gain K^i appears in the estimation error dynamics, which is not the case in a standard Luenberger observer. Therefore, it is important to also take into account the control law when designing the distributed observer, as is done in this chapter.

12.4.4 Estimation and Control System Architecture with Quantized Communications

To solve the problem formulated in section 12.3, this chapter proposes a general architecture consisting of a quantized consensus and a Luenberger observer update, together with a control input computation block at each agent, as depicted in the diagram of Figure 12.2.

The purpose of each of the blocks is the following:

- *Luenberger observer update* - Provides the local Luenberger observer contribution $z_{t,0}^i$ to be averaged, given the local measurement y_t^i and the current state estimate $\hat{x}_t^i$.
- *Quantized consensus* - Provides an approximation of the average $\frac{1}{N}\sum_{i\in\mathcal{N}} z_{t,0}^i$ of the local Luenberger observer contributions, which serves as the local state estimate $\hat{x}_t^i$, while performing over the time interval between t and $t+1$ a finite number of iterations of a consensus algorithm through the transmission of messages with a limited, fixed, number of bits.
- *Control input* - Computes the local control input u_t^i given the local state estimate $\hat{x}_t^i$.

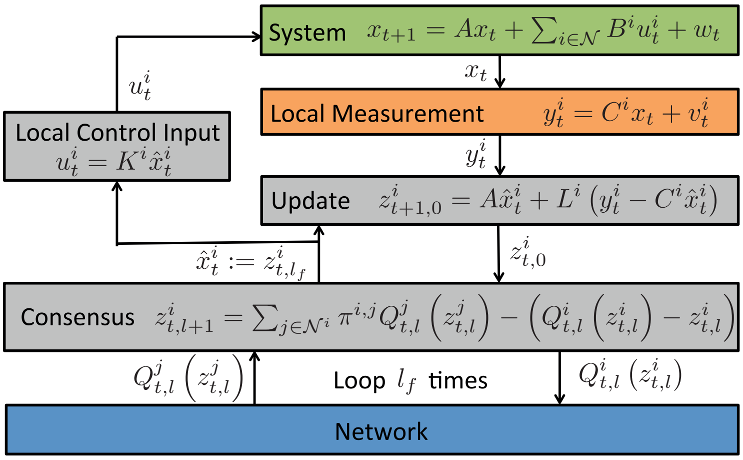

Figure 12.2 – Control architecture diagram.

12.5 Main Result

In this section we describe the proposed distributed Luenberger observer with quantized communications and we present the main result of this chapter, which establishes the ultimate boundedness of the state estimation error and the system state under the proposed distributed observer and controller.

12.5.1 Distributed Luenberger Observer with Quantized Communications

We now consider the distributed Luenberger observer given in Subsection 12.4.3. Because we assume that starting at each time step, between two measurements, a limited number of data packages containing a limited number of bits are exchanged among agents, we consider that the averaging is performed with the quantized consensus algorithm given in Chapter 7 with a limited number of iterations.

The quantized consensus algorithm consists of initializing each agent with $z_{t,0}^j := z_t^j$ and then performing l_f times the following update rule in between discrete time instants t and $t+1$.

$$z_{t,l+1}^i = \sum_{j\in\mathcal{N}^i} \pi^{i,j} Q_{t,l}^j\left(z_{t,l}^j\right) - \left(Q_{t,l}^i\left(z_{t,l}^i\right) - z_{t,l}^i\right). \tag{12.6}$$

During the consensus step the quantities $z_{t,l}^j$ are quantized through $Q_{t,l}^j(\cdot)$ with mid-value $\bar{z}_{t,l+1}^j := Q_{t,l}^j\left(z_{t,l}^j\right)$ for $l > 0$ and $\bar{z}_{t,0}^j = AQ_{t-1,l_f-1}^j\left(z_{t-1,l_f-1}^j\right)$, and quantization interval $\Lambda_{t,l} := \left(a\beta^t + b\right)\alpha^l$, where we initialize the parameters a and b and the decreasing rates α and β so as to satisfy the conditions of Theorem 21 given below. We initialize the mid-values $\bar{z}_{0,0}^j$, and the estimated states before consensus with the same value in all the nodes, i.e. $\bar{z}_{0,0}^i = z_0^i = z_0^j$, $\forall i, j \in \mathcal{N}$. Finally, we consider that the local estimate of the state is defined as $\hat{x}_t^i := z_{t,l_f}^i$, the end result of the consensus step. The local control input u_t^i given the local state estimate $\hat{x}_t^i$ is computed as $u_t^i = K^i\hat{x}_t^i$. The distributed Luenberger observer with quantized communications can be summarized in the form of the following algorithm, which consists of two steps, the consensus and the update steps.

Algorithm:
Quantized Distributed Luenberger Observer

Initialization:

• Choose L such that $\rho(A-LC)<1$.
• Choose the decrease rates α and β
satisfying conditions (12.7) and (12.8) respectively.
• Choose the quantizer parameters a and b
satisfying condition (12.9).

Consensus:

for $l = 0,1,\dots,l_f-1$ **do**

$\Lambda_{t,l} = \left(a\beta^t + b\right)\alpha^l$

$z^i_{t,l+1} = \sum_{j\in\mathcal{N}^i}\pi^{i,j}Q^j_{t,l}\left(z^j_{t,l}\right) - \left(Q^i_{t,l}\left(z^i_{t,l}\right)-z^i_{t,l}\right)$

$\bar{z}^j_{t,l+1} = Q^j_{t,l}\left(z^j_{t,l}\right), \forall j\in\mathcal{N}^i$

end for

$\bar{z}^j_{t+1,0} = (A+BK)Q^j_{t,l_f-1}\left(z^j_{t,l_f-1}\right), \forall j\in\mathcal{N}^i$

$\hat{x}^i_t := z^i_{t,l_f}$

$u^i_t = K^i\hat{x}^i_t$

Update:

sample the measurement y^i_t

$z^i_{t+1,0} = (A+BK)\hat{x}^i_t + L^i\left(y^i_t - C^i\hat{x}^i_t\right)$

Before proceeding to the main result of this chapter and its proof, the following definitions are required. We define the matrices $\Phi^i := A - L^iC^i$, $\Gamma := \mathrm{diag}\left(\Phi^i+BK\right) - \mathbf{1}\otimes\mathrm{row}\left(B^iK^i\right)$, and the error dynamics matrix as $\Phi := \frac{1}{N}\,\mathrm{col}\left(\Phi^i\right)\mathbf{1}^T\otimes I_n$. Based on these matrices we define the parameters

$$
\begin{aligned}
\bar{\Phi} &:= \|\Phi\|_{I_N\otimes P_1} = \frac{M(\mathrm{col}\left(\Phi^i\right)^T I_N\otimes P_1\,\mathrm{col}\left(\Phi^i\right), P_1)}{\sqrt{N}},\\
\hat{\Phi} &:= \left\|\frac{1}{N}\mathbf{1}\otimes I_n\,\mathrm{row}\left(\Phi^i+BK\right)\right\|_{I_N\otimes P_1} = \left\|P_1^{\frac{1}{2}}\,\mathrm{row}\left(\Phi^i+BK\right)I_N\otimes P_1^{-\frac{1}{2}}\right\|,\\
\tilde{\Phi} &:= \|\Gamma\|_{I_N\otimes P_1}.
\end{aligned}
$$

See Appendix F.2 for the derivation of the above equalities. Because Γ is of size $Nn\times Nn$, the direct computation of $\|\Gamma\|_{I_N\otimes P_1}$ is very costly if the number of agents N is large. For this reason, it is preferable to use, instead of $\tilde{\Phi}$, its upper bound

$$
\tilde{\Phi} \le \max\left(\left\|\Phi^i+BK\right\|_{P_1}\right) + N\left\|P_1^{\frac{1}{2}}\,\mathrm{row}\left(B^iK^i\right)I_N\otimes P_1^{-\frac{1}{2}}\right\|,
$$

which is derived in Appendix F.2.

We also define the local and global estimation errors $e^i_{t,l} := x_t - z^i_{t,l}$ and $e_{t,l} := \mathrm{col}(e^i_{t,l})$, respectively, the global noise bound $\epsilon := \sqrt{\sum_{i\in\mathcal{N}}\left(M(L^{iT}P_1L^i)\epsilon_{v^i} + M(P_1)\epsilon_w\right)^2}$, and the design parameters given in Appendix F.1. We now state the main result of this chapter.

Theorem 21. Let Assumptions A2-A3 and A14-A16 hold and adopt the quantized distributed Luenberger observer algorithm with L such that $\tilde{\beta} := \|A-LC\|_{P_1} < 1$. Further let the number of bits transmitted n_b satisfy $n_b > \log_2(\max(c_2,d_2)+2)$, the number of iterations of the consensus step satisfy $l_f \ge 1$ or, if $\sigma_2 > 0$, $l_f > \log_{\sigma_2}\left(\frac{1-\tilde{\beta}}{\bar{\Phi}}\min\left(1,\frac{\tilde{\beta}}{\bar{\Phi}}\right)\right)$, α and β satisfy

$$
\sigma_2 < \alpha < \bar{\alpha}, \tag{12.7}
$$

$$\bar{\beta} < \beta < 1. \tag{12.8}$$

where $\bar{\beta} := \tilde{\beta} + \alpha^{l_f}\tilde{\Phi}\max\left(1, \frac{\bar{\Phi}}{\tilde{\beta}}\right)$, and $\bar{\alpha} := \min\left(\sqrt[l_f]{\frac{1-\tilde{\beta}}{\bar{\Phi}}\min\left(1, \frac{\tilde{\beta}}{\bar{\Phi}}\right)}, 1\right)$.

Consider also the parameters $c_1 - c_2$, $d_1 - d_2$, $k_1 - k_4$, defined in (F.1). If the parameters a and b satisfy

$$c_1 \le \left(1 - \frac{c_2}{2^{n_b} - 2}\right)\frac{a}{2}, \qquad d_1 \le \left(1 - \frac{d_2}{2^{n_b} - 2}\right)\frac{b}{2}, \tag{12.9}$$

then for any $t \ge 0$ the norm of the estimation error e_{t,l_f} satisfies

$$\|e_{t,l_f}\|_{I_N \otimes P_1} \le \beta^t \left[k_1 \|e_{0,0}\|_{I_N \otimes P_1} + k_2\right] + k_3\epsilon + k_4. \tag{12.10}$$

The proof of this theorem will be given in the next section.

We can observe that the lower bound on l_f depends heavily on the choice of L since the parameters $\tilde{\beta}$ and $\bar{\Phi}$ depend directly on L by definition.

In general, for an arbitrary network we have a lower bound on the number of iterations of the consensus step l_f, since in general $\sigma_2 > 0$ and we have to satisfy the condition $l_f > \log_{\sigma_2}\left(\frac{1-\tilde{\beta}}{\bar{\Phi}}\min\left(1, \frac{\tilde{\beta}}{\bar{\Phi}}\right)\right)$. However, in the case of a full network where each node can broadcast its message to all other nodes, we may have $\sigma_2 = 0$ and in this case we can set $l_f = 1$.

It can be observed from inequality (12.10) that the norm of the estimation error $\|e_{t,l_f}\|_{I_N \otimes P_1}$ becomes bounded above by $k_3\epsilon + k_4$ when t goes to infinity, and the error is thus ultimately bounded. This bound depends directly on the disturbance bounds through ϵ and on the choice of the constant component of the quantization interval length b.

It is worth noticing that for the noise-free case, when the number of the exchanged bits n_b and the number of consensus iterations l_f tend to infinity, we recover perfect convergence of the estimation error to the origin. Moreover, the convergence rate of the algorithm β is lower bounded by $\bar{\beta}$ which tends to, but never reaches exactly (since $\bar{\beta} > \tilde{\beta}$ always), the convergence rate of the centralized case $\tilde{\beta} := \|A - LC\|_{P_1}$ as the number of iterations of the consensus algorithm l_f tends to infinity.

Note also that if in Assumption A16 $\|w_t\|_{P_w} \le \epsilon_w$ for some symmetric positive definite matrix P_w, then we must replace $M(P_1)$ by $M(P_1, P_w)$ in the definition of ϵ. Similarly, if in Assumption A16 $\|v_t^i\|_{P_{v^i}} \le \epsilon_{v^i}$ for some symmetric positive definite matrix P_{v^i}, we must replace $M\left(L^{iT}P_1L^i\right)$ by $M\left(L^{iT}P_1L^i, P_{v^i}\right)$ on the definitions of ϵ and d_1.

Finally, one of the key elements of the proposed algorithm is to set the quantization interval at the beginning of the consensus step to $a\beta^t + b$. With this setting we can observe that as t goes to infinity, the first term $a\beta^t$ goes to zero and only the second term b is functioning. Moreover, we can note that from condition (12.9) only b relates to the noise bound ϵ and only a depends on the initial estimation error.

12.5.2 Ultimate Boundedness of the System State

The proposed distributed observer and the linear feedback control law with $\rho(A + BK) < 1$ can be described by the dynamical system

$$x_{t+1} = (A + BK)\,x_t + w_t - B\,\mathrm{diag}\left(K^i\right) e_{t,l_f}. \tag{12.11}$$

Because the gain matrix K is computed so that $\rho(A+BK)<1$ and the process disturbance w_t and estimation errors e_{t,l_f} are ultimately bounded, it follows that the state x_t is ultimately bounded. More specifically, choosing a symmetric positive definite matrix Q_2 of size $n\times n$ and computing a matrix P_2 such that the Lyapunov equation $P_2-(A+BK)^T P_2(A+BK)=Q_2$ holds, defining $\tilde{\gamma}:=\|A+BK\|_{P_2}<1$, and choosing a positive scalar γ such that $1>\gamma>\max(\tilde{\gamma},\beta)$, we have the following result

Theorem 22. Let Assumptions A2-A3 and A14-A16 hold and let a quantized distributed Luenberger observer algorithm be adopted such that the assumptions of Theorem 21 are satisfied. Then, the system state norm $\|x_t\|_{P_2}$ is bounded as follows:

$$\|x_t\|_{P_2}\le\gamma^t\left[\|x_0\|_{P_2}+\frac{M^*\beta}{\beta-\tilde{\gamma}}(k_1\|e_{0,0}\|_{I_N\otimes P_1}+k_2)\right]+\frac{M(P_2)\epsilon_w+M^*(k_3\epsilon+k_4)}{1-\tilde{\gamma}},$$

where $M^*:=M\left(\mathrm{diag}\left(K^{iT}\right)B^T P_2 B\,\mathrm{diag}\left(K^i\right),I_n\otimes P_1\right)$.

The proof is given in Appendix F.5. Again, if in Assumption A16 $\|w_t\|_{P_w}\le\epsilon_w$ for some symmetric positive definite matrix P_w then we must replace $M(P_2)$ by $M(P_2,P_w)$ in Theorem 22.

12.6 Proof of Ultimate Boundedness of Estimation Error

Before proceeding with the proof of Theorem 21, the following definitions are required. We define the vector of averages $z_{t,l}^{\text{avg}}:=\frac{1}{N}\left(\mathbf{1}\mathbf{1}^T\right)z_{t,l}$, its difference to $z_{t,l}$ as $q_{t,l}:=z_{t,l}-z_{t,l}^{\text{avg}}$, the vector of mid-values $\bar{z}_{t,l}:=\mathrm{col}\left(\bar{z}_{t,l}^i\right)$, the average of the estimation errors $e_{t,l}^{\text{avg}}:=\frac{1}{N}\left(\mathbf{1}\mathbf{1}^T\right)\otimes I_n e_{t,l}$, the local and global noise contributions to the error dynamics as $\omega_t^i:=w_t-L^i v_t^i$, $\omega_t:=\mathrm{col}\left(\omega_t^i\right)$, the local and global consensus error contribution to the error dynamics as $\xi_t^i:=\Phi^i q_{t,l_f}^i-\sum_{j\in\mathcal{N}}B^j K^j\left(q_{t,l_f}^j-q_{t,l_f}^i\right)$, and $\xi_t:=\mathrm{col}\left(\xi_t^i\right)$. We can observe that $\xi_t=\Gamma q_{t,l_f}$. We also require the parameters c_1-c_8, d_1-d_8, k_1-k_6 which are defined in (F.1) in Appendix F.1.

12.6.1 Conditions for Convergence of Consensus Step

As a first step we can apply directly the results of Section 7 in the consensus step of the distributed Luenberger observer to get conditions on how to bound the difference between the estimates $z_{t,l}$ and the vector of averages $z_{t,l}^{\text{avg}}$, i.e. how to bound $q_{t,l}$. Applying Theorem 8 we have the following result

Lemma 14. Let Assumptions A2-A3 hold and the quantized distributed Luenberger observer algorithm be adopted with $l_f\ge 1$. If $\sigma_2<\alpha<1$ and the number of bits n_b and the parameters a and b satisfy

$$c_3+k_5\frac{a}{2^{n_b+1}-4}\le\frac{a}{2},\qquad d_3+k_5\frac{b}{2^{n_b+1}-4}\le\frac{b}{2},\tag{12.12}$$

where k_5 is defined in (F.1) in Appendix F.1 and c_3 and d_3 satisfy

$$c_3\beta^t+d_3\ge m(P_1)^{-1}\left(\frac{\alpha+1}{\alpha}\|q_{t,0}\|_{I_N\otimes P_1}+\|\bar{z}_{t,0}-z_{t,0}^{\text{avg}}\|_{I_N\otimes P_1}\right),\tag{12.13}$$

then for any $l\ge 0$ the values of $q_{t,l}:=z_{t,l}-z_{t,l}^{\text{avg}}$ satisfy

$$\|q_{t,l}\|_{I_N\otimes P_1}\le\alpha^l\left[\|q_{t,0}\|_{I_N\otimes P_1}+k_6\frac{a\beta^t+b}{2^{n_b}-2}\right].\tag{12.14}$$

Proof. Noting that if condition (12.12) holds then we have

$$c_3\beta^t+d_3+k_5\frac{a\beta^t+b}{2^{n_b+1}-4}\le\frac{a\beta^t+b}{2},$$

and the lemma follows from Theorem 8 with $z_{t,l}$ as z_l, $a\beta^t + b$ as r. □

12.6.2 Error Dynamics

Combining the fact that the consensus algorithm preserves averages, i.e. that $z_{t,l}^{\text{avg}} = z_{t,l+1}^{\text{avg}}$, the system dynamics (12.1), the measurement equations (12.2), and the distributed observer algorithm (12.4), we obtain the following result which describes the dynamics of the estimation errors $e_{t+1,0}^i$, $e_{t+1,0}$ and the dynamics of the average of the estimation errors $e_{t,0}^{\text{avg}}$.

Lemma 15. Let the quantized distributed Luenberger observer algorithm be adopted with $l_f \geq 1$; then, the estimation errors obey the recursion

$$e_{t+1,0}^i = \sum_{j \in \mathcal{N}} \frac{1}{N} \Phi^i e_{t,0}^j - \xi_t^i + \omega_t^i, \tag{12.15}$$

for any $i \in \mathcal{N}$, and globally,

$$e_{t+1,0} = \Phi e_{t,0} - \xi_t + \omega_t. \tag{12.16}$$

Moreover,

$$e_{t+1,0} = \operatorname{diag}\left(\Phi^i\right) e_{t,0}^{\text{avg}} - \xi_t + \omega_t, \tag{12.17}$$

and

$$e_{t+1,0}^{\text{avg}} = I_N \otimes (A - LC)\, e_{t,0}^{\text{avg}} + \frac{1}{N}\left(\mathbf{1}\mathbf{1}^T\right) \otimes I_n \left(\omega_t - \xi_t\right). \tag{12.18}$$

We now derive results on the norms of $e_{t,0}$ and $e_{t,0}^{\text{avg}}$ by taking the norms of both sides of equations (12.17) and (12.18), respectively. For this purpose we compute upper bounds of the norms of the terms ξ_t and ω_t in Appendix F, where we show that if Assumption A16 holds we have $\|\omega_t\|_{I_N \otimes P_1} \leq \epsilon$, and if at time t the conditions of Lemma 14 are observed, then

$$\|\xi_t\|_{I_N \otimes P_1} \leq \tilde{\Phi} \alpha^{l_f} \left[\|e_{t,0}\|_{I_N \otimes P_1} + k_6 \frac{a\beta^p + b}{2^{n_b} - 2} \right].$$

Therefore, we can bound $\|e_{t+1,0}^{\text{avg}}\|_{I_N \otimes P_1}$ and $\|e_{t+1,0}\|_{I_N \otimes P_1}$ by taking the norm of (12.18) and (12.17), as follows:

$$\|e_{t+1,0}^{\text{avg}}\|_{I_N \otimes P_1} \leq \tilde{\beta} \|e_{t,0}^{\text{avg}}\|_{I_N \otimes P_1} + \tilde{\Phi} \alpha^{l_f} \left[\|e_{t,0}\|_{I_N \otimes P_1} + k_6 \frac{a\beta^t + b}{2^{n_b} - 2} \right] + \epsilon, \tag{12.19}$$

$$\|e_{t+1,0}\|_{I_N \otimes P_1} \leq \bar{\Phi} \|e_{t,0}^{\text{avg}}\|_{I_N \otimes P_1} + \tilde{\Phi} \alpha^{l_f} \left[\|e_{t,0}\|_{I_N \otimes P_1} + k_6 \frac{a\beta^t + b}{2^{n_b} - 2} \right] + \epsilon. \tag{12.20}$$

Since, for reasons that will become clear later in the proof of Lemma 16, we need an upper bound of $\|e_{t+1,0}\|_{I_N \otimes P_1}$ which is equal to the upper bound of $\|e_{t+1,0}^{\text{avg}}\|_{I_N \otimes P_1}$ times a constant, we upper bound $\|e_{t+1,0}\|_{I_N \otimes P_1}$ as follows:

$$\|e_{t+1,0}\|_{I_N \otimes P_1} \leq \max\left(1, \frac{\bar{\Phi}}{\tilde{\beta}}\right) \left(\tilde{\beta} \|e_{t,0}^{\text{avg}}\|_{I_N \otimes P_1} + \tilde{\Phi} \alpha^{l_f} \left[\|e_{t,0}\|_{I_N \otimes P_1} + k_6 \frac{a\beta^t + b}{2^{n_b} - 2} \right] + \epsilon \right). \tag{12.21}$$

We now choose β such that $\tilde{\beta} < \beta < 1$ and derive the conditions in a, b, and n_b to ensure ultimate boundedness.

12.6.3 Proof of Theorem 21

Theorem 21 is proven by induction. We show that if we satisfy, for all time instants p such that $0 \le p \le t$, the conditions of Lemma 14 and if inequality (12.7) holds, then inequality (12.10) follows. For this purpose we apply equations (12.19) and (12.21) recursively to obtain bounds on $\|e^{\text{avg}}_{t,0}\|_{I_N\otimes P_1}$ and $\|e_{t,0}\|_{I_N\otimes P_1}$ depending explicitly in time. Moreover, since we want that the conditions of Lemma 14, and more specifically inequality (12.13), hold we also need to provide bounds in $\bar{z}_{t+1,0} - z^{\text{avg}}_{t+1,0}$. These results are presented in the following Lemma, the proof of which is given in Appendix F.4.

Lemma 16. Let Assumptions A2-A3 and A14-A16 hold and let the quantized distributed Luenberger observer algorithm be adopted with L such that $\tilde{\beta} := \|A - LC\|_{P_1} < 1$. If α and $l_f \ge 1$ are adopted such that

$$\alpha^{l_f} \le \frac{1-\tilde{\beta}}{\bar{\Phi}} \min\left(1, \frac{\tilde{\beta}}{\bar{\Phi}}\right),$$

$\sigma_2 < \alpha < 1$, β satisfy $\bar{\beta} < \beta < 1$, and the conditions of Lemma 14 are satisfied for all $0 \le p \le t$, then $\|e^{\text{avg}}_{p,0}\|_{I_N\otimes P_1}$, $\|e_{p,0}\|_{I_N\otimes P_1}$, $\|q_{p,l}\|_{I_N\otimes P_1}$, $\|\bar{z}_{p+1,0} - z^{\text{avg}}_{p+1,0}\|_{I_N\otimes P_1}$ and $\|e_{p,l_f}\|_{I_N\otimes P_1}$ satisfy

$$\begin{aligned}
\|e^{\text{avg}}_{p,0}\|_{I_N\otimes P_1} &\le \beta^p \left[\|e_{0,0}\|_{I_N\otimes P_1} + c_8 \tfrac{a}{2^{n_b}-2}\right] + \tfrac{\epsilon}{1-\tilde{\beta}} + d_8 \tfrac{b}{2^{n_b}-2}, \forall t+1 \ge p \ge 0;\\
\|e_{p,0}\|_{I_N\otimes P_1} &\le \max\left(1, \tfrac{\bar{\Phi}}{\tilde{\beta}}\right)\left(\beta^p \left[\|e_{0,0}\|_{I_N\otimes P_1} + c_8 \tfrac{a}{2^{n_b}-2}\right] + \tfrac{\epsilon}{1-\tilde{\beta}} + d_8 \tfrac{b}{2^{n_b}-2}\right), \forall t+1 \ge p \ge 0;\\
\|q_{p,l}\|_{I_N\otimes P_1} &\le \alpha^l \left[\beta^p \left[\max\left(1, \tfrac{\bar{\Phi}}{\tilde{\beta}}\right)\|e_{0,0}\|_{I_N\otimes P_1} + c_7 \tfrac{a}{2^{n_b}-2}\right] + \tfrac{\max\left(1,\frac{\bar{\Phi}}{\tilde{\beta}}\right)\epsilon}{1-\tilde{\beta}} + d_7 \tfrac{b}{2^{n_b}-2}\right], \forall t \ge p \ge 0, l_f \ge l \ge 0;\\
\|\bar{z}_{p+1,0} - z^{\text{avg}}_{p+1,0}\|_{I_N\otimes P_1} &\le \beta^p \left[c_5 \|e_{0,0}\|_{I_N\otimes P_1} + c_6 \tfrac{a}{2^{n_b}-2}\right] + d_5 + d_6 \tfrac{b}{2^{n_b}-2}, \forall t \ge p \ge 0;\\
\|e_{p,l_f}\|_{I_N\otimes P_1} &\le \beta^p \left[k_1 \|e_{0,0}\|_{I_N\otimes P_1} + k_2\right] + k_3\epsilon + k_4, \forall t \ge p \ge 0.
\end{aligned}$$

Proof of Theorem 21. We prove by induction that $z^j_{t,l}$ falls inside the quantization interval of $Q_{t,l}$, i.e. $\|z^j_{t,l} - \bar{z}^j_{t,l}\|_\infty \le \frac{\Lambda_{t,l}}{2}$ for $t \ge 0$, which, combined with Lemma 16 concludes the proof of Theorem 21. In light of Lemma 14, we need to prove that the conditions

$$c_1 + c_2 \frac{a}{2^{n_b+1}-4} \le \frac{a}{2}, \qquad d_1 + d_2 \frac{b}{2^{n_b+1}-4} \le \frac{b}{2},$$

are equivalent to

$$c_3 + k_5 \frac{a}{2^{n_b+1}-4} \le \frac{a}{2}, \qquad d_3 + k_5 \frac{b}{2^{n_b+1}-4} \le \frac{b}{2},$$

Since c_2 and d_2 are defined as in (F.1), i.e. as $c_2 := c_4 + k_5$ and $d_2 := d_4 + k_5$, this equivalence is achieved by defining c_3 and d_3 as

$$c_3 := c_1 + c_4 \frac{a}{2^{n_b+1}-4},\ d_3 := d_1 + d_4 \frac{b}{2^{n_b+1}-4}.$$

Now, to satisfy all the conditions of Lemma 14, it remains to show that, for $t \ge 0$,

$$c_3\beta^t + d_3 \ge \frac{\frac{\alpha+1}{\alpha}\|q_{t,0}\|_{I_N\otimes P_1} + \|\bar{z}_{t,0} - z^{\text{avg}}_{t,0}\|_{I_N\otimes P_1}}{m(P_1)}.$$

We will prove the above by induction. The base case is given by assumption, since $q_{0,0} = \bar{z}_{0,0} - z^{\text{avg}}_{0,0} = 0$. For the induction step we first note that if, for some $t \ge 0$,

$$c_3\beta^p + d_3 \ge \frac{\frac{\alpha+1}{\alpha}\|q_{p,0}\|_{I_N\otimes P_1} + \|\bar{z}_{p,0} - z^{\text{avg}}_{p,0}\|_{I_N\otimes P_1}}{m(P_1)},$$

and applying Lemma 16 and inequality (F.2) we obtain

$$
\begin{aligned}
&\frac{\frac{\alpha+1}{\alpha}\|q_{t+1,0}\|_{I_N\otimes P_1}+\|\bar{z}_{t+1,0}-z^{\text{avg}}_{t+1,0}\|_{I_N\otimes P_1}}{m(P_1)} \leq \\
\leq\quad & \frac{(\alpha+1)}{m(P_1)\alpha}\left[\beta^{t+1}\max\left(1,\frac{\bar{\Phi}}{\tilde{\beta}}\right)\left[\|e_{0,0}\|_{I_N\otimes P_1}+c_8\frac{a}{2^{n_b}-2}\right]+\frac{\epsilon}{1-\tilde{\beta}}+d_8\frac{b}{2^{n_b}-2}\right]+\frac{\beta^{t+1}\left[\frac{c_5}{\beta}\|e_{0,0}\|_{I_N\otimes P_1}+\frac{c_6}{\beta}\frac{a}{2^{n_b}-2}\right]+d_5+d_6\frac{b}{2^{n_b}-2}}{m(P_1)} \\
=\quad & \left[c_1+c_4\frac{a}{2^{n_b+1}-4}\right]\beta^{t+1}+d_1+d_4\frac{b}{2^{n_b+1}-4} \\
=\quad & c_3\beta^{t+1}+d_3.
\end{aligned}
$$

We have proven that, under the assumptions of the theorem, the base case holds, i.e. $z^j_{0,l}$ falls inside the quantization interval $\left[\bar{z}^j_{0,l}-\frac{(a+b)\alpha^l}{2},\bar{z}^j_{0,l}+\frac{(a+b)\alpha^l}{2}\right]$ for $0\leq l\leq l_f$. The recursion step guarantees that if $z^j_{t,l}$ is inside its quantization interval for $0\leq l\leq l_f$, then $z^j_{t+1,l}$ is too.

Then, by induction we have shown, for all $0\leq t$ and $0\leq l\leq l_f$, that:

$$
z^j_{t,l}\in\left[\bar{z}^j_{t,l}-\frac{(a\beta^t+b)\alpha^l}{2},\bar{z}^j_{t,l}+\frac{(a\beta^t+b)\alpha^l}{2}\right],
$$

and the theorem is proven. □

12.7 Numerical Results

As a design example we consider a system composed by a network system of 20 agents, a communication network $(\mathcal{N},\mathcal{A})$ that is bidirectional and randomly generated, and a consensus matrix computed as $\Pi = h_\Pi I_N+(1-h_\Pi)\Pi_{\text{Metro}}$, where Π_{Metro} is computed with Metropolis weights, and h_Π is selected to minimize σ_2. In this example we consider a network where the second singular value of Π is $\sigma_2 = 0.6913$. We also consider an objective network $(\mathcal{N},\mathcal{A}_{\text{obj}})$ which is also randomly generated, and for each agent we define the objective neighbour set as $\mathcal{N}^i_{\text{obj}} := \{j\in\mathcal{N}:(j,i)\in\mathcal{A}_{\text{obj}}\}$. The communication and objective networks are represented graphically in Figures 12.3 and 12.4, respectively.

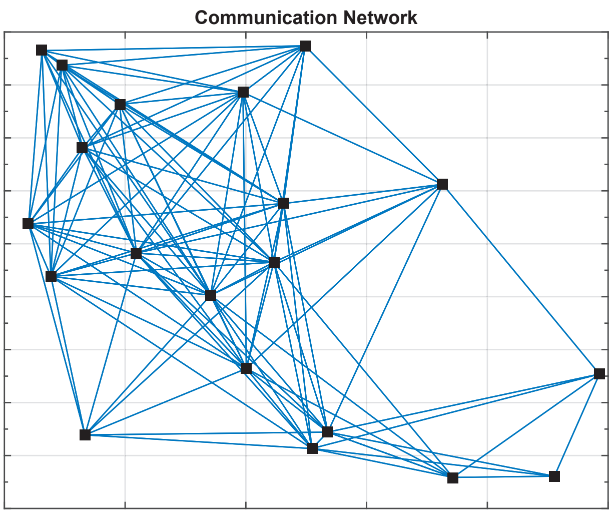

Figure 12.3 – Graphical representation of the communication network.

Remark. *For the communication network of this example the value of h_Π that minimizes σ_2 is $h_\Pi = -0.73$, which yields a consensus matrix that has some negative elements, and is therefore does not satisfy the assumption*

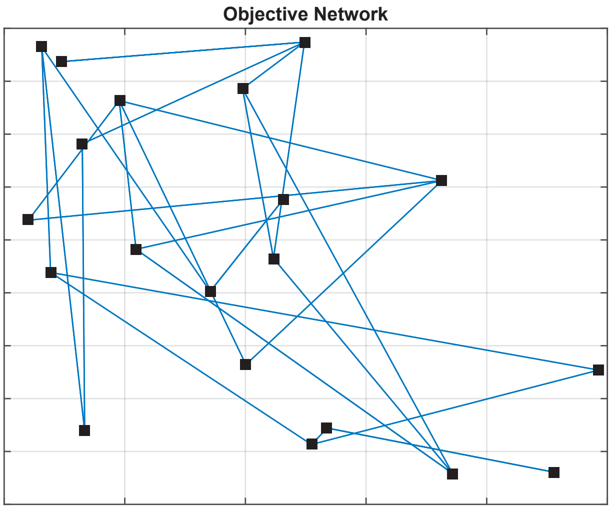

Figure 12.4 – Graphical representation of the objective network.

that Π *is a non-negative matrix. However, since the resulting matrix is doubly stochastic and primitive, the results of Theorems 21 and 22 still hold.*

Each agent has 3 states, locally referred to as x^1, x^2 and x^3. The first two states of each agent correspond to a double integrator with the following dynamics with disturbances:

$$x^1_{t+1} = x^1_t + u_t + w^1_t,$$
$$x^2_{t+1} = x^2_t + x^1_t + w^2_t,$$

where u_t is the agent's input and w^1_t and w^2_t are bounded disturbances. We consider also a local colored noise signal with dynamics

$$x^3_{t+1} = 0.95x^3_t + w^3_t,$$

where w^3_t is a bounded disturbance. All local states x^1, x^2, and x^3 are observed with some measurement noise by each agent. The objective of each agent is to have x^2 track x^3 (that is, drive x^2 as close as possible to x^3) and also to coordinate the states x^2 of the agents among themselves (that is, drive the state $x^{2,i}$ of an agent as close as possible to $\frac{1}{|\mathcal{N}^i_{\text{obj}}|}\sum_{j\in\mathcal{N}^i_{\text{obj}}} x^{2,j}$, where in $x^{2,i}$, $i \in \mathcal{N}$ is the index of the agent). This setting aims to represent the case where several agents try to track separate signals while coordinating among themselves. This example translates to a system described by (12.1) with

$$A = I_{20} \otimes \begin{bmatrix} 1 & 0 & 0 \\ 1 & 1 & 0 \\ 0 & 0 & 0.95 \end{bmatrix}.$$

The output matrix C^i for each agent is

$$C^i = \begin{bmatrix} (\boldsymbol{e}_i - \boldsymbol{e}_{i+1})^T \\ (\boldsymbol{e}_{i-1} - \boldsymbol{e}_i)^T \end{bmatrix} \otimes I_3,$$

where $\boldsymbol{e}_i$ is a vector of size 20×1 with 0 on every element except on the ith, which is 1. The local input matrix

B^i for each agent is

$$B^i = \boldsymbol{e}_i \otimes \begin{bmatrix} 1 \\ 0 \\ 0 \end{bmatrix}.$$

It is straightforward to show that in this example we have global observability but not local observability.

The measurement and process noise are selected at random with a Gaussian distribution centered at zero, with a covariance of

$$\begin{bmatrix} 10^{-6} & 0 & 0 \\ 0 & 10^{-8} & 0 \\ 0 & 0 & 10^{-4} \end{bmatrix},$$

for the local measurement noise, and

$$I_{20} \otimes \begin{bmatrix} 10^{-8} & 0 & 0 \\ 0 & 10^{-4} & 0 \\ 0 & 0 & 0.25 \end{bmatrix},$$

for the process noise. The measurement and process noises are saturated so as to satisfy Assumption A16 with $\epsilon_v^i = 1.5 \times 10^{-3}$ and $\epsilon_w = 0.5$. To compute the controller gain matrix K, notice that the objective stated previously, of having x^2 tracking x^3 and coordinating the states x^2 of the agents among themselves, can be converted into that of minimizing the cost function

$$\sum_{t=0}^{\infty} \left(x_t^T Q x_t + u_t^T R u_t \right), \tag{12.22}$$

where Q and R are defined as $R := 20 I_{20}$ and

$$Q := I_{20} \otimes \left(C_{\mathrm{loc}}^T C_{\mathrm{loc}} \right) + L_{\mathrm{obj}} \otimes \left(C_{\mathrm{dist}}^T C_{\mathrm{dist}} \right)$$

with

$$L_{\mathrm{obj}}^{ij} := \begin{cases} 1 & \text{if } i = j, \\ -\frac{1}{\left|\mathcal{N}_{\mathrm{obj}}^i\right|} & \text{if } j \in \mathcal{N}_{\mathrm{obj}}^i, \\ 0 & \text{otherwise.} \end{cases},$$

$$C_{\mathrm{loc}} := [0,\ 1,\ -1],$$

$$C_{\mathrm{dist}} := [0,\ 1,\ 0],$$

Given the above matrices, let P be the unique positive definite solution of the algebraic Riccati equation (ARE)

$$P = Q + A^T P A - A^T P B \left(R + B^T P B \right)^{-1} B^T P A,$$

and compute the controller gain as

$$K = \left(R + B^T P B \right)^{-1} B^T P A.$$

It is well known from LQR theory that this selection of control gain minimizes the cost (12.22) for a system without disturbances when the state is measured directly. Notice from the definition of K that

$$A^T P B \left(R + B^T P B \right)^{-1} B^T P A = A^T P B K = K^T (B^T P B + R) K.$$

Therefore, the ARE becomes

$$(A-BK)^T P(A-BK) - P + Q + K^T RK = 0,$$

which, combined with the proof of Property P2 results in $\|A-BK\|_{P_2} = \sqrt{1-\sigma_{\min}\left(Q_2^{\frac{1}{2}} P_2^{-\frac{1}{2}}\right)^2}$, where $P_2 := P$ and $Q_2 := Q + K^T RK$.

To compute the observer gain matrix L we define the matrices $V := I_{60}$ and $W := I_{60}$ and compute the solution Σ to the algebraic Riccati equation

$$\Sigma = W + A\Sigma A^T - A\Sigma C^T \left(V + C\Sigma C^T\right)^{-1} C\Sigma A^T,$$

from which follows the observer gain L given by

$$L = A\Sigma C^T \left(V + C\Sigma C^T\right)^{-1}.$$

This choice of observer gain is known from Kalman filtering theory to asymptotically minimize the mean of the square estimation error for the centralized case, when the measurement noise covariance is V^{-1} and the process noise covariance is W^{-1}. Following the derivations in Subsection 6.3.3 of Chapter 6, we define $\tilde{\Sigma} := \left(\Sigma^{-1} + CV^{-1}C^T\right)^{-1}$, $P_1 := \Sigma^{-1}\tilde{\Sigma}\Sigma^{-1}$, and $Q_1 := \Sigma^{-1}\left(\tilde{\Sigma}^{-1} + A^T \tilde{W}^{-1} A\right)\Sigma^{-1}$, which is positive definite since Σ and $\tilde{\Sigma}$ are positive definite, yielding $\|A-LC\|_{P_1} = \sqrt{1-\sigma_{\min}\left(Q_1^{\frac{1}{2}} P_1^{-\frac{1}{2}}\right)^2}$.

The computed minimum number of consensus iterations for guaranteed stability was 24. Setting $l_f = 29$, the minimum number of bits sent such that stability can be guaranteed was 17, and the number of bits used was 18. The obtained estimated states for two sensors in the network are represented in Figure 12.5, where the initial condition for each state is either 5 or -5 and the initial estimate for all the states is 0.

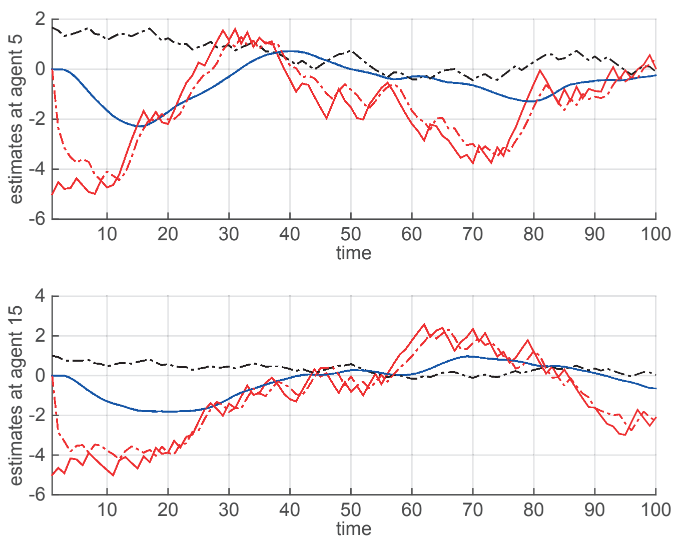

Figure 12.5 – Estimated states z^i_{t,l_f} in two sensors (states 14 (in blue) and 15 (in red) above, states 44 (in blue) and 45 (in red) below). The solid lines represent the real states, and the black dashed lines near the origin represent the average of the states $x^{2,j}$, $j \in \mathcal{N}^i_{\text{obj}}$, that is $\frac{1}{\left|\mathcal{N}^i_{\text{obj}}\right|}\sum_{j\in\mathcal{N}^i_{\text{obj}}} x^{2,j}$.

We can observe that, for the settings of this problem, at each time step consensus is almost achieved and therefore we are not able to distinguish the estimates for different states since the estimates $z_t^i(T)$ are almost equal for all the states. We also note that the estimated states (dashed lines) remain close to the actual states (solid lines) thus indicating that the observer fulfills its purpose. Finally, we observe that the objectives mentioned earlier, of having x^2 track x^3 and coordinate the states x^2 of the agents among themselves, were achieved. That is, we note that for both represented agents, 5 and 15, the local x^2 states (blue lines) remain at a close distance from both the x^3 states and the average of the other x^2 states, $\frac{1}{\left|\mathcal{N}_{\text{obj}}^i\right|}\sum_{j\in\mathcal{N}_{\text{obj}}^i} x^{2,j}$ (black dashed lines). This was achieved while guaranteeing input to state stability with a limited number of consensus iterations, 29, at each time step and using exchanged messages with a determined number of bits, 18 in this case.

This number of transmitted bits and consensus iterations guaranteeing stability of the observer, which stems from the analysis in this chapter, is a conservative upper bound. In order to assess how conservative these upper bounds are, we computed the estimation error and objective cost of the system coupled with the estimation and control algorithm for different values of the number of transmitted bits n_b, and consensus iterations l_f, maintaining the values of a, b, α and β. In Figure 12.6, we plot the base 10 logarithm of the average control objective cost of the system defined by

$$AEE := \frac{1}{t_f}\sum_{t=0}^{t_f} \|e_t\|,$$

where $t_f > 0$ is the final time of the simulation, and in Figure 12.7, we plot the base 10 logarithm of the average estimation error of the observers defined by

$$ACC := \frac{1}{t_f}\sum_{t=0}^{t_f} x_t^T Q x_t.$$

In both Figure 12.6 and 12.7 we plot the isocontours of the base 10 logarithm of the data rate defined by

$$DR := n n_b l_f,$$

the values for each point of n_b and l_f represent the average of 5 realizations of the system for $t_f = 100$. We only plot the values for points where the average estimation errors are smaller than 10^2. Also for both figures we represent a dashed dotted line, obtained by linear regression, defined by $l_f = 41.4 - 2.47n_b$, where above it the average estimation error is smaller than 20. We also represent a line $l_f = 41.4 - 2.47n_b$ where above it the average estimation error is in general smaller than 11.5.

We can observe from Figures 12.6 and 12.7 that in practice above the line $l_f = 41.4 - 2.47n_b$, represented by a dashed line, we obtain a performance similar to the centralized Luenberger observer, and below that line the performance of the algorithm degrades quickly when reducing the number of consensus iterations or the number of transmitted bits. In Figures 12.8 and 12.9 we plot the average estimation error and the average control objective cost along the line $l_f = \lceil 41.4 - 2.47n_b \rceil$.

From Figures 12.8 and 12.9 one can observe that the performance of the algorithm does not change significantly along the line $l_f = \lceil 41.4 - 2.47n_b \rceil$. Along that line the required data rate (DR) is shown in Figure 12.10. We can conclude from Figure 12.10 that the two best settings that yield a performance similar to that of a centralized observer are transmitting 3 bits and a performing a 35 consensus iterations, yielding a data rate of 8100 bits/s, or exchanging 17 bits and performing 10 consensus iterations, yielding a data rate of 10200 bits/s. In this case the better strategy would be to to transmit 17 bits and performing 10 consensus iterations. However, since the difference is not large, we can envision that in some cases transmitting a low number of bits and performing a large number of iterations would be more advantageous.

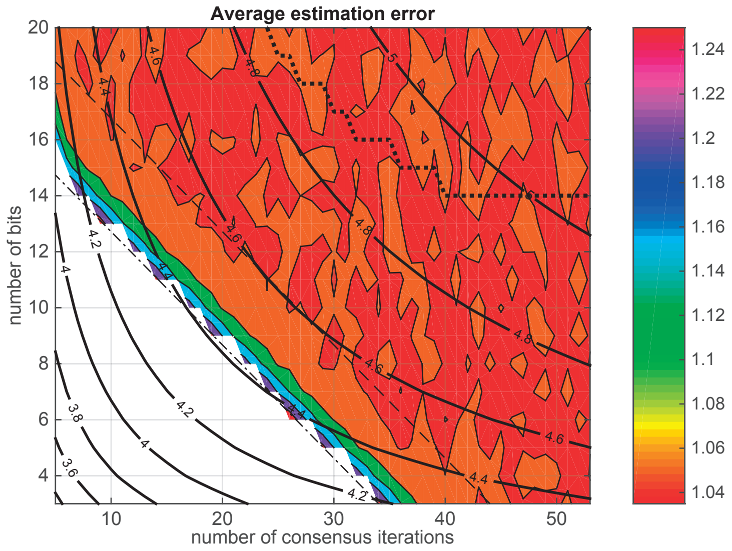

Figure 12.6 – Base 10 logarithm of the average estimation error ($\log_{10}(AEE)$) for different numbers of bits transmitted n_b and consensus iterations l_f. The base 10 logarithm of the required data rate ($\log_{10}(Bw)$) contour lines are plotted in labeled solid black lines. The dotted black lines represent the theoretical bounds for stability of Theorem 21.

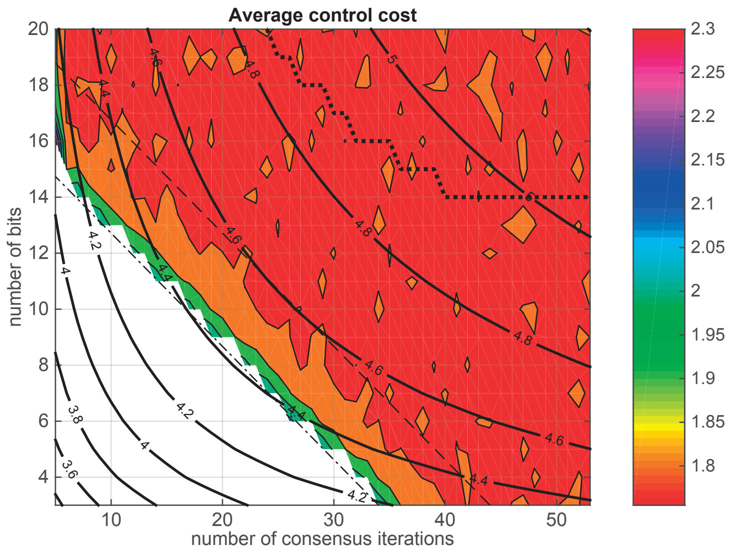

Figure 12.7 – Base 10 logarithm of the average objective control cost ($\log_{10}(ACC)$) for different numbers of bits transmitted n_b and consensus iterations l_f. The base 10 logarithm of the required data rate ($\log_{10}(Bw)$) contour lines are plotted in labeled solid black lines. The dotted black lines represent the theoretical bounds for stability of Theorem 21.

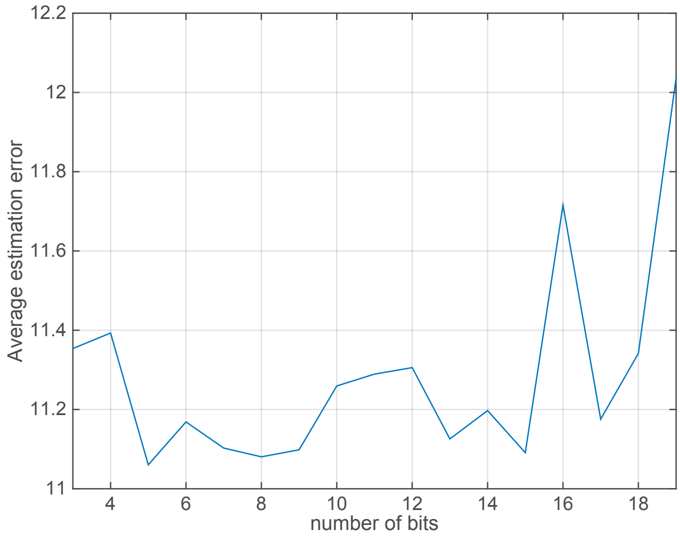

Figure 12.8 – Average estimation error (AEE) along the line $l_f = \lceil 41.4 - 2.47 n_b \rceil$.

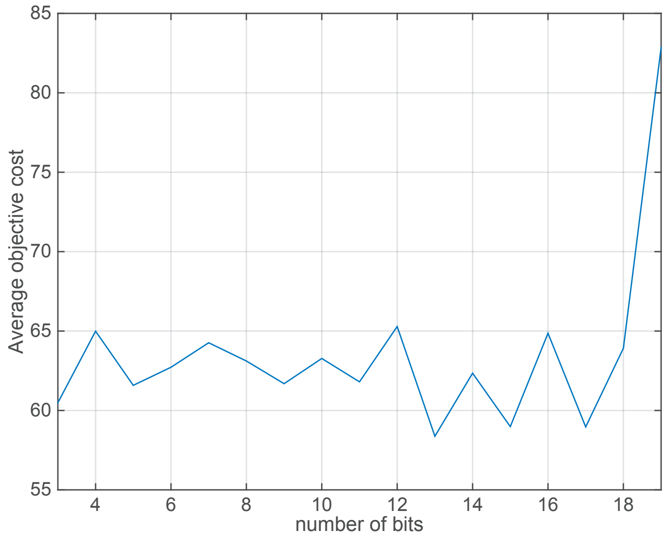

Figure 12.9 – Average control objective cost (ACC) along the line $l_f = \lceil 41.4 - 2.47 n_b \rceil$.

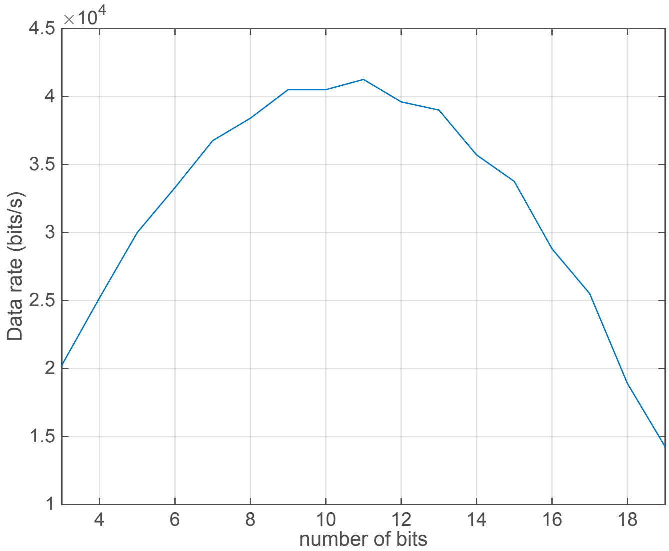

Figure 12.10 – Required data rate along the line $l_f = \lceil 41.4 - 2.47 n_b \rceil$.

Tests with Real Vehicles Part VI

13 Range-Based Formation Control

In order to prepare the Medusa-class autonomous underwater vehicles (AUVs) for more complex tests, in the scope of the MORPH project Abreu et al. [2015], and to introduce a scenario which can profit from the use of distributed estimation methods, as will be seen in Chapter 15, in this chapter we propose controllers for formation control of AUVs in a scenario where we have two surface vehicles (the anchor vehicles) which are equipped with GPS, so as to follow desired paths and one or more follower vehicles which are required to reach and maintain a desired formation with the anchors, relying on measurements of the distances to the leading vehicles and exchanging complementary data. This chapter proposes a control strategy for the follower vehicle that uses simple feedback laws for speed and heading commands to drive along track and cross track errors to zero. Simulation results using a realistic model of an existing marine vehicle are described and discussed. The performance of the algorithm that we propose is demonstrated in sea trials with the same vehicles, equipped with acoustic modems and ranging devices affected by noise, outliers, and communication losses.

13.1 Problem formulation

The range based formation control problem addressed in this chapter can be understood by referring to Fig. 13.1. The objective is to execute a triangular formation keeping maneuver, that is, to drive and maintain a vehicle, henceforth known as the follower, at a desired position with respect to two leader vehicles that run a cooperative path following controller Ghabcheloo et al. [2009]. The follower obtains, via an acoustic ranging and communication device, range measurements to each leader, as well as their headings. These measurements have a period of multiple seconds.

The kinematic model for the AUV is written in terms of its speed and heading. In the figure, the follower is at position p with controlled speed v and heading angle ψ measured with respect to an inertial reference frame. The leaders move in cooperation, with equal reference speed and heading denoted v_l and ψ_l, respectively. For simplicity, we assume that the course and heading angles are equal, i.e. there is no current and side-slip is negligible. The two leaders, denoted x_1 and x_2, move at a fixed distance d from each other.

To describe the geometry of the formation we define an $x-y$ frame with origin at the midpoint between the leaders. The y axis points from x_1 to x_2 and the x axis points 90° clockwise from the y axis. The desired position of the follower, denoted p_d, is at a distance d_1 from x_1 and d_2 from x_2. To disambiguate the two possible locations of p_d we introduce a flag x_d so that if $x_d = 1$ then p_d is on the negative side of the x axis, and if $x_d = -1$ then p_d is on the positive side of the x axis.

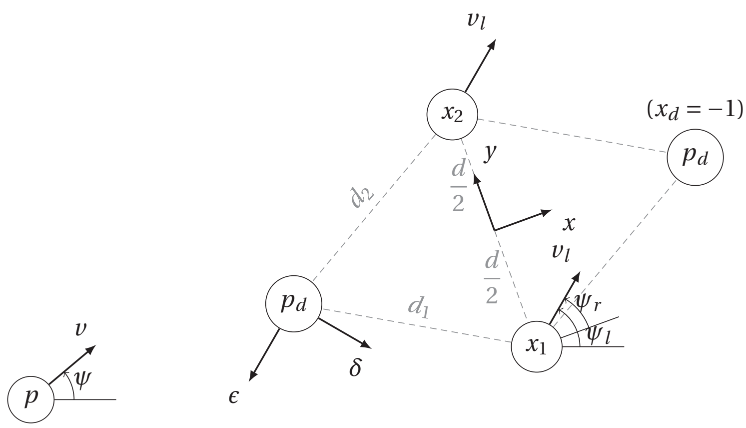

Figure 13.1 – Formation diagram.

For controller design purposes we define the along track - cross track, $\epsilon - \delta$ reference frame with origin at p_d. The along track axis ϵ points in a direction opposite to that specified by the heading of the leaders, that is, $\psi_l + 180°$. The δ axis points 90° anti-clockwise from the ϵ axis. Written in the $\epsilon - \delta$ frame, the kinematics of the follower vehicle are as follows:

$$\dot{p}_\epsilon = v_l - v\cos(\psi - \psi_l) \tag{13.1}$$

$$\dot{p}_\delta = -v\sin(\psi - \psi_l). \tag{13.2}$$

where p_ϵ and p_δ are the ϵ and δ coordinates of p, respectively. The goal is to derive outer-loop feedback laws in p_ϵ and p_δ to drive the follower vehicle to the desired position p_d, specified by the desired distances d_1 and d_2 and by the flag x_d (see Fig. 13.1). If the errors p_ϵ and p_δ go to zero, then p converges to p_d.

13.2 Related Work

Representative work in the area of relative formation control includes that of Desai et al. [1998, 2001] on the so-called leader-follower formation control problem for a formation graph with an arbitrary number of vehicles. In the work cited, two approaches were proposed using either range-bearing or range-range control, depending on the available sensors. In both approaches, knowledge of the leader motion was assumed. A different strategy is employed in Cao and Morse [2007, 2008], where a solution is proposed for a 4-vehicle station keeping problem, requiring exclusively range measurements and a decentralized control policy using switched adaptive control. The vehicle dynamics correspond to single integrators in 2D.

In the more recent work of Cao et al. [2011], the authors advance algorithms to coordinate a formation of mobile agents when the agents can only measure the distances to their respective neighbors. This solution requires that subsets of non-neighbor agents cyclically localize the relative positions of their respective neighbor agents while these are held stationary and only then move to reduce the value of a cost function; the latter is nonnegative and assumes the zero value precisely when the inter-vehicle distances in the formation are the pre-specified desired distances. Again, it is assumed that the mobile agents can be described by kinematic points.

Additional related work includes that of Anderson and Yu [2011], which provides conditions on the range measurements required for each vehicle to infer the relative positions of its neighbors in its own coordinate frame. In the work of Kim et al. [2007], a method is presented for formation keeping of an unmanned aerial vehicle using relative range information. The proposed controller is designed using classical input-out feedback linearization methods. It is important to observe that the performance of any of these methods depends on the accuracy of the range measurements, which are often subject to sensor noise and only available at discrete times. To cope with this limitation, an extended Kalman filter, such as the one proposed in Alcocer et al. [2007], can be useful as part of a range based formation keeping algorithm. A similar approach has been proposed for merging inertial and range information for localization purposes (e.g. Allotta et al. [2011]).

Motivated by the above considerations, Soares et al. [2012, 2013] addressed the simplified problem of maintaining an autonomous vehicle in a moving triangular formation with respect to two leader vehicles that move at the same speed and with constant separation. The follower vehicle has no a priori knowledge of the path described by the leaders and its goal is to follow them by regulating its relative position to a desired point in the formation, using range measurements and the heading of the leaders.

The present chapter borrows the framework and control structure proposed in Soares et al. [2012]. However, it departs from it in that it deals with a flexible geometry, where the formation is not restricted to the case where the distance to the two leader vehicles is identical and the two-leaders travel side by side. Rather, the leaders follow the same path with one trailing the other. To cope with this new situation, instead of regulating the common- and differential- mode errors defined in the previous work, suitably defined along track and cross track errors are regulated to zero. This set-up is strongly influenced by the mission scenarios adopted in the scope of the EU FP7 project MORPH (Kalwa et al. [2013]), where a formation is spearheaded by a single vehicle equipped with a multibeam echosounder and trailed by a communication coordination vehicle.

13.3 Controller design

The control system, depicted in Fig. 13.2, consists of multiple discrete modules. The follower vehicles receive periodically, with an acoustic modem, messages from the leader vehicles. These messages contain the heading of the leader ψ_l^{aco}, and through a Dynamic Long Baseline (DLBL) method one can compute the message travel time between the leader and the follower in the acoustic medium t^{aco}. These signals are then processed to exclude outliers and filtered through Kalman filters yielding estimates of the distance between the follower and x_1 ($\hat{z}_1$), the distance between the follower and x_2 ($\hat{z}_2$), and the circular mean of the leaders' angle ($\hat{\psi}_l$). The distance estimates $\hat{z}_1$ and $\hat{z}_2$ are used to compute (p_ϵ, p_δ), the estimated position of the follower in the $\epsilon - \delta$ frame. Using the ϵ coordinate, a velocity controller computes a command of desired speed u_d which is then linearly transformed to a common mode command. Finally, with the leaders' heading estimate $\hat{\psi}_l$ and the δ coordinate, a heading controller yields a reference for the follower's heading angle ψ_d. The details of each module are presented in the subsections below.

13.3.1 Outer-loop feedback

One distinctive characteristic of this work is the use of simple control laws that separately regulate the desired linear velocity u_d and heading ψ_d. These are then fed to inner loop controllers specific to the vehicle.

The control law for the desired velocity is given by

$$u_d = \mathrm{sat}\left(k_{up} p_\epsilon + k_{ui} \int_0^t p_\epsilon d\tau + v_{l_{nom}}\right), \tag{13.3}$$

where k_{up} is the proportional gain, k_{ui} is the integral gain and $v_{l_{nom}}$ is a scenario-configurable nominal velocity. While not strictly required, the use of a $v_{l_{nom}}$ close to the leader speed accelerates the convergence to the desired speed and position. The final value is run through a saturation function that limits the output to $[v_{\min}, v_{\max}]$. An integration clamping anti-windup scheme is adopted, *i.e.* the integration is interrupted when the control variable

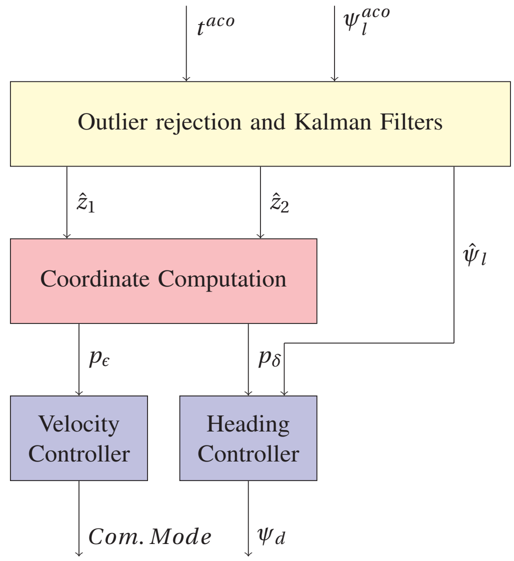

Figure 13.2 – Control system diagram.

saturates and the control error and control variable have the same sign.

The control law for ψ_d is given by

$$\psi_d = \hat{\psi}_l + \text{sat}\left(k_{\psi p} p_\delta + k_{\psi i} \int_0^t p_\delta d\tau\right). \tag{13.4}$$

The heading controller tracks the reference heading estimated from the information sent by the leaders, and adds a PI controller on the error p_δ. The output of the PI controllers is saturated to $[-0.5rad, 0.5rad]$ so that, even for large errors, the vehicle does not move in a direction opposite the leaders'. As in the case of the velocity control law, an integration clamping anti-windup scheme is implemented.

With these control laws, defining $\eta := v_l - k_{ui} \int_0^t p_\epsilon d\tau - v_{l_{nom}}$ and $\xi := -k_{\psi i} \int_0^t p_\delta d\tau$ and neglecting the inner loop dynamics, i.e. considering $v = u_d$ and $\psi = \psi_d$ we may linearize the kinematics of the follower about the desired position p_d and about heading $\psi = \psi_l$ and speed $v = v_l$ yielding, from (13.1) and (13.2),

$$\begin{bmatrix} \dot{p}_\epsilon \\ \dot{\eta} \end{bmatrix} = \begin{bmatrix} -k_{up} & 1 \\ -k_{ui} & 0 \end{bmatrix} \begin{bmatrix} p_\epsilon \\ \eta \end{bmatrix}, \tag{13.5}$$

and

$$\begin{bmatrix} \dot{p}_\delta \\ \dot{\xi} \end{bmatrix} = \begin{bmatrix} -v_l k_{\psi p} & v_l \\ -k_{\psi i} & 0 \end{bmatrix} \begin{bmatrix} p_\delta \\ \xi \end{bmatrix}. \tag{13.6}$$

The characteristic polynomial for the p_ϵ dynamics is $s^2 + sk_{up} + k_{ui}$ and the characteristic polynomial for the p_δ dynamics is $s^2 + sv_l k_{\psi p} + v_l k_{\psi i}$. Therefore, we may select the gains for p_δ as $k_{up} := 2\zeta_u \omega_{nu}$ and $k_{ui} := \omega_{nu}^2$ and the gains for p_ϵ as $k_{\psi p} := \zeta_\psi \omega_{n\psi} / v_l$ and $k_{\psi i} := \omega_{n\psi}^2 / v_l$.

13.3.2 Outlier rejection

Due to the nature of acoustic ranging, erroneous readings are frequent, especially in shallow waters with irregular seabed topography. Therefore, the range samples received must be filtered for outliers. A measurement m is accepted if it is inside the interval

$$[a - s_{max} \cdot (t - t_l), a + s_{max} \cdot (t - t_l)]\,. \tag{13.7}$$

For $z := v_{sound} \cdot t^{aco}$ to be accepted, we consider $s_{max} = v_{max}$, the maximum speed of the vehicle, and for ψ_l^{aco} to be accepted we consider $s_{max} = \omega_{max}$, the preset maximum angular speed.

When a measurement is accepted, a and t_l are updated according to $t_l = t$ and $a(k+1) = (1 - k_{acc}) \cdot a(k) + k_{acc} \cdot m$, where $k_{acc} = 0.5$. When a measurement is not accepted but is inside the interval

$$[a - 4s_{max} \cdot (t - t_l), a + 4s_{max} \cdot (t - t_l)]\,, \tag{13.8}$$

then a is updated as $a_{k+1} = (1 - k_{rej}) \cdot a_k + k_{rej} \cdot m$, where $k_{rej} = 0.25$. A measurement outside these ranges is discarded.

13.3.3 Kalman filter

The long period between samples and relatively fast error dynamics require the use of an estimator to improve the behavior of the controllers. The problem is further exacerbated in the presence of packet loss, frequent for some scenarios and particular modem alignment conditions. The estimated states are $\hat{z}_1$, $\hat{z}_2$ and $\hat{\psi}_l$ with one Kalman filter for each state, and their respective discrete-time increase or decrease rate. In precise terms, we chose to use a Kalman filter, with a design model as follows:

$$x_{k+1} = Ax_k + w, \tag{13.9}$$

where A is defined as

$$A = \begin{bmatrix} 1 & 1 \\ 0 & 1 \end{bmatrix}, \tag{13.10}$$

and w is process noise with covariance matrix Q. The output equation is

$$y_k = Hx_k + v_k, \tag{13.11}$$

where H is defined as

$$H = [1\ 0], \tag{13.12}$$

and v_k is process noise with covariance matrix R. The sampling period considered is 0.2 seconds. Notice that we only perform the update step when a measurement is received, *i.e.* during most samples only the prediction step is performed.

The Kalman filters are updated each time a new measurement is accepted. The estimated ranges $\hat{z}_i$ are updated with $y = v_{sound}\ t_i^{aco}$ and the estimated leaders' average heading $\hat{\psi}_l$ is updated with the circular mean of the last accepted headings from each leader.

13.4 Simulation results

Simulations were carried out in order to evaluate the performance of the algorithm in preparation for the sea trials. For this purpose, we used a Simulink model of the MEDUSA AMV shown in Fig. 13.3, with the inner loop controller for heading described in Ribeiro et al. [2012].

Figure 13.3 – The Medusa vehicles.

The two leaders follow the same path at $0.5m/s$ with the follower at starboard of the leaders. Each vehicle is $15m$ away from the others, that is, $\psi_l = -\pi/2$, $x_p = 1$ and $d_1 = d_2 = d = 15m$. The acoustic modems of each of the leader vehicles transmit information with a period of $4s$. The simulation time step is of $0.2s$. Sensing and ranging imperfection are taken into account, with a packet loss rate of 40% and added Gaussian ranging noise with a standard deviation of $\sigma = 0.45m$. The parameters of the ROF controller are the following:

- ω_{nu} - 0.041,
- ζ_u - 0.82,
- $\omega_{n\psi}$ - 0.0022,
- ζ_ψ - 8.9.

The simulated paths of the vehicles can be seen in Fig. 13.4 and the along track and cross track errors are shown in Fig. 13.5.

From Figures 13.4 and 13.5 we can conclude that the control algorithm achieves the objective of keeping the vehicles in formation, and is able to cope with packet losses and sensor noise with a standard deviation of $0.45m$.

After an initial transient phase, the along track and cross track errors are bounded between $-5m$ and $5m$. There is, nevertheless, room for improvement on the range measurement filters, especially to mitigate the effect of packet losses. A possible enhancement would be using an extended Kalman filter (EKF) that takes into account the input commands.

13.5 Sea trials

To verify the performance of the ROF controller, trials were performed at Parque das Nações, Lisbon, Portugal, in a closed harbor with shallow waters and no boat traffic. The MEDUSA AMVS, developed at the LARSyS/ ISR/IST, Lisbon, Portugal, were used in the sea trials.

The vehicles implement a Dynamic Long Baseline method conceived by the NATO Center for Maritime Research and Experimentation (CMRE) atop functionalities present in the EvoLogics modems (Kebkal et al. [2012]). Each node has the ability to accurately time-stamp, in a local clock, the incoming and outgoing packets. Every packet

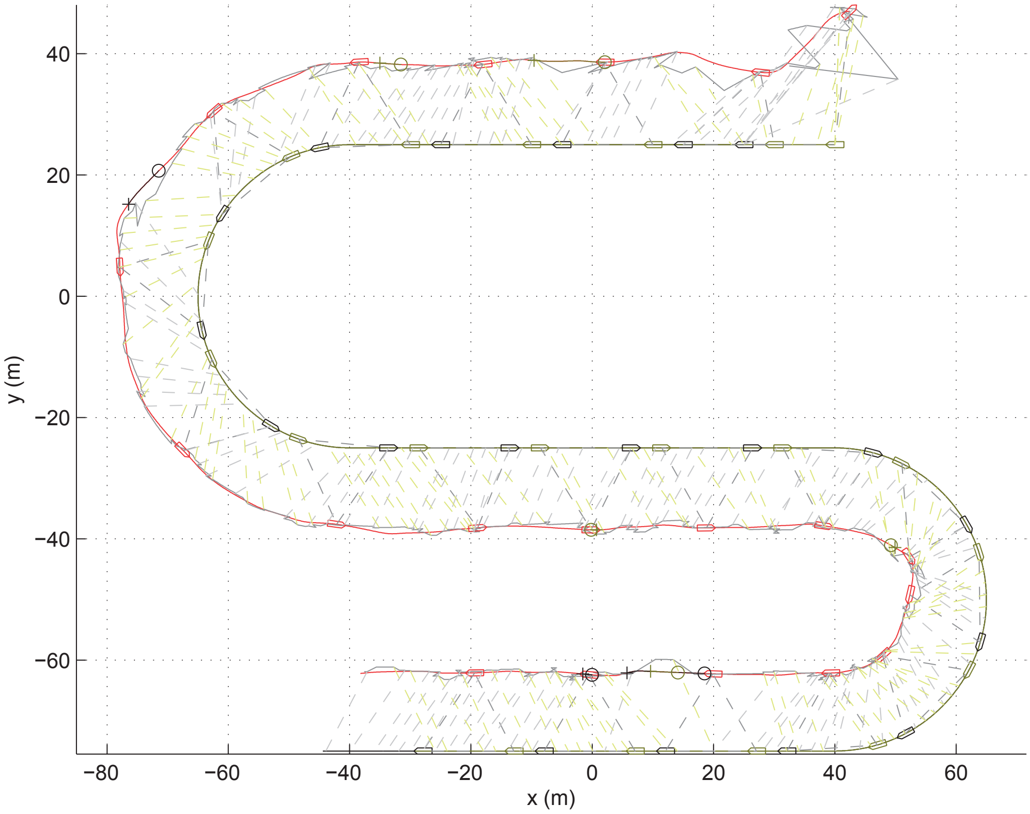

Figure 13.4 – Simulated vehicle paths. The solid red line is the actual path followed by the vehicle, the gray solid line represents the computed path with range measurements, and the dashed lines represent range measurements. The segments between a circle and a cross represent periods during which no range measurement was received from one of the vehicles in the preceding 12 seconds.

sent is then used as a query and yields N-1 replies in a distributed LBL scheme, considering the time differences between queries receptions and reply transmission. Since the nodes are at close distance, rigid time-division multiple access (TDMA) is used without incurring a large penalty in channel capacity. Heading exchanges are piggybacked on these localization packets. At the end of each round, and in the absence of losses, all vehicles will know the distance to and heading of every other vehicle in communication range. This is an improvement over the simple ping-reply model used in Soares et al. [2013].

During this trial, we again considered the mission described in Section 13.4. The paths described by the vehicles during the trial are shown in Fig. 13.6 and the along track and cross track errors are shown in Fig. 13.7. Aside from minimal disturbances, the follower is able to better track the leaders than observed in the simulation. This suggests that either our vehicle model is not a sufficiently accurate representation of the real vehicles and/or that our simulation overestimates sensor noise and packet losses. The latter is found to be true, with packet loss during trials recorded as 8.12%, compared to the 40% rate used in simulation.

13.6 Conclusions

This chapter proposed a solution to a three-vehicle formation keeping problem where a follower moves in a triangular formation with two leader vehicles. The follower has no knowledge of the path taken by the leaders, and uses only inter-vehicle range measurements, the predefined relative position between the two leaders and their headings.

Preliminary simulation results were described for a lawnmower motion using a dynamic model of the Medusa

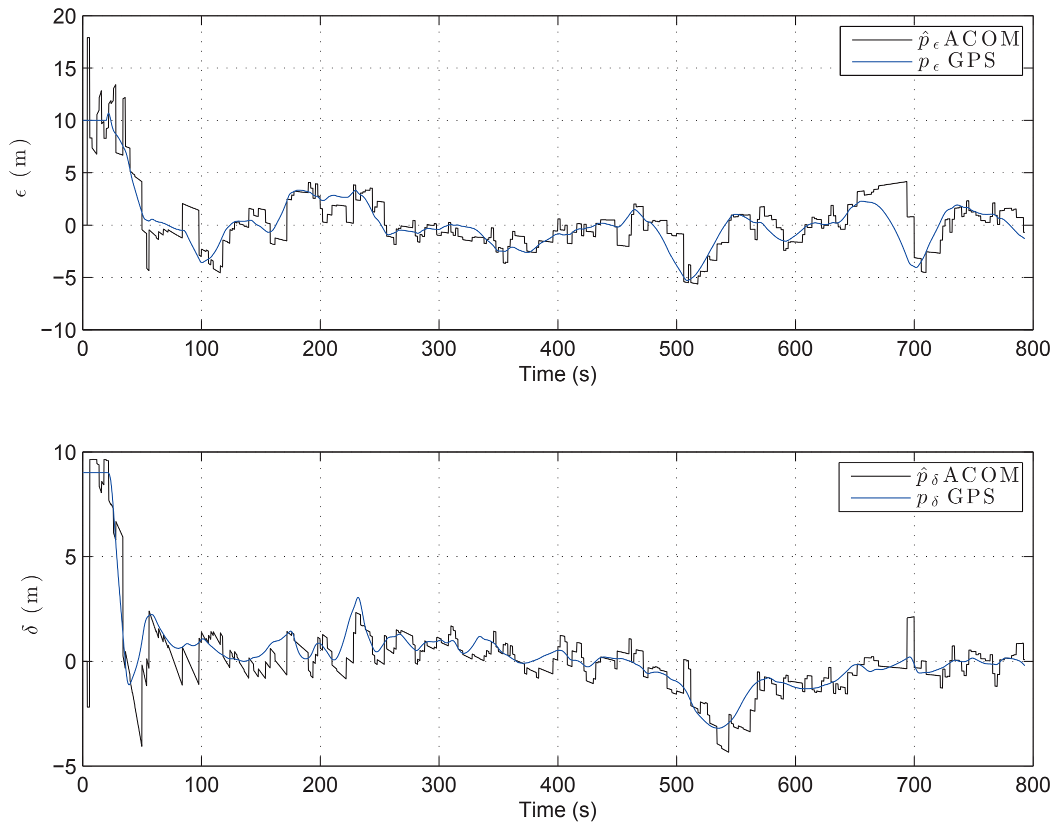

Figure 13.5 – Along track (p_ϵ) and cross track (p_δ) errors during simulation. The black line represents the estimated errors from the ranges measured by the virtual acoustic modems. The blue line indicates the exact along track and cross track errors, as if they were computed using continuous exact measurements.

vehicles developed at ISR/IST. The results show good performance with error bounded to a $5m$ window.

We have also addressed the implementation and testing of the algorithm in marine scenarios using real marine vehicles. The algorithm is able to deal with range measurements that are only available at discrete points in time, with a period of several seconds. Furthermore, these measurements are affected by sensor noise and outliers, as well as communication delays and temporary losses.

Future steps will include the analysis of the performance and robustness of the algorithm proposed. A simple but significant improvement would be to use estimators with accurate vehicle dynamics, taking into account the commands given to the vehicle, as well as other data, namely from inertial sensors.

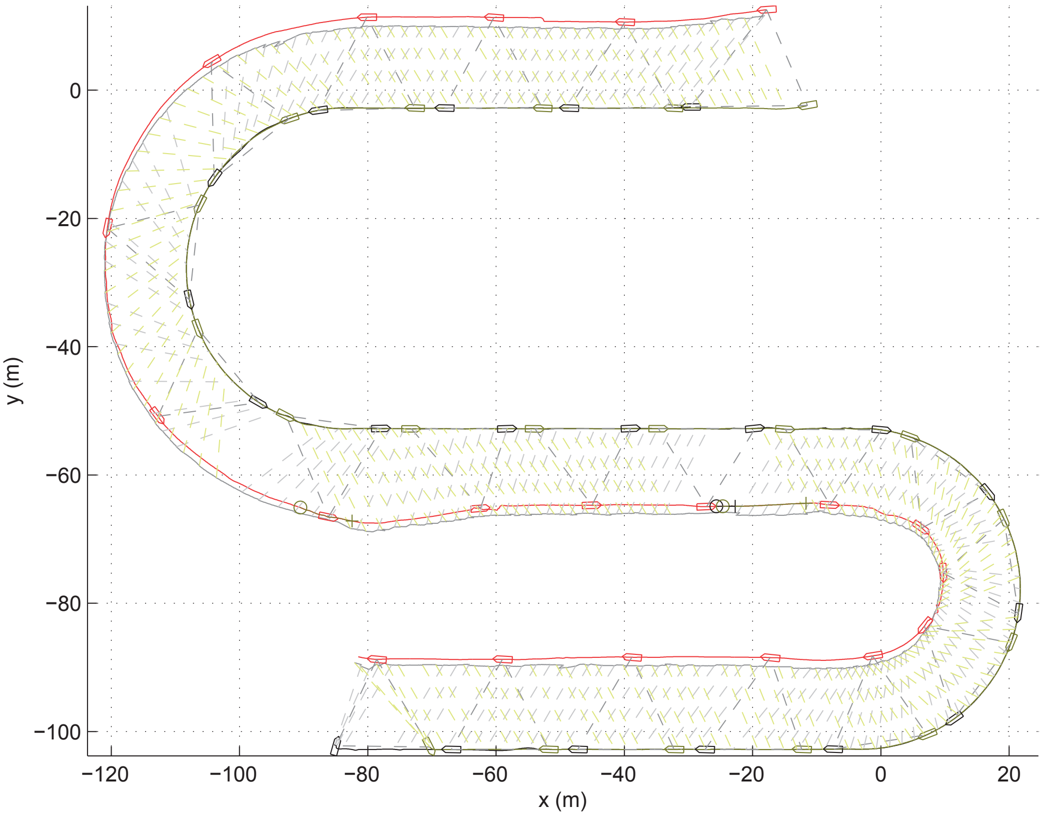

Figure 13.6 – Vehicle paths during trials. The follower vehicle is plotted in red and the leaders are plotted in black and yellow.

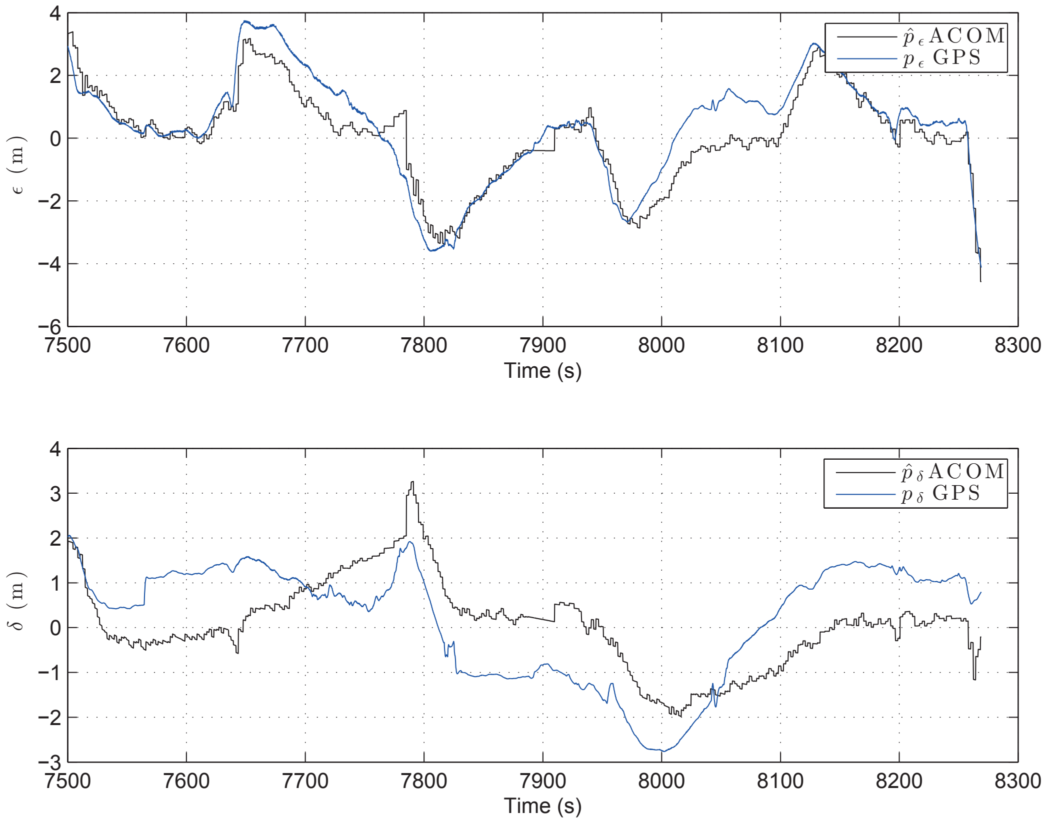

Figure 13.7 – Along track (p_ϵ) and cross track (p_δ) errors during trials. The black line represents the estimated errors from the ranges measured by the acoustic modems. The blue line indicates the along track and cross track errors computed using RTK GPS measurements.

14 Cooperative Path-Following with Event-Based Communications Field Tests

This chapter contains the results of field trials with autonomous marine vehicles that illustrate the efficacy of the event-triggered coordinated path following algorithm derived in Chapter 10. In addition, on each test, a saturation of the RPM control signal in one of the vehicles (the so-called Medusa-black vehicle) is temporarily enforced in order to test the resilience of the proposed algorithms to transient events that may have a negative impact on coordination.

14.1 Test Set-up

The field tests were performed with 3 Medusa-class AUVs, the properties developed by DSOR/ISR. We name the vehicles with the Black, Red and Yellow MEDUSAs, corresponding to their colors. The vehicles and its operation during the test are illustrated by Figure 14.1. Each Medusa vehicle is equipped with a navigation system using GPS that allows it to access its own position. The communications among the vehicles take place using a wi-fi connection. For further details on the technology used in the Medusa vehicles, we refer to Abreu et al. [2016].

a - Medusa vehicles

b - Red, Yellow and Black Medusas operating at sea

Figure 14.1 – Medusa surface vehicles and an aerial snapshot during the tests.

The communication topology between the vehicles used during the field tests is shown in Figure 14.2.

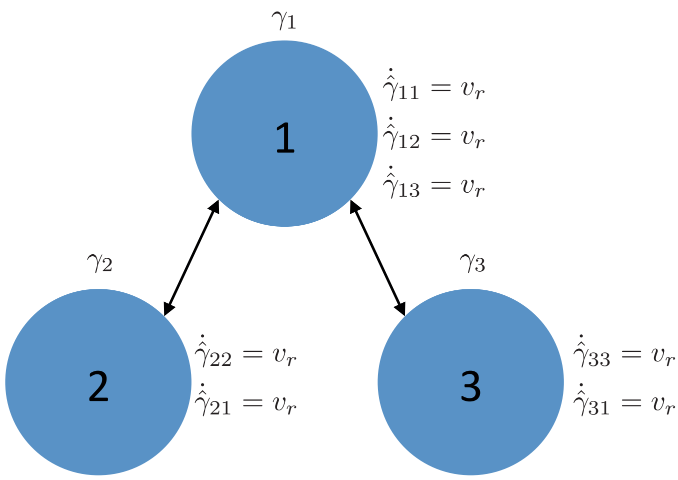

Figure 14.2 – Communication topology and filters running at each vehicle. Vehicle 1 is the Red vehicle, vehicle 2 is the Black vehicle, and vehicle 3 is the Yellow vehicle.

The performed mission in all the reported trials was the following:

- Nominal path for the RED vehicle: Lawnmower trajectory with 30m length for straight line segments and 12m radius for circle segments,
- Formation: Alongside alignment, 5m of separation with the red vehicle at the center following the nominal path,
- Nominal speed along the nominal path: $v_r = 0.5$m/s.

In the following plots, when displaying the dimensionless path-following variable, the latter corresponds to the arc-length in meters along the nominal path, i.e. the path taken by the red vehicle.

In the field tests the following algorithms were tested:

- Coordinated path-following with event-triggered communications with $\epsilon = 0.2$m, $\epsilon = 0.6$m, and $\epsilon = 1.4$m,
- Coordinated path-following with event-triggered communications with $\epsilon = 0.6$m, subjected to packet losses (with a probability of communication loss of 20%) considering delays up to 2 seconds[1].

14.2 Periodic Communications

To evaluate the performance of the controllers developed in the best case scenario, we tested the coordinated path-following algorithm with periodic communications with a period of 0.2 seconds, which is equal to the sampling period of the controller. The enforced saturation of motor propeller speed of the black vehicle occurs at the beginning of the third circular segment, 400 seconds after the start of the mission, until 550 seconds after the start of the mission. The trajectories of the vehicles are shown in Figure 14.3 and the evolution of the path-following variables is displayed in 14.4.

We can observe from both Figure 14.3 and 14.4 that coordination is achieved from the beginning of the mission and is maintained throughout the mission, even during the saturation of motor propeller speed of the black

[1] Since we are using a wi-fi network, message transmissions are virtually instantaneous. However, we assume that delays of up to 2 seconds could be possible and therefore in the case of a packet loss a message will only be resent after 2 seconds.

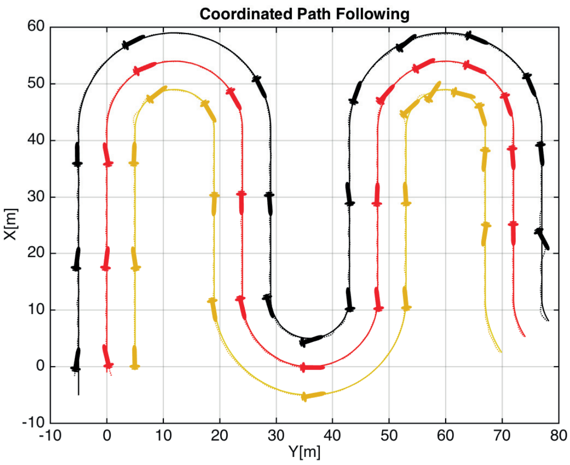

Figure 14.3 Vehicle paths for CPF with periodic communications.

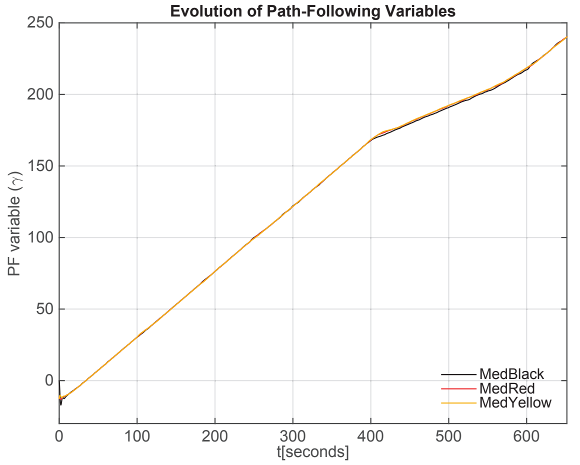

Figure 14.4 Path-following variables for CPF with periodic communications.

vehicle. It is apparent also from Figure 14.4 that, since the black vehicle is not able to follow its assigned speed, all the vehicles follow their assigned paths with a speed lower than the pre-defined.

14.3 Trajectory Tracking

Since all the vehicles have synchronized clocks, when the vehicles perform trajectory tracking they evolve in a coordinated formation without requiring communications. The trajectory of the vehicles is shown in Figure 14.3. The saturation of the black vehicle propeller rotation occurs in the beginning of the second straight line. This was done to avoid that the black vehicle will depart from its path and collide with other vehicles, since it is not able to follow its assigned position. This possibility highlights the advantage of cooperative path-following with respect to trajectory tracking, for its resilience to events that force one or more vehicles away from its defined position.

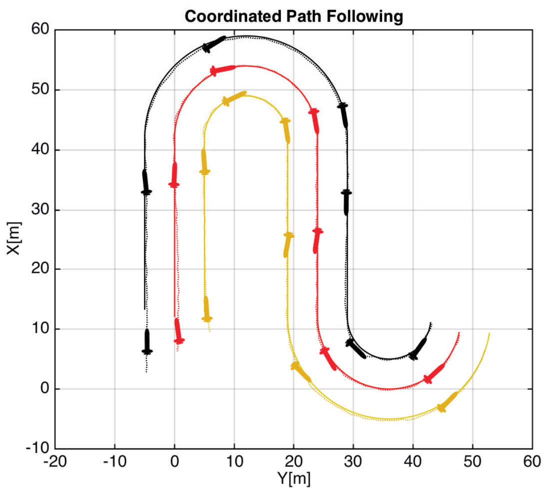

Figure 14.5 – Vehicle paths performing trajectory tracking.

It is clear that, because the vehicles are not aligned and not moving at the beginning of the mission, they do not align during the whole first straight line, and they only coordinate during the first circular segment. In contrast with the behaviour of the cooperative path-following, uncoordination is very apparent during the saturation. However, after the saturation is removed the vehicles become aligned again.

14.4 Event-triggered Communications

This section contains the main results of this chapter, where it is shown the results of the field tests of the cooperative path-following algorithm with event-triggered algorithms for values of ϵ of 0.2, 0.6 and 1.4. For all the performed tests in this section a saturation of the propeller rotation was introduced in the black vehicle, between 400 and 550 seconds from the beginning of the mission, which corresponds to the period from the beginning of the third circular segment to the middle of the fourth straight line segment.

14.4.1 Test with $\epsilon = 0.2$

Figures 14.6 and 14.7 contain the trajectories of the vehicles and the evolution of the path-following variables for $\epsilon = 0.2$.

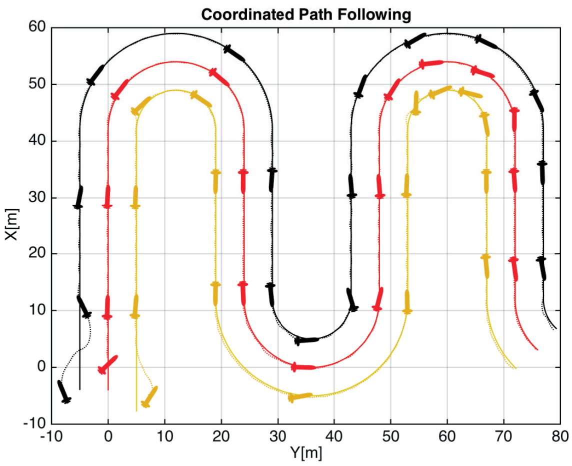

Figure 14.6 Vehicle paths for event-triggered communications with $\epsilon = 0.2$.

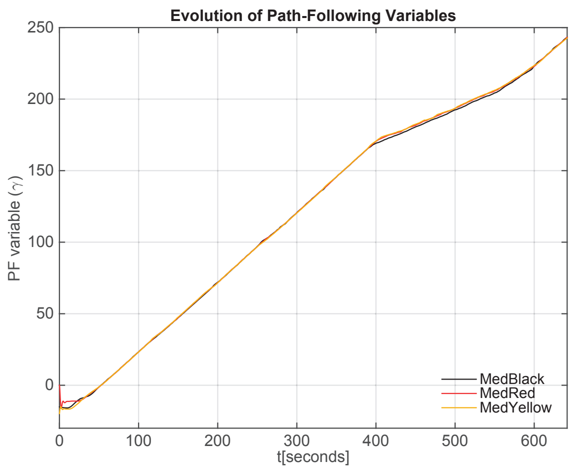

Figure 14.7 Path-following variables for event-triggered communications with $\epsilon = 0.2$.

One can observe from Figures 14.6 and 14.7 that coordination is maintained throughout the test with the vehicles running at a lower speed during the enforced saturation. The communication events between the vehicles and the estimation errors are plotted in Figures 14.8, 14.9 and 14.10.

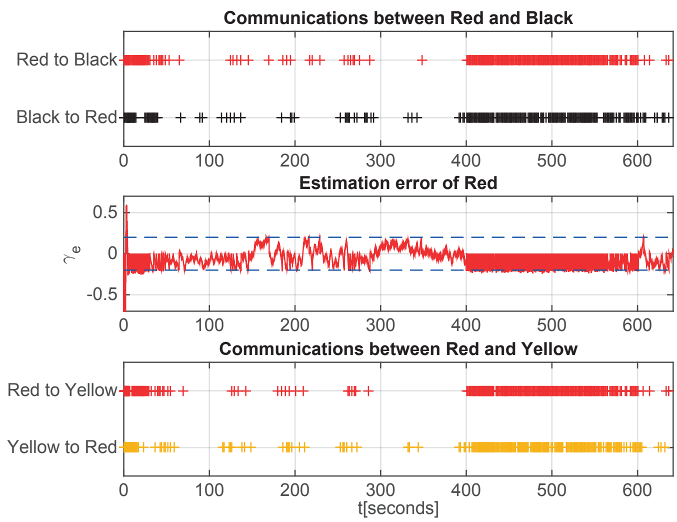

Figure 14.8 – Communication events and estimation error on the red vehicle for $\epsilon = 0.2$.

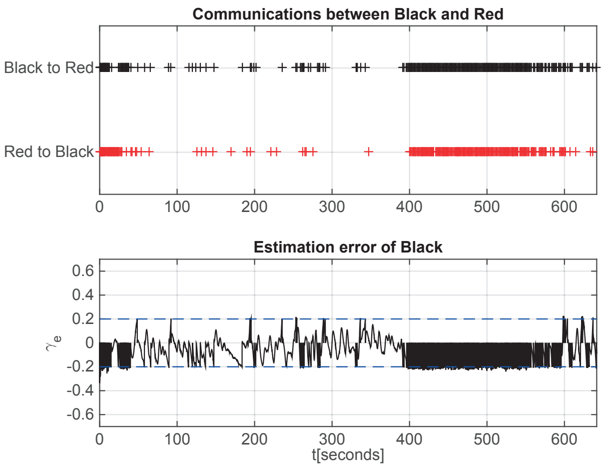

Figure 14.9 Communication events and estimation error on the black vehicle for $\epsilon = 0.2$.

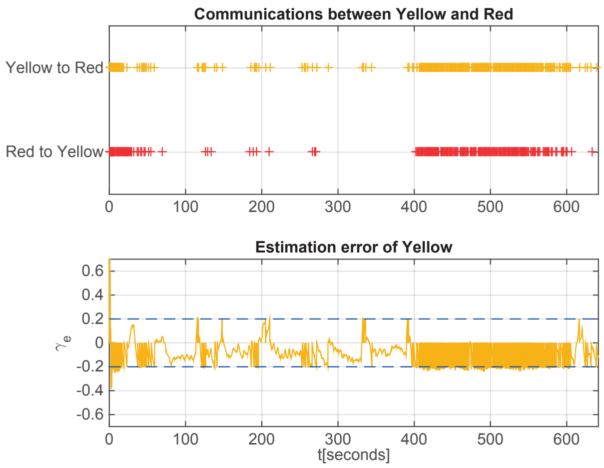

Figure 14.10 Communication events and estimation error on the yellow vehicle for $\epsilon = 0.2$.

From Figures 14.8, 14.9 and 14.10, one can observe large periods without communications after the initial period when the vehicles are still converging to the paths from their initial positions and before the enforced saturation. However, the number of communications is still elevated. During the enforced saturation, since the vehicles move at a speed which is lower than the reference, the estimates of the path, the vehicles communicate almost periodically. As expected, since we do not have packet losses in this test, the estimation error of all the vehicles never surpasses 0.2.

14.4.2 Test with $\epsilon = 0.6$

For $\epsilon = 0.6$ the trajectories and path following-variable evolution of the three vehicles were the ones plotted in Figures 14.11 and 14.12.

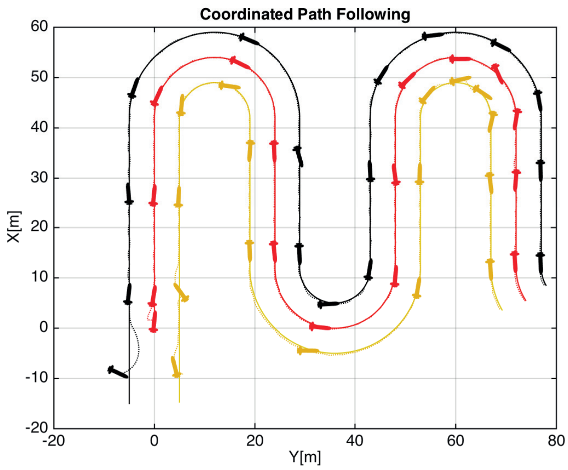

Figure 14.11 Vehicle paths for event-triggered communications with $\epsilon = 0.6$.

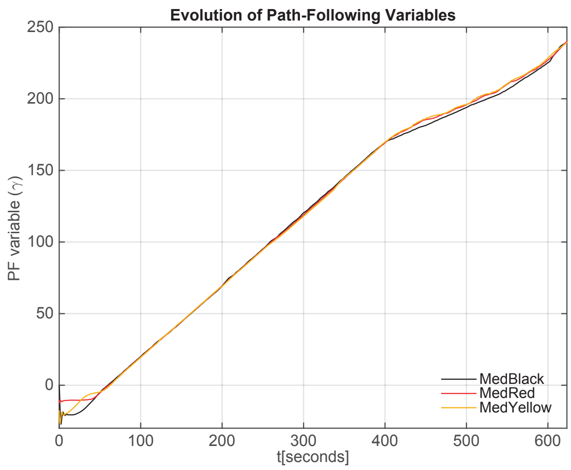

Figure 14.12 Path-following variables for event-triggered communications with $\epsilon = 0.6$.

From both Figure 14.11 and 14.12 it is visible a slightly worse performance during the saturation than for the case with $\epsilon = 0.2$. Figures 14.13, 14.14 and 14.15 contain the communication instants and estimation errors of the path-following variables of all the vehicles.

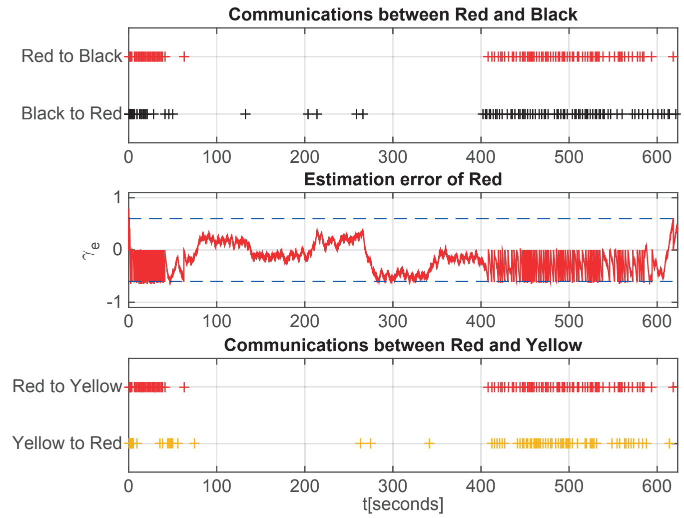

Figure 14.13 – Communication events and estimation error on the red vehicle for $\epsilon = 0.6$.

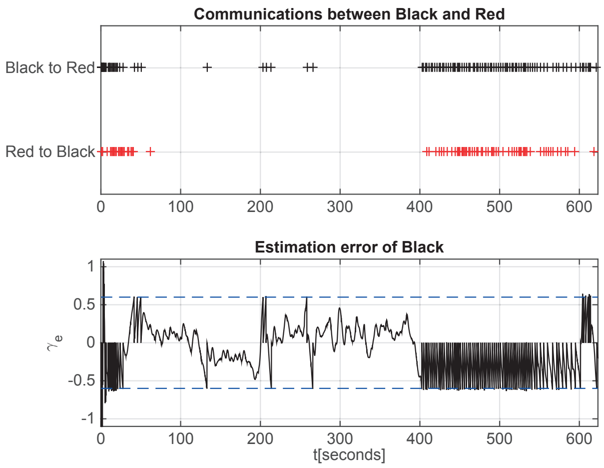

Figure 14.14 Communication events and estimation error on the black vehicle for $\epsilon = 0.6$.

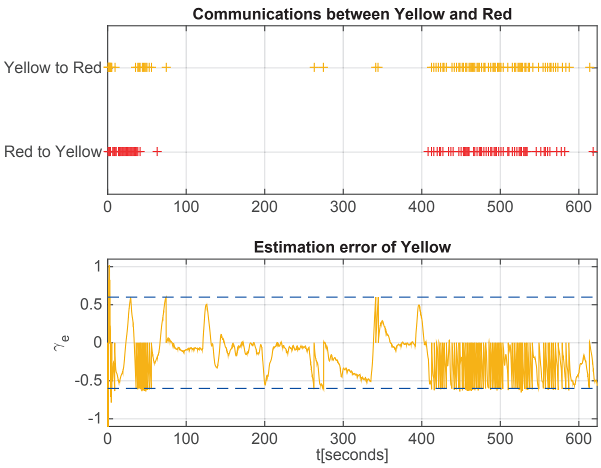

Figure 14.15 Communication events and estimation error on the yellow vehicle for $\epsilon = 0.6$.

From Figures 14.13, 14.14 and 14.15 one can observe that after the initial convergence and before the enforced saturation the communications are sporadic and occur only at the instants when the vehicles enter or leave the circular segments. This is the case since the outer and inner vehicles on the circular segment are required to respectively accelerate and decelerate instantaneously to follow their pre-defined paths.

14.4.3 Test with $\epsilon = 1.4$

For $\epsilon = 1.4$ the trajectories followed by the vehicles and the path-following variables of the vehicles were the ones shown in Figures 14.16 and 14.17 respectively.

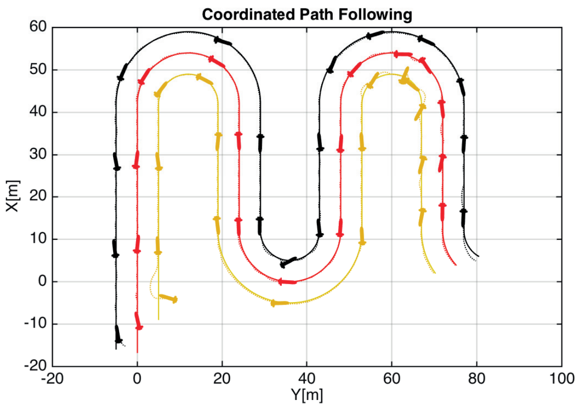

Figure 14.16 Vehicle paths for event-triggered communications with $\epsilon = 1.4$.

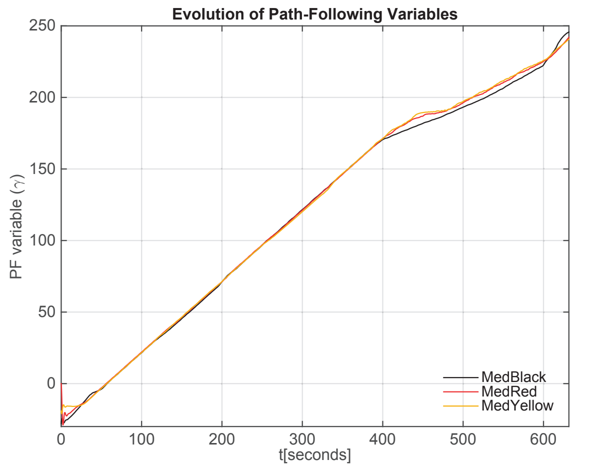

Figure 14.17 Path-following variables for event-triggered communications with $\epsilon = 1.4$.

During most of the mission the vehicles are coordinated. However, it is apparent that during the enforced saturation we have a much worse performance than in the previous cases with the black vehicle further behind the other two vehicles. Also, during the enforced saturation, one can observe oscillations in the heading of the yellow vehicle. This is likely due to sudden variations of reference speed whenever a message is received. The communications events between the vehicles were the ones shown in Figures 14.18, 14.19 and 14.20.

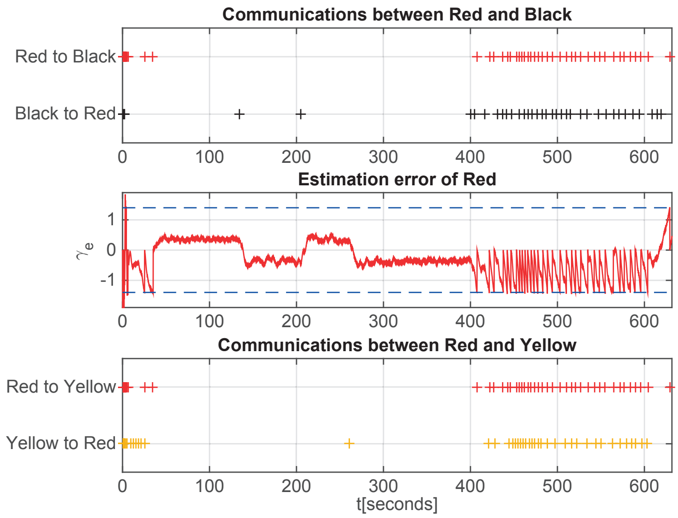

Figure 14.18 – Communication events and estimation error on the red vehicle for $\epsilon = 1.4$.

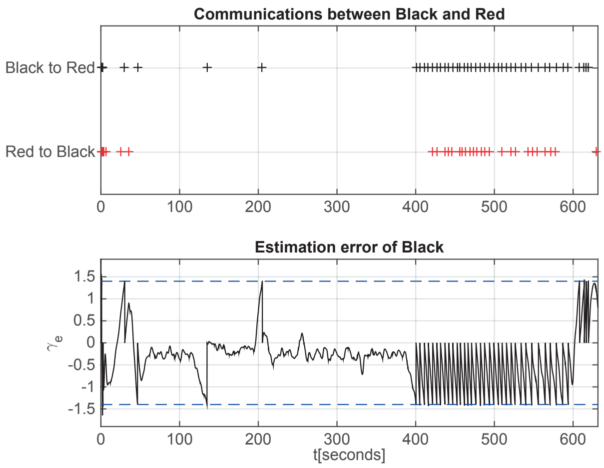

Figure 14.19 Communication events and estimation error on the black vehicle for $\epsilon = 1.4$.

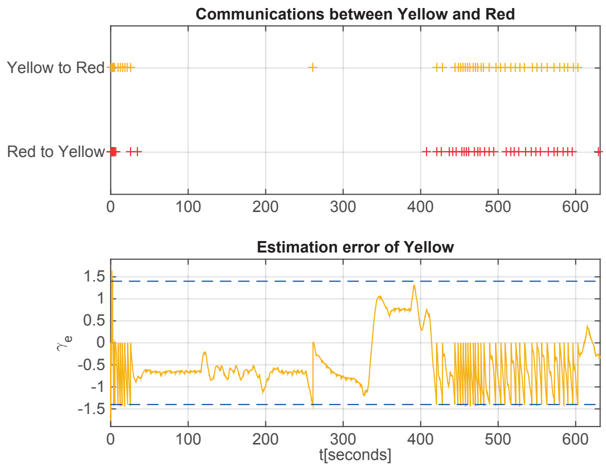

Figure 14.20 Communication events and estimation error on the yellow vehicle for $\epsilon = 1.4$.

In this case we obtain a very low number of exchanged messages after the vehicles reach coordination and before the saturation. In total after coordination and before saturation we can count only two communications from the black vehicle and one from the yellow.

14.5 Event-triggered Communications with Packet Losses

To check the predicted performance with acoustic communications we perform tests with packet losses and delays for $\epsilon = 0.6$. The saturation only takes 40 seconds and occurs at the start of the third straight line.

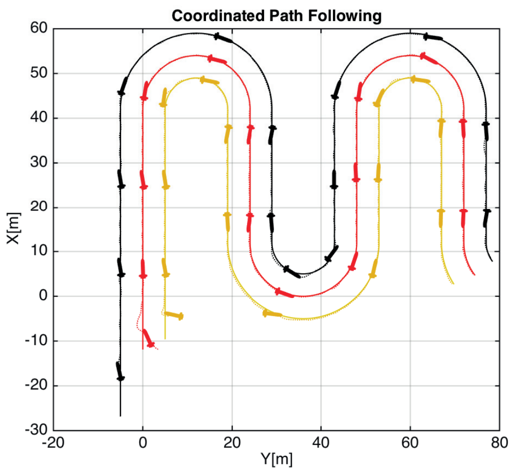

Figure 14.21 Vehicle paths for event-triggered communications with $\epsilon = 0.6$ and packet losses.

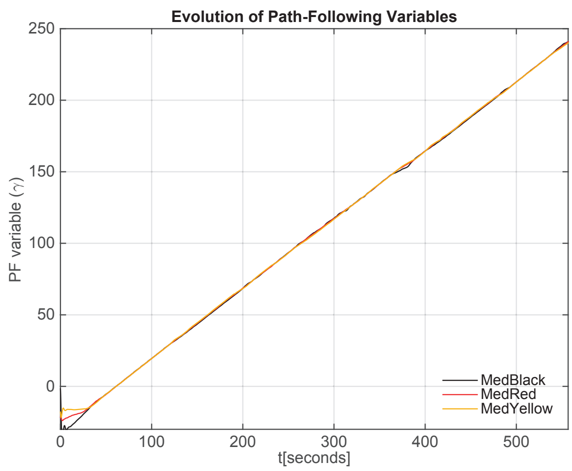

Figure 14.22 Path-following variables for event-triggered communications with $\epsilon = 0.6$ and packet losses.

We can observe from Figures 14.21 and 14.22 that the performance is similar to the case without packet losses and $\epsilon = 0.6$. The communications among vehicles are shown in Figures 14.23, 14.24 and 14.25.

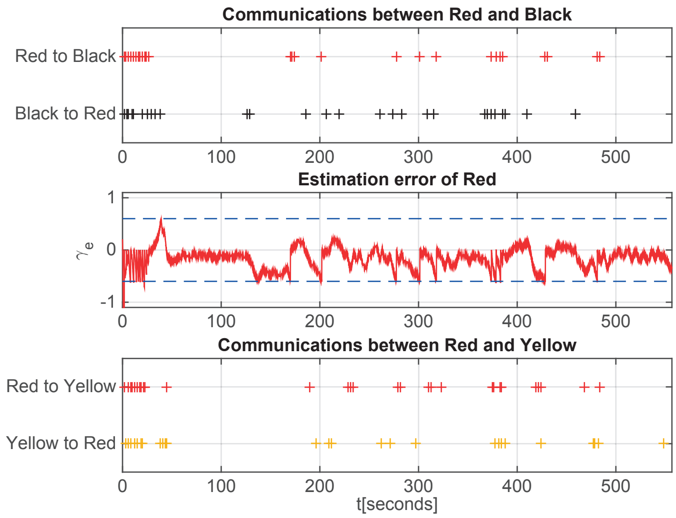

Figure 14.23 – Communication events and estimation error on the red vehicle for $\epsilon = 0.6$ and packet losses.

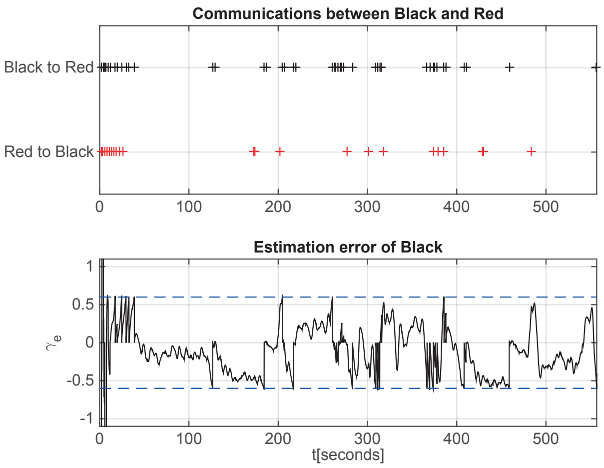

Figure 14.24 Communication events and estimation error on the black vehicle for $\epsilon = 0.6$ and packet losses.

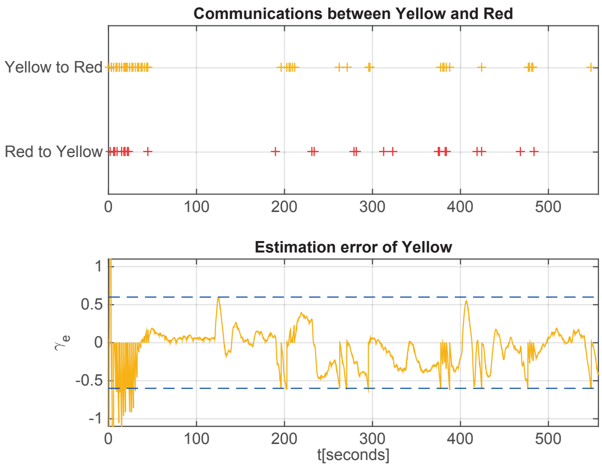

Figure 14.25 Communication events and estimation error on the yellow vehicle for $\epsilon = 0.6$ and packet losses.

One can observe that the communications events are still sparse in this situation. However, the numbers of exchanged messages is much larger than in the case without packet losses.

15 Cooperative Navigation with Quantized Communications Tests

15.1 Test setup

To test the performance of the algorithms described in Chapter 12 a set-up was mounted composed by three model cars (AMZ Atomic) controlled with an R/C radio connected to a computer with a PcTX cable, a cable that transmits pulse width modulated (PWM) commands to the R/C radio that will be relayed to the steering servo and the electronic speed controllers in the model cars. The tests were conducted in a room equipped with an OptiTrack vision tracking system which measured the position of the vehicles. The algorithms controlling the cars were implemented in MATLAB.

15.2 Distributed Luenberger Observer

The trials consist of three vehicles which can only measure ranges to neighbours and communicate with neighbour vehicles. The vehicles are also able to measure the range to a virtual beacon vehicle with a known position. Those measurements are used on a distributed Luenberger observer, which is used to estimate the vehicle's positions by exchanging estimates. The position estimate is then used to control the cars using a trajectory tracking algorithm. This set-up emulates the situation where we have a fleet of AUVs equipped with acoustic modems capable of measuring ranges to a limited set of neighbours.

In the setting of these trials all the non-beacon vehicles communicate with each other and measure ranges to each other and to a set of beacon vehicles $\mathscr{B}^i$. Only one communication with a finite number of bits, which will vary on each test, is allowed after each vehicle makes the range measurements. We consider a fully connected network and therefore one communication is sufficient to guarantee the conditions of Chapter 12. The number of bits might not satisfy the requirements of Chapter 12, since we do not have an accurate model of the effect of the control input. However, we show here that with a low number of transmitted bits we obtain a stable closed loop system.

We consider that the pre-defined paths of the vehicles, $\boldsymbol{p}_d^i(t)$, define a formation with fixed distances between the cars, that is, $\left\|\boldsymbol{p}_d^i(t) - \boldsymbol{p}_d^j(t)\right\|$ is constant for $t \in \mathbb{R}^+$ and $i, j \in \mathscr{N}$, where $\mathscr{N}$ is the set of non-beacon vehicles. To design the distributed Luenberger observer, we take into consideration the deviation from the desired position in the formation frame

$$\bar{e}^i := R_d(\boldsymbol{p}^i - \boldsymbol{p}_d^i),$$

where R_d is the rotation matrix between the inertial frame and the tangent to the path at the center of the formation, and $\boldsymbol{p}^i$ is the position of the ith vehicle. The Luenberger observer is designed on the assumption that the deviation from the desired position has the following discrete time dynamics.

$$\bar{e}^i_{k+1} = \bar{e}^i_k + \xi^i_{k+1} + w^{1i}_k,$$
$$\xi^i_{k+1} = \xi^i_{k+1} + w^{2i}_k,$$

where $w^{1i}_k \in \mathbb{R}^2$ and $w^{2i}_k \in \mathbb{R}^2$ are bounded process disturbances. Note that it is possible to recover $\boldsymbol{p}^i$ knowing $\bar{e}^i$ through $\boldsymbol{p}^i = R_d^T \bar{e}^i + \boldsymbol{p}^i_d$. The state of the system that will be observed by the Luenberger observer is then

$$x_k = \mathrm{col}\left(\begin{bmatrix} \bar{e}^i_k \\ \xi^i_k \end{bmatrix}, i \in \mathcal{N}\right)$$

which is assumed to follow the discrete time dynamics

$$x_k := I_3 \otimes A + w_k$$

where $w_k \in \mathbb{R}^1 2$ is a bounded process noise and A is defined as

$$A := \begin{bmatrix} I_2 & I_2 \\ \mathbf{0} & I_2 \end{bmatrix}.$$

The measurement equation for each vehicle is

$$h^i(x) := \begin{bmatrix} \mathrm{col}\left(\|\boldsymbol{p}^i - \boldsymbol{p}^{bj}\|, j \in \mathcal{B}^i\right) \\ \mathrm{col}\left(\|\boldsymbol{p}^i - \boldsymbol{p}^j\|, j \in \mathcal{N}\right) \end{bmatrix},$$

where $\mathcal{B}^i$ is the set of beacon vehicles from where i measures ranges and $\boldsymbol{p}^{bj}$ is the position of beacon j. The set of measurements that is assumed to be available to each vehicle is

$$y^i_k = h^i(x_k) + v^i_k,$$

where v^i_k is a bounded measurement noise. The observation matrix matrix for each vehicle is computed as the linearization of the measurement equation when the vehicles are at their defined positions, that is, it is defined as

$$C^i := \frac{\partial h^i}{\partial x}(\mathbf{0}).$$

The observer gain L of the Distributed Luenberger observer was computed by solving an ARE as proposed in Subsection 6.3.3 of Chapter 6 which provides a positive definite matrix P and a matrix L such that $\|I_3 \otimes A - LC\|_P < 1$, where $C := \mathrm{col}(C^i)$. The matrix L is then partitioned in local sub-matrices such that $L = \mathrm{row}(L^i)$ and a decrease rate β is selected such that $\|I_3 \otimes A - LC\|_P < \beta < 1$. The distributed Luenberger observer is the following

$$\hat{x}^i_k = \frac{1}{3}\left(\sum_{j \in \mathcal{N}} Q^j_k\left(\bar{x}^j_k\right)\right) + \bar{x}^i_k - Q^i_k\left(\bar{x}^i_k\right),$$

where

$$\bar{x}^i_{k+1} = I_3 \otimes A\hat{x}^i_k + 3L^i\left(y^i_k - h^i(0) - C^i\hat{x}^i_k\right),$$

Regarding the quantizer parameters, a decrease rate of β of the quantization interval was implemented. However, since it is difficult to obtain a-priori bounds on the process noise, the quantization interval is determined according to a zoom-in, zoom-out approach, that is, it is defined as

$$\Lambda_{k+1}^{i} = \begin{cases} \beta\Lambda_k^i & \text{if } \left\|\bar{x}_k^i - Q_k^i\left(\bar{x}_k^i\right)\right\| \\ 2\Lambda_k^i & \text{otherwise} \end{cases}.$$

The number of bits for each dimension of the state, n_b, was set to a different value on each test.

15.3 Trajectory Tracking Controller

A trajectory tracking controller was implemented that drives the vehicles to their assigned paths $\boldsymbol{p}_d$ by controlling the desired surge speed u_d and yaw rate r_d of the vehicles.

Dropping the vehicle index, and defining $\hat{\boldsymbol{e}} := R(\hat{\boldsymbol{p}} - \boldsymbol{p}_d)$ where R is the rotation matrix from the inertial frame to the body frame of the vehicle, and $\hat{\boldsymbol{p}}$ is the estimated position of the vehicle, the trajectory tracking control law is the following

$$\begin{bmatrix} u_d \\ r_d \end{bmatrix} = \Delta^{-1}\left(-K(\hat{\boldsymbol{e}} - \boldsymbol{\delta}) + R^T\dot{\boldsymbol{p}}_d\right), \tag{15.1}$$

where K is a positive diagonal matrix, and for a positive constant $\delta > 0$,

$$\Delta := \begin{bmatrix} 1 & 0 \\ 0 & -\delta \end{bmatrix},$$

and $\boldsymbol{\delta} := [\delta,\, 0]^T$. The speed of the vehicle is controlled by a PI controller which assigns commands to the motor of the vehicle to drive the surge speed to u_d. Finally, the yaw rate of the car is driven to r_d by commanding the steering angle of the vehicle, which is determined by inverting a mapping between the steering angle and yaw rate.

15.4 Mission

The formation of the three non-beacon vehicles and the two beacon vehicles along with the measured ranges is shown in Figure 15.1.

It can be seen from Figure 15.1 that each non-beacon vehicle is not able to determine its own position only by its own range measurements to the beacons, thus it is necessary that the vehicles communicate among themselves to estimate their positions. The trajectory followed by the vehicles during the trials is a cyclical trajectory composed by two straight lines and two half-circles. The nominal assigned speed is 0.8m/s. During the trials, the frequency of the algorithm is 10Hz, which corresponds to the frequency at which each vehicle measures ranges and the frequency at which each vehicle exchanges its estimate with the others.

15.5 Test with $n_b := 16$

The first test performed the number of transmitted bits for each dimension of the state n_b was set to 16. For that test the trajectories followed by the cars and the estimated positions are shown in Figure 15.2. The position errors are shown in Figure 15.3.

We can observe from Figures 15.2 and 15.3 that the vehicles follow their assigned paths with a deviation of up to 0.2 meters. The estimation errors during the test are displayed in Figure 15.4 and the quantization interval size is

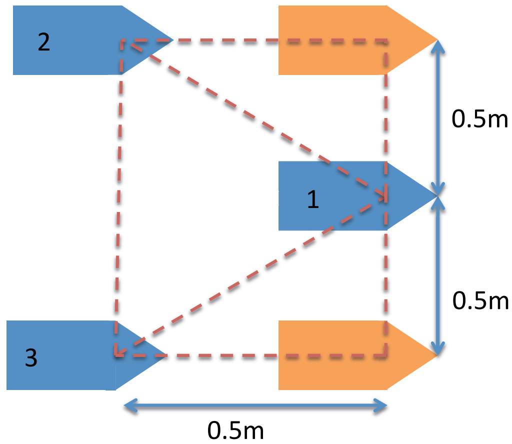

Figure 15.1 – Formation of the cars during the trials. The orange vehicles correspond to virtual beacon vehicles that are assumed to follow perfectly their assigned paths. The dashed red lines correspond to the measured ranges.

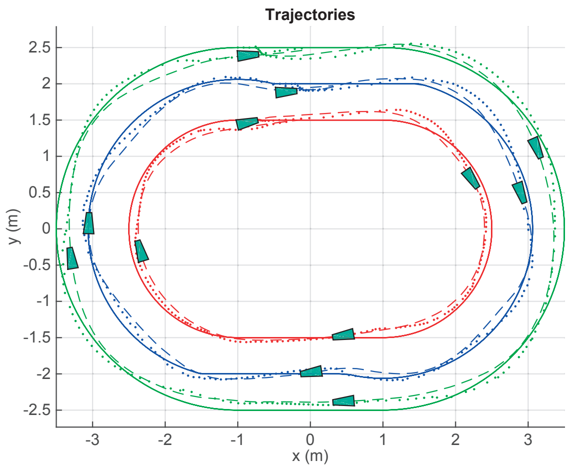

Figure 15.2 Trajectory of the vehicles during the first cycle of the trial for $n_b := 16$. The solid lines are the pre-defined trajectories, the dashed lines are the cars trajectories and the dots are the estimated positions.

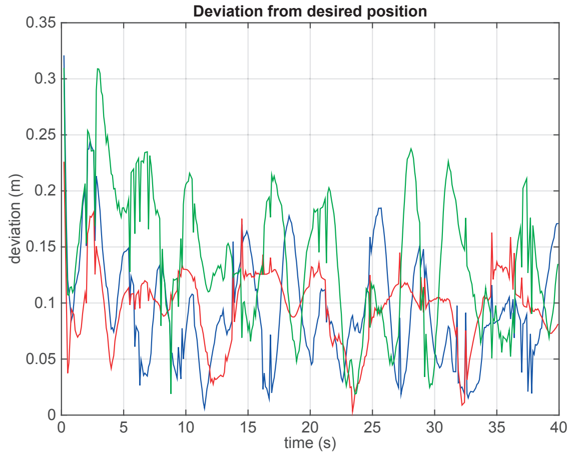

Figure 15.3 Deviation from the assigned position for $n_b := 16$.

shown in Figure 15.5. One can see from Figure 15.4 that the estimation errors are of the same size as deviation to the assigned position. We are assuming a linearized system and therefore the estimation error is expected to be proportional to the distance to the desired position. From Figure 15.5 it is visible that the quantization interval size remains bellow 0.1 throughout most of the test, while surpassing 0.3 for brief periods.

15.6 Test with $n_b := 4$

For the test with $n_b := 4$ the trajectories followed by the cars and the estimated positions are shown in Figure 15.6. The position errors are shown in Figure 15.7.

From Figures 15.6 and 15.7 one can observe that the performance is similar to the case of $n_b = 16$, and that the algorithm is robust to a challenging initial condition. The estimation errors during the test are displayed in Figure 15.8 and the quantization interval size is shown in Figure 15.9.

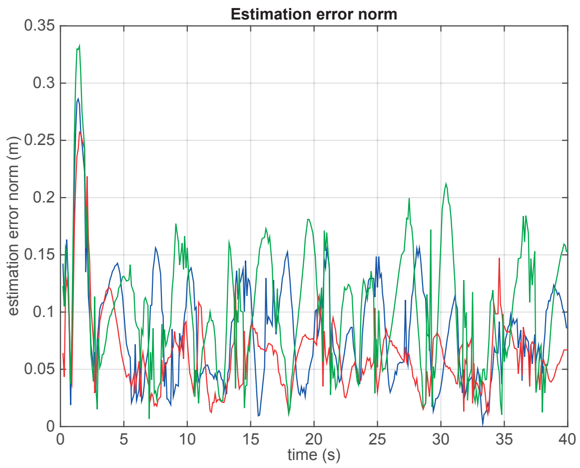

Figure 15.4 Estimation errors for $n_b := 16$.

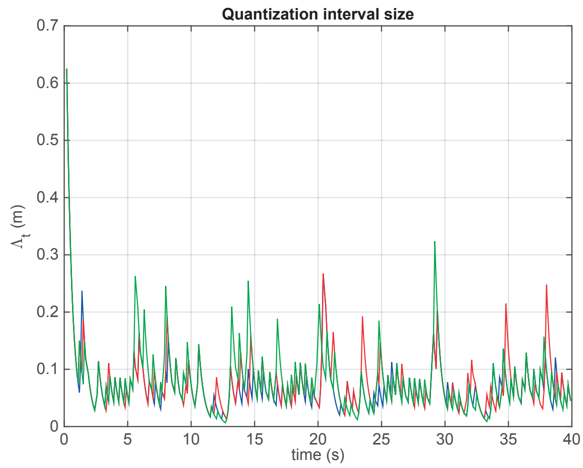

Figure 15.5 Quantization interval evolution for $n_b := 16$.

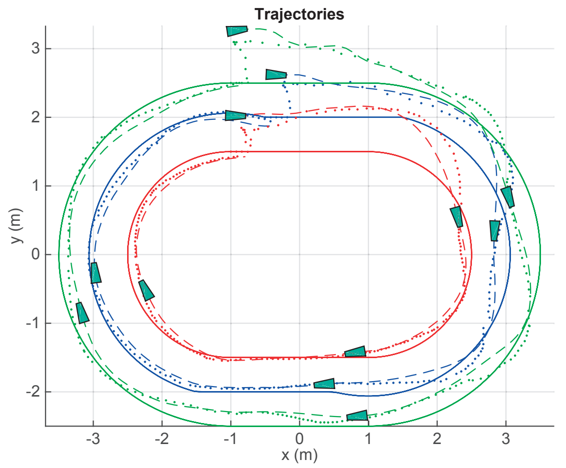

Figure 15.6 Trajectory of the vehicles during the first cycle of the trial for $n_b := 4$.

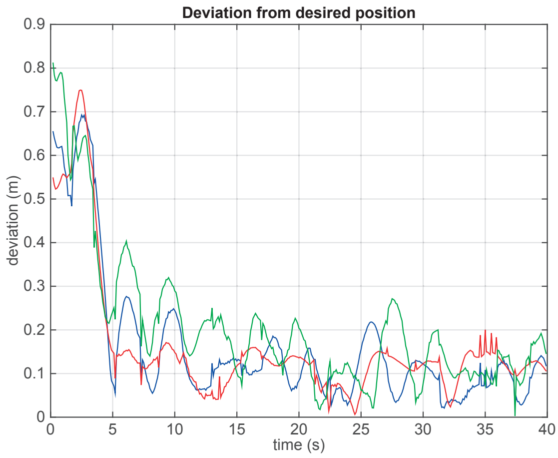

Figure 15.7 Deviation from the assigned position for $n_b := 4$.

From Figures 15.8 and 15.9 one can see that the estimation error size is similar to the trial with $n_b = 16$ indicating that the quantization errors contribute little to the estimation error in this case. The quantization intervals are greater than for $n_b = 16$ indicating that the quantization errors are also larger.

15.7 Test with $n_b := 3$

Finally, the trajectories followed by the cars and the estimated positions for the test with $n_b := 3$ are shown in Figure 15.10 and the position errors are shown in Figure 15.11.

It can be seen that the behaviour of the estimation errors is very different from the previous cases, since the quantization error has a greater impact on the estimation performance. During the first cycle the vehicles followed their assigned paths. However, it is visible from Figure 15.11 that the cars diverge slowly from their assigned paths. The estimation errors are shown in Figure 15.12 and the quantization interval size are plotted in Figure 15.13, where it is visible that the path-following control system is unstable in this case.

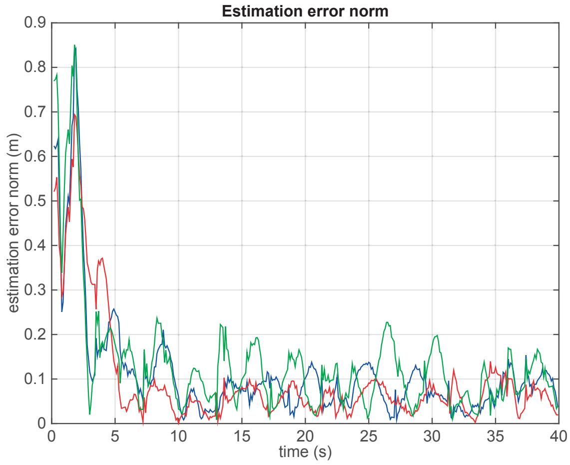

Figure 15.8 Estimation errors for $n_b := 4$.

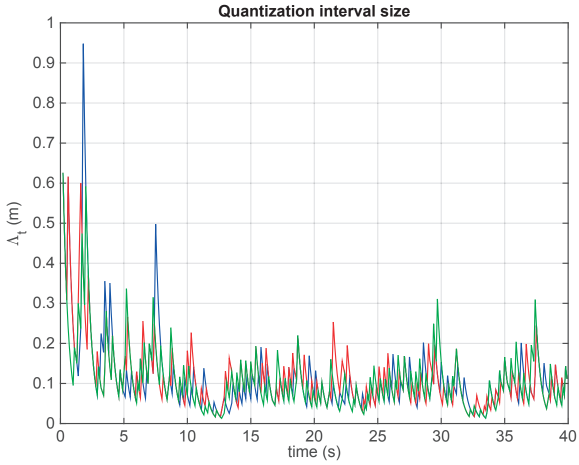

Figure 15.9 Quantization interval evolution for $n_b := 4$.

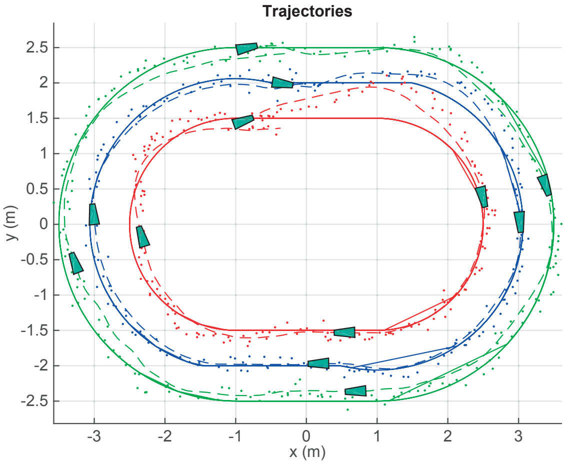

Figure 15.10 Trajectory of the vehicles during the first cycle of the trial for $n_b := 3$.

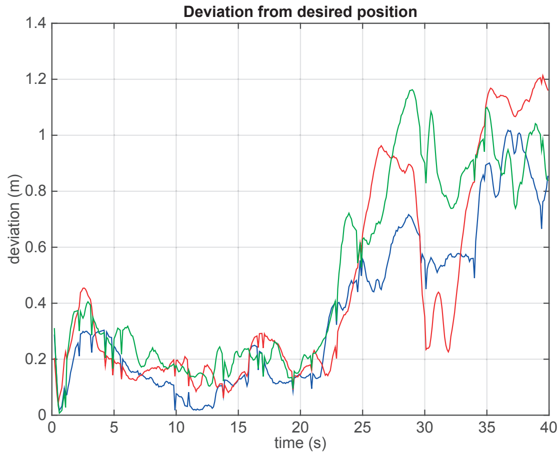

Figure 15.11 Deviation from the assigned position for $n_b := 3$.

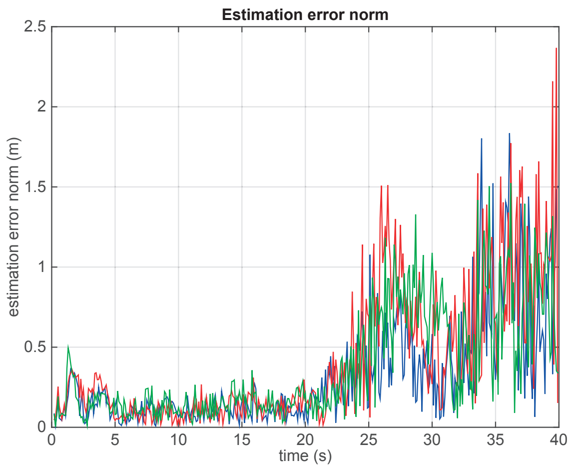

Figure 15.12 Estimation errors for $n_b := 3$.

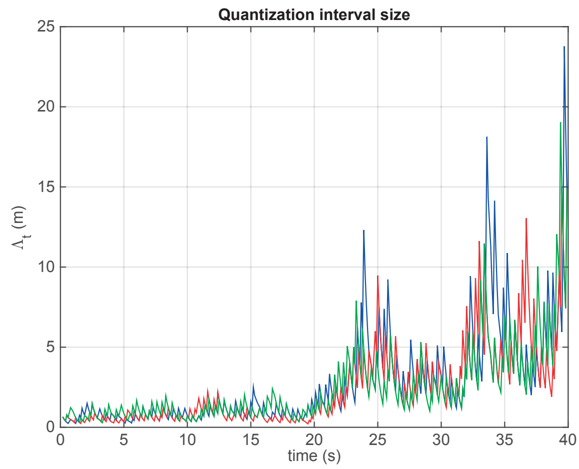

Figure 15.13 Quantization interval evolution for $n_b := 3$.

Discussion Part VII

16 Conclusions

In this thesis we proposed a number of algorithms for distributed state estimation and cooperative path-following that take into account explicitly the bandwidth limitations of the communications medium.

It was shown that the proposed quantized consensus algorithm achieves consensus asymptotically and that there are explicit convergence conditions yielding convergence rates that can be as close as one wishes to the case of unquantized communications, depending on the number of transmitted bits, and compute explicitly upper bounds on the deviation from average of each node. We have also shown that when the value stored at each node is disturbed by a bounded noise the ultimate bound on the difference to the average of a node is proportional to the magnitude of the noise.

We also proposed a new design method for a distributed state estimation algorithm for linear systems with guaranteed stability for collectively observable systems, that only requires the broadcasting of the node's state estimate at each discrete time instant. We demonstrated with simulations that, for some particular conditions, the algorithm has a lower estimation error norm than the other methods that use the same bandwidth and yield stable estimation errors for unstable systems.

We proposed a cooperative path-following algorithm with self-triggered communications that is robust to delays and packet losses and we proved that the closed-loop system is input to state stable with respect to disturbances. We have shown through simulations and with tests in real vehicles that the self-triggered cooperative path-following algorithm has adequate performance for formation control of autonomous marine vehicles. Moreover, the algorithm only requires communications when the vehicles are converging to their paths and into formation, and after that phase the vehicles practically do not need to communicate. From the tests with real vehicles it was found that cooperative path-following is a safer approach to formation control than trajectory tracking, since formation is maintained even when for some reason one vehicle lags behind temporarily, avoiding possible collisions.

We have also shown that with an appropriate parameter choice and given that the system is collective detectable, the distributed estimation and control algorithm with progressive quantization proposed in this thesis yields a bounded estimation error and state in every agent, with bounds proportional to the process and measurement noise.

We demonstrated in simulations that in a particular example the two best possible strategies in terms of bandwidth, that yield estimation errors with the same magnitude of the centralized case, are either transmitting 3 bits and performing a large number of consensus iterations between two discrete time instants, or performing the least possible number of consensus iterations guaranteeing adequate performance while communicating a large number of bits.

Finally, it was shown in tests with model cars that distributed estimation with quantized consensus is a feasible strategy for formation control using only range measurements between the vehicles, and, in that case, stability was achieved when each vehicle broadcast 10 times per second a vector of dimension 12 with each element coded with 4 bits. That is, we required a data rate of $10 \times 12 \times 4 = 480$ bits per second.

17 Future Work

We have determined conditions under which quantized distributed estimation and self-triggered cooperative path-following are input to state stable with respect to disturbance and measurement noise. However, in order to assess the performance in practice of the devised algorithms, a rigorous analysis of the trade-off between the available bandwidth and the performance of the algorithms would be useful.

A strong assumption in quantized consensus and, consequently, in quantized distributed estimation is the assumption that there are no packet losses, and therefore that each node knows exactly what data was received by the out-neighbours. A possible method to cope with packet losses is the adaptation of protocols such as the method in Saab et al. [2017] to ensure that all the agents know which information each observer used to update its own state.

To complete the analysis of the application of quantized distributed estimation to cooperative navigation of Chapter 15, a potential future work to assess the suitableness of the algorithm in real conditions is to perform sea trials with Medusa vehicles using acoustic modems. Also, another limitation of the tests of Chapter 15 is that, since the noise bound is not known beforehand, the quantization interval was selected according to a zoom-in zoom-out method, instead of the progressive quantization method proposed in Chapter 12. Both methods are similar, in that the quantization interval decreases with a pre-determined decrease rate. However, in the method of Chapter 15 the quantization interval length does not reach asymptotically a fixed value but instead it increases whenever the quantized value is outside the quantization interval. A theoretical analysis of the method in Chapter 15 in terms of stability would be useful.

Since in underwater environments there are few available positioning systems and we usually have to rely on range measurements to other vehicles or beacons, and in Chapter 10 we assumed that the agents have knowledge of their positions, we should investigate the stability of the coupling between cooperative navigation with range measurements, as is done in Chapter 15, and cooperative path-following with quantized or event-triggered communications, instead of trajectory tracking as in Chapter 15.

Another potential improvement to the theory in this thesis is the use of the results in Almeida et al. [2012], which state that cooperative path-following with periodic communications is stable, to relax some of the assumptions in Theorem 18, such as that the initial conditions must be within a neighbourhood of the origin.

A potential breakthrough in the theory of distributed estimation would be to determine under which conditions in the distributed estimation method of Section 8.7 in Chapter 8 the global covariance matrix converges to a fixed value. In that case it is expected that we would obtain the advantages of the method with known cross-correlations of Section 8.7, which is optimal in the stochastic sense, with the light on-line computational burden of a distributed Luenberger observer.

Another potential research topic in the field of distributed state estimation for linear systems is to investigate under which conditions it is possible to stabilize a system using distributed observers to estimate the state and using these state estimates to perform feedback control. This problem is not trivial since each node does not have knowledge of the control action the other nodes apply. In particular, the application of model-predictive control for constraint satisfaction is particularly challenging in this context since each agent must guarantee that the constraints are not violated without knowledge of the state estimate present in the other agents.

Finally, a possible extension to the quantized distributed estimation methods is to extend the developed methods to non-linear systems using methods similar to the extended Kalman filter.

A Appendices of Chapter 6

A.1 Proofs of Ellipsoidal norm Properties

Proof of property P1.

$$\|AB\|_P := \sup_{y=Bx, \|x\|_P=1} \|Ay\|_P \le \sup_{\|y\|_P=\|B\|_P=1} \|Ay\|_P = \|A\|_P \|B\|_P.$$

$\square$

Proof of property P2. Because $\rho(A) < 1$, given any positive definite matrix Q there is a positive definite P such that $A^T PA - P = -Q$. Multiplying on the right by $P^{-\frac{1}{2}}$ and on the left by $P^{-\frac{1}{2}T}$ one obtains

$$P^{-\frac{1}{2}T} QP^{-\frac{1}{2}} = I_n - P^{-\frac{1}{2}T} A^T PAP^{-\frac{1}{2}}.$$

Moreover, since Q and P are positive definite, and thus $P^{-\frac{1}{2}T} QP^{-\frac{1}{2}}$, and because $P^{-\frac{1}{2}T} A^T PAP^{-\frac{1}{2}}$ is positive semidefinite, it follows that

$$0 < \sigma_{\min}(Q^{\frac{1}{2}} P^{-\frac{1}{2}}) < 1.$$

As a consequence,

$$\begin{aligned}
\|A\|_P &:= \sup_{\|x\|_P=1} \sqrt{x^T A^T PAx} = \sup_{\|x\|_P=1} \sqrt{\|x\|_P^2 - x^T Qx} = \sqrt{1 - \min_{\|x\|_P=1} \|x\|_Q^2} \\
&= \sqrt{1 - \min_{\|x\|=1} \|Q^{\frac{1}{2}} P^{-\frac{1}{2}} x\|^2} = \sqrt{1 - \sigma_{\min}(Q^{\frac{1}{2}} P^{-\frac{1}{2}})^2} < 1.
\end{aligned}$$

$\square$

Proof of property P3.
Given the ellipsoid $\mathscr{Y}_\alpha := \{y | \|y\|_P \le \alpha\}$, define its support function as

$$h_{\mathscr{Y}_\alpha}(\gamma) := \max_{x \in \mathscr{Y}_\alpha} \gamma^T x.$$

Performing the change of variables $y := P^{\frac{1}{2}}x$ we have

$$h_{\mathcal{Y}_\alpha}(\gamma) := \max_{\|y\|\leq\alpha} \gamma^T P^{-\frac{1}{2}} y,$$

which can be solved by inspection to yield

$$h_{\mathcal{Y}_\alpha}(\gamma) := \gamma^T P^{-\frac{1}{2}} \frac{P^{-\frac{1}{2}}\gamma}{\left\|P^{-\frac{1}{2}}\gamma\right\|}\alpha = \|P^{-\frac{1}{2}}\gamma\|\alpha.$$

Therefore,

$$\begin{aligned}\min_{\|y\|_\infty=1} \|y\|_P &= \max_{\mathcal{Y}_\alpha\subseteq\mathcal{H}} \alpha = \max_{h_{\mathcal{Y}_\alpha}(F_i)\leq f_i} \alpha = \max_{\left\|P^{-\frac{1}{2}}F_i\right\|\alpha\leq f_i} \alpha \\ &= \min_{1\leq i\leq n} \frac{f_i}{\left\|P^{-\frac{1}{2}}F_i^T\right\|} := m(P).\end{aligned}$$

Furthermore,

$$\max_{\|y\|_\infty=1} \|y\|_P = \max_{y\in\mathcal{H}} \|y\|_P = \max_{1\leq i\leq 2^n} \|v_i\|_P := M(P).$$

Given two positive definite matrices P_1 and P_2 of size $n_1 \times n_1$ and $n_2 \times n_2$, respectively and defining F_i^1 as the ith row of the matrix $F^1 := [I_{n_1}, -I_{n_1}]^T$, and F_i^1 as the ith row of the matrix $F^2 := [I_{n_2}, -I_{n_2}]^T$ it follows, using property P5 and the usual properties of the Kronecker product, that

$$\begin{aligned}m(P_1 \otimes P_2) &= \min_{1\leq i\leq n_1, 1\leq j\leq n_2} \frac{1}{\left\|P_1^{-\frac{1}{2}} \otimes P_2^{-\frac{1}{2}} F_i^{1T} \otimes F_j^{2T}\right\|} \\ &= \min_{1\leq i\leq n_1, 1\leq j\leq n_2} \frac{1}{\left\|P_1^{-\frac{1}{2}} F_i^{1T}\right\| \left\|P_2^{-\frac{1}{2}} F_j^{2T}\right\|} = m(P_1)m(P_2).\end{aligned}$$

Furthermore, defining v_i^1 as the ith vertex of the hypercube $\mathcal{H}^1 := \{y|F^1 y \leq 1\}$ and v_i^2 as the ith vertex of the hypercube $\mathcal{H}^2 := \{y|F^2 y \leq 1\}$ we have

$$M(P_1 \otimes P_2) = \max_{1\leq i\leq 2^{n_1}, 1\leq j\leq 2^{n_2}} \left\|v_i^1 \otimes v_j^2\right\|_{P_1\otimes P_2} = \max_{1\leq i\leq 2^{n_1}, 1\leq j\leq 2^{n_2}} \|v_i^1\|_{P_1} \left\|v_j^2\right\|_{P_2} = M(P_1)M(P_2).$$

□

Proof of property P4.

$$\min_{\|y\|_{P_2}=1} \|y\|_{P_1} = \min_{\|v\|=1} \left\|P_2^{-\frac{1}{2}} v\right\|_{P_1} = \sigma_{\min}(P_1^{\frac{1}{2}} P_2^{-\frac{1}{2}}) := m(P_1, P_2).$$

Similarly,

$$\max_{\|y\|_{P_2}=1} \|y\|_{P_1} = \sigma_{\max}(P_1^{\frac{1}{2}} P_2^{-\frac{1}{2}}) := M(P_1, P_2).$$

□

Proof of property P5. Using the mixed product property of the Kronecker product gives

$$\|A \otimes B\|_{P_1 \otimes P_2} = \max_{\|x\|_{P_1 \otimes P_2} = 1} \|A \otimes Bx\|_{P_1 \otimes P_2}.$$

Doing the transformation $x := y \otimes z$ one obtains

$$\begin{aligned}\|A \otimes B\|_{P_1 \otimes P_2} &= \max_{\|y^T \otimes z^T\|_{P_1 \otimes P_2} = 1} \left\| y^T \otimes z^T \right\|_{A^T \otimes B^T P_1 \otimes P_2 A \otimes B} = \max_{y^T P_1 y z^T P_2 z = 1} \sqrt{y^T A^T P_1 A y z^T B^T P_2 B z} \\ &= \max_{y^T P_1 y = 1} \sqrt{y^T A^T P_1 A y} \max_{z^T P_2 z = 1} \sqrt{z^T B^T P_2 B z} = \|A\|_{P_1} \|B\|_{P_2}.\end{aligned}$$

□

B Appendices of Chapter 7

B.1 Proofs of Standard Consensus Lemmas

Before proving Lemma 1 the following result, based on the theorems in Tifenbach [2011], is required.

Lemma 17. If Assumptions A2-A3 are satisfied then $\sigma_{\max}(\Pi) = 1$ and $\sigma_2 < 1$.

Proof. If Assumption A3 is satisfied, then $\Pi^T\Pi$ has the same or a larger number of non-zero elements than Π, and if Π is doubly stochastic then $\Pi^T\Pi$ is doubly stochastic. Therefore, from Assumption A2 it follows that $\Pi^T\Pi$ is non-negative, doubly stochastic, and primitive.

Since $\Pi^T\Pi$ is doubly stochastic, $\frac{1}{\sqrt{N}}\mathbf{1}$ is both the left- and right-eigenvector associated with the eigenvalue 1. Therefore, it follows from the Perron-Frobenius Theorem that the eigenvalue 1 is a simple eigenvalue of $\Pi^T\Pi$ and the norm of the other eigenvalues is smaller than 1.

Finally, since the singular values of Π are the eigenvalues of $\Pi^T\Pi$, we obtain $\sigma_{\max}(\Pi) = 1$ and $\sigma_2 < 1$. □

We can now prove Lemma 1.

Proof of Lemma 1. We start by proving the first implication, i.e. if $\lim_{l\to\infty} z_l^i = \sum_{j\in\mathcal{N}} \frac{1}{N} z_0^j,\ \forall i \in \mathcal{N}$ then Assumption A2 is satisfied. Defining $z_l := col(z_l^i)$ we can write (7.3) as

$$z_{l+1} = \Pi z_l.$$

We can also write the property

$$\lim_{l\to\infty} z_l^i = \sum_{j\in\mathcal{N}} \frac{1}{N} z_0^j,\ \forall i \in \mathcal{N},$$

as

$$\lim_{l\to\infty} z_l = \frac{1}{N}\mathbf{1}\mathbf{1}^T z_0,$$

which is equivalent to

$$\lim_{l\to\infty}\Pi^l = \frac{1}{N}\mathbf{1}\mathbf{1}^T.$$

This implies that $\Pi\frac{1}{N}\mathbf{1}\mathbf{1}^T = \frac{1}{N}\mathbf{1}\mathbf{1}^T\Pi = \frac{1}{N}\mathbf{1}\mathbf{1}^T$, which is only possible if Π is doubly stochastic. Moreover, since $\lim_{l\to\infty}\Pi^l$ is positive, there is an integer $k > 0$ such that Π^k is positive, i.e. Π is primitive.

If Assumption A2 is satisfied, then the conditions of Lemma 17 apply and therefore $\sigma_{\max}(\Pi) = 1$ and $\sigma_2 < 1$. We can also observe that since Π is doubly stochastic, $\frac{1}{\sqrt{N}}\mathbf{1}$ is both a left- and a right-singular vector associated with $\sigma_{\max}(\Pi) = 1$ and the left- and a right-eigenvector associated with $\lambda_1 = 1$. Therefore, from the Perron-Frobenius theorem (see e.g. Bullo et al. [2009]), we have that $\lim_{t\to\infty}\Pi^t$ is the Perron projection $\frac{1}{N}\mathbf{1}\mathbf{1}^T$.

Finally, given that Assumption A2 is satisfied we can perform an SVD decomposition of Π as

$$\Pi = U\begin{bmatrix} 1 & & 0 \\ & \sigma_2 & \\ 0 & & \ddots \end{bmatrix}V^T,$$

from which it follows that

$$\frac{1}{N}\mathbf{1}\mathbf{1}^T = U\begin{bmatrix} 1 & & 0 \\ & 0 & \\ 0 & & 0 \end{bmatrix}V^T,$$

and $\|\Pi - \frac{1}{N}\mathbf{1}\mathbf{1}^T\| = \sigma_{\max}(\Pi - \frac{1}{N}\mathbf{1}\mathbf{1}^T) = \sigma_2 < 1.$ □

A proof of Lemma 2 is given in Theorem 3 of Hartfiel and Spellmann [1972]. In what follows we give an alternative proof that departs considerably from that in Hartfiel and Spellmann [1972] and has the benefit of being constructive. The proof presented here relies on graph theoretical considerations and on the Birkhoff-von Neumann Theorem given next.

Theorem 23 (Birkhoff-von Neumann theorem, In Horn and Johnson [2012], Theorem 8.7.1)**.** A square matrix is doubly stochastic if and only if it is a convex combination of permutation matrices.

Proof of Lemma 2. The implication that if Assumption A2 is satisfied then the network $(\mathcal{N},\mathcal{A})$ is strongly connected, stems from the fact that if Π is primitive then it is irreducible, i.e. we cannot partition $\mathcal{N}$ into two disjoint sets $\mathcal{N}_1$ and $\mathcal{N}_2$, $\mathcal{N}_1\cup\mathcal{N}_2 = \mathcal{N}$, $\mathcal{N}_1\cap\mathcal{N}_2 = \emptyset$, such that $\pi^{i,j} > 0$ for $i \in \mathcal{N}_1$ and $j \in \mathcal{N}_2$, and from the well known result that if Π is irreducible then $G(\Pi)$ is strongly connected.

The converse implication, i.e. that if self loops are allowed and the network $(\mathcal{N},\mathcal{A})$ is strongly connected then there exists a matrix Π such that Assumption A2 is satisfied, is proven as follows. If the network $(\mathcal{N},\mathcal{A})$ is strongly connected then each edge $(i,j)\in\mathcal{A}$ is included in a cycle of edges contained in $\mathcal{A}$. This is due to the fact that since the network is strongly connected, for every edge $(i,j)\in\mathcal{A}$ there is a path without repeated nodes starting in j and ending in i. Therefore, there is a finite set of $n > 0$ cycles $\mathcal{C}_k$, $k = \{1\ldots,n\}$ such that $\bigcup_{k=1}^n\mathcal{C}_k = \mathcal{A}$. Since self loops are allowed, for every cycle we can define a permutation matrix P_k, whose $G(P_k)$ is a subgraph of $(\mathcal{N},\mathcal{A})$, by defining its ijth component $p_k^{i,j}$ as

$$p_k^{i,j} := \begin{cases} 1, & \text{if}\begin{cases} (i,j)\in\mathcal{C}_k \\ \text{or} \\ \text{if } i = j, \text{ and } \forall k\in\mathcal{N},\ (i,k)\notin\mathcal{C}_k \end{cases} \\ 0, & \text{otherwise} \end{cases}.$$

We can now define $\Pi := \sum_{k+1}^{n} \alpha_k P_k$, with $\alpha_k > 0$ for $k = \{1,\dots,n\}$ and $\sum_{k+1}^{n} \alpha_k = 1$. We can see that $G(\Pi) = (\mathcal{N},\mathcal{A})$. Since the network is strongly connected and aperiodic (because it contains self-loops), we have that $G(\Pi)$ is strongly connected and aperiodic, and therefore Π is primitive. Moreover, since Π is a convex combination of permutation matrices, from Theorem 23 Π is doubly stochastic. This concludes the proof. $\square$

B.2 Proof of Theorem 8

To prove the main result of this section we need the following.

Lemma 18. Consider the quantizer Q_l defined in (7.1) in Section 7.1 with n_b bits and where $\Lambda_l = r\alpha^l$, with $0 < \sigma_2 < \alpha < 1$. Let Assumption A2 hold. Given the linear consensus system with quantized communications (7.7), if, given l, for all $0 \le p < l$ the values of z_p fall inside the quantization interval, i.e. $\|z_p - \bar{z}_p\|_\infty \le \frac{\Lambda_p}{2}$, then $\|q_l\|_{I_N \otimes P}$ satisfies

$$\|q_l\|_{I_N\otimes P} \le \alpha^l \left[\|q_0\|_{I_N\otimes P} + \frac{\sqrt{N}M(P)}{\alpha - \sigma_2}\left(\frac{r}{2^{n_b}-2}\right)\right]. \tag{B.1}$$

Proof. If Assumption A2 holds, then from (7.8) it follows that

$$q_{p+1} = \left(\Pi - \frac{1}{N}\mathbf{1}\mathbf{1}^T\right)^{p+1} \otimes I_n q_0 + \sum_{i=0}^{p}\left[\left(\Pi - \frac{1}{N}\mathbf{1}\mathbf{1}^T\right)^{i}(\Pi - I_N)\right] \otimes I_n \eta_{p-i}.$$

The same assumption implies that $\|\Pi - \frac{1}{N}\mathbf{1}\mathbf{1}^T\| = \sigma_2 < 1$, $\|\Pi - I_N\| \le \|\Pi\| + \|I_N\| \le 2$, and that $\|I_N - \frac{1}{N}\mathbf{1}\mathbf{1}^T\| = 1$, and therefore

$$\begin{aligned}
\|q_{p+1}\|_{I_N\otimes P} &\le \left\|\Pi - \frac{1}{N}\mathbf{1}\mathbf{1}^T\right\|^{p+1} \|q_0\|_{I_N\otimes P} + \sum_{i=0}^{p}\left\|\Pi - \frac{1}{N}\mathbf{1}\mathbf{1}^T\right\|^{i} \|\Pi - I_N\| \|\eta_{p-i}\|_{I_N\otimes P} \\
&= \sigma_2^{p+1}\|q_0\|_{I_N\otimes P} + \sum_{i=0}^{p}\sigma_2^i\left(2\|\eta_{p-i}\|_{I_N\otimes P}\right),
\end{aligned}$$

where we used Properties P1 and P5. From the assumption that $\|\eta_p\|_\infty \le \frac{\Lambda_p}{2^{n_b+1}-4}$, and Property P3, we have

$$\|\eta_p\|_{I_N\otimes P} \le \sqrt{N}M(P)\|\eta_p\|_\infty \le \frac{\Lambda_p\sqrt{N}M(P)}{2^{n_b+1}-4} \le \frac{r\sqrt{N}M(P)}{2^{n_b+1}-4}\alpha^p.$$

Therefore,

$$\begin{aligned}
\|q_{p+1}\|_{I_N\otimes P} &\le \sigma_2^{p+1}\|q_0\|_{I_N\otimes P} + \frac{r}{2^{n_b}-2}\sqrt{N}M(P)\sum_{i=0}^{p}\sigma_2^i\alpha^{p-i} \\
&\le \alpha^{p+1}\|q_0\|_{I_N\otimes P} + \frac{r}{2^{n_b}-2}\sqrt{N}M(P)\sum_{i=0}^{p}\sigma_2^i\alpha^{p-i} \\
&\le \alpha^{p+1}\left[\|q_0\|_{I_N\otimes P} + \frac{r}{2^{n_b}-2}\sqrt{N}M(P)\sum_{i=0}^{p}\frac{\sigma_2^i}{\alpha^{i+1}}\right].
\end{aligned}$$

Since $\sigma_2 < \alpha < 1$, by using the convergence property of the geometric series, we get that the expression above is equivalent to

$$\|q_{p+1}\|_{I_N\otimes P} \le \alpha^{p+1}\left[\|q_0\|_{I_N\otimes P} + \frac{r}{2^{n_b}-2}\frac{\sqrt{N}M(P)\left(1-\left(\frac{\sigma_2}{\alpha}\right)^{p+1}\right)}{\alpha\left(1-\frac{\sigma_2}{\alpha}\right)}\right]$$

$$\leq \alpha^{p+1}\left[\|q_0\|_{I_N\otimes P}+\frac{r}{2^{n_b}-2}\frac{\sqrt{N}M(P)}{\alpha-\sigma_2}\right].$$

□

Proof of Theorem 8. We prove by induction that z_l falls inside the quantization interval of Q_l, i.e. $\|z_l-\bar{z}_l\|_\infty \leq \frac{\Lambda_l}{2}$ for $l \geq 0$. This, combined with Lemma 19 concludes the proof of Theorem 8.

The base case that $\|z_0-\bar{z}_0\|_\infty \leq \frac{\Lambda_0}{2}$ is given by assumption, since from equation (7.10), using the norm Property P3, and the definitions of q_l and z_l^{avg} we can state that

$$\|z_0-\bar{z}_0\|_\infty = \|q_0+z_0^{\text{avg}}-\bar{z}_0\|_\infty \leq \frac{\|q_0\|_{I_N\otimes P}+\|z_0^{\text{avg}}-\bar{z}_0\|_{I_N\otimes P}}{m(P)} \leq s_1 \leq \frac{r}{2} \leq \frac{r\alpha^0}{2} = \frac{\Lambda_0}{2}.$$

We must now prove the induction step, that is, if $\|z_l-\bar{z}_l\|_\infty \leq \frac{\Lambda_l}{2}$ then $\|z_{l+1}-\bar{z}_{l+1}\|_\infty \leq \frac{\Lambda_{l+1}}{2}$. From (7.8), and the fact that the algorithm preserves averages, i.e. $z_{l+1}^{\text{avg}} = z_l^{\text{avg}}$, we have

$$\begin{aligned}\|z_{l+1}-\bar{z}_{l+1}\|_\infty &= \|z_{l+1}-Q_l(z_l)\|_\infty \\ &= \|q_{l+1}-q_l-\eta_l\|_\infty \leq \|q_{l+1}\|_\infty+\|q_l\|_\infty+\|\eta_l\|_\infty \\ &\leq \frac{\|q_{l+1}\|_{I_N\otimes P}}{m(P)}+\frac{\|q_l\|_{I_N\otimes P}}{m(P)}+\|\eta_l\|_\infty. \end{aligned} \tag{B.2}$$

Combining (B.2) with Lemma 18, and the assumption of the induction, i.e. the assumption that $\|z_l-\bar{z}_l\|_\infty \leq \frac{\Lambda_l}{2}$, it follows that

$$\|z_{l+1}-\bar{z}_{l+1}\|_\infty \leq \frac{\alpha^{l+1}}{m(P)}\left[\|q_0\|_{I_N\otimes P}+\frac{\sqrt{N}M(P)r}{2^{n_b}(\alpha-\sigma_2)}\right]+\frac{\alpha^l}{m(P)}\left[\|q_0\|_{I_N\otimes P}+\frac{\sqrt{N}M(P)r}{2^{n_b}(\alpha-\sigma_2)}\right]+\frac{r}{2^{n_b+1}}\alpha^l.$$

Rearranging the right hand side of the last inequality one obtains

$$\begin{aligned}\|z_{l+1}-\bar{z}_{l+1}\|_\infty &\leq \alpha^{l+1}\left[\frac{(\alpha+1)\|q_0\|_{I_N\otimes P}}{m(P)\alpha}+\frac{2\sqrt{N}M(P)(\alpha+1)+m(P)(\alpha-\sigma_2)}{m(P)\alpha(\alpha-\sigma_2)}\frac{r}{2^{n_b+1}}\right] \\ &\leq \alpha^{l+1}\left[s_1+s_2\frac{r}{2^{n_b+1}}\right],\end{aligned}$$

where the last inequality stems from the definitions of s_1, s_2 and the fact that $\|\bar{z}_0-z_0^{\text{avg}}\|_{I_N\otimes P} \geq 0$. From the assumptions of Theorem 8 we obtain

$$\|z_{l+1}-\bar{z}_{l+1}\|_\infty \leq \alpha^{l+1}\left[s_1+s_2\frac{r}{2^{n_b+1}}\right] \leq \frac{r\alpha^{l+1}}{2} = \frac{\Lambda_{l+1}}{2}.$$

□

B.3 Proof of Theorem 9

Before proving the main result of this section we first need the following preparatory result:

Lemma 19. Consider a quantizer Q_l from (7.1) with n_b bits and where $\Lambda_l = r_1\alpha^l + r_2$, with $0 < \sigma_2 < \alpha < 1$ and $\alpha_v < \alpha$. Let Assumptions A2, A3 and A4 hold. Given the linear consensus system with quantized communications (7.7), if, given l, for all $0 \leq p < l$ the values of z_p fall inside the quantization interval, i.e.

$\|\eta_p\|_\infty \leq \frac{\Lambda_p}{2}$ then $\|q_l\|$ satisfies

$$\|q_l\|_{I_N\otimes P} \leq \alpha^l \left[\|q_0\|_{I_N\otimes P} + \frac{\sqrt{N}M(P)}{\alpha-\sigma_2}\left(\frac{r_1}{2^{n_b}-2}+\epsilon_v\right)\right] + \frac{\sqrt{N}M(P)}{1-\sigma_2}\left(\frac{r_2}{2^{n_b}-2}+\delta_v\right). \tag{B.3}$$

Proof. Given that Assumptions A2, A3 hold, from (7.8) we have

$$\begin{aligned} q_{p+1} &= \left(\Pi - \frac{1}{N}\mathbf{1}\mathbf{1}^T\right)^{p+1} \otimes I_n q_0 \\ &+ \sum_{i=0}^{p}\left[\left(\Pi - \frac{1}{N}\mathbf{1}\mathbf{1}^T\right)^i (\Pi - I_N)\right] \otimes I_n \eta_{p-i} \\ &+ \sum_{i=0}^{p}\left[\left(\Pi - \frac{1}{N}\mathbf{1}\mathbf{1}^T\right)^i \left(I_N - \frac{1}{N}\mathbf{1}\mathbf{1}^T\right)\right] \otimes I_n v_{p-i}. \end{aligned}$$

Noting that, from Assumptions A2 and A3, $\|\Pi - \frac{1}{N}\mathbf{1}\mathbf{1}^T\| = \sigma_2 < 1$, $\|\Pi - I_N\| \leq \|\Pi\| + \|I_N\| \leq 2$, and that $\|I_N - \frac{1}{N}\mathbf{1}\mathbf{1}^T\| = 1$, from Property P5, and the fact that $\|I_n\|_P = 1$, we have

$$\begin{aligned} \|q_{p+1}\|_{I_N\otimes P} &\leq \left\|\Pi - \frac{1}{N}\mathbf{1}\mathbf{1}^T\right\|^{t+1} \|q_0\|_{I_N\otimes P} \\ &+ \sum_{i=0}^{p}\left\|\Pi - \frac{1}{N}\mathbf{1}\mathbf{1}^T\right\|^i \|\Pi - I_N\| \|\eta_{p-i}\|_{I_N\otimes P} \\ &+ \sum_{i=0}^{p}\left\|\Pi - \frac{1}{N}\mathbf{1}\mathbf{1}^T\right\|^i \|I_N - \frac{1}{N}\mathbf{1}\mathbf{1}^T\| \|v_{p-i}\|_{I_N\otimes P} \\ &= \sigma_2^{p+1}\|e_0\|_{I_N\otimes P} + \sum_{i=0}^{p}\sigma_2^i\left(2\|\eta_{p-i}\|_{I_N\otimes P} + \|v_{p-i}\|_{I_N\otimes P}\right). \end{aligned}$$

From the assumption that $\|\eta_p\|_\infty \leq \frac{\Lambda_p}{2^{n_b+1}-4}$ we obtain

$$\|\eta_p\|_{I_N\otimes P} \leq \sqrt{N}M(P)\|\eta_p\|_\infty \leq \frac{\Lambda_p\sqrt{N}M(P)}{2^{n_b+1}-4} \leq \frac{r_1\sqrt{N}M(P)}{2^{n_b+1}-4}\alpha^p + \frac{r_2\sqrt{N}M(P)}{2^{n_b+1}-4}.$$

Also, assumption A4 yields

$$\begin{aligned} \|v_p\|_{I_N\otimes P} &\leq \sqrt{N}M(P)\|v_p\|_\infty \leq \sqrt{N}M(P)\epsilon_v\alpha_v^p + \sqrt{N}M(P)\delta_v \\ &\leq \sqrt{N}M(P)\epsilon_v\alpha^p + \sqrt{N}M(P)\delta_v, \end{aligned}$$

where we used the fact that $\alpha_v \leq \alpha$, and therefore

$$\begin{aligned} \|q_{p+1}\|_{I_N\otimes P} &\leq \sigma_2^{p+1}\|q_0\|_{I_N\otimes P} + \left(\frac{r_1}{2^{n_b}-2}+\epsilon_v\right)\sqrt{N}M(P)\sum_{i=0}^{p}\sigma_2^i k^{p-i}\left(\frac{r_2}{2^{n_b}-2}+\delta_v\right)\sqrt{N}M(P)\sum_{i=0}^{p}\sigma_2^i \\ &\leq \alpha^{p+1}\|q_0\|_{I_N\otimes P} + \left(\frac{r_1}{2^{n_b}-2}+\epsilon_v\right)\sqrt{N}M(P)\sum_{i=0}^{p}\sigma_2^i\alpha^{p-i} + \left(\frac{r_2}{2^{n_b}-2}+\delta_v\right)\sqrt{N}M(P)\sum_{i=0}^{p}\sigma_2^i \\ &\leq \alpha^{p+1}\left[\|q_0\|_{I_N\otimes P} + \left(\frac{r_1}{2^{n_b}-2}+\epsilon_v\right)\sqrt{N}M(P)\sum_{i=0}^{p}\frac{\sigma_2^i}{\alpha^{i+1}}\right] + \left(\frac{r_2}{2^{n_b}-2}+\delta_v\right)\sqrt{N}M(P)\sum_{i=0}^{p}\sigma_2^i. \end{aligned}$$

Since $0 < \alpha < 1$, by using the property of the geometric series, we get that the expression above is equal to

$$
\begin{aligned}
\|q_{p+1}\|_{I_N\otimes P} \le \alpha^{p+1} & \left[\|q_0\|_{I_N\otimes P} + \left(\frac{r_1}{2^{n_b}-2} + \epsilon_v\right) \frac{\sqrt{N}M(P)\left(1-\left(\frac{\sigma_2}{\alpha}\right)^{p+1}\right)}{\alpha\left(1-\frac{\sigma_2}{\alpha}\right)} \right] \\
& + \left(\frac{r_2}{2^{n_b}-2} + \delta_v\right) \frac{\sqrt{N}M(P)\left(1-\sigma_2^{p+1}\right)}{1-\sigma_2} \\
& \le \alpha^{p+1} \left[\|q_0\|_{I_N\otimes P} + \left(\frac{r_1}{2^{n_b}-2} + \epsilon_v\right) \frac{\sqrt{N}M(P)}{\alpha-\sigma_2} \right] + \left(\frac{r_2}{2^{n_b}-2} + \delta_v\right) \frac{\sqrt{N}M(P)}{1-\sigma_2}.
\end{aligned}
$$

□

Proof of Theorem 9. We prove by induction that z_l falls inside the quantization interval of Q_l, i.e. $\|z_l - \bar{z}_l\|_\infty \le \frac{\Lambda_l}{2}$ for $l \ge 0$ which, combined with Lemma 19, concludes the proof of Theorem 9.

The base case is given by assumption, since from equation (7.17), the definitions of q_l and z_l^{avg}, Property P3, and the fact that $m(I_N) = 1$ we can state that

$$
\begin{aligned}
\|z_0 - \bar{z}_0\|_\infty = \|q_0 + z_0^{\text{avg}} - \bar{z}_0\|_\infty & \le m(P)^{-1}\left(\|q_0\|_{I_N\otimes P} + \|z_0^{\text{avg}} - \bar{z}_0\|_{I_N\otimes P}\right) \\
& \le a_1 \le \frac{r_1}{2} \le \frac{r_1\alpha^0 + r_2}{2} = \frac{\Lambda_0}{2}.
\end{aligned}
$$

We now have to prove the induction step, that is, given that $\|z_l - \bar{z}_l\|_\infty \le \frac{\Lambda_l}{2}$ we have $\|z_{l+1} - \bar{z}_{l+1}\|_\infty \le \frac{\Lambda_{l+1}}{2}$. From (7.8), and the fact that the vector of averages follows the dynamics $z_{l+1}^{\text{avg}} = z_l^{\text{avg}} + \frac{1}{N}\left(\mathbf{1}\mathbf{1}^T\right) \otimes I_n v_l$, we have

$$
\begin{aligned}
\|z_{l+1} - \bar{z}_{l+1}\|_\infty & = \|z_{l+1} - \hat{z}_l\|_\infty = \|q_{l+1} - q_l + \tfrac{1}{N}\left(\mathbf{1}\mathbf{1}^T\right)\otimes I_n v_l - \eta_l\|_\infty \\
& \le \|q_{l+1}\|_\infty + \|q_l\|_\infty + \|\tfrac{1}{N}\left(\mathbf{1}\mathbf{1}^T\right)\otimes I_n v_l\|_\infty + \|\eta_l\|_\infty \\
& \le m(P)^{-1}\left(\|q_{l+1}\|_{I_N\otimes P} + \|q_l\|_{I_N\otimes P}\right) + \|v_l\|_\infty + \|\eta_l\|_\infty.
\end{aligned}
\tag{B.4}
$$

Combining (B.4) with Lemma 19, assumption A4 and the assumption of the induction, i.e. the assumption that $\|z_l - \bar{z}_l\|_\infty \le \frac{\Lambda_l}{2}$, it follows that

$$
\begin{aligned}
\|z_{l+1} - \bar{z}_{l+1}\|_\infty \le & \frac{\alpha^{l+1}}{m(P)} \left[\|q_0\|_{I_N\otimes P} + \frac{\sqrt{N}M(P)\epsilon_v}{\alpha-\sigma_2} + \frac{\sqrt{N}M(P)r_1}{(2^{n_b}-2)(\alpha-\sigma_2)} \right] \\
& + \frac{\alpha^l}{m(P)} \left[\|q_0\|_{I_N\otimes P} + \frac{\sqrt{N}M(P)\epsilon_v}{\alpha-\sigma_2} + \frac{\sqrt{N}M(P)r_1}{(2^{n_b}-2)(\alpha-\sigma_2)} \right] \\
& + \frac{2\sqrt{N}M(P)}{m(P)(1-\sigma_2)}\delta_v + \frac{2\sqrt{N}M(P)r_2}{m(P)(1-\sigma_2)(2^{n_b}-2)} + \epsilon_v\alpha^l + \delta_v + \frac{r_1}{2^{n_b+1}-4}\alpha^l + \frac{r_2}{2^{n_b+1}-4}.
\end{aligned}
$$

Rearranging the right hand side of the last inequality one obtains

$$
\begin{aligned}
\|z_{l+1} - \bar{z}_{l+1}\|_\infty \le \alpha^{l+1} & \left[\frac{(\alpha+1)\|q_0\|_{I_N\otimes P}}{m(P)\alpha} + \left(\frac{\sqrt{N}M(P)(\alpha+1)}{\alpha(\alpha-\sigma_2)} + \frac{1}{\alpha}\right)\epsilon_v \right. \\
& \left. + \left(\frac{2\sqrt{N}M(P)(\alpha+1)}{m(P)\alpha(\alpha-\sigma_2)} + \frac{1}{\alpha}\right)\frac{r_1}{2^{n_b+1}-4} \right] \\
& + \left(\frac{2\sqrt{N}M(P)}{m(P)(1-\sigma_2)} + 1\right)\delta_v + \left(\frac{4\sqrt{N}M(P)}{m(P)(1-\sigma_2)} + 1\right)\frac{r_2}{2^{n_b+1}-4} \\
& \le \alpha^{l+1}\left[a_1 + a_2\frac{r_1}{2^{n_b+1}-4}\right] + b1 + b_2\frac{r_2}{2^{n_b+1}-4},
\end{aligned}
$$

where the last inequality stems from the definitions of a_1, a_2, b_1, b_2 and the fact that $\|\bar{z}_0 - z_0^{\text{avg}}\|_{I_N\otimes P} \ge 0$. From the assumptions of Theorem 9 we have that

$$
\begin{aligned}
\|z_{l+1} - \bar{z}_{l+1}\|_\infty &\le \alpha^{l+1}\left[a_1 + a_2 \frac{r_1}{2^{n_b+1}-4}\right] + b_1 + b_2 \frac{r_2}{2^{n_b+1}-4} \\
&\le \frac{r_1 \alpha^{l+1} + r_2}{2} = \frac{\Lambda_{l+1}}{2}.
\end{aligned}
$$

□

C Appendices of Chapter 8

C.1 General Solution for a Non-invertible Matrix A

Given a dynamic system described by (8.1) and (8.2), where $w_t = 0$ and $v_t^i = 0$, one can express it in a basis that transforms the A matrix in its Jordan form, i.e. we can find a matrix M such that $J = M^{-1}AM$ is a block diagonal matrix in the Jordan form diag(J_i), where for each i in $\{1,\dots,p\}$, the sub-matrix J_i is the ith real Jordan block.

If the matrix A is non-invertible, we can partition the state between modes associated with the zero eigenvalues, and modes associated with the non-zero eigenvalues. That is, without loss of generality we consider that there exists a an integer p_0 such that $J_{p_0+1},\dots,J_p$ are all the Jordan blocks associated with the zero eigenvalue. This implies that there exists a positive integer k_0 for which $J_i^k = 0$ for all $k \geq k_0$ and $i \in \{p_0+1,\dots,p\}$.

By applying a similarity transform to the system with M, we obtain the following state-space equation:

$$\begin{bmatrix} x_{t+1}^a \\ x_{t+1}^b \end{bmatrix} = \begin{bmatrix} A_a & \mathbf{0} \\ \mathbf{0} & A_b \end{bmatrix} \begin{bmatrix} x_t^a \\ x_t^b \end{bmatrix},$$

$$y_t = \begin{bmatrix} C_a & C_b \end{bmatrix} \begin{bmatrix} x_t^a \\ x_t^b \end{bmatrix},$$

where $\begin{bmatrix} x_t^a \\ x_t^b \end{bmatrix} = M^{-1}x_t$, $A_a = \text{diag}(J_i, i \in \{1,\dots,p_0\})$, $A_b = \text{diag}(J_i, i \in \{p_0+1,\dots,p\})$, and $\begin{bmatrix} C_a & C_b \end{bmatrix} = CM$. With this partition x_t^a contains the modes associated with the non-zero eigenvalues, therefore the A_a matrix is invertible. The state x_t^b contains the modes associated with the zero eigenvalue, therefore A_b is nilpotent, i.e. there exists a positive integer t_0 such that $A_b^t = \mathbf{0}$ for $t \geq t_0$, and therefore it holds that $x_t^b = 0$ for all $t \geq t_0$.

Since all the modes associated with the zero eigenvalues will converge to zero asymptotically we can derive the following state-space equation:

$$\begin{aligned} x_{t+1}^a &= A_a x_{t+1}^a, \\ y_t &= C_a x_t^a, \end{aligned}$$

for $t \geq t_0$. Therefore we can design a stable estimator for x_t using Assumption A6 by only estimating the state x_t^a, from which the state x_t can be obtained using the relation $x_t = M \begin{bmatrix} x_t^a \\ \mathbf{0} \end{bmatrix}$.

C.2 Proofs

Before proceeding to the convergence results, the following result is required.

Lemma 20 (Lemma 1 of Battistelli and Chisci [2014])**.** Define $\psi(\Omega) := \left(A\Omega^{-1}A^T + Q\right)^{-1}$, with $Q > 0$. Then, if A is invertible, for any positive definite matrices $\mathring{\Omega}$ and $\breve{\Omega}$ there exist positive scalars $\mathring{\beta} < 1$ and $\breve{\beta} \leq 1$ such that:

I) For any $\Omega \geq \mathring{\Omega} > 0$ we obtain $\psi(\Omega) \leq \mathring{\beta}A^{-T}\Omega A^{-1}$.

II) For any $\breve{\Omega} \geq \Omega > 0$ we obtain $\psi(\Omega) \geq \breve{\beta}A^{-T}\Omega A^{-1}$.

Proof of Lemma 20. Since $Q > 0$, there exists a positive constant $\tilde{\gamma} > 0$ such that

$$A^{-1}QA^{-T} \geq \tilde{\gamma}\mathring{\Omega}^{-1},$$

and therefore since $\Omega \geq \mathring{\Omega} > 0$ we obtain

$$A^{-1}QA^{-T} \geq \mathring{\gamma}\Omega^{-1},$$

and part I of the lemma follows with $\mathring{\beta} := \frac{1}{1+\mathring{\gamma}}$.

For part II, we note that since $\breve{\Omega} > 0$, for each positive constant $\alpha > 0$ there exists a positive constant $\bar{\gamma}(\alpha) > 0$ such that

$$A^{-1}QA^{-T} \leq \bar{\gamma}(\alpha)\left(\breve{\Omega} + \alpha I_n\right)^{-1} \leq \bar{\gamma}(\alpha)\left(\Omega + \alpha I_n\right)^{-1}.$$

One can observe that $\bar{\gamma}(\alpha)$ decreases with α. The conclusion follows by taking the limit

$$\breve{\gamma} := \lim_{\alpha \to 0} \bar{\gamma}(\alpha),$$

and defining $\breve{\beta} := \frac{1}{1+\breve{\gamma}}$. □

Proof of Theorem 10. To prove boundedness of the covariance matrix we first note that, from (8.6), $P_t \leq (W+S)^{-1}$ for $t \geq 1$. Applying part II of Lemma 20 with $\breve{\Omega} := W + S$ yields

$$P_{t+1}^{-1} \geq S + \breve{\beta}A^{-T}\Omega_t A^{-1}. \tag{C.1}$$

Therefore, applying recursively (C.1) yields, for $t \geq n$,

$$P_t^{-1} \geq \sum_{i=0}^{n-1} \breve{\beta}\left(A^{-i}\right)^T SA^{-i} := \mathring{\Omega} > 0,$$

and, for $t \geq n$, we obtain $P_t \leq \breve{P}$ with $\mathring{P} := \mathring{\Omega}^{-1}$.

For $1 \leq t < n$, if one considers that initially $P_0 > 0$ then, from (8.6), one has that $P_t > 0$ within that interval and since the set $1 \leq t < n$ is finite, there exists a maximum $\max_{1 \leq t < n} P_t$ and therefore the covariance P_t is bounded from above for all time t. □

Proof of Theorem 11. Noting that, for $t \geq n$,

$$\mathring{\Omega} := \sum_{i=0}^{n-1} \breve{\beta}\left(A^{-i}\right)^T SA^{-i} \leq \Omega_t \leq \breve{\Omega} := W + S,$$

from the covariance prediction equation (8.4) one can bound the disturbance vector $\varepsilon_t := C^T V v_{t+1} - \bar{\Omega}_t w_t$ as

$$\begin{aligned}\|\varepsilon_t\| &\leq \|C^T V\| \|v_{t+1}\| + \|\bar{\Omega}_t\| \|w_t\| \\ &\leq \|C^T V\| \sqrt{m}\epsilon_v + \frac{1}{\sigma_m\left(A^T \breve{\Omega}^{-1} A + Q\right)} \sqrt{n}\epsilon_w := \epsilon_M.\end{aligned}$$

We now define a candidate Lyapunov function as

$$V_t(e_t) := e_t^T \Omega_t e_t.$$

From Theorem 10 can conclude that $V_t(\cdot)$ is positive definite, and that, for $t \geq n$, $\sigma_m\left(\mathring{\Omega}\right) x^2 \leq V_t(x) \leq \sigma_M\left(\breve{\Omega}\right) x^2$.

Now we prove the convergence to zero of the estimation error for the noiseless case, i.e. when $w_t = \mathbf{0}$ and $v_t = \mathbf{0}$. We first note, from (8.4) that $P_t \preceq \bar{P}_t$ and from part I of Lemma 20 with $\mathring{\Omega} := \sum_{i=0}^{n-1} \breve{\beta}\left(A^{-i}\right)^T C^T R^{-1} C A^{-i}$, that $P_t^{-1} \preceq \mathring{\beta} A^{-1} \bar{P}_t^{-1} A^{-T}$. Then the Lyapunov function candidate has the following decrease property for the noiseless case

$$\begin{aligned}V_{t+1}(e_{t+1}) &= e_{t+1}^T \Omega_{t+1} e_{t+1} = \bar{e}_{t+1}^T \bar{\Omega}_{t+1} P_{t+1} \bar{\Omega}_{t+1} \bar{e}_{t+1} \\ &\leq \bar{e}_{t+1}^T \bar{\Omega}_{t+1} \bar{e}_{t+1} = e_t^T A^T \bar{\Omega}_{t+1} A e_t \\ &\leq \mathring{\beta} e_t^T \Omega_t e_t = \mathring{\beta} V_t(e_t).\end{aligned}$$

Therefore, for the noiseless case, the estimation error converges to zero.

In the noisy case, choosing a positive constant θ such that $0 < \theta < 1 - \mathring{\beta}$, from (8.11) we obtain

$$\begin{aligned}V_{t+1}(e_{t+1}) &\leq \mathring{\beta} V_t(e_t) + 2 e_t^T A^T \bar{\Omega}_{t+1} P_{t+1} \varepsilon_t + \varepsilon_t^T P_{t+1} \varepsilon_t \\ &\leq (\mathring{\beta} + \theta) V_t(e_t) + 2\left(\|e_t\| \frac{\|A\|}{\sigma_m(A^T \breve{\Omega}^{-1} A + Q)\sigma_m(\mathring{\Omega})} \epsilon_M - \frac{\theta}{2} \sigma_m(\mathring{\Omega}) \|e_t\|^2\right) + \frac{1}{\sigma_m(\mathring{\Omega})} \epsilon_M^2.\end{aligned}$$

To guarantee that $V_t(e_t)$ decreases, one must first ensure that

$$\frac{\theta}{2} \sigma_m(\mathring{\Omega}) \|e_t\|^2 \geq \frac{\|A\|}{\sigma_m(A^T \breve{\Omega}^{-1} A + Q)\sigma_m(\mathring{\Omega})} \epsilon_M.$$

Therefore if e_t satisfies

$$\|e_t\| \geq \frac{2\|A\|}{\theta \sigma_m(A^T \breve{\Omega}^{-1} A + Q)\sigma_m^2(\mathring{\Omega})} \epsilon_M,$$

we obtain

$$V_{t+1}(e_{t+1}) \leq \left(\mathring{\beta} + \theta\right) V_t(e_t) + \frac{1}{\sigma_m(\mathring{\Omega})} \epsilon_M^2.$$

In this case, we can guarantee that $V_{t+1}(e_{t+1}) \leq V_t(e_t)$ when

$$\left(\mathring{\beta} + \theta\right) V_t(e_t) + \frac{1}{\sigma_m(\mathring{\Omega})} \epsilon_M^2 \leq V_t(e_t),$$

which is equivalent to, using the fact that $V_t(e_t) \leq \sigma_M\left(\breve{\Omega}\right) \|e_t\|^2$,

$$\frac{\epsilon_M}{\sigma_m\left(\mathring{\Omega}\right) \sqrt{1 - \mathring{\beta} - \theta}} \leq \|e_t\|.$$

Therefore, if

$$\xi := \frac{1}{\sigma_m\left(\mathring{\Omega}\right)} \max\left(\frac{2\|A\|}{\theta\sigma_m(A^T\breve{\Omega}^{-1}A+Q)\sigma_m(\mathring{\Omega})}, \frac{1}{\sqrt{1-\mathring{\beta}-\theta}}\right)\epsilon_m \le \|e_t\|^2,$$

we can guarantee that $V_t(e_t)$ decreases. Since $V_t(e_t) \le \sigma_M\left(\breve{\Omega}\right)\|e_t\|^2$, if $\sigma_M\left(\breve{\Omega}\right)\xi^2 \le V_t(e_t)$ then $\xi \le \|e_t\|$ and therefore $V_t(e_t)$ decreases according to

$$\max\left(V_{t+1}(e_{t+1}) - \sigma_M\left(\breve{\Omega}\right)\xi^2, 0\right) \le \left(\mathring{\beta}+\theta\right)\max\left(V_t(e_t) - \sigma_M\left(\breve{\Omega}\right)\xi^2, 0\right),$$

hence

$$\lim_{t\to\infty} \max\left(V_t(e_t) - \sigma_M\left(\breve{\Omega}\right)\xi^2, 0\right) = 0,$$

and from the fact that $\sigma_m\left(\mathring{\Omega}\right)\|e_t\|^2 \le V_t(e_t)$ the theorem follows. □

Proof of Theorem 12. After the agents communicate among themselves, we wish to compute $\tilde{x}_t^i$, the BLU estimate given the estimates of the neighbours, i.e. given $\bar{x}_t^j, j \in \mathcal{N}^i$, where $\mathcal{N}^i$ is the set of neighbours of i. The estimate $\tilde{x}_t^i$, can be computed as follows. Then, the estimate $\tilde{x}_t^i$ is the BLUE of x_t such that $\eta_i\bar{x}_t = \mathbf{1}_i x_t + \epsilon_t$ with $\epsilon_t \sim \mathcal{N}\left(0, \eta_i\bar{P}_t\eta_i^T\right)$. Therefore from Lemma 3, if $\bar{P}_t^{ii}$ is full rank, we obtain

$$\tilde{x}_t^i = \left(\tilde{\Omega}_t^i\right)^{-1}\mathbf{1}_i^T\left(\eta_i\bar{P}_t\eta_i^T\right)^{\dagger}\eta_i\bar{x}_t,$$

and $\tilde{x}_t^i$ has the following characteristics:

$$\begin{aligned} E\left[\tilde{x}_t^i - x_t\right] &= 0, \\ E\left[\left(\tilde{x}_t^i - x_t\right)\left(\tilde{x}_t^i - x_t\right)^T\right] &= \left(\tilde{\Omega}_t^i\right)^{-1}, \end{aligned}$$

where $\tilde{\Omega}_t^i := \mathbf{1}_i^T\left(\eta_i\bar{P}_t\eta_i^T\right)^{\dagger}\mathbf{1}_i$. We can also express $\tilde{x}_t^i$ as

$$\tilde{x}_t^i = \left(\tilde{\Omega}_t^i\right)^{-1}\mathbf{1}_i^T\left(\eta_i\bar{P}_t\eta_i^T\right)^{\dagger}\sum_{j\in\mathcal{N}^i}\Gamma_{ij}\bar{x}_t^j.$$

After taking a measurement, one wishes to compute $\hat{x}_t^i$, the BLUE of x_t given $\tilde{x}_t^i$ and y_t^i. This can be obtained directly as

$$\hat{x}_t^i = \left(\Omega_t^i\right)^{-1}\left(\tilde{\Omega}_t^i\tilde{x}_t^i + \left(C^i\right)^T\left(R^i\right)^{-1}y_t^i\right).$$

Finally, we do the prediction, i.e. we compute the estimate of x_{t+1} given $\hat{x}_t^i$, which is simply

$$\bar{x}_{t+1}^i = A\hat{x}_t^i.$$

We are still left to compute the next global covariance matrix $\bar{P}_{t+1}$. For this purpose we must analyze the error dynamics, i.e. the dynamics of $\bar{e}_t^i := \bar{x}_t^i - x_t$. The dynamics of the estimate $\bar{x}_t^i$ can be written as follows:

$$\bar{x}_{t+1}^i = A\left(\Omega_t^i\right)^{-1}\left(\sum_{j\in\mathcal{N}^i}\mathbf{1}_i^T\left(\eta_i\bar{P}_t\eta_i^T\right)^{\dagger}\Gamma_{ij}\bar{x}_t^j + \left(C^i\right)^T\left(R^i\right)^{-1}y_t^i\right)$$

$$= A\left(\Omega_t^i\right)^{-1}\left(\sum_{j\in\mathcal{N}^i} \mathbf{1}_i^T\left(\eta_i\bar{P}_t\eta_i^T\right)^{\dagger}\Gamma_{ij}\bar{x}_t^j + S^i x_t\right) + A\left(\Omega_t^i\right)^{-1}\left(C^i\right)^T\left(R^i\right)^{-1} v_t^i.$$

Given that $\bar{\Omega}_t^i = \sum_{j\in\mathcal{N}^i} \mathbf{1}_i^T\left(\eta_i\bar{P}_t\eta_i^T\right)^{\dagger}\Gamma_{ij}$ (from the fact that $\sum_{j\in\mathcal{N}^i}\Gamma_{ij} = \mathbf{1}_i$) the state dynamics can be expressed as

$$\begin{aligned} x_{t+1} = Ax_t + w_t &= A\left(\Omega_t^i\right)^{-1}\left(\bar{\Omega}_t^i x_t + S^i x_t\right) + w_t \\ &= A\left(\Omega_t^i\right)^{-1}\left(\sum_{j\in\mathcal{N}^i} \mathbf{1}_i^T\left(\eta_i\bar{P}_t\eta_i^T\right)^{\dagger}\Gamma_{ij}x_t + S^i x_t\right) + w_t. \end{aligned}$$

The error dynamics can then be written according to

$$e_{t+1}^i = A\left(\Omega_t^i\right)^{-1}\left(\sum_{j\in\mathcal{N}^i} \mathbf{1}_i^T\left(\eta_i\bar{P}_t\eta_i^T\right)^{\dagger}\Gamma_{ij}e_t^j\right) + A\left(\Omega^i\right)^{-1}\left(C^i\right)^T\left(R^i\right)^{-1} v_t^i - w_t. \tag{C.2}$$

Defining $v_t = \mathrm{col}(v_t^i)$ yields

$$e_{t+1} = T_t e_t + K v_t + \mathbf{1}_N \otimes I_n w_t.$$

with $K := \mathrm{diag}\left(A\left(\Omega_t^i\right)^{-1}\left(C^i\right)^T\left(R^i\right)^{-1}\right)$. Finally, we can compute the update law for $\bar{P}_t$, (8.16). □

Lemma 21 (Lemma 2 of Battistelli and Chisci [2014])**.** Given an integer $N \geq 2$, N positive definite matrices $M_1,\ldots,M_N$, and N vectors $v_1,\ldots,v_N$, the following inequality holds

$$\left(\sum_{i=1}^N M_i v_i\right)^T\left(\sum_{i=1}^N M_i\right)^{-1}\left(\sum_{i=1}^N M_i v_i\right) \leq \sum_{i=1}^N v_i^T M_i v_i. \tag{C.3}$$

Proof of Theorem 13. Defining the matrix

$$\phi_t^{ij} := \pi^{ij} A P_t^i \bar{\Omega}_t^j,$$

we obtain, from the distributed consensus-based Kalman filter equations (8.19)-(8.22) the following error dynamics

$$\bar{e}_{t+1}^i = \sum_{j\in\mathcal{N}} \phi_t^{ij}\bar{e}_t^j + AP_t^i\left(C^i\right)^T V^i v_t^i + w_t.$$

We now consider the noiseless case where $v_t^i = \mathbf{0}$, $i\in\mathcal{N}$, and $w_t = \mathbf{0}$, and define the matrix $\Pi := \left[\pi^{i,j}\right]_{i,j\in\mathcal{N}}$. It follows from the properties of Π that we can find a vector $p := \mathrm{col}(p^i)$ such that $p^T\Pi = p^T$. Then, the Lyapunov function used to prove convergence is the following:

$$V_t(\bar{e}_t) = \sum_{i\in\mathcal{N}} p^i\left(\bar{e}_t^i\right)\bar{\Omega}_t^i\bar{e}_t^i. \tag{C.4}$$

From Lemma 20 and boundedness of information matrix (Lemma 1 of Battistelli et al. [2015]) it follows that

$$\begin{aligned} \left(\bar{e}_{t+1}^i\right)^T\bar{\Omega}_{t+1}^i\bar{e}_{t+1}^i &= \left(\sum_{j\in\mathcal{N}}\phi_t^{ij}\bar{e}_t^j\right)^T\bar{\Omega}_{t+1}^i\sum_{j\in\mathcal{N}}\phi_t^{ij}\bar{e}_t^j \\ &\leq \mathring{\beta}\left(\sum_{j\in\mathcal{N}}\pi^{ij}\bar{\Omega}_t^j\bar{e}_t^j\right)^T P_t^i\sum_{j\in\mathcal{N}}\pi^{ij}\bar{\Omega}_{t|t-1}^j\bar{e}_t^j \end{aligned}$$

$$\leq \mathring{\beta} \sum_{j\in\mathcal{N}} \pi^{ij} \left(\bar{e}_t^j\right)^T \bar{\Omega}_t^j \bar{e}_t^j.$$

We can now establish the decreasing property of the Lyapunov function as follows:

$$\begin{aligned} V_{t+1}(\bar{e}_{t+1}) &= \sum_{i\in\mathcal{N}} p^i \left(\bar{e}_{t+1}^i\right) \bar{\Omega}_{t+1}^i \bar{e}_{t+1}^i \\ &\leq \mathring{\beta} \sum_{i,j\in\mathcal{N}} p^i \pi_L^{ij} \left(\bar{e}_t^j\right)^T \bar{\Omega}_t^j \bar{e}_t^j \\ &= \mathring{\beta} \sum_{i,j\in\mathcal{N}} p^i \left(\bar{e}_t^i\right)^T \bar{\Omega}_t^i \bar{e}_t^i = \mathring{\beta} V_t(\bar{e}_t), \end{aligned}$$

thus proving that for the noiseless case the estimation errors converge to zero. Since we assume additive bounded noise and the dynamics are linear, ultimate boundedness of the estimation error follows. □

Proof of Theorem 14. Before proceeding with the proof, we define $q_t := \mathrm{col}\left(q_t^i\right)$, $e_{t,0}^i := z_{t,0}^i - x_t$, $e_{t,0} := \mathrm{col}\left(e_{t,0}^i\right)$, and the local and global noise contributions to the error dynamics $\omega_t^i := w_t - L^i v_t^i$, $\omega_t := \mathrm{col}\left(\omega_t^i\right)$. Combining the fact that the consensus algorithm preserves averages, i.e. that $\frac{1}{N}\sum_{j\in\mathcal{N}} z_{t,l}^j = \frac{1}{N}\sum_{j\in\mathcal{N}} z_{t,l+1}^j$, and the error dynamics (8.25), we obtain the following result which describes the dynamics of the estimation errors $e_{t+1,0}$ and the dynamics of the average of the estimation errors before consensus e_t^{avg}. Let the distributed Luenberger observer algorithm be adopted with $l_f \geq 1$; then, the estimation errors obey the recursion

$$e_{t+1,0} = \mathrm{col}\left(A - L^i C^i\right) e_{t,0}^{\mathrm{avg}} + \mathrm{diag}\left(A - L^i C^i\right) q_t + \omega_t, \tag{C.5}$$

and

$$e_{t+1}^{\mathrm{avg}} = (A - LC)\, e_t^{\mathrm{avg}} + \frac{1}{N}\mathbf{1}^T \otimes I_n \left(\omega_t + \mathrm{diag}\left(A - L^i C^i\right) q_t\right). \tag{C.6}$$

We consider now the noiseless case where $\omega_t = 0$ for all $t \geq 0$ and derive results on the norms of $e_{t,0}$ and e_t^{avg} by taking the norms of both sides of equations (C.5) and (C.6), respectively. From Theorem 7 we obtain

$$\|q_t\|_{I_N\otimes P_1} \leq \sigma_2^{l_f} \|e_{t,0}\|_{I_N\otimes P_1}.$$

Therefore, we can bound $\left\|e_{t+1}^{\mathrm{avg}}\right\|_{P_1}$ and $\|e_{t+1,0}\|_{I_N\otimes P}$ by taking the norm of (12.18) and (12.17), as follows:

$$\left\|e_{t+1}^{\mathrm{avg}}\right\|_{P_1} \leq \|A - LC\|_{P_1} \left\|e_t^{\mathrm{avg}}\right\|_{P_1} + \max\left(\left\|A - L^i C^i\right\|_{P_1}\right) \sigma_2^{l_f} \frac{1}{\sqrt{N}} \|e_{t,0}\|_{I_N\otimes P_1}, \tag{C.7}$$

$$\|e_{t+1,0}\|_{I_N\otimes P_1} \leq \max\left(\left\|A - L^i C^i\right\|_P\right) \sqrt{N} \left\|e_t^{\mathrm{avg}}\right\|_{P_1} + \max\left(\left\|A - L^i C^i\right\|_{P_1}\right) \sigma_2^{l_f} \|e_{t,0}\|_{I_N\otimes P_1}.$$

We need an upper bound of $\|e_{t+1,0}\|_{I_N\otimes P_1}$ which is equal to the upper bound of $\|e_{t+1}^{\mathrm{avg}}\|_P$ times a constant, we upper bound $\|e_{t+1,0}\|_{I_N\otimes P_1}$ as follows:

$$\begin{aligned} &\|e_{t+1,0}\|_{I_N\otimes P_1} \\ &\leq \sqrt{N} \max\left(1, \frac{\left\|A - L^i C^i\right\|_{P_1}}{\|A - LC\|_{P_1}}\right) \left(\|A - LC\|_{P_1} \left\|e_t^{\mathrm{avg}}\right\|_{P_1} + \max\left(\left\|A - L^i C^i\right\|_{P_1}\right) \sigma_2^{l_f} \frac{1}{\sqrt{N}} \|e_{t,0}\|_{I_N\otimes P_1}\right). \end{aligned} \tag{C.8}$$

It is given by assumption that for $t \leq p \leq 0$ we are under the conditions of Lemma 14, then equations (12.19) and (12.21) hold. Note that since we initialized the algorithm with $z_{0,0}^i = z_{0,0}^j$ for any $i, j \in \mathcal{N}$, we obtain $e_{0,0} = \mathbf{1} e_0^{\mathrm{avg}}$, and therefore $\|e_{0,0}\|_{I_N\otimes P_1} = \sqrt{N} \left\|e_0^{\mathrm{avg}}\right\|_{P_1} \leq \sqrt{N} \max\left(1, \frac{\|A - L^i C^i\|_{P_1}}{\|A - LC\|_{P_1}}\right) \left\|e_0^{\mathrm{avg}}\right\|_{I_N\otimes P_1}$. Applying equations (C.7) and

(C.8) at $p = 1$ we obtain

$$\begin{aligned}
\|e_1^{\text{avg}}\|_{P_1} &\leq \|A - LC\|_{P_1} \|e_0^{\text{avg}}\|_{I_N \otimes P_1} + \max\left(\left\|A - L^i C^i\right\|_{P_1}\right) \sigma_2^{l_f} \frac{1}{\sqrt{N}} \|e_{0,0}\|_{I_N \otimes P_1} \leq \bar{\beta} \|e_{0,0}\|_{I_N \otimes P_1}, \\
\|e_{1,0}\|_{I_N \otimes P_1} &\leq \sqrt{N} \max\left(1, \frac{\|A - L^i C^i\|_{P_1}}{\|A - LC\|_{P_1}}\right) \bar{\beta} \|e_0^{\text{avg}}\|_{P_1},
\end{aligned}$$

where $\bar{\beta}$ is defined as

$$\bar{\beta} := \|A - LC\|_{P_1} + \sigma_2^{l_f} \max\left(\left\|A - L^i C^i\right\|_{P_1}\right) \max\left(1, \frac{\|A - L^i C^i\|_{P_1}}{\|A - LC\|_{P_1}}\right),$$

and is strictly positive and smaller than 1 by assumption. At $p = 2$ we obtain

$$\begin{aligned}
\|e_2^{\text{avg}}\|_{P_1} &= \bar{\beta}^2 \|e_0^{\text{avg}}\|_{P_1} \\
\|e_{2,0}\|_{I_N \otimes P_1} &\leq \sqrt{N} \max\left(1, \frac{\|A - L^i C^i\|_{P_1}}{\|A - LC\|_{P_1}}\right) \bar{\beta}^2 \|e_0^{\text{avg}}\|_{P_1}.
\end{aligned}$$

Repeating this step p times yields

$$\left\|e_{p+1,0}^{\text{avg}}\right\|_{I_N \otimes P_1} \leq \bar{\beta}^{p+1} \|e_{0,0}\|_{I_N \otimes P_1}.$$

Similarly to the previous point, applying equations (C.7) and (C.8) recursively, and following the same steps we have for $\|e_{p,0}\|$ and for any p such that $t + 1 \geq p \geq 0$.

$$\|e_{p+1,0}\|_{I_N \otimes P_1} \leq \sqrt{N} \max\left(1, \frac{\|A - L^i C^i\|_{P_1}}{\|A - LC\|_{P_1}}\right) \bar{\beta}^{p+1} \|e_0^{\text{avg}}\|_{P_1}.$$

We have thus proved that in the noiseless case the estimation errors converge to zero. Since we assume additive bounded noise and the dynamics are linear, ultimate boundedness of the estimation error follows. □

D Appendices of Chapter 10

D.1 Proofs

Proof of Lemma 5. The proof exploits the use of the Lyapunov function $V = \frac{1}{2}\|\eta_e\|^2 = \frac{1}{2}\left(\|\boldsymbol{e}-\boldsymbol{\delta}\|^2 + c_\omega \omega^2\right)$.

From (10.19) and (10.20) we have, when $\dot{\tilde{v}}_r$ is defined,

$$\dot{\omega} = \ddot{\gamma} - \dot{v}_r - \dot{\tilde{v}}_r = -k_\omega \omega + \frac{1}{c_\omega}(\boldsymbol{e}-\boldsymbol{\delta})^T R^T \frac{\partial \boldsymbol{p}_d}{\partial \gamma}, \tag{D.1}$$

and since ω is continuous and $-k_\omega\omega + \frac{1}{c_\omega}(\boldsymbol{e}-\boldsymbol{\delta})^T R^T \frac{\partial \boldsymbol{p}_d}{\partial \gamma}$ is also continuous we have that $\dot{\omega}$ is continuous and (D.1) holds at all times.

From (10.18) and (10.21) we have

$$\dot{\boldsymbol{e}} = -S(r)(\boldsymbol{e}-\boldsymbol{\delta}) - K_k(\boldsymbol{e}-\boldsymbol{\delta}) - R^T \frac{\partial \boldsymbol{p}_d}{\partial \gamma}\omega - \begin{bmatrix} 0 \\ \delta\tilde{r} \end{bmatrix} + \begin{bmatrix} \tilde{u} \\ v_w + \tilde{v}_c \end{bmatrix}.$$

Noting that $x^T S(r) x = 0$, $\forall x \in \mathbb{R}^2$, computing the time derivative of V yields

$$\begin{aligned}
\dot{V} &= (\boldsymbol{e}-\boldsymbol{\delta})^T \left(-K_k(\boldsymbol{e}-\boldsymbol{\delta}) - \begin{bmatrix} 0 \\ \delta\tilde{r} \end{bmatrix} + \begin{bmatrix} \tilde{u} \\ v_w + \tilde{v}_c \end{bmatrix}\right) - k_\omega c_\omega \omega^2 \\
&= -(\boldsymbol{e}-\boldsymbol{\delta})^T K_k(\boldsymbol{e}-\boldsymbol{\delta}) - c_\omega k_\omega \omega^2 + (\boldsymbol{e}-\boldsymbol{\delta})^T \left(-\begin{bmatrix} 0 \\ \delta\tilde{r} \end{bmatrix} + \begin{bmatrix} \tilde{u} \\ v_w + \tilde{v}_c \end{bmatrix}\right).
\end{aligned}$$

Defining $K_e := \mathrm{diag}\{k_x, k_y, k_\omega\}$ we obtain the following result

$$\begin{aligned}
\dot{V} \le & -\eta_e^T K_e \eta_e + \|\eta_e\| \Bigg(\sqrt{\epsilon_{\tilde{u}}^2 + \left(\epsilon_v + \epsilon_{v_c}\right)^2} + \delta\epsilon_{\tilde{r}} \\
& + \sqrt{\left(\beta^{\tilde{u}}\left(\|\boldsymbol{x}_{il}^0\|, t\right)\right)^2 + \left(\beta^{v}\left(\|\boldsymbol{x}_{il}^0\|, t\right)\right)^2} + \delta\beta^{\tilde{r}}\left(\|\boldsymbol{x}_{il}^0\|, t\right) + \beta^{v_c}\left(\|\boldsymbol{x}_{v_c}^0\|, t\right)\Bigg).
\end{aligned} \tag{D.2}$$

The rest of the proof involves dominating all positive terms of (D.2) by $-\eta_e^T K_e \eta_e \le -\min(k_x, k_y, k_\omega)\|\eta_e\|^2$. To do this, notice from (D.2) that

$$\dot{V} \leq -(1-\theta)\min(k_x,k_y,k_\omega)\|\eta_e\|^2 + \|\eta_e\|\left(\sqrt{\epsilon_{\tilde{u}}^2 + \left(\epsilon_v + \epsilon_{v_c}\right)^2} + \delta\epsilon_{\tilde{r}}\right.$$
$$\left. + \sqrt{\left(\beta^{\tilde{u}}\left(\|\boldsymbol{x}_{il}^0\|,t\right)\right)^2 + \left(\beta^{v}\left(\|\boldsymbol{x}_{il}^0\|,t\right)\right)^2} + \delta\beta^{\tilde{r}}\left(\|\boldsymbol{x}_{il}^0\|,t\right) + \beta^{v_c}\left(\|\boldsymbol{x}_{v_c}^0\|,t\right) - \theta\min(k_x,k_y,k_\omega)\|\eta_e\|\right),$$

and therefore, defining

$$\beta_{il}(x,t) := \frac{\sqrt{\left(\beta^{\tilde{u}}(x,t)\right)^2 + \left(\beta^{v}(x,t)\right)^2} + \delta\beta^{\tilde{r}}(x,t)}{\theta\min(k_x,k_y,k_\omega)},$$
$$\beta_{obs}(x,t) := \frac{\beta^{v_c}(x,t)}{\theta\min(k_x,k_y,k_\omega)},$$
$$\varepsilon_e := \frac{\sqrt{\epsilon_{\tilde{u}}^2 + \left(\epsilon_v + \epsilon_{v_c}\right)^2} + \delta\epsilon_{\tilde{r}}}{\theta\min(k_x,k_y,k_\omega)},$$

where $0 < \theta < 1$ we have

$$\dot{V} \leq -(1-\theta)\min(k_x,k_y,k_\omega)\|\eta_e\|^2, \forall \|\eta_e\| \geq \beta_{il}\left(\|x_{il}^0\|,t\right) + \beta_{obs}\left(\|\boldsymbol{x}_{v_c}^0\|,t\right) + \varepsilon_e,$$

from which (10.23) follows with $\beta^e(x,t) := xe^{-(1-\theta)\min(k_x,k_y,k_\omega)t}$, where $\beta_{il}^e(x,t)$ and $\beta_{obs}^e(x,t)$ are defined such that $\beta_{il}^e(x,0) := \beta_{il}(x,0)$, $\beta_{obs}^e(x,0) := \beta_{obs}(x,0)$ and, assuming without loss of generality that $\beta_{il}(x,t)$ and $\beta_{obs}(x,t)$ are differentiable in t (one can always upper bound a $\mathcal{KL}$ function by a differentiable $\mathcal{KL}$ function)

$$\frac{\partial}{\partial t}\beta_{il}^e(x,t) = \begin{cases} -(1-\theta)\min(k_x,k_y,k_\omega)\beta_{il}^e(x,t) & \text{if } \beta_{il}^e(x,t) > \beta_{il}(x,t) \\ \max\left(-(1-\theta)\min(k_x,k_y,k_\omega)\beta_{il}^e(x,t),\ \frac{\partial}{\partial t}\beta_{il}(x,t)\right) & \text{if } \beta_{il}^e(x,t) = \beta_{il}(x,t) \end{cases},$$
$$\frac{\partial}{\partial t}\beta_{obs}^e(x,t) = \begin{cases} -(1-\theta)\min(k_x,k_y,k_\omega)\beta_{obs}^e(x,t) & \text{if } \beta_{obs}^e(x,t) > \beta_{obs}(x,t) \\ \max\left(-(1-\theta)\min(k_x,k_y,k_\omega)\beta_{obs}^e(x,t),\ \frac{\partial}{\partial t}\beta_{obs}(x,t)\right) & \text{if } \beta_{obs}^e(x,t) = \beta_{obs}(x,t) \end{cases}.$$

□

Proof of Lemma 6. Defining

$$\bar{\gamma} := \frac{1}{N}\mathbf{1}^T\gamma,$$

we can decompose γ as

$$\gamma = \mathbf{1}\bar{\gamma} + \xi.$$

Using this fact and recalling that $v_r(\gamma)$ is assumed to be globally Lipschitz we can conclude that

$$\xi^T\Gamma\bar{v}_r = \xi^T\Gamma\left(\mathbf{1}v_r(\bar{\gamma}) - (\mathbf{1}v_r(\bar{\gamma}) - \bar{v}_r)\right) = \xi^T\Gamma\left(\bar{v}_r - \mathbf{1}v_r(\bar{\gamma})\right) \leq l\|\xi\|^2.$$

We can now bound the time derivative of V with

$$\dot{V} \leq -k\xi^T\boldsymbol{L}\xi + l\|\xi\|^2 + \xi^T\Gamma\bar{\omega} + k\xi^T\Gamma\tilde{\gamma} \leq -k\sigma_2\|\xi\|^2 + l\|\xi\|^2 + \|\xi\|\|\bar{\omega}\| + kd^*\|\xi\|\|\tilde{\gamma}\|.$$

We can then conclude that $\dot{V} < -(1-\theta)(k\sigma_2 - l)\|\xi\|^2$ for $\|\xi\| \geq \sigma_\omega^\xi(\|\bar{\omega}\|_{[0,t]}) + \sigma_{\tilde{\gamma}}^\xi(\|\tilde{\gamma}\|_{[0,t]})$, for $1 > \theta > 0$, where $\sigma_\omega^\xi(s) := \dfrac{1}{(k\sigma_2 - l)\theta}s$, $\sigma_{\tilde{\gamma}}^\xi(s) := \dfrac{kd^*}{(k\sigma_2 - l)\theta}s$. The conclusion of the lemma follows with $\beta^\xi(x,t) := xe^{-(1-\theta)(k\sigma_2 - l)t}$. □

Proof of Lemma 7. The proof is based on Lemmas 5 and 6 together with Theorem 16.

Lemma 5 implies that $\Sigma_i^{pf}, i \in \mathcal{N}$ solve the path-following problem with $\sigma_{\tilde{v}_r}^{e}(s) := \alpha s$, for $\alpha > 0$ with α arbitrarily small. Lemma 6 states that $\Sigma_i^{cc}, i \in \mathcal{N}$ solve the coordination control problem. Since α can be arbitrarily small, Theorem 16 implies that Σ^{cl} solves robustly the CPF problem.

From the proofs of Lemmas 5 and 6 one can also bound $\|\xi\|$ as

$$\begin{aligned}\|\xi\| \le \beta^{\xi}(\|\xi(0)\|,t) + \beta^{\xi}_{e\omega}\left(\max_{i\in\mathcal{N}}\|\eta_{e_i}(0)\|,t\right) + \beta^{\xi}_{il}\left(\max_{i\in\mathcal{N}}\|\boldsymbol{x}^0_{il_i}\|,t\right) + \beta^{\xi}_{obs}\left(\max_{i\in\mathcal{N}}\|\boldsymbol{x}^0_{v_{ci}}\|,t\right)\\ + \sigma^{\xi}_{\tilde{\gamma}}\left(\max_{i\in\mathcal{N},j\in\mathcal{N}^i}\|\tilde{\gamma}_i^j\|_{[0,t]}\right) + \varepsilon_{e\xi},\end{aligned}$$

with

$$\begin{aligned}\beta^{\xi}_{e\omega}(x,t) &:= \frac{\sqrt{N/c_\omega}}{\theta\,(k\sigma_2 - l)}\, x e^{-(1-\theta)\min(k_x,k_y,k_\omega,k\sigma_2-l)},\\ \varepsilon_{e\xi} &:= \frac{\sqrt{N/c_\omega}}{\theta\,(k\sigma_2 - l)}\varepsilon_e,\\ \beta^{\xi}_{il}(x,t) &:= \frac{\sqrt{N/c_\omega}}{\theta\,(k\sigma_2 - l)}\tilde{\beta}_{il}(x,t),\\ \beta^{\xi}_{obs}(x,t) &:= \frac{\sqrt{N/c_\omega}}{\theta\,(k\sigma_2 - l)}\tilde{\beta}_{obs}(x,t),\end{aligned}$$

and with $\tilde{\beta}_{il}(x,t)$ and $\tilde{\beta}_{obs}(x,t)$ defined such that $\tilde{\beta}_{il}(x,0) := \beta_{il}(x,0)$, $\tilde{\beta}_{obs}(x,0) := \beta_{obs}(x,0)$, and

$$\begin{aligned}\frac{\partial}{\partial t}\tilde{\beta}_{il}(x,t) &= \begin{cases} -(1-\theta)\min\left(k_x,k_y,k_\omega,\,k\sigma_2-l\right)\tilde{\beta}_{il}(x,t) & \text{if } \tilde{\beta}_{il}(x,t) > \beta_{il}(x,t)\\ 0 & \text{otherwise}\end{cases},\\ \frac{\partial}{\partial t}\tilde{\beta}_{obs}(x,t) &= \begin{cases} -(1-\theta)\min\left(k_x,k_y,k_\omega,k\sigma_2-l\right)\tilde{\beta}_{obs}(x,t) & \text{if } \tilde{\beta}_{obs}(x,t) > \beta_{obs}(x,t)\\ 0 & \text{otherwise}\end{cases}.\end{aligned}$$

□

Proof of Lemma 8. If $\left\|\tilde{\gamma}_i^j\left(\left(t_k^{ij}+2\bar{\tau}\right)^+\right)\right\| < \varepsilon$ is satisfied, for any time t_k^{ij} when the data messages sent from agent i to j are received by j, defining $t_{CTC}\left(t_k^{ij}\right) \le t_k^{ij}$ the time when the last data message was sent triggered by a communication triggering condition (CTC) we have that $\left\|\tilde{\gamma}_i^j\left(t_{CTC}\left(t_k^{ij}\right)\right)\right\| = \varepsilon$ and $t_k^{ij} - t_{CTC}\left(t_k^{ij}\right) \le 2(N_{\max}-1)\bar{\tau}$.

From the definition of $\tilde{\gamma}_i^j$, the facts that $\dot{\gamma}_i = v_r(\gamma_i) + \tilde{v}_{r_i} + \omega_i$ and $\dot{\hat{\gamma}}_i^j = v_r\left(\hat{\gamma}_i^j\right)$, when the derivative is defined, we have for $t \in \left[t_{CTC}\left(t_k^{ij}\right), t_k^{ij}+2\bar{\tau}\right)$

$$\dot{\tilde{\gamma}}_i^j = v_r\left(\hat{\gamma}_i^j\right) - v_r(\gamma_i) - \tilde{v}_{r_i} - \omega_i \le l\left\|\tilde{\gamma}_i^j\right\| + kd^\star \max_{o\in\mathcal{N},p\in\mathcal{N}^o}\left\|\tilde{\gamma}_p^o\right\| + k\|\xi\| + \|\omega_i\|.$$

From the comparison lemma in Khalil [1996] (Lemma 3.4) we have for $t \in \left[t_{CTC}\left(t_k^{ij}\right), t_k^{ij}+2\bar{\tau}\right]$, $\left\|\tilde{\gamma}_i^j\right\| < \Gamma(t)$ where $\Gamma : \left[t_{CTC}\left(t_k^{ij}\right),\infty\right) \to [\varepsilon,\infty)$ is defined with $\Gamma\left(t_{CTC}\left(t_k^{ij}\right)\right) = \varepsilon$ and

$$\dot{\Gamma} = l\Gamma + kd^\star \max_{o\in\mathcal{N},p\in\mathcal{N}^o}\|\tilde{\gamma}_p^o\| + k\|\xi\|_{\left[t_{CTC}\left(t_k^{ij}\right),t_k^{ij}+2\bar{\tau}\right]} + \|\omega_i\|_{\left[t_{CTC}\left(t_k^{ij}\right),t_k^{ij}+2\bar{\tau}\right]}.$$

It follows that

$$
\begin{aligned}
\left\|\tilde{\gamma}_i^j\left(t_k^{ij}+2\bar{\tau}\right)\right\| &\leq \Gamma\left(t_k^{ij}+2\bar{\tau}\right)\\
&= \varepsilon e^{l\left(t_k^{ij}+2\bar{\tau}-t_{CTC}\left(t_k^{ij}\right)\right)} + z\left(l, t_k^{ij}+2\bar{\tau}-t_{CTC}\left(t_k^{ij}\right)\right) kd^\star \max_{o\in\mathcal{N}, p\in\mathcal{N}^o} \|\tilde{\gamma}_p^o\|\\
&\quad + z\left(l, t_k^{ij}+2\bar{\tau}-t_{CTC}\left(t_k^{ij}\right)\right)\left(k\|\xi\|_{\left[t_{CTC}(t_k^{ij}),t_k^{ij}+2\bar{\tau}\right]} + \|\omega_i\|_{\left[t_{CTC}(t_k^{ij}),t_k^{ij}+2\bar{\tau}\right]}\right)\\
&\leq \varepsilon e^{2lN_{\max}\bar{\tau}} + z\left(l, 2N_{\max}\bar{\tau}\right) kd^\star \max_{o\in\mathcal{N}, p\in\mathcal{N}^o} \|\tilde{\gamma}_p^o\|\\
&\quad + z\left(l, 2N_{\max}\bar{\tau}\right)\left(k\|\xi\|_{\left[t_k^{ij}-2(N_{\max}-1)\bar{\tau},t_k^{ij}+2\bar{\tau}\right]} + \|\omega_i\|_{\left[t_k^{ij}-2(N_{\max}-1)\bar{\tau},t_k^{ij}+2\bar{\tau}\right]}\right),
\end{aligned}
$$

where

$$
z(l,t) := \begin{cases} \frac{e^{lt}-1}{l}, & \text{if} \quad l>0\\ t, & \text{if} \quad l=0 \end{cases}.
$$

Therefore noting that $\max_{i\in\mathcal{N}, j\in\mathcal{N}^i, t\in\mathbb{R}^+} \|\tilde{\gamma}_i^j(t)\| \leq \max_{i\in\mathcal{N}, j\in\mathcal{N}^i, k\in\mathbb{N}^+} \|\tilde{\gamma}_i^j(t_k^{ij}+2\bar{\tau})\|$, if $N_{\max}$ and $\bar{\tau}$ are small enough such that $kd^\star z(l, 2N_{\max}\bar{\tau}) \leq 1$, we have

$$
\begin{aligned}
\max_{i\in\mathcal{N}, j\in\mathcal{N}^i, t\in\mathbb{R}^+} \|\tilde{\gamma}_i^j(t)\| &\leq \varepsilon e^{2lN_{\max}\bar{\tau}} + z(l, 2N_{\max}\bar{\tau}) kd^\star \max_{i\in\mathcal{N}, j\in\mathcal{N}^i, t\in\mathbb{R}^+} \|\tilde{\gamma}_i^j(t)\|\\
&\quad + z(l, 2N_{\max}\bar{\tau})\left(k\|\xi\|_{[t-2N_{\max}\bar{\tau},t]} + \max_{i\in\mathcal{N}} \|\omega_i\|_{[t-2N_{\max}\bar{\tau},t]}\right).
\end{aligned}
$$

Finally we have

$$
\begin{aligned}
\max_{i\in\mathcal{N}, j\in\mathcal{N}^i, t\in\mathbb{R}^+} \|\tilde{\gamma}_i^j(t)\| &\leq \varepsilon \frac{e^{2lN_{\max}\bar{\tau}}}{1-kd^\star z(l, 2N_{\max}\bar{\tau})}\\
&\quad + \frac{z(l, 2N_{\max}\bar{\tau})}{1-kd^\star z(l, 2N_{\max}\bar{\tau})}\left(k\|\xi\|_{[t-2N_{\max}\bar{\tau},t]} + \max_{i\in\mathcal{N}} \|\omega_i\|_{[t-2N_{\max}\bar{\tau},t]}\right),
\end{aligned}
$$

and (10.29) holds with $\alpha^\varepsilon(x) := \frac{e^{2lx}}{1-kd^\star z(l,2x)}$, $\alpha^\xi(x) := \frac{kz(l,2x)}{1-kd^* z(l,2x)}$ and $\alpha^\omega(x) := \frac{z(l,2x)}{1-kd^* z(l,2x)}$. □

Proof of Lemma 9. We wish to determine the bound $\max_{i\in\mathcal{N}, j\in\mathcal{N}^i}\left\|\tilde{\gamma}_i^j(t)\right\| \leq \breve{\gamma}(t) := \tilde{\alpha}^\xi(N_{\max}\bar{\tau})\beta^\xi(\|\xi(0)\|, t) + \tilde{\alpha}^\omega(N_{\max}\bar{\tau})\breve{\omega}(t) + \tilde{\alpha}^\varepsilon(N_{\max}\bar{\tau})\varepsilon$, where

$$
\breve{\omega}(t) := \beta_{e\omega}^{\tilde{\gamma}}\left(\max_{i\in\mathcal{N}}\left\|\eta_{e_i}(0)\right\|, t\right) + \beta_{il}^{\tilde{\gamma}}\left(\max_{i\in\mathcal{N}}\left\|\boldsymbol{x}_{il_i}^0\right\|, t\right) + \beta_{obs}^{\tilde{\gamma}}\left(\max_{i\in\mathcal{N}}\left\|\boldsymbol{x}_{v_{ci}}^0\right\|, t\right) + \varepsilon_e.
$$

We first note that, from Lemma 5 and the definitions of $\tilde{\beta}_{il}$ and $\tilde{\beta}_{obs}$ in the proof of Lemma 7, defining $\tilde{\beta}(x,t) := xe^{-(1-\theta)\min(k_x,k_y,k_\omega,k\sigma_2-l)}$ $\omega_i(t)$ can be bounded as

$$
\max_{i\in\mathcal{N}}\|\omega_i(t)\| \leq \tilde{\omega}(t) := \frac{1}{\sqrt{c_\omega}}\left(\tilde{\beta}\left(\max_{i\in\mathcal{N}}\left\|\eta_{e_i}(0)\right\|, t\right) + \tilde{\beta}_{il}\left(\max_{i\in\mathcal{N}}\left\|\boldsymbol{x}_{il_i}^0\right\|, t\right) + \tilde{\beta}_{obs}\left(\max_{i\in\mathcal{N}}\left\|\boldsymbol{x}_{v_{ci}}^0\right\|, t\right) + \varepsilon_e\right).
$$

Also, we note that, if the bound $\max_{i\in\mathcal{N}, j\in\mathcal{N}^i}\left\|\tilde{\gamma}_i^j(t)\right\| \leq \breve{\gamma}(t)$ is defined for $t \leq \bar{t} \in \mathbb{R}^+$, and $\frac{\partial}{\partial t}\breve{\gamma}(t) \geq -(1-\theta)(k\sigma_2-l)\breve{\gamma}(t)$, since from the definitions of $\tilde{\beta}$, $\tilde{\beta}_{il}$ and $\tilde{\beta}_{obs}$, $\frac{\partial}{\partial t}\tilde{\omega}(t) \geq -(1-\theta)(k\sigma_2-l)\tilde{\omega}(t)$, from the proof of Lemma 6, we can bound $\|\xi(t)\|$ by

$$
\|\xi(t)\| \leq \beta^\xi(\|\xi(0)\|, t) + \frac{\sqrt{N}}{\theta(k\sigma_2-l)}\tilde{\omega}(t) + \frac{kd^\star}{\theta(k\sigma_2-l)}\breve{\gamma}(t). \tag{D.3}
$$

We first define $\breve{\gamma}(t)$ in the interval $t \in [0, 2N_{\max}\bar{\tau}]$ such that it is guaranteed that $\max_{i\in\mathcal{N}, j\in\mathcal{N}^i}\left\|\tilde{\gamma}_i^j(t)\right\| \leq \breve{\gamma}(t)$,

$\forall t \in [0, 2N_{\max}\bar{\tau}]$. From equations (10.29) and (D.3) one can observe that

$$\begin{aligned}
\max_{i\in\mathcal{N}, j\in\mathcal{N}^i} \left\|\tilde{\gamma}_i^j\right\|_{[0,\,2N_{\max}\bar{\tau}]} \leq\ & \alpha^{\varepsilon}(N_{\max}\bar{\tau})\varepsilon + \alpha^{\xi}(N_{\max}\bar{\tau})\left(\beta^{\xi}\left(\|\xi(0)\|, 0\right) + \frac{\sqrt{N}}{\theta(k\sigma_2 - l)}\tilde{\omega}(0)\right) \\
& + \alpha^{\xi}(N_{\max}\bar{\tau})\frac{kd^{\star}}{\theta(k\sigma_2 - l)} \max_{i\in\mathcal{N}, j\in\mathcal{N}^i} \left\|\tilde{\gamma}_i^j\right\|_{[0,\,2N_{\max}\bar{\tau}]} \\
& + \alpha^{\omega}(N_{\max}\bar{\tau})\tilde{\omega}(0),
\end{aligned}$$

We define $\breve{\gamma}(t)$ to be constant on the period $t \in [0, 2N_{\max}\bar{\tau}]$. Therefore one has for $t \in [0,\, 2N_{\max}\bar{\tau}]$ that $\breve{\gamma}(t) \geq \max_{i\in\mathcal{N}, j\in\mathcal{N}^i} \|\tilde{\gamma}_i^j(t)\|$ if one defines $\breve{\gamma}(t)$ in the period $t \in [0,\, 2N_{\max}\bar{\tau}]$ satisfying

$$\breve{\gamma}(t) = \alpha^{\varepsilon}(N_{\max}\bar{\tau})\varepsilon + \alpha^{\xi}(N_{\max}\bar{\tau})\left(\beta^{\xi}\left(\|\xi(0)\|, 0\right) + \frac{\sqrt{N}}{\theta(k\sigma_2 - l)}\tilde{\omega}(0) + \frac{kd^{\star}}{\theta(k\sigma_2 - l)}\breve{\gamma}(t)\right) + \alpha^{\omega}(N_{\max}\bar{\tau})\tilde{\omega}(0),$$

which is possible if $\bar{\tau}$ is sufficiently small such that $\alpha^{\xi}(N_{\max}\bar{\tau})\frac{kd^{\star}}{\theta(k\sigma_2 - l)} < 11$. This is equivalent to

$$\begin{aligned}
\breve{\gamma}(t) =\ & \frac{1}{1 - \frac{kd^{\star}\alpha^{\xi}(N_{\max}\bar{\tau})}{\theta(k\sigma_2 - l)}}\left(\alpha^{\varepsilon}(N_{\max}\bar{\tau})\varepsilon + \alpha^{\xi}(N_{\max}\bar{\tau})\beta^{\xi}\left(\|\xi(0)\|, 0\right)\right) \\
& + \frac{1}{1 - \frac{kd^{\star}\alpha^{\xi}(N_{\max}\bar{\tau})}{\theta(k\sigma_2 - l)}}\left(\alpha^{\xi}(N_{\max}\bar{\tau})\frac{\sqrt{N}}{\theta(k\sigma_2 - l)} + \alpha^{\omega}(N_{\max}\bar{\tau})\right)\tilde{\omega}(0),
\end{aligned}$$

which holds by defining

$$\begin{aligned}
& \tilde{\alpha}^{\varepsilon}(x) := \frac{1}{1 - \frac{kd^{\star}\alpha^{\xi}(x)}{\theta(k\sigma_2 - l)}}\alpha^{\varepsilon}(x),\ \tilde{\alpha}^{\xi}(x) := \frac{1}{1 - \frac{kd^{\star}\alpha^{\xi}(x)}{\theta(k\sigma_2 - l)}}\alpha^{\xi}(x), \\
& \tilde{\alpha}^{\omega}(x) := \frac{1}{1 - \frac{kd^{\star}\alpha^{\xi}(x)}{\theta(k\sigma_2 - l)}}\left(\alpha^{\xi}(x)\frac{\sqrt{N}}{\theta(k\sigma_2 - l)} + \alpha^{\omega}(x)\right),
\end{aligned}$$

and if $\breve{\omega}(t) = \tilde{\omega}(0)$ for $t < 2N_{\max}\bar{\tau}$, which is the case if, for $t < 2N_{\max}\bar{\tau}$, $\beta_{e\omega}^{\tilde{\gamma}}(x,t) = \frac{1}{\sqrt{c_\omega}}\beta^{e}(x,0)$, $\beta_{il}^{\tilde{\gamma}}(x,t) = \frac{1}{\sqrt{c_\omega}}\tilde{\beta}_{il}(x,0)$, and $\beta_{obs}^{\tilde{\gamma}}(x,t) = \frac{1}{\sqrt{c_\omega}}\tilde{\beta}_{obs}(x,0)$. One can also observe that $\breve{\gamma}(0)$ is an absolute upper bound on $\max_{i\in\mathcal{N}, j\in\mathcal{N}^i} \|\tilde{\gamma}_i^j(t)\|$ for $t \in \mathbb{R}^+$.

If on the interval $t \in \left[\bar{t} - 2\bar{k}N_{\max}\bar{\tau},\ \bar{t}\right]$ we have $\breve{\gamma}(t) \geq \max_{i\in\mathcal{N}, j\in\mathcal{N}^i}\left\|\tilde{\gamma}_i^j(t)\right\|$ and $\frac{\partial}{\partial t}\breve{\gamma}(t) \geq -(1-\theta)(k\sigma_2 - l)\breve{\gamma}(t)$, and on the interval $t \in \left[\bar{t} - 2\bar{k}N_{\max}\bar{\tau},\ \bar{t} - 2\bar{k}N_{\max}\bar{\tau} + \bar{\tau}\right]$ we have $\breve{\gamma}(t) \geq \max_{i\in\mathcal{N}, j\in\mathcal{N}^i}\left\|\tilde{\gamma}_i^j\right\|_{[t,\, t+2N_{\max}\bar{\tau}]}$, from equations (10.29) and (D.3) we obtain on the interval $t \in \left[\bar{t},\ \bar{t} + \bar{\tau}\right]$

$$\begin{aligned}
\max_{i\in\mathcal{N}, j\in\mathcal{N}^i}\left\|\tilde{\gamma}_i^j(t)\right\| \leq\ & \alpha^{\varepsilon}(N_{\max}\bar{\tau})\varepsilon + \alpha^{\omega}(N_{\max}\bar{\tau})\tilde{\omega}(t - 2N_{\max}\bar{\tau}) + \alpha^{\xi}(N_{\max}\bar{\tau})\left(\frac{kd^{\star}}{\theta(k\sigma_2 - l)}\breve{\gamma}(t - 2N_{\max}\bar{\tau})\right) \\
& + \alpha^{\xi}(N_{\max}\bar{\tau})\left(\beta^{\xi}\left(\|\xi(0)\|, t - 2N_{\max}\bar{\tau}\right) + \frac{\sqrt{N}}{\theta(k\sigma_2 - l)}\tilde{\omega}(t - 2N_{\max}\bar{\tau})\right),
\end{aligned}$$

and therefore we have that $\breve{\gamma}(t) \geq \max_{i\in\mathcal{N}, j\in\mathcal{N}^i}\left\|\tilde{\gamma}_i^j(t)\right\|$, $\forall t \in \left[2(\bar{k}+1)N_{\max}\bar{\tau},\ 2(\bar{k}+2)N_{\max}\bar{\tau}\right]$, if

$$\begin{aligned}
\breve{\gamma}(t) \geq\ & \alpha^{\varepsilon}(N_{\max}\bar{\tau})\varepsilon + \alpha^{\omega}(N_{\max}\bar{\tau})\tilde{\omega}(t - 2N_{\max}\bar{\tau}) + \alpha^{\xi}(N_{\max}\bar{\tau})\left(\frac{kd^{\star}}{\theta(k\sigma_2 - l)}\breve{\gamma}(t - 2N_{\max}\bar{\tau})\right) \\
& + \alpha^{\xi}(N_{\max}\bar{\tau})\left(\beta^{\xi}\left(\|\xi(0)\|, t - 2N_{\max}\bar{\tau}\right) + \frac{\sqrt{N}}{\theta(k\sigma_2 - l)}\tilde{\omega}(t - 2N_{\max}\bar{\tau})\right),
\end{aligned}$$

which holds if $\tilde{\alpha}^{\epsilon}$, $\tilde{\alpha}^{\xi}$ and $\tilde{\alpha}^{\omega}$ are defined as before, and $\beta^{\tilde{\gamma}}_{e\omega}(x,t)$, $\beta^{\tilde{\gamma}}_{il}(x,t)$ and $\beta^{\tilde{\gamma}}_{obs}(x,t)$ are defined as

$$\beta^{\tilde{\gamma}}_{e\omega}(x,t) := \begin{cases} \frac{1}{\sqrt{c_\omega}}\beta^{e}(x,0), & \text{if } t \le 2N_{\max}\bar{\tau} \\ \frac{kd^\star \alpha^{\xi}(x)}{\theta(k\sigma_2-l)}\beta^{\tilde{\gamma}}_{e\omega}(x,t-2N_{\max}\bar{\tau}) + \left(1-\frac{kd^\star\alpha^{\xi}(x)}{\theta(k\sigma_2-l)}\right)\frac{1}{\sqrt{c_\omega}}\beta^{e}(x,t-2N_{\max}\bar{\tau}), & \text{otherwise}\end{cases},$$

$$\beta^{\tilde{\gamma}}_{il}(x,t) := \begin{cases} \frac{1}{\sqrt{c_\omega}}\tilde{\beta}_{il}(x,0), & \text{if } t \le 2N_{\max}\bar{\tau} \\ \frac{kd^\star \alpha^{\xi}(x)}{\theta(k\sigma_2-l)}\beta^{\tilde{\gamma}}_{il}(x,t-2N_{\max}\bar{\tau}) + \left(1-\frac{kd^\star\alpha^{\xi}(x)}{\theta(k\sigma_2-l)}\right)\frac{1}{\sqrt{c_\omega}}\tilde{\beta}_{il}(x,t-2N_{\max}\bar{\tau}), & \text{otherwise}\end{cases},$$

$$\beta^{\tilde{\gamma}}_{obs}(x,t) := \begin{cases} \frac{1}{\sqrt{c_\omega}}\tilde{\beta}_{obs}(x,0), & \text{if } t \le 2N_{\max}\bar{\tau} \\ \frac{kd^\star \alpha^{\xi}(x)}{\theta(k\sigma_2-l)}\beta^{\tilde{\gamma}}_{obs}(x,t-2N_{\max}\bar{\tau}) + \left(1-\frac{kd^\star\alpha^{\xi}(x)}{\theta(k\sigma_2-l)}\right)\frac{1}{\sqrt{c_\omega}}\tilde{\beta}_{obs}(x,t-2N_{\max}\bar{\tau}), & \text{otherwise}\end{cases}.$$

With the above definitions one can observe that $\breve{\gamma}(t)$ is continuous and $\frac{\partial}{\partial t}\breve{\gamma}(t) \ge -(1-\theta)(k\sigma_2 - l)\breve{\gamma}(t)$ when the derivative is defined.

Because we can establish that $\max_{i\in\mathcal{N},j\in\mathcal{N}^i}\left\|\tilde{\gamma}^j_i(t)\right\|_{[0,\,\bar{t}+\bar{\tau}]} \le \breve{\gamma}(0)$, from the proof of Lemma 8 one can observe that, when $\dot{\tilde{\gamma}}^j_i(t)$ is defined, $\max_{i\in\mathcal{N},j\in\mathcal{N}^i}\left\|\dot{\tilde{\gamma}}^j_i(t)^j_i(t)\right\| \le v_{\dot{\tilde{\gamma}}}$, where $v_{\dot{\tilde{\gamma}}}$ depends on $\|\xi(0)\|$, $\max_{i\in\mathcal{N}}\|\eta_{e_i}(0)\|$, $\max_{i\in\mathcal{N}}\|\boldsymbol{x}^0_{il_i}\|$, $\max_{i\in\mathcal{N}}\|\boldsymbol{x}^0_{v_{ci}}\|$, ε_e and ε but not on time.

Since $\breve{\gamma}(t)$ is decreasing we have that $\breve{\gamma}(t) \ge \max_{i\in\mathcal{N},j\in\mathcal{N}^i}\left\|\tilde{\gamma}^j_i(t)\right\|_{[t,\,t+2N_{\max}\bar{\tau}]}$ is valid for t in the interval $\left[\bar{t}-2\bar{k}N_{\max}\bar{\tau}+\bar{\tau},\ \bar{t}-2\bar{k}N_{\max}\bar{\tau}+\bar{\tau}+\min\left(N_{\max}\bar{\tau},\ \frac{\breve{\gamma}(\bar{t}-\bar{k}N_{\max}\bar{\tau}+\bar{\tau})-\breve{\gamma}(\bar{t}+\bar{\tau})}{2v_{\dot{\tilde{\gamma}}}}\right)\right]$.

Finally, by induction we verify that $\max_{i\in\mathcal{N},j\in\mathcal{N}^i}\left\|\tilde{\gamma}^j_i(t)\right\| \le \breve{\gamma}(t)$ holds for $t\in\mathbb{R}$. □

Proof of Lemma 10. The post reset estimation error can be expressed as

$$\tilde{\gamma}^j_i\left(\left(t^i_k+2\bar{\tau}\right)^+\right) = \hat{\gamma}^j_i\left(\left(t^i_k+2\bar{\tau}\right)^+\right) - \gamma_i\left(t^i_k+2\bar{\tau}\right) = \Gamma_r\left(2\bar{\tau}-t^i_k+T_r\left(\gamma_i\left(t^i_k\right)\right)\right) - \gamma_i\left(t^i_k+2\bar{\tau}\right).$$

Defining, on the interval $t\in\left[t^i_k t^i_k+2\bar{\tau}\right]$ the function $\eta(t) := \Gamma_r\left(t-t^i_k+T_r\left(\gamma_i\left(t^i_k\right)\right)\right)-\gamma_i(t)$ we have $\eta\left(t^i_k\right)=0$ and $\eta\left(t^i_k+2\bar{\tau}\right) = \tilde{\gamma}^j_i\left(\left(t^i_k+2\bar{\tau}\right)^+\right)$.

From the derivative of the inverse function we have

$$\dot{\eta} = v_r\left(\Gamma_r\left(t-t^i_k+T_r\left(\gamma_i\left(t^i_k\right)\right)\right)\right) - \dot{\gamma}_i = v_r(\gamma_i+\eta) - v_r(\gamma_i) - \tilde{v}_{r_i} - \omega_i,$$

and taking the norm yields

$$\begin{aligned}\|\dot{\eta}\| &\le l\|\eta\| + kd^\star\breve{\gamma}(0) + \bar{\omega}(0) + k\left(\beta^{\xi}(\|\xi(0)\|,0) + \frac{\sqrt{N}}{\theta(k\sigma_2-l)}\bar{\omega}(0) + \frac{kd^\star}{\theta(k\sigma_2-l)}\breve{\gamma}(0)\right)\\ &\le l\|\eta\| + k\beta^{\xi}(\|\xi(0)\|,0) + kd^\star\left(1+\frac{k}{\theta(k\sigma_2-l)}\right)\breve{\gamma}(0) + \left(1+\frac{k\sqrt{N}}{\theta(k\sigma_2-l)}\right)\bar{\omega}(0).\end{aligned}$$

Following the derivations of Lemma 8 of this proof, it follows that

$$
\begin{aligned}
\left\|\tilde{\gamma}_i^j\left(\left(t_k^i+2\bar{\tau}\right)^+\right)\right\| &= \left\|\eta\left(t_k^i+2\bar{\tau}\right)\right\| \\
&\leq z(l,2\bar{\tau})\left(k\beta^{\xi}\left(\|\xi(0)\|,0\right)+kd^{\star}\left(1+\frac{k}{\theta(k\sigma_2-l)}\right)\breve{\gamma}(0)+\left(1+\frac{k\sqrt{N}}{\theta(k\sigma_2-l)}\right)\tilde{\omega}(0)\right) \\
&\leq z(l,2\bar{\tau})\left(kd^{\star}\left(1+\frac{k}{\theta(k\sigma_2-l)}\right)\tilde{\alpha}^{\varepsilon}(N_{\max}\bar{\tau})\varepsilon\right. \\
&+\left(k+kd^{\star}\left(1+\frac{k}{\theta(k\sigma_2-l)}\right)\tilde{\alpha}^{\xi}(N_{\max}\bar{\tau})\right)\beta^{\xi}\left(\|\xi(0)\|,0\right) \\
&\left.+\left(\frac{kd^{\star}}{\sqrt{c_\omega}}\left(1+\frac{k}{\theta(k\sigma_2-l)}\right)+\left(1+\frac{k\sqrt{N}}{\theta(k\sigma_2-l)}\right)\right)\tilde{\omega}(0)\right).
\end{aligned}
$$

Finally we have that $\|\tilde{\gamma}_i^j((t_k^i+2\bar{\tau})^+)\|<\varepsilon$ if the time delays $\bar{\tau}$ and maximum number of failed communications $N_{\max}$ are sufficiently small such that

$$
kd^{\star}z(l,2\bar{\tau})\tilde{\alpha}^{\varepsilon}(N_{\max}\bar{\tau})\left(1+\frac{k}{\theta(k\sigma_2-l)}\right)<1,
$$

and for sufficiently small values of $\|\xi(0)\|$, $\max_{i\in\mathcal{N}}\|\eta_{e_i}(0)\|$, $\max_{i\in\mathcal{N}}\|\boldsymbol{x}^0_{il_i}\|$, $\max_{i\in\mathcal{N}}\|\boldsymbol{x}^0_{v_{ci}}\|$ and ε_e such that

$$
\begin{aligned}
\varepsilon > &\frac{z(l,2\bar{\tau})}{1-kd^{\star}z(l,2\bar{\tau})\tilde{\alpha}^{\varepsilon}(N_{\max}\bar{\tau})\left(1+\frac{k}{\theta(k\sigma_2-l)}\right)}\left(\left(k+kd^{\star}\left(1+\frac{k}{\theta(k\sigma_2-l)}\right)\tilde{\alpha}^{\xi}(N_{\max}\bar{\tau})\right)\beta^{\xi}\left(\|\xi(0)\|,0\right)\right. \\
&\left.+\left(\frac{kd^{\star}}{\sqrt{c_\omega}}\left(1+\frac{k}{\theta(k\sigma_2-l)}\right)+\left(1+\frac{k\sqrt{N}}{\theta(k\sigma_2-l)}\right)\right)\tilde{\omega}(0)\right).
\end{aligned}
$$

□

Proof of Lemma 11. The proof exploits the use of the Lyapunov function $V=\frac{1}{2}\|\eta_e\|^2=\frac{1}{2}\left(\|\boldsymbol{e}-\delta\|^2+c_\omega e_{\dot{\gamma}}^2\right)$.

From (10.32) and (10.33) we have

$$
\dot{e}_{\dot{\gamma}}=\ddot{\gamma}-\dot{v}_r=-k_\omega e_{\dot{\gamma}}+k_\omega\tilde{v}_r+\frac{1}{c_\omega}(\boldsymbol{e}-\boldsymbol{\delta})^T R_d^T\frac{\partial\boldsymbol{p}_d}{\partial\gamma}. \tag{D.4}
$$

From (10.31) and (10.34) we have

$$
\dot{\boldsymbol{e}}=-S\left(\dot{\psi}_d\right)(\boldsymbol{e}-\boldsymbol{\delta})-K_k(\boldsymbol{e}-\boldsymbol{\delta})+\tilde{R}\begin{bmatrix}\tilde{u}\\ v_w+\tilde{v}_c\end{bmatrix}-R_d^T\frac{\partial\boldsymbol{p}_d}{\partial\gamma}(\tilde{v}_r-e_{\dot{\gamma}}). \tag{D.5}
$$

Computing the time derivative of V yields

$$
\begin{aligned}
\dot{V}&=(\boldsymbol{e}-\boldsymbol{\delta})^T\left(-K_k(\boldsymbol{e}-\boldsymbol{\delta})+\tilde{R}\begin{bmatrix}\tilde{u}\\ v_w+\tilde{v}_c\end{bmatrix}+R_d^T\frac{\partial\boldsymbol{p}_d}{\partial\gamma}\tilde{v}_r\right)+c_\omega e_{\dot{\gamma}}\left(-k_\omega(e_{\dot{\gamma}}-\tilde{v}_r)\right) \\
&=(\boldsymbol{e}-\boldsymbol{\delta})^T K_k(\boldsymbol{e}-\boldsymbol{\delta})-c_\omega k_\omega e_{\dot{\gamma}}^2+c_\omega k_\omega e_{\dot{\gamma}}\tilde{v}_r+(\boldsymbol{e}-\boldsymbol{\delta})^T\left(R_d^T\frac{\partial\boldsymbol{p}_d}{\partial\gamma}\tilde{v}_r+\tilde{R}\begin{bmatrix}\tilde{u}\\ v_w+\tilde{v}_c\end{bmatrix}\right).
\end{aligned}
$$

Defining $K_e:=\operatorname{diag}(k_x,k_y,k_\omega)$ we have the following result

$$
\begin{aligned}
\dot{V}\leq&-\eta_e^T K_e\eta_e \\
&+\|\eta_e\|\left(\max\left(\sqrt{c_\omega}k_\omega,\ \sup_{\gamma\in\mathbb{R}}\left\|\frac{\partial\boldsymbol{p}_d}{\partial\gamma}\right\|\right)\|\tilde{v}_r\|+\sqrt{\epsilon_{\tilde{u}}^2+\left(\epsilon_v+\epsilon_{v_c}\right)^2}\right)
\end{aligned} \tag{D.6}
$$

$$+\|\eta_e\|\left(\sqrt{\left(\beta^{\bar{u}}\left(\|\boldsymbol{x}_{il}^0\|,t\right)\right)^2+\left(\beta^{v}\left(\|\boldsymbol{x}_{il}^0\|,t\right)\right)^2}+\beta^{v_c}\left(\|\boldsymbol{x}_{v_c}^0\|,t\right)\right). \tag{D.7}$$

The rest of the proof amounts to dominating all positive terms of (D.6) by $-\eta_e^T K_e \eta_e \leq -\min(k_x,k_y,k_\omega)\|\eta_e\|^2$. That is, we note that from (D.6) we have

$$\begin{aligned}\dot{V} \leq & -(1-\theta_e)\min(k_x,k_y,k_\omega)\|\eta_e\|^2\\ &+\|\eta_e\|\left(\max\left(\sqrt{c_\omega}k_\omega,\ \sup_{\gamma\in\mathbb{R}}\left\|\frac{\partial \boldsymbol{p}_d}{\partial\gamma}\right\|\right)\|\tilde{v}_r\|+\sqrt{\epsilon_{\bar{u}}^2+\left(\epsilon_v+\epsilon_{v_c}\right)^2}\right)\\ &+\|\eta_e\|\left(\sqrt{\left(\beta^{\bar{u}}\left(\|\boldsymbol{x}_{il}^0\|,t\right)\right)^2+\left(\beta^{v}\left(\|\boldsymbol{x}_{il}^0\|,t\right)\right)^2}+\beta^{v_c}\left(\|\boldsymbol{x}_{v_c}^0\|,t\right)-\theta_e\min(k_x,k_y,k_\omega)\|\eta_e\|\right),\end{aligned}$$

and therefore, defining $\beta_{il}^e\left(\|x_{il}^0\|,t\right):=\frac{\sqrt{\left(\beta^{\bar{u}}\left(\|\boldsymbol{x}_{il}^0\|,t\right)\right)^2+\left(\beta^{v}\left(\|\boldsymbol{x}_{il}^0\|,t\right)\right)^2}}{\theta_e\min(k_x,k_y,k_\omega)}$ and $\beta_{obs}^e\left(\|\boldsymbol{x}_{v_c}^0\|,t\right):=\frac{\beta^{v_c}\left(\|\boldsymbol{x}_{v_c}^0\|,t\right)}{\theta_e\min(k_x,k_y,k_\omega)}$ we have

$$\dot{V}\leq-(1-\theta_e)\min(k_x,k_y,k_\omega)\|\eta_e\|^2,\forall\|\eta_e\|\geq\beta_{il}^e\left(\|x_{il}^0\|,t\right)+\beta_{obs}^e\left(\|\boldsymbol{x}_{v_c}^0\|,t\right)+\sigma_{\tilde{v}_r}^e\left(\|\tilde{v}_r\|_{[0,t]}\right)+\varepsilon_e,$$

and therefore (10.35) follows with $\beta^e\left(\|\eta_e(0)\|,t\right):=\|\eta_e(0)\|e^{-(1-\theta_e)\min(k_x,k_y,k_\omega)t}$. □

Proof of Lemma 12. Defining

$$\bar{\gamma}:=\frac{1}{N}\mathbf{1}^T\gamma,$$

we can decompose γ as

$$\gamma=\mathbf{1}\bar{\gamma}+\xi.$$

Using this fact and recalling that $v_r(\gamma)$ is assumed to be globally Lipschitz we can conclude that

$$\xi^T\Gamma\bar{v}_r=\xi^T\Gamma\left(\mathbf{1}v_r(\bar{\gamma})-(\mathbf{1}v_r(\bar{\gamma})-\bar{v}_r)\right)=\xi^T\Gamma(\bar{v}_r-\mathbf{1}v_r(\bar{\gamma}))\leq l\|\xi\|^2.$$

We can now bound the time derivative of V with

$$\dot{V}\leq-k\xi^T\boldsymbol{L}\xi+l\|\xi\|^2+\xi^T\Gamma\bar{\omega}\leq-k\sigma_2\|\xi\|^2+l\|\xi\|^2+\|\xi\|\|\bar{\omega}\|.$$

Then we can conclude that $\dot{V}<0$ for $\|\xi\|\geq\left[(k\sigma_2-l)\theta_\xi\right]^{-1}\|\bar{\omega}\|$, for $1>\theta_\xi>0$. □

Proof of Lemma 13. The proof is based on the Lyapunov function $V=\frac{1}{2}\|\eta_\omega\|^2=\frac{1}{2}\left(\|\boldsymbol{e}_\delta\|^2+c_\omega\|\bar{\omega}\|^2\right)$.

From (D.5) we have in vector form

$$\dot{\boldsymbol{e}}_\delta=-\operatorname{diag}\left(S\left(\dot{\psi}_{d_i}\right)\right)\boldsymbol{e}_\delta-\boldsymbol{K}_k(\boldsymbol{e}-\boldsymbol{\delta})+\operatorname{col}\left(\begin{bmatrix}\tilde{u}_i\\ v_{w_i}+\tilde{v}_{c_i}\end{bmatrix}+R_{d_i}^T\frac{\partial\boldsymbol{p}_{d_i}}{\partial\gamma_i}\left(-\omega_i+k\sum_{j\in\mathcal{N}^i}\tilde{\gamma}_j^i\right)\right).$$

From (D.4)

$$\begin{aligned}\dot{\omega}_i=\dot{e}_{\dot{\gamma}_i}-\dot{\bar{v}}_{r_{d_i}}&=-k_\omega\omega_i+k_\omega k\sum_{j\in\mathcal{N}^i}\tilde{\gamma}_j^i+\frac{1}{c_\omega}(\boldsymbol{e}_i-\boldsymbol{\delta})^T R_{d_i}^T\frac{\partial\boldsymbol{p}_{d_i}}{\partial\gamma_i}+k\sum_{j\in\mathcal{N}^i}\left(\dot{\gamma}_i-\dot{\gamma}_j\right)\\ &=-k_\omega\omega_i+k_\omega k\sum_{j\in\mathcal{N}^i}\tilde{\gamma}_j^i+\frac{1}{c_\omega}(\boldsymbol{e}_i-\boldsymbol{\delta})^T R_{d_i}^T\frac{\partial\boldsymbol{p}_{d_i}}{\partial\gamma_i}+k\sum_{j\in\mathcal{N}^i}\left(v_{r_i}-v_{r_j}+\omega_i-\omega_j+k\sum_{k\in\mathcal{N}^j}\left(\gamma_i-\gamma_j\right)\right).\end{aligned}$$

and in vector form we have

$$\dot{\bar{\omega}} = -k_\omega \bar{\omega} + k_\omega \bar{\gamma} + k\boldsymbol{L}\bar{v}_r + k^2 \boldsymbol{L}^2 \xi + k\boldsymbol{L}\bar{\omega} + \boldsymbol{e}_\delta^T \operatorname{col}\left(R_{d_i}^T \frac{\partial \boldsymbol{p}_{d_i}}{\partial \gamma_i} \right).$$

Computing the time derivative of V yields

$$\begin{aligned}\dot{V} = \boldsymbol{e}_\delta^T &\left(-\boldsymbol{K}_k \boldsymbol{e}_\delta + \operatorname{col}\left(\tilde{R}_i \begin{bmatrix} \tilde{u}_i \\ v_{w_i} + \tilde{v}_{c_i} \end{bmatrix} + R_{d_i}^T \frac{\partial \boldsymbol{p}_{d_i}}{\partial \gamma_i} \sum_{j \in \mathcal{N}^i} \tilde{\gamma}_j^i \right) \right) \\ &+ c_\omega \bar{\omega}^T \left(-k_\omega \bar{\omega} + k_\omega \bar{\gamma} + k\boldsymbol{L}(\bar{v}_r + k\boldsymbol{L})\xi + k\boldsymbol{L}\bar{\omega} \right),\end{aligned}$$

where $\boldsymbol{K}_k := \operatorname{diag}(K_k, \ldots, K_k)$. Noting the fact that $\|\bar{\gamma}\| \leq \ d^* \left\|\tilde{\gamma}\right\|$, where $d^* := \max_{i \in \mathcal{N}} \|\mathcal{N}^i\|$, we have the following result

$$\begin{aligned}\dot{V} \leq &-\min(k_x, k_y, k_\omega)\|\eta_\omega\|^2 + \max\left(\sqrt{c_\omega} k_\omega, \sup_{\gamma \in \mathbb{R}, i \in \mathcal{N}} \left\| \frac{\partial \boldsymbol{p}_{d_i}(\gamma)}{\partial \gamma} \right\| \right) d^* \left\|\eta_\omega\right\| \left\|\tilde{\gamma}\right\| \\ &+ \sqrt{N} \left(\sqrt{\epsilon_{\tilde{u}}^2 + \left(\epsilon_v + \epsilon_{v_c}\right)^2} + \sqrt{\left(\beta^{\tilde{u}} \left(\left\| \operatorname{col}\left(\boldsymbol{x}_{il_i}^0 \right) \right\|, t \right) \right)^2 + \left(\beta^v \left(\left\| \operatorname{col}\left(\boldsymbol{x}_{il_i}^0 \right) \right\|, t \right) \right)^2} \right) \|\eta_\omega\| \\ &+ \sqrt{N} \beta^{v_c} \left(\left\| \operatorname{col}\left(\boldsymbol{x}_{v_{c_i}}^0 \right) \right\|, t \right) \|\eta_\omega\| + \sqrt{c_\omega} k\sigma_N (l + k\sigma_N) \|\xi\| \|\eta_\omega\| + k\sigma_N \|\eta_\omega\|^2.\end{aligned} \tag{D.8}$$

The rest of the proof involves dominating all positive terms of (D.8) by $-\min(k_x, k_y, k_\omega)\|\eta_\omega\|^2$. That is, we note that from (D.8) we have

$$\begin{aligned}\dot{V} \leq &-(1-\theta_\omega)(\min(k_x, k_y, k_\omega) - k\sigma_N)\|\eta_\omega\|^2 \\ &+ \left\|\eta_\omega\right\| \left(\max\left(\sqrt{c_\omega} k_\omega, \sup_{\gamma \in \mathbb{R}} \left\| \frac{\partial \boldsymbol{p}_d}{\partial \gamma} \right\| \right) d^* \left\|\tilde{\gamma}\right\| + \sqrt{c_\omega} k\sigma_N (l + k\sigma_N)\|\xi\| + \sqrt{N}\sqrt{\epsilon_{\tilde{u}}^2 + \left(\epsilon_v + \epsilon_{v_c}\right)^2} \right. \\ &+ \sqrt{N} \sqrt{\left(\beta^{\tilde{u}} \left(\left\| \operatorname{col}\left(\boldsymbol{x}_{il_i}^0 \right) \right\|, t \right) \right)^2 + \left(\beta^v \left(\left\| \operatorname{col}\left(\boldsymbol{x}_{il_i}^0 \right) \right\|, t \right) \right)^2} + \sqrt{N} \beta^{v_c} \left(\left\| \operatorname{col}\left(\boldsymbol{x}_{v_{c_i}}^0 \right) \right\|, t \right) \\ &\left. - \theta_\omega (\min(k_x, k_y, k_\omega) - k\sigma_N)\|\eta_\omega\| \right),\end{aligned}$$

and therefore, defining

$$\begin{aligned}\beta_{il}^e(x, t) &:= \frac{\sqrt{N}\sqrt{(\beta^{\tilde{u}}(x,t))^2 + (\beta^v(x,t))^2}}{\theta_\omega(\min(k_x, k_y, k_\omega) - k\sigma_N)}, \\ \beta_{obs}^e(\|x\|, t) &:= \frac{\sqrt{N}\beta^{v_c}(x,t)}{\theta_\omega(\min(k_x, k_y, k_\omega) - k\sigma_N)}, \\ \sigma_{\tilde{\gamma}}^\omega(s) &:= \frac{\max\left(\sqrt{c_\omega} k_\omega, \sup_{\gamma \in \mathbb{R}} \left\| \frac{\partial \boldsymbol{p}_d}{\partial \gamma} \right\| \right) d^*}{\theta_\omega(\min(k_x, k_y, k_\omega) - k\sigma_N)} s, \\ \varepsilon_\omega &:= \frac{\sqrt{N}\sqrt{\epsilon_{\tilde{u}}^2 + \left(\epsilon_v + \epsilon_{v_c}\right)^2}}{\theta_\omega(\min(k_x, k_y, k_\omega) - k\sigma_N)},\end{aligned}$$

we obtain

$$\begin{aligned}&\dot{V} \leq -(1-\theta_\omega)(\min(k_x, k_y, k_\omega) - k\sigma_N)\|\eta_\omega\|^2, \\ &\forall \|\eta_\omega\| \geq \beta_{il}^\omega \left(\left\| \operatorname{col}\left(\boldsymbol{x}_{il_i}^0 \right) \right\|, t \right) + \beta_{obs}^\omega \left(\left\| \operatorname{col}\left(\boldsymbol{x}_{v_{c_i}}^0 \right) \right\|, t \right) + \sigma_\xi^\omega \left(\|\xi\|_{[0,t]} \right) + \sigma_{\tilde{\gamma}}^\omega \left(\left\|\tilde{\gamma}\right\|_{[0,t]} \right) + \varepsilon_\omega,\end{aligned}$$

from which (10.41) follows with $\beta^\omega(x, t) := xe^{-(1-\theta_\omega)(\min(k_x, k_y, k_\omega) - k\sigma_N)t}$. □

E Appendices of Chapter 11

E.1 Proof of Theorem 20

Proof. First, we introduce the Lyapunov function $V(z) = \frac{1}{2}z'z = \frac{1}{2}\|z\|^2$. We can bound the derivative of the Lyapunov function as

$$\begin{aligned}\dot{V}(z) &= -k_\xi \xi'\xi - k_\eta \eta^2 + \omega'\xi \\ &= -(1-\theta)(k_\xi \xi'\xi + k_\eta \eta^2) \\ &+ (\omega'\xi - \theta k_\xi \xi'\xi - \theta k_\eta \eta^2) \\ &\le -(1-\theta)k_m \|z\|^2 + (\|\omega\|\|z\| - \theta k_m \|z\|^2) \\ &= -(1-\theta)k_m 2V(z) + (\|\omega\|\sqrt{2V(z)} - \theta k_m 2V(z)).\end{aligned}$$

Noting that $\|\omega\|\sqrt{2V(z)} - \theta k_m 2V(z)$ is always negative for $V(z) \ge \frac{1}{2}\left(\frac{\epsilon_\omega}{\theta k_m}\right)^2$ we have that

$$\dot{V}(z) \le -(1-\theta)k_m 2V(z) \quad \forall z : V(z) \ge \frac{1}{2}\left(\frac{\epsilon_\omega}{\theta k_m}\right)^2.$$

Applying the comparison lemma (see e.g. Khalil [1996]) we have

$$V(z) \le \max\left(V(z(0))e^{-(1-\theta)k_m 2t}, \frac{1}{2}\left(\frac{\epsilon_\omega}{\theta k_m}\right)^2\right).$$

And finally we can bound $\|z(t)\|$ as

$$\|z(t)\| \le \|z(0)\|e^{-(1-\theta)k_m t} + \frac{\epsilon_\omega}{\theta k_m}. \tag{E.1}$$

□

F Appendices of Chapter 12

F.1 Glossary of Formulas

$$c_1 := \frac{\frac{\alpha+1}{\alpha}\max\left(1,\frac{\bar{\Phi}}{\bar{\beta}}\right)+\frac{1}{\beta}c_5}{m(P_1)}\|e_0\|_{I_N\otimes P_1}, \tag{F.1a}$$

$$c_2 := c_4 + k_5, \tag{F.1b}$$

$$c_4 := \frac{2}{m(P_1)}\left(\frac{\alpha+1}{\alpha}\max\left(1,\frac{\bar{\Phi}}{\tilde{\beta}}\right)c_8+\frac{c_6}{\beta}\right), \tag{F.1c}$$

$$c_5 := \left(\|A+BK\|_{P_1}\alpha^{l_f-1}+\hat{\Phi}\alpha^{l_f}+\|LC\|_{P_1}\right)\max\left(1,\frac{\bar{\Phi}}{\tilde{\beta}}\right), \tag{F.1d}$$

$$c_6 := \|A+BK\|_{P_1}\alpha^{l_f-1}\left[\frac{\sqrt{N}M(P_1)}{2}+c_7\right]+\hat{\Phi}\alpha^{l_f}c_7+\|LC\|_{P_1}\max\left(1,\frac{\bar{\Phi}}{\tilde{\beta}}\right)c_8, \tag{F.1e}$$

$$c_7 := \max\left(1,\frac{\bar{\Phi}}{\tilde{\beta}}\right)c_8+k_6, \tag{F.1f}$$

$$c_8 := \alpha^{l_f}k_6\frac{\tilde{\Phi}}{\beta-\bar{\beta}}, \tag{F.1g}$$

$$d_1 := \frac{\alpha+1}{m(P_1)\alpha}\frac{\max\left(1,\frac{\bar{\Phi}}{\tilde{\beta}}\right)\epsilon}{1-\bar{\beta}}+\frac{d_5}{m(P_1)}, \tag{F.1h}$$

$$d_2 := d_4 + k_5, \tag{F.1i}$$

$$d_4 := \frac{2}{m(P_1)}\left(\frac{\alpha+1}{\alpha}\max\left(1,\frac{\bar{\Phi}}{\tilde{\beta}}\right)d_8+d_6\right), \tag{F.1j}$$

$$d_5 := \left(\|A+BK\|_{P_1}\alpha^{l_f-1}+\hat{\Phi}\alpha^{l_f}+\|LC\|_{P_1}\right)\frac{\max\left(1,\frac{\bar{\Phi}}{\tilde{\beta}}\right)\epsilon}{1-\bar{\beta}}+\frac{\sum_{j\in\mathcal{N}}M(L^{jT}P_1L^j)\epsilon_v^j}{\sqrt{N}}, \tag{F.1k}$$

$$d_6 := \|A+BK\|_{P_1}\alpha^{l_f-1}\left[\frac{\sqrt{N}M(P_1)}{2}+d_7\right]+\hat{\Phi}\alpha^{l_f}d_7+\|LC\|_{P_1}\max\left(1,\frac{\bar{\Phi}}{\tilde{\beta}}\right)d_8, \tag{F.1l}$$

$$d_7 := \max\left(1,\frac{\bar{\Phi}}{\tilde{\beta}}\right)d_8+k_6, \tag{F.1m}$$

$$d_8 := \alpha^{l_f}k_6\frac{\tilde{\Phi}}{1-\bar{\beta}}, \tag{F.1n}$$

$$k_1 := \left(1+\alpha^{l_f}\max\left(1,\frac{\bar{\Phi}}{\tilde{\beta}}\right)\right), \tag{F.1o}$$

$$k_2 := \left(c_8+\alpha^{l_f}c_7\right)\frac{a}{2^{n_b}-2}, \tag{F.1p}$$

$$k_3 := \left(1+\alpha^{l_f}\max\left(1,\frac{\bar{\Phi}}{\tilde{\beta}}\right)\right)\frac{1}{1-\tilde{\beta}}, \tag{F.1q}$$

$$k_4 := \left(d_8+\alpha^{l_f}d_7\right)\frac{b}{2^{n_b}-2}, \tag{F.1r}$$

$$k_5 := \frac{2\sqrt{N}M(P_1)(\alpha+1)+m(P_1)(\alpha-\sigma_2)}{m(P_1)\alpha(\alpha-\sigma_2)}, \tag{F.1s}$$

$$k_6 := \frac{\sqrt{N}M(P_1)}{\alpha-\sigma_2}. \tag{F.1t}$$

F.2 Derivation of $\bar{\Phi}$, $\hat{\Phi}$, and the Upper Bound on $\tilde{\Phi}$

To compute $\bar{\Phi}$, notice that

$$\begin{aligned}\bar{\Phi} &:= \|\Phi\|_{I_N\otimes P_1} = \frac{1}{N}\max_{\|x\|_{I_N\otimes P_1}=1}\|\operatorname{col}\left(\Phi^i\right)\mathbf{1}^T\otimes I_n x\|_{I_N\otimes P_1}\\ &= \frac{1}{\sqrt{N}}\max_{\|y\|_{P_1}=1}\|\operatorname{col}\left(\Phi^i\right)y\|_{I_N\otimes P_1} = \frac{M(\operatorname{col}\left(\Phi^i\right)^T I_N\otimes P_1\operatorname{col}\left(\Phi^i\right),P_1)}{\sqrt{N}},\end{aligned}$$

where we used the transformation $y := \frac{1}{\sqrt{N}}\mathbf{1}^T\otimes I_n x$ and the fact that $\max_{\|x\|_{I_N\otimes P_1}=1}\|\mathbf{1}^T\otimes I_n x\|_{I_N\otimes P_1} = \sqrt{N}$ with $x = \mathbf{1}\otimes I_n y$ and $\|y\|_{P_1} = 1$, which can be easily verified.

The parameter $\hat{\Phi}$ can be derived as follows:

$$\begin{aligned}\hat{\Phi} &:= \left\|\frac{1}{N}\mathbf{1}\otimes I_n\operatorname{row}\left(\Phi^i+BK\right)\right\|_{I_N\otimes P_1} = \frac{1}{N}\max_{\|x\|_{I_N\otimes P_1}=1}\left\|\mathbf{1}\otimes I_n\operatorname{row}\left(\Phi^i+BK\right)x\right\|_{I_N\otimes P_1}\\ &= \frac{1}{N}\max_{\|x\|_{I_N\otimes P_1}=1}\|x\|_{\operatorname{row}(\Phi^i+BK)^T(\mathbf{1}^T\mathbf{1})\otimes P_1\operatorname{row}(\Phi^i+BK)} = \max_{\|x\|_{I_N\otimes P_1}=1}\|x\|_{\operatorname{row}(\Phi^i+BK)^T P_1\operatorname{row}(\Phi^i+BK)}\\ &= \left\|P_1^{\frac{1}{2}}\operatorname{row}\left(\Phi^i+BK\right)I_N\otimes P_1^{-\frac{1}{2}}\right\|.\end{aligned}$$

To upper-bound $\tilde{\Phi}$ we use the definition of Γ as follows:

$$\begin{aligned}\tilde{\Phi} &:= \|\Gamma\|_{I_N\otimes P_1} = \|\operatorname{diag}\left(\Phi^i+BK\right)+\mathbf{1}\otimes\operatorname{row}\left(B^iK^i\right)\|_{I_N\otimes P_1}\\ &\le \|\operatorname{diag}\left(\Phi^i+BK\right)\|_{I_N\otimes P_1}+\|\mathbf{1}\otimes\operatorname{row}\left(B^iK^i\right)\|_{I_N\otimes P_1}\\ &= \max(\|\Phi^i+BK\|_{P_1})+N\left\|P_1^{\frac{1}{2}}\operatorname{row}\left(B^iK^i\right)I_N\otimes P_1^{-\frac{1}{2}}\right\|.\end{aligned}$$

F.3 Derivation of Upper Bounds on the Norms of ω_t and ξ_t

If Assumption A16 holds, then, from property P3, we have

$$\|\omega_t\|_{I_N\otimes P_1} = \sqrt{\sum_{i\in\mathcal{N}}\left(\|\omega_t^i\|_{P_1}\right)^2} = \sqrt{\sum_{i\in\mathcal{N}}\left(\|w_t - L^i v_t^i\|_{P_1}\right)^2}$$

$$\leq \sqrt{\sum_{i\in\mathcal{N}} \left(\|w_t\|_{P_1} + \|L^i v_t^i\|_{P_1}\right)^2} \leq \sqrt{\sum_{i\in\mathcal{N}} \left(M(P_1)\|w_t\|_\infty + M(L^{iT}P_1L^i)\|v_t^i\|_\infty\right)^2}$$
$$\leq \sqrt{\sum_{i\in\mathcal{N}} \left(M(L^{iT}P_1L^i)\epsilon_{v^i} + M(P_1)\epsilon_w\right)^2} := \epsilon.$$

To bound $\|\xi_t\|_{I_N\otimes P_1}$ first note that, since $z_{t,0} = \mathbf{1}\otimes x_t - e_{t,0}$ and $\left(I_N - \frac{1}{N}\mathbf{1}\mathbf{1}^T\right)\mathbf{1} = 0$ one has

$$q_{t,0} = -\left(I_N - \frac{1}{N}\mathbf{1}\mathbf{1}^T\right)\otimes I_n e_{t,0}.$$

Since $\|I_N - \frac{1}{N}\mathbf{1}\mathbf{1}^T\| = 1$ we have

$$\|q_{t,0}\|_{I_N\otimes P_1} \leq \|e_{t,0}\|_{I_N\otimes P_1}. \tag{F.2}$$

Then, if at time t the conditions of Lemma 14 apply, it follows from inequality (F.2), the definitions of ξ_t and $\tilde{\Phi}$ and the fact that $\xi_t = \Gamma q_{t,l_f}$, that

$$\|\xi_t\|_{I_N\otimes P_1} \leq \tilde{\Phi}\alpha^{l_f}\left[\|e_{t,0}\|_{I_N\otimes P_1} + k_6\frac{a\beta^p + b}{2^{n_b}-2}\right].$$

F.4 Proofs of Lemmas

Proof of Lemma 15. We first define $q_{t,l}^i := z_{t,l}^i - \sum_{j\in\mathcal{N}}\frac{1}{N}z_{t,l}^j$, which is the component of $q_{t,l}$ corresponding to the node i. Then, we can express the state estimates z_{t,l_f}^i as the average of the state estimates plus an error q_{t,l_f}^i as

$$z_{t,l_f}^i = \sum_{j\in\mathcal{N}}\frac{1}{N}z_{t,l_f}^j + q_{t,l_f}^i.$$

Because the consensus algorithm preserves averages, $\sum_{j\in\mathcal{N}}\frac{1}{N}z_{t,l_f}^j = \sum_{j\in\mathcal{N}}\frac{1}{N}z_{t,0}^j$, we obtain

$$z_{t,l_f}^i = \sum_{j\in\mathcal{N}}\frac{1}{N}z_{t,0}^j + q_{t,l_f}^i.$$

Then, from the state dynamics and filter update equations (12.1) and (12.4), the definitions of Φ^i in section 12.5.1, and ω_t^i and ξ_t^i in Section 12.6, we obtain equation (12.15) as follows:

$$\begin{aligned}
e_{t+1,0}^i &= A(x_t - z_{t,l_f}^i) - L^i(C^i x_t + v_t^i - C^i z_{t,l_f}^i) + \sum_{j\in\mathcal{N}} B^j K^j (z_{t,l_f}^j - z_{t,l_f}^i) + w_t \\
&= A\left(x_t - \sum_{j\in\mathcal{N}}\frac{1}{N}z_{t,0}^j - q_{t,l_f}^i\right) - L^i\left(C^i x_t + v_t^i - C^i\sum_{j\in\mathcal{N}}\frac{1}{N}z_{t,0}^j - C^i q_{t,l_f}^i\right) + \sum_{j\in\mathcal{N}} B^j K^j (q_{t,l_f}^j - q_{t,l_f}^i) + w_t \\
&= \Phi^i\left(x_t - \sum_{j\in\mathcal{N}}\frac{1}{N}z_{t,0}^j\right) - \xi_t^i + \omega_t^i = \sum_{j\in\mathcal{N}}\frac{1}{N}\Phi^i e_{t,0}^j - \xi_t^i + \omega_t^i.
\end{aligned}$$

From the definitions of Φ, ξ_t and ω_t we obtain directly equation (12.16), given by

$$e_{t+1,0} = \Phi e_{t,0} - \xi_t + \omega_t = \frac{1}{N}\mathrm{col}\left(\Phi^i\right)\mathbf{1}^T \otimes I_n e_{t,0} - \xi_t + \omega_t.$$

Because $\operatorname{col}\left(\Phi^i\right)$ is equal to $\operatorname{diag}\left(\Phi^i\right)\mathbf{1}\otimes I_n$, the previous equation is equivalent to

$$e_{t+1,0}=\frac{1}{N}\operatorname{diag}\left(\Phi^i\right)\mathbf{1}\otimes I_n\mathbf{1}^T\otimes I_n e_{t,0}-\xi_t+\omega_t.$$

Using this equation, the mixed-product property of the Kronecker product, and the definition of $e^{\text{avg}}_{t,0}$, we obtain equation (12.17) as:

$$e_{t+1,0}=\operatorname{diag}\left(\Phi^i\right)\frac{1}{N}\left(\mathbf{1}\mathbf{1}^T\right)\otimes I_n e_{t,0}-\xi_t+\omega_t=\operatorname{diag}\left(\Phi^i\right)e^{\text{avg}}_{t,0}-\xi_t+\omega_t.$$

Finally, from the definition of $e^{\text{avg}}_{t+1,0}$ and equation (12.17) we obtain

$$e^{\text{avg}}_{t+1,0}=\frac{1}{N}\left(\mathbf{1}\mathbf{1}^T\right)\otimes I_n e_{t+1,0}=\frac{1}{N}\left(\mathbf{1}\mathbf{1}^T\right)\otimes I_n\left(\operatorname{diag}\left(\Phi^i\right)e^{\text{avg}}_{t,0}-\xi_t+\omega_t\right).$$

Since $\mathbf{1}^T\otimes I_n\operatorname{diag}\left(\Phi^i\right)$ is equal to $\operatorname{row}\left(\Phi^i\right)$, using the mixed-product property of the Kronecker product yields

$$e^{\text{avg}}_{t+1,0}=\frac{1}{N}\mathbf{1}\otimes I_n\operatorname{row}\left(\Phi^i\right)e^{\text{avg}}_{t,0}+\frac{1}{N}\left(\mathbf{1}\mathbf{1}^T\right)\otimes I_n\left(\omega_t-\xi_t\right).$$

Noting that $\frac{1}{N}\left(\mathbf{1}\mathbf{1}^T\right)\otimes I_n e^{\text{avg}}_{t,0}$ is equal to $e^{\text{avg}}_{t,0}$ we have

$$e^{\text{avg}}_{t+1,0}=\frac{1}{N}\mathbf{1}\otimes I_n\operatorname{row}\left(\Phi^i\right)\frac{1}{N}\left(\mathbf{1}\mathbf{1}^T\right)\otimes I_n e^{\text{avg}}_{t,0}+\frac{1}{N}\left(\mathbf{1}\mathbf{1}^T\right)\otimes I_n\left(\omega_t-\xi_t\right).$$

Using the mixed-product property and the fact that $\operatorname{row}\left(\Phi^i\right)\frac{1}{N}\mathbf{1}\otimes I_n=\frac{1}{N}\sum_{j\in\mathcal{N}}\Phi^j=A-LC$ the previous equation is equivalent to

$$e^{\text{avg}}_{t+1,0}=\frac{1}{N}\mathbf{1}\otimes I_n\left(A-LC\right)\mathbf{1}^T\otimes I_n e^{\text{avg}}_{t,0}+\frac{1}{N}\left(\mathbf{1}\mathbf{1}^T\right)\otimes I_n\left(\omega_t-\xi_t\right).$$

Again, using the mixed-product property we have that

$$\mathbf{1}\otimes I_n\left(A-LC\right)=I_N\otimes\left(A-LC\right)\mathbf{1}\otimes I_n,$$

from which it follows that

$$e^{\text{avg}}_{t+1,0}=I_N\otimes\left(A-LC\right)\frac{1}{N}\mathbf{1}\otimes I_n\mathbf{1}^T\otimes I_n e^{\text{avg}}_{t,0}+\frac{1}{N}\left(\mathbf{1}\mathbf{1}^T\right)\otimes I_n\left(\omega_t-\xi_t\right).$$

Finally, from the last equation, the definition of $e^{\text{avg}}_{t,0}$, and the mixed-product property, we obtain equation (12.18). □

Proof of Lemma 16. The proof of each inequality is given in each of the following points.

1. The first inequality follows from the assumption that for $t\le p\le 0$ we are under the conditions of Lemma 14, thus equations (12.19) and (12.21) hold. Note that since we initialized the algorithm with $z^i_{0,0}=z^j_{0,0}$ for any $i,j\in\mathcal{N}$, we obtain $e^{\text{avg}}_{0,0}=e_{0,0}$, and therefore $\|e_{0,0}\|_{I_N\otimes P_1}\le\left\|e^{\text{avg}}_{0,0}\right\|_{I_N\otimes P_1}\le\max\left(1,\frac{\tilde{\Phi}}{\tilde{\beta}}\right)\left\|e^{\text{avg}}_{0,0}\right\|_{I_N\otimes P_1}$. Since Assumption A16 holds, applying equations (12.19) and (12.21) at $p=1$ we obtain

$$\begin{aligned}\left\|e^{\text{avg}}_{1,0}\right\|_{I_N\otimes P_1}&\le\tilde{\beta}\left\|e^{\text{avg}}_{0,0}\right\|_{I_N\otimes P_1}+\tilde{\Phi}\alpha^{l_f}\|e_{0,0}\|_{I_N\otimes P_1}+\tilde{\Phi}\alpha^{l_f}k_6\frac{a\beta^p+b}{2^{n_b}-2}+\epsilon\\&\le\bar{\beta}\|e_{0,0}\|_{I_N\otimes P_1}+\tilde{\Phi}\alpha^{l_f}k_6\frac{a\beta^p+b}{2^{n_b}-2}+\epsilon,\end{aligned}$$

$$\|e_{1,0}\|_{I_N\otimes P_1} \leq \max\left(1, \frac{\bar{\Phi}}{\tilde{\beta}}\right)\left(\bar{\beta}\|e_{0,0}\|_{I_N\otimes P_1} + \tilde{\Phi}\alpha^{l_f}k_6\frac{a\beta^p+b}{2^{n_b}-2}+\epsilon\right),$$

where $\bar{\beta}$ is defined in the statement of Theorem 21 as $\bar{\beta} := \tilde{\beta} + \alpha^{l_f}\tilde{\Phi}\max\left(1, \frac{\bar{\Phi}}{\tilde{\beta}}\right)$ and is strictly positive and smaller than 1 by assumption. At $p = 2$ we obtain

$$\begin{aligned}
\left\|e_{2,0}^{\text{avg}}\right\|_{I_N\otimes P_1} &\leq \bar{\beta}\left(\bar{\beta}\|e_{0,0}\|_{I_N\otimes P_1} + \tilde{\Phi}\alpha^{l_f}k_6\frac{a\beta^{p-1}+b}{2^{n_b}-2}+\epsilon\right) + \tilde{\Phi}\alpha^{l_f}k_6\frac{a\beta^p+b}{2^{n_b}-2}+\epsilon\\
&= \bar{\beta}^2\|e_{0,0}\|_{I_N\otimes P_1} + \sum_{\tau=0}^{1}\bar{\beta}^\tau\left(\tilde{\Phi}\alpha^{l_f}k_6\frac{a\beta^{p-\tau}+b}{2^{n_b}-2}+\epsilon\right),\\
\|e_{2,0}\|_{I_N\otimes P_1} &\leq \max\left(1, \frac{\bar{\Phi}}{\tilde{\beta}}\right)\left(\bar{\beta}^2\|e_{0,0}\|_{I_N\otimes P_1} + \sum_{\tau=0}^{1}\bar{\beta}^\tau\left(\tilde{\Phi}\alpha^{l_f}k_6\frac{a\beta^{p-\tau}+b}{2^{n_b}-2}+\epsilon\right)\right),
\end{aligned}$$

Repeating this step p times yields

$$\begin{aligned}
&\left\|e_{p+1,0}^{\text{avg}}\right\|_{I_N\otimes P_1} \leq \bar{\beta}^{p+1}\|e_{0,0}\|_{I_N\otimes P_1} + \sum_{\tau=0}^{p}\bar{\beta}^\tau\left(\tilde{\Phi}\alpha^{l_f}k_6\frac{a\beta^{p-\tau}+b}{2^{n_b}-2}+\epsilon\right)\\
&\leq \bar{\beta}^{p+1}\left[\|e_{0,0}\|_{I_N\otimes P_1} + \alpha^{l_f}\tilde{\Phi}k_6\frac{a}{2^{n_b}-2}\sum_{\tau=0}^{p}\bar{\beta}^{\tau-p-1}\beta^{p-\tau}\right] + \epsilon\sum_{\tau=0}^{p}\bar{\beta}^\tau + \tilde{\Phi}\alpha^{l_f}k_6\frac{b}{2^{n_b}-2}\sum_{\tau=0}^{p}\bar{\beta}^\tau\\
&\leq \beta^{p+1}\left[\|e_{0,0}\|_{I_N\otimes P_1} + \alpha^{l_f}\tilde{\Phi}k_6\frac{a}{2^{n_b}-2}\sum_{\tau=0}^{p}\frac{\bar{\beta}^\tau}{\beta^{\tau+1}}\right] + \epsilon\sum_{\tau=0}^{p}\bar{\beta}^\tau + \tilde{\Phi}\alpha^{l_f}k_6\frac{b}{2^{n_b}-2}\sum_{\tau=0}^{p}\bar{\beta}^\tau.
\end{aligned}$$

Since $0 < \beta < 1$, using the property of the geometric series, we obtain that the expression above is equivalent to

$$\begin{aligned}
\left\|e_{p+1,0}^{\text{avg}}\right\|_{I_N\otimes P_1} &\leq \beta^{p+1}\left[\|e_{0,0}\|_{I_N\otimes P_1} + \frac{\tilde{\Phi}\alpha^{l_f}k_6\left(1-\left(\frac{\bar{\beta}}{\beta}\right)^{p+1}\right)}{\beta\left(1-\frac{\bar{\beta}}{\beta}\right)}\frac{a}{2^{n_b}-2}\right] + \frac{\epsilon}{1-\bar{\beta}} + \frac{\tilde{\Phi}\alpha^{l_f}k_6}{1-\bar{\beta}}\frac{b}{2^{n_b}-2}\\
&\leq \beta^{p+1}\left[\|e_{0,0}\|_{I_N\otimes P_1} + \frac{\tilde{\Phi}\alpha^{l_f}k_6}{\beta-\bar{\beta}}\frac{a}{2^{n_b}-2}\right] + \frac{\epsilon}{1-\bar{\beta}} + \frac{\tilde{\Phi}\alpha^{l_f}k_6}{1-\bar{\beta}}\frac{b}{2^{n_b}-2}.
\end{aligned}$$

2. Similarly to the previous point, applying equations (12.19) and (12.21) recursively, and following the same steps we have for $\|e_{p,0}\|$ and for any p such that $t+1 \geq p \geq 0$.

$$\|e_{p,0}\|_{I_N\otimes P_1} \leq \max\left(1, \frac{\bar{\Phi}}{\tilde{\beta}}\right)\left(\beta^p\left[\|e_{0,0}\|_{I_N\otimes P_1} + \frac{\tilde{\Phi}\alpha^{l_f}k_6}{\beta-\bar{\beta}}\frac{a}{2^{n_b}-2}\right] + \frac{\epsilon}{1-\bar{\beta}} + \frac{\tilde{\Phi}\alpha^{l_f}k_6}{1-\bar{\beta}}\frac{b}{2^{n_b}-2}\right).$$

3. From (F.2),

$$\begin{aligned}
\|q_{p,0}\|_{I_N\otimes P_1} &\leq \|e_{t,0}\|_{I_N\otimes P_1}\\
&\leq \max\left(1, \frac{\bar{\Phi}}{\tilde{\beta}}\right)\left(\beta^p\left[\|e_{0,0}\|_{I_N\otimes P_1} + c_8\frac{a}{2^{n_b}-2}\right] + \frac{\epsilon}{1-\bar{\beta}} + d_8\frac{b}{2^{n_b}-2}\right), \forall\, t+1 \geq p \geq 0.
\end{aligned}$$

Moreover, from Lemma 14, we have

$$\begin{aligned}
&\|q_{p,l}\|_{I_N\otimes P_1} \leq \alpha^l\left[\|q_{p,0}\|_{I_N\otimes P_1} + k_6\frac{a\beta^p+b}{2^{n_b}-2}\right]\\
&\leq \alpha^l\left[\beta^p\left[\max\left(1, \frac{\bar{\Phi}}{\tilde{\beta}}\right)\|e_{0,0}\|_{I_N\otimes P_1} + c_7\frac{a}{2^{n_b}-2}\right] + \frac{\max\left(1, \frac{\bar{\Phi}}{\tilde{\beta}}\right)\epsilon}{1-\bar{\beta}} + d_7\frac{b}{2^{n_b}-2}\right], \forall\, t \geq p \geq 0, l_f \geq l \geq 0.
\end{aligned}$$

4. Noting that since $z_{p,l_f} = q_{p,l_f} + z^{\text{avg}}_{p,l_f} = q_{p,l_f} + z^{\text{avg}}_{p,0}$, from the fact that the consensus algorithm preserves averages, and $x_p = \frac{1}{N}\sum_{i\in\mathcal{N}} e^i_{p,0} + z^i_{p,0}$, from the definitions of $e^i_{p,0}$ and $z^i_{p,0}$, one obtains

$$
\begin{aligned}
z^i_{p+1,0} &= (A+BK)z^i_{p,l_f} + L^i\left(y^i_p - C^i z^i_{p,l_f}\right) = (\Phi^i + BK)z^i_{p,l_f} + L^i y^i_p \\
&= (\Phi^i + BK)z^i_{p,l_f} + L^i\left(C^i x_p + v^i_p\right) = (\Phi^i + BK)z^i_{p,l_f} + L^i C^i x_p + L^i v^i_p \\
&= (\Phi^i + BK)\left(q^i_{p,l_f} + \frac{1}{N}\sum_{j\in\mathcal{N}} z^j_{p,0}\right) + L^i C^i\left(\frac{1}{N}\sum_{j\in\mathcal{N}} e^j_{p,0} + z^j_{p,0}\right) + L^i v^i_p \\
&= (\Phi^i + BK)q^i_{p,l_f} + (A+BK)\frac{1}{N}\sum_{j\in\mathcal{N}} z^j_{p,0} + L^i C^i \frac{1}{N}\sum_{j\in\mathcal{N}} e^j_{p,0} + L^i v^i_p.
\end{aligned}
$$

Therefore,

$$
z_{p+1,0} = \operatorname{diag}\left(\Phi^i + BK\right) q_{p,l_f} + I_N \otimes A z^{\text{avg}}_{p,0} + \operatorname{diag}\left(L^i C^i\right)\frac{1}{N}\left(\mathbf{1}\mathbf{1}^T\right)\otimes I_n e_{p,0} + \operatorname{col}\left(L^i v^i_p\right),
$$

and, noting that $\sum_{i\in\mathcal{N}}\left(L^i C^i\right) = NLC$, we obtain

$$
\begin{aligned}
z^{\text{avg}}_{p+1,0} = &\frac{1}{N}\left(\mathbf{1}\mathbf{1}^T\right)\otimes I_n \operatorname{diag}\left(\Phi^i + BK\right) q_{p,l_f} + I_N \otimes (A+BK) z^{\text{avg}}_{p,0} \\
&+ I_N \otimes (LC)\frac{1}{N}\left(\mathbf{1}\mathbf{1}^T\right)\otimes I_n e_{p,0} + \frac{1}{N}\left(\mathbf{1}\mathbf{1}^T\right)\otimes I_n \operatorname{col}\left(L^i v^i_p\right).
\end{aligned}
$$

For $\bar{z}_{p+1,0}$ we have

$$
\begin{aligned}
\bar{z}_{p+1,0} &= I_N \otimes (A+BK) Q_{p,l_f-1}\left(z_{p,l_f-1}\right) \\
&= I_N \otimes (A+BK)\left[Q_{p,l_f-1}\left(z_{p,l_f-1}\right) - z_{p,l_f-1}\right] + I_N \otimes (A+BK) z_{p,l_f-1} \\
&= I_N \otimes (A+BK)\left[Q_{p,l_f-1}\left(z_{p,l_f-1}\right) - z_{p,l_f-1}\right] + I_N \otimes (A+BK) q_{p,l_f-1} + I_N \otimes (A+BK) z^{\text{avg}}_{p,0},
\end{aligned}
$$

and finally,

$$
\begin{aligned}
&\|\bar{z}_{p+1,0} - z^{\text{avg}}_{p+1,0}\|_{I_N\otimes P_1} \leq \\
&\leq \|A+BK\|_{P_1}\frac{\left(a\beta^p + b\right)\alpha^{l_f-1}\sqrt{N}M(P_1)}{2^{n_b+1}-4} + \|A+BK\|_{P_1}\|q_{p,l_f-1}\|_{I_N\otimes P_1} \\
&+ \hat{\Phi}\|q_{p,l_f}\|_{I_N\otimes P_1} + \|LC\|_{P_1}\|e_{p,0}\|_{I_N\otimes P_1} + \frac{\sum_{j\in\mathcal{N}} M(L^{jT}P_1 L^j)\epsilon^j_v}{\sqrt{N}} \\
&\leq c_5\beta^p\|e_{0,0}\|_{I_N\otimes P_1} + c_6\beta^t\frac{a}{2^{n_b}-2} + d_5 + d_6\frac{b}{2^{n_b}-2}.
\end{aligned}
$$

5. Since $z_{p,l_f} = q_{p,l_f} + z^{\text{avg}}_{p,0}$ we may subtract both sides by $\mathbf{1}\otimes x_p$, yielding $e_{p,l_f} = q_{p,l_f} + e^{\text{avg}}_{p,0}$. Then we obtain

$$
\begin{aligned}
\|e_{p,l_f}\|_{I_N\otimes P_1} &\leq \|q_{p,l_f}\|_{I_N\otimes P_1} + \|e^{\text{avg}}_{p,0}\|_{I_N\otimes P_1} \\
&\leq \beta^p\left[\left(1 + \alpha^{l_f}\max\left(1, \frac{\bar{\Phi}}{\tilde{\beta}}\right)\right)\|e_{0,0}\|_{I_N\otimes P_1} + \left(c_8 + \alpha^{l_f}c_7\right)\frac{a}{2^{n_b}-2}\right] \\
&+ \left(1 + \alpha^{l_f}\max\left(1, \frac{\bar{\Phi}}{\tilde{\beta}}\right)\right)\frac{\epsilon}{1-\tilde{\beta}} + \left(d_8 + \alpha^{l_f}d_7\right)\frac{b}{2^{n_b}-2}, \forall\, t+1 \geq p \geq 1,
\end{aligned}
$$

$\square$

F.5 Proof of Theorem 22

Proof. Given the system dynamics (12.11) we can express x_{t+1} as

$$x_{t+1} = (A+BK)^{t+1} x_0 + \sum_{j=0}^{t} (A+BK)^j \left(w_{t-j} - B \operatorname{diag}\left(K^i\right) e_{t-j,l_f} \right). \tag{F.3}$$

From Theorem 21 and using Property P4 we have

$$\left\| B \operatorname{diag}\left(K^i\right) e_{t-j,l_f} \right\|_{P_2} \le M^* \| e_{t-j,l_f} \|_{I_N \otimes P_1} \le M^* \left(\beta^{t-j} \left[k_1 \| e_{0,0} \|_{I_N \otimes P_1} + k_2 \right] + k_3 \epsilon + k_4 \right).$$

Taking the norm of (F.3) and using Property P3, together with the convergence properties of the geometric series, yields

$$\begin{aligned}
\| x_{t+1} \|_{P_2} &\le \tilde{\gamma}^{t+1} \| x_0 \|_{P_2} + \sum_{j=0}^{t} \tilde{\gamma}^j \left(M(P_2) \epsilon_w + M^* \left(\beta^{t-j} \left[k_1 \| e_{0,0} \|_{I_N \otimes P_1} + k_2 \right] + k_3 \epsilon + k_4 \right) \right) \\
&\le \gamma^t \left[\| x_0 \|_{P_2} + \sum_{j=0}^{t} \left(\frac{\tilde{\gamma}}{\beta} \right)^j M^* (k_1 \| e_{0,0} \|_{I_N \otimes P_1} + k_2) \right] + \sum_{j=0}^{t} \tilde{\gamma}^j M(P_2) \epsilon_w + M^* (k_3 \epsilon + k_4) \\
&\le \gamma^t \left[\| x_0 \|_{P_2} + \frac{M^* \beta}{\beta - \tilde{\gamma}} (k_1 \| e_{0,0} \|_{I_N \otimes P_1} + k_2) \right] + \frac{M(P_2) \epsilon_w + M^* (k_3 \epsilon + k_4)}{1 - \tilde{\gamma}}.
\end{aligned}$$

□

Bibliography

K. Aberer, S. Sathe, D. Chakraborty, A. Martinoli, G. Barrenetxea, B. Faltings, and L. Thiele. OpenSense: Open community driven sensing of environment. In *Proceedings of the ACM SIGSPATIAL International Workshop on GeoStreaming*, pages 39–42. ACM, 2010.

P. C. Abreu, M. Bayat, J. Botelho, P. Góis, J. P. Gomes, A. M. Pascoal, J. Ribeiro, M. Ribeiro, M. Rufino, L. Sebastião, and H. Silva. Cooperative navigation and control: The EU MORPH project. In *OCEANS 2015 - MTS/IEEE Washington*, pages 1–10, 2015.

P. C. Abreu, J. Botelho, P. Góis, A. M. Pascoal, J. Ribeiro, M. Ribeiro, M. Rufino, L. Sebastião, and H. Silva. The MEDUSA class of autonomous marine vehicles and their role in EU projects. In *Proceedings of OCEANS 2016*, pages 1–10. IEEE, 2016.

A. P. Aguiar and J. P. Hespanha. Trajectory-tracking and path-following of underactuated autonomous vehicles with parametric modeling uncertainty. *IEEE Transactions on Automatic Control*, 52(8):1362–1379, 2007.

A. P. Aguiar, A. Rucco, and A. Alessandretti. A sampled-data model predictive framework for cooperative path following of multiple robotic vehicles. In *Sensing and Control for Autonomous Vehicles*, pages 473–494. Springer, 2017.

I. F. Akyildiz, W. Su, Y. Sankarasubramaniam, and E. Cayirci. A survey on sensor networks. *IEEE Communications Magazine*, 40(8):102–114, 2002.

A. Alcocer, P. Oliveira, and A. M. Pascoal. Study and implementation of an EKF GIB-based underwater positioning system. *Control engineering practice*, 15(6):689–701, 2007.

A. Alessandretti, A. P. Aguiar, and C. N. Jones. Trajectory-tracking and path-following controllers for constrained underactuated vehicles using model predictive control. In *2013 European Control Conference (ECC)*, pages 1371–1376. IEEE, 2013.

B. Allotta, L. Pugi, R. Costanzi, and G. Vettori. Localization algorithm for a fleet of three AUVs by INS, DVL and range measurements. In *2011 15th International Conference on Advanced Robotics (ICAR)*, pages 631–636, 2011.

J. Almeida, C. Silvestre, and A. M. Pascoal. Cooperative control of multiple surface vessels with discrete-time periodic communications. *International Journal of Robust and Nonlinear Control*, 22(4):398–419, 2012.

J. Almeida, C. Silvestre, and A. M. Pascoal. Synchronization of multiagent systems using event-triggered and self-triggered broadcasts. *IEEE Transactions on Automatic Control*, 62(9):4741–4746, 2017.

P. Alriksson and A. Rantzer. Distributed Kalman filtering using weighted averaging. In *Proceedings of the 17th International Symposium on Mathematical Theory of Networks and Systems*, pages 2445–2450, 2006.

B. D. O. Anderson and J. B. Moore. Optimal filtering. *Englewood Cliffs*, 21:22–95, 1979.

B. D. O. Anderson and C. Yu. Range-only sensing for formation shape control and easy sensor network localization. In *2011 Chinese Control and Decision Conference (CCDC)*, pages 3310–3315. IEEE, 2011.

A. Anta and P. Tabuada. To sample or not to sample: Self-triggered control for nonlinear systems. *IEEE Transactions on Automatic Control*, 55(9):2030–2042, 2010.

A. Astolfi, P. Bolzern, and A. Locatelli. Path-tracking of a tractor-trailer vehicle along rectilinear and circular paths: a Lyapunov-based approach. *IEEE Transactions on Robotics and Automation*, 20(1):154–160, 2004.

K. J. Aström. Event based control. *Analysis and design of nonlinear control systems*, 3:127–147, 2008.

T. C. Aysal, M. J. Coates, and M. G. Rabbat. Distributed average consensus with dithered quantization. *IEEE Transactions on Signal Processing*, 56(10):4905–4918, 2008.

A. Bahr, J. J. Leonard, and M. F. Fallon. Cooperative localization for autonomous underwater vehicles. *The International Journal of Robotics Research*, 28(6):714–728, 2009.

Y. Bar-Shalom. On the track-to-track correlation problem. *IEEE Transactions on Automatic Control*, 26(2): 571–572, 1981.

P. Barooah. *Estimation and control with relative measurements: Algorithms and scaling laws*. PhD thesis, University of California, Santa Barbara, 2007.

P. Barooah, W. J. Russell, and J. P. Hespanha. Approximate distributed Kalman filtering for cooperative multi-agent localization. In *International Conference on Distributed Computing in Sensor Systems*, pages 102–115. Springer, 2010.

T. Basary, S. R. Etesami, and A. Olshevsky. Fast convergence of quantized consensus using Metropolis chains. In *2014 IEEE 53rd Annual Conference on Decision and Control (CDC)*, pages 1330–1334. IEEE, 2014.

G. Battistelli and L. Chisci. Kullback-Leibler average, consensus on probability densities, and distributed state estimation with guaranteed stability. *Automatica*, 50(3):707–718, 2014.

G. Battistelli and L. Chisci. Stability of consensus extended Kalman filter for distributed state estimation. *Automatica*, 68:169–178, 2016.

G. Battistelli, A. Benavoli, and L. Chisci. Data-driven communication for state estimation with sensor networks. *Automatica*, 48(5):926–935, 2012.

G. Battistelli, L. Chisci, G. Mugnai, A. Farina, and A. Graziano. Consensus-based linear and nonlinear filtering. *IEEE Transactions on Automatic Control*, 60(5):1410–1415, 2015.

A. R. Benaskeur. Consistent fusion of correlated data sources. In *IEEE 2002 28th Annual Conference of the Industrial Electronics Society. IECON 02.*, volume 4, pages 2652–2656. IEEE, 2002.

B. Bethke, M. Valenti, and J. How. Cooperative vision based estimation and tracking using multiple UAVs. In *Advances in Cooperative Control and Optimization*, pages 179–189. Springer, 2007.

V. D. Blondel and A. Olshevsky. How to decide consensus? A combinatorial necessary and sufficient condition and a proof that consensus is decidable but NP-hard. *SIAM Journal on Control and Optimization*, 52(5): 2707–2726, 2014.

V. D. Blondel, Y. Nesterov, and J. Theys. On the accuracy of the ellipsoid norm approximation of the joint spectral radius. *Linear Algebra and its Applications*, 394:91–107, 2005.

R. S. Blum, S. A. Kassam, and H. V. Poor. Distributed detection with multiple sensors II. Advanced topics. *Proceedings of the IEEE*, 85(1):64–79, 1997.

V. Borkar and P. Varaiya. Asymptotic agreement in distributed estimation. *IEEE Transactions on Automatic Control*, 27(3):650–655, 1982.

F. Bullo, J. Cortés, and S. Martínez. *Distributed control of robotic networks: A mathematical approach to motion coordination algorithms*. Princeton series in applied mathematics. Princeton University Press, 2009.

G. C. Calafiore and F. Abrate. Distributed linear estimation over sensor networks. *International Journal of Control*, 82(5):868–882, 2009.

M. Cao and A. S. Morse. Station keeping in the plane with range-only measurements. In *American Control Conference, 2007. ACC'07*, pages 5419–5424. IEEE, 2007.

M. Cao and A. S. Morse. The use of dwell-time switching to maintain a formation with only range sensing. In *3rd International Symposium on Communications, Control and Signal Processing, 2008. ISCCSP 2008.*, pages 954–959. IEEE, 2008.

M. Cao, C. Yu, and B. Anderson. Formation control using range-only measurements. *Automatica*, 47(4): 776–781, 2011.

R. Carli, F. Bullo, and S. Zampieri. Quantized average consensus via dynamic coding/decoding schemes. *International Journal of Robust and Nonlinear Control*, 20(2):156–175, 2010.

L. C. Carrillo-Arce, E. D. Nerurkar, J. L. Gordillo, and S. I. Roumeliotis. Decentralized multi-robot cooperative localization using covariance intersection. In *2013 IEEE/RSJ International Conference on Intelligent Robots and Systems (IROS)*, pages 1412–1417. IEEE, 2013.

D. W. Casbeer and R. Beard. Distributed information filtering using consensus filters. In *American Control Conference, ACC'09*, pages 1882–1887. IEEE, 2009.

F. S. Cattivelli and A. H. Sayed. Diffusion strategies for distributed Kalman filtering and smoothing. *IEEE Transactions on Automatic Control*, 55(9):2069–2084, 2010.

Z. Chair and P. K. Varshney. Optimal data fusion in multiple sensor detection systems. *IEEE Transactions on Aerospace and Electronic Systems*, (1):98–101, 1986.

J.-F. Chamberland and V. V. Veeravalli. Decentralized detection in sensor networks. *IEEE Transactions on Signal Processing*, 51(2):407–416, 2003.

B. Charron-Bost. Orientation and connectivity based criteria for asymptotic consensus. *arXiv preprint arXiv:1303.2043*, 2013.

J. Cortes. Distributed Kriged Kalman filter for spatial estimation. *IEEE Transactions on Automatic Control*, 54 (12):2816–2827, 2009.

O. H. Dagci, U. Y. Ogras, and U. Ozguner. Path following controller design using sliding mode control theory. In *Proceedings of the 2003 American Control Conference*, volume 1, pages 903–908, 2003.

S. Das and J. M. F. Moura. Distributed state estimation in multi-agent networks. In *2013 IEEE International Conference on Acoustics, Speech and Signal Processing (ICASSP)*, pages 4246–4250. IEEE, 2013a.

S. Das and J. M. F. Moura. Distributed Kalman filtering. In *2013 Proceedings of the 21st European Signal Processing Conference (EUSIPCO)*, pages 1–5. IEEE, 2013b.

S. Das and J. M. F. Moura. Distributed linear estimation of dynamic random fields. In *2013 51st Annual Allerton Conference on Communication, Control, and Computing (Allerton)*, pages 1120–1125. IEEE, 2013c.

S. Das and J. M. F. Moura. Distributed Kalman filtering with dynamic observations consensus. *IEEE Transactions on Signal Processing*, 63(17):4458–4473, 2015.

Sailer R. De Persis, C. and F. Wirth. On a small-gain approach to distributed event-triggered control. *IFAC Proceedings Volumes*, 44(1):2401–2406, 2011.

V. Delouille, R. Neelamani, and R. Baraniuk. Robust distributed estimation in sensor networks using the embedded polygons algorithm. In *Proceedings of the 3rd international symposium on Information processing in sensor networks*, pages 405–413. ACM, 2004.

J. P. Desai, J. Ostrowski, and V. Kumar. Controlling formations of multiple mobile robots. In *Proceedings of the 1998 IEEE International Conference on Robotics and Automation*, volume 4, pages 2864–2869. IEEE, 1998.

J. P. Desai, J. P. Ostrowski, and V. Kumar. Modeling and control of formations of nonholonomic mobile robots. *IEEE Transactions on Robotics and Automation*, 17(6):905–908, 2001.

D. V. Dimarogonas and K. H. Johansson. Event-triggered control for multi-agent systems. In *Proceedings of the 48th IEEE Conference on Decision and Control, 2009 held jointly with the 2009 28th Chinese Control Conference. CDC/CCC 2009.*, pages 7131–7136. IEEE, 2009.

D. V. Dimarogonas, E. Frazzoli, and K. H. Johansson. Distributed event-triggered control for multi-agent systems. *IEEE Transactions on Automatic Control*, 57(5):1291–1297, 2012.

H. Dong, X. Bu, N. Hou, Y. Liu, F. E. Alsaadi, and T. Hayat. Event-triggered distributed state estimation for a class of time-varying systems over sensor networks with redundant channels. *Information Fusion*, 36 (Supplement C):243–250, 2017.

W. Dong. On consensus algorithms of multiple uncertain mechanical systems with a reference trajectory. *Automatica*, 47(9):2023–2028, 2011.

M. C. F. Donkers and W. P. M. H. Heemels. Output-based event-triggered control with guaranteed $\mathscr{L}_\infty$-gain and improved and decentralized event-triggering. *IEEE Transactions on Automatic Control*, 57(6):1362–1376, 2012.

M. Doostmohammadian and U. A. Khan. On the genericity properties in distributed estimation: Topology design and sensor placement. *IEEE Journal of Selected Topics in Signal Processing*, 7(2):195–204, 2013.

J. Du, S. Ma, Y.-C. Wu, S. Kar, and J. M. F. Moura. Convergence analysis of distributed inference with vector-valued Gaussian belief propagation. *arXiv preprint arXiv:1611.02010*, 2016.

J. Du, S. Ma, Y.-C. Wu, S. Kar, and J. M. F. Moura. Convergence analysis of the information matrix in Gaussian belief propagation. *arXiv preprint arXiv:1704.03969*, 2017.

H. F. Durrant-Whyte. A beginner's guide to decentralised data fusion. *Technical Document of Australian Centre for Field Robotics, University of Sydney, Australia*, pages 1–27, 2000.

N. Elia and S. K. Mitter. Stabilization of linear systems with limited information. *IEEE Transactions on Automatic Control*, 46(9):1384–1400, 2001.

P. Encarnação and A. M. Pascoal. 3D path following for autonomous underwater vehicle. In *Proceedings of the 39th IEEE Conference on Decision and Control*, volume 3, pages 2977–2982, 2000.

Y. Fan, G. Feng, Y. Wang, and C. Song. Distributed event-triggered control of multi-agent systems with combinational measurements. *Automatica*, 49(2):671–675, 2013.

J. Fang and H. Li. An adaptive quantization scheme for distributed consensus. In *IEEE International Conference on Acoustics, Speech and Signal Processing. ICASSP 2009.*, pages 2777–2780. IEEE, 2009.

M. Farina, G. Ferrari-Trecate, and R. Scattolini. Distributed moving horizon estimation for linear constrained systems. *IEEE Transactions on Automatic Control*, 55(11):2462–2475, 2010.

M. Farina, G. Ferrari-Trecate, and R. Scattolini. Distributed moving horizon estimation for nonlinear constrained systems. *International Journal of Robust and Nonlinear Control*, 22(2):123–143, 2012.

A. L. Flåten and E. F. Brekke. Stability of line-of-sight based trajectory-tracking in two dimensions. In *2017 IEEE Conference on Control Technology and Applications (CCTA)*, pages 760–765, 2017.

T. I. Fossen and K. Y. Pettersen. On uniform semiglobal exponential stability (USGES) of proportional line-of-sight guidance laws. *Automatica*, 50(11):2912–2917, 2014.

Powell J. D. Franklin, G. F. and M. L. Workman. *Digital control of dynamic systems*, volume 3. Addison-wesley Menlo Park, CA, 1998.

P. Frasca, R. Carli, F. Fagnani, and S. Zampieri. Average consensus on networks with quantized communication. *International Journal of Robust and Nonlinear Control*, 19(16):1787–1816, 2009.

E. Garcia, Y. Cao, and D. W. Casbeer. Cooperative control with general linear dynamics and limited communication: Centralized and decentralized event-triggered control strategies. In *2014 American Control Conference (ACC)*, pages 159–164. IEEE, 2014.

F. Garin and L. Schenato. A survey on distributed estimation and control applications using linear consensus algorithms. In *Networked Control Systems*, pages 75–107. Springer, 2010.

R. Ghabcheloo, A. P. Aguiar, A. M. Pascoal, C. Silvestre, I. Kaminer, and J. Hespanha. Coordinated path-following control of multiple underactuated autonomous vehicles in the presence of communication failures. In *2006 45th IEEE Conference on Decision and Control*, pages 4345–4350, 2006.

R. Ghabcheloo, A. M. Pascoal, C. Silvestre, and I. Kaminer. Non-linear co-ordinated path following control of multiple wheeled robots with bidirectional communication constraints. *International Journal of Adaptive Control and Signal Processing*, 21(2-3):133–157, 2007.

R. Ghabcheloo, A. P. Aguiar, A. M. Pascoal, C. Silvestre, I. Kaminer, and J. Hespanha. Coordinated path-following in the presence of communication losses and time delays. *SIAM Journal on Control and Optimization*, 48(1):234–265, 2009.

F. Giulietti, L. Pollini, and M. Innocenti. Autonomous formation flight. *Control Systems, IEEE*, 20(6):34–44, 2000.

C. Godsil and G. F. Royle. *Algebraic graph theory*, volume 207. Springer Science & Business Media, 2013.

G. Guo, L. Ding, and Q. Han. A distributed event-triggered transmission strategy for sampled-data consensus of multi-agent systems. *Automatica*, 50(5):1489–1496, 2014.

D. L. Hall and J. Llinas, editors. *Handbook of multisensor data fusion*. The Electrical engineering and applied signal processing series. CRC Press, 2001.

D. J. Hartfiel. Concerning diagonal similarity of irreducible matrices. *Proceedings of the American Mathematical Society*, 30(3):419, 1971.

D. J. Hartfiel and J. W. Spellmann. A role for doubly stochastic matrices in graph theory. *Proceedings of the American Mathematical Society*, 36(2):389–394, 1972.

H. R. Hashemipour, S. Roy, and A. J. Laub. Decentralized structures for parallel Kalman filtering. *IEEE Transactions on Automatic Control*, 33(1):88–94, 1988.

A. J. Healey and D. Lienard. Multivariable sliding mode control for autonomous diving and steering of unmanned underwater vehicles. *IEEE Journal of Oceanic Engineering*, 18(3):327–339, 1993.

J. P. Hespanha. *Linear systems theory*. Princeton university press, 2009.

R. A. Horn and C. R. Johnson. *Matrix analysis*. Cambridge university press, 2012.

I.-A. F. Ihle, M. Arcak, and T. I. Fossen. Passivity-based designs for synchronized path-following. *Automatica*, 43:1508–1518, 2006.

H. Ishii and T. Başar. Remote control of LTI systems over networks with state quantization. *Systems & Control Letters*, 54(1):15–31, 2005.

J.-J. Xiao, S. Cui, Z.-Q. Luo, and A.J. Goldsmith. Power scheduling of universal decentralized estimation in sensor networks. *IEEE Transactions on Signal Processing*, 54(2):413–422, 2006.

A. Jadbabaie, Jie Lin, and A.S. Morse. Coordination of groups of mobile autonomous agents using nearest neighbor rules. *IEEE Transactions on Automatic Control*, 48(6):988–1001, 2003.

R. P. Jain, A. P. Aguiar, and J. Sousa. Self-triggered cooperative path following control of fixed wing unmanned aerial vehicles. In *2017 International Conference on Unmanned Aircraft Systems (ICUAS)*, pages 1231–1240, 2017.

L. Jetto and V. Orsini. Event-triggered internally stabilizing sporadic control for MIMO plants with non measurable state. In *IFAC World congres*, page 10, 2011.

Z.-P. Jiang, A. R. Teel, and L. Praly. Small-gain theorem for ISS systems and applications. *Mathematics of Control, Signals, and Systems (MCSS)*, 7:95–120, 1994.

S. Julier and J. K. Uhlmann. General decentralized data fusion with covariance intersection (CI). In *Multisensor Data Fusion*. CRC Press, 2001.

S. J. Julier and J. K. Uhlmann. A non-divergent estimation algorithm in the presence of unknown correlations. In *Proceedings of the 1997 American Control Conference*, volume 4, pages 2369–2373. IEEE, 1997.

T. Kailath, A. H. Sayed, and B. Hassibi. *Linear estimation*, volume 1. Prentice Hall Upper Saddle River, NJ, 2000.

J. Kalwa, A. M. Pascoal, P. Ridao, A. Birk, M. Eichhorn, L. Brignone, M. Caccia, J. Alves, and R.S. Santos. The european R&D-project morph: Marine robotic systems of self-organizing, logically linked physical nodes. In *Proceedings of MCMC 2012*, 2013.

M. Kamgarpour and C. Tomlin. Convergence properties of a decentralized Kalman filter. In *47th IEEE Conference on Decision and Control, 2008. CDC 2008.*, pages 3205–3210. IEEE, 2008.

S. Kar and J. M. F. Moura. Distributed consensus algorithms in sensor networks: Quantized data and random link failures. *IEEE Transactions on Signal Processing*, 58(3):1383–1400, 2010.

A. Kashyap, T. Başar, and R. Srikant. Quantized consensus. *Automatica*, 43(7):1192–1203, 2007.

O. Kebkal, K. Kebkal, and R. Bannasch. Long-baseline hydro-acoustic positioning using D-MAC communication protocol. In *Proceedings of OCEANS 2012*, pages 1–7, 2012.

H. K Khalil. *Nonlinear Systems*. Prentice-Hall, New Jersey, 1996.

U. A. Khan and A. Jadbabaie. On the stability and optimality of distributed Kalman filters with finite-time data fusion. In *2011 American Control Conference (ACC)*, pages 3405–3410. IEEE, 2011.

U. A. Khan and J. M. F. Moura. Distributed Kalman filters in sensor networks: Bipartite fusion graphs. In *2007 IEEE/SP 14th Workshop on Statistical Signal Processing*, pages 700–704. IEEE, 2007.

U. A. Khan and J. M. F. Moura. Distributing the Kalman filter for large-scale systems. *IEEE Transactions on Signal Processing*, 56(10):4919–4935, 2008.

U. A. Khan, S. Kar, A. Jadbabaie, and J. MF Moura. On connectivity, observability, and stability in distributed estimation. In *2013 IEEE/RSJ International Conference on Decision and Control (CDC)*, pages 6639–6644. IEEE, 2010.

A. Y. Kibangou. Distributed estimation over unknown fading channels. *IFAC Proceedings Volumes*, 43(19): 317–322, 2010.

K. H. Kim. Development of track to track fusion algorithms. volume 1, pages 1037–1041. IEEE, 1994.

S. Kim, C. Ryoo, K. Choi, and C. Park. Multi-vehicle formation using range-only measurement. In *International Conference on Control, Automation and Systems, 2007. ICCAS'07.*, pages 2104–2109. IEEE, 2007.

L. Lapierre, D. Soetanto, and A. M. Pascoal. Nonlinear path following control of autonomous underwater vehicles. *IFAC Proceedings Volumes*, 36(4):25–30, 2003.

S. H. Lee and M. West. Performance comparison of the distributed extended Kalman filter and Markov chain distributed particle filter (MCDPF). *IFAC Proceedings Volumes*, 43(19):151–156, 2010.

S. H. Lee and M. West. Convergence of the Markov chain distributed particle filter (MCDPF). *IEEE Transactions on Signal Processing*, 61(4):801–812, 2013.

D. Li, S. Kar, F. E. Alsaadi, A. M. Dobaie, and S. Cui. Distributed Kalman filtering with quantized sensing state. *IEEE Transactions on Signal Processing*, 63(19):5180–5193, 2015a.

H. Li and J. Fang. Distributed adaptive quantization and estimation for wireless sensor networks. *IEEE Signal Processing Letters*, 14(10):669–672, 2007.

T. Li, M. Fu, L. Xie, and J. Zhang. Distributed consensus with limited communication data rate. *IEEE Transactions onAutomatic Control*, 56(2):279–292, 2011.

W. Li, Z. Wang, G. Wei, L. Ma, J. Hu, and D. Ding. A survey on multisensor fusion and consensus filtering for sensor networks. *Discrete Dynamics in Nature and Society*, 2015, 2015b.

X. R. Li. Optimal linear estimation fusion, Part VII: Dynamic systems. In *Proceedings of the 2003 International Conference on Information Fusion*, pages 445–462, 2003.

X. R. Li and J. Wang. Unified optimal linear estimation fusion - Part II: discussions and examples. In *Proceedings of the 2000 International Conference on Information Fusion*, 2000.

X. R. Li and K. S. Zhang. Optimal linear estimation fusion - Part IV: Optimality and efficiency of distributed fusion. In *Proceedings of the 2001 International Conference on Information Fusion*, 2001a.

X.-R. Li and P. Zhang. Optimal linear estimation fusion - Part III: Cross-correlation of local estimation errors. In *Proceedings of the 2001 International Conference on Information Fusion*, 2001b.

X. R. Li, K. Zhang, J. Zhao, and Y. Zhu. Optimal linear estimation fusion. Part V. Relationships. In *Proceedings of the Fifth International Conference on Information Fusion*, volume 1, pages 497–504. IEEE, 2002.

X. R. Li, Y. Zhu, J. Wang, and C. Han. Optimal linear estimation fusion. I. Unified fusion rules. *IEEE Transactions on Information Theory*, 49(9):2192–2208, 2003.

Y. Li and R. G. Sanfelice. Robust distributed state observers with performance guarantees and optimized communication graph. In *American Control Conference (ACC)*, pages 1090–1095. IEEE, 2014.

H. Long, Z. Qu, X. Fan, and S. Liu. Distributed extended Kalman filter based on consensus filter for wireless sensor network. In *2012 10th World Congress on Intelligent Control and Automation (WCICA)*, pages 4315–4319. IEEE, 2012.

J. Lunze and D. Lehmann. A state-feedback approach to event-based control. *Automatica*, 46(1):211–215, 2010.

C. Q. Ma and J. F. Zhang. Necessary and sufficient conditions for consensusability of linear multi-agent systems. *IEEE Transactions on Automatic Control*, 55(5):1263–1268, 2010.

M. S. Mahmoud and H. M. Khalid. Distributed Kalman filtering: a bibliographic review. *IET Control Theory & Applications*, 7(4):483–501, 2013.

A. Makarenko and H. Durrant-Whyte. Decentralized data fusion and control in active sensor networks. In *Proceedings of the Seventh International Conference on Information Fusion*, volume 1, pages 479–486, 2004.

I. L. Manuel and A. N. Bishop. Distributed Monte Carlo information fusion and distributed particle filtering. *IFAC Proceedings Volumes*, 47(3):8681–8688, 2014.

J. Manyika. *An Information-Theoretic Approach to Data Fusion and Sensor Management*. PhD thesis, University of Oxford, 1993.

I. Matei and J. S. Baras. Consensus-based linear distributed filtering. *Automatica*, 48(8):1776–1782, 2012.

M. Mazo and P. Tabuada. Decentralized event-triggered control over wireless sensor/actuator networks. *IEEE Transactions on Automatic Control*, 56(10):2456–2461, 2011.

M. Mazo, A. Anta, and P. Tabuada. An ISS self-triggered implementation of linear controllers. *Automatica*, 46 (8):1310–1314, 2010.

M. Mesbahi and M. Egerstedt. *Graph theoretic methods in multiagent networks*. Princeton University Press, 2010.

C. D. Meyer. *Matrix analysis and applied linear algebra*, volume 2. SIAM, 2000.

A. Micaelli and C. Samson. *Trajectory tracking for unicycle-type and two-steering-wheels mobile robots*. PhD thesis, INRIA, 1993.

A. Mitra and S. Sundaram. An approach for distributed state estimation of LTI systems. In *2016 54th Annual Allerton Conference on Communication, Control, and Computing (Allerton)*, pages 1088–1093. IEEE, 2016.

L. Moreau. Stability of multiagent systems with time-dependent communication links. *IEEE Transactions on Automatic Control*, 50(2):169–182, 2005.

C. Mosquera and S. K. Jayaweera. Entangled Kalman filters for cooperative estimation. In *5th IEEE Sensor Array and Multichannel Signal Processing Workshop, SAM*, pages 279–283. IEEE, 2008.

C. Mosquera, R. López-Valcarce, and S. K. Jayaweera. Stepsize sequence design for distributed average consensus. *Signal Processing Letters, IEEE*, 17(2):169–172, 2010.

E. J. Msechu, S. I. Roumeliotis, A. Ribeiro, and G. B. Giannakis. Decentralized quantized Kalman filtering with scalable communication cost. *IEEE Transactions on Signal Processing*, 56(8):3727–3741, 2008.

A. G. O. Mutambara. *Decentralized estimation and control for multisensor systems*. CRC Press, 1998.

E. F. Nakamura, A. A. F. Loureiro, and A. C. Frery. Information fusion for wireless sensor networks: Methods, models, and classifications. *ACM Computing Surveys*, 39(3), 2007.

A. Nedić, A. Olshevsky, A. Ozdaglar, and J. N. Tsitsiklis. On distributed averaging algorithms and quantization effects. *IEEE Transactions on Automatic Control*, 54(11):2506–2517, 2009.

K. Ogata. *Discrete-time Control Systems*. Prentice-Hall, Inc., 1995.

P. Ogren, M. Egerstedt, and X. Hu. A control Lyapunov function approach to multiagent coordination. *IEEE Transactions on Robotics and Automation*, 18(5):847–851, 2002.

R. Olfati-Saber. Distributed Kalman filter with embedded consensus filters. In *44th IEEE Conference on Decision and Control, 2005 and 2005 European Control Conference. CDC-ECC'05.*, pages 8179–8184. IEEE, 2005.

R. Olfati-Saber. Kalman-consensus filter: Optimality, stability, and performance. In *CDC/CCC 2009. Proceedings of the 48th IEEE Conference on Decision and Control, 2009 held jointly with the 2009 28th Chinese Control Conference*, pages 7036–7042. IEEE, 2009.

R. Olfati-Saber and P. Jalalkamali. Coupled distributed estimation and control for mobile sensor networks. *IEEE Transactions on Automatic Control*, 57(10):2609–2614, 2012.

L. Orihuela, P. Millán, C. Vivas, and F. R. Rubio. Reduced-order H_2 / H_∞ distributed observer for sensor networks. *International Journal of Control*, 86(10):1870–1879, 2013.

S. Park and N. C. Martins. Design of distributed LTI observers for state omniscience. *IEEE Transactions on Automatic Control*, 2016.

F. Pasqualetti, R. Carli, A. Bicchi, and F. Bullo. Distributed estimation and detection under local information. *IFAC Proceedings Volumes*, 43(19):263–268, 2010.

J. Plaskonka. The path following control of a unicycle based on the chained form of a kinematic model derived with respect to the serret-frenet frame. In *2012 17th International Conference on Methods and Models in Automation and Robotics (MMAR)*, pages 617–620a, 2012.

U. Prathap, D. P. Shenoy, K. R. Venugopal, and L. M. Patnaik. Wireless sensor networks applications and routing protocols: Survey and research challenges. In *2012 International Symposium on Cloud and Services Computing (ISCOS)*, pages 49–56. IEEE, 2012.

Y. Pu, M. N. Zeilinger, and C. N. Jones. Quantization design for unconstrained distributed optimization. In *The 2015 American Control Conference*, 2015.

Y. Pu, M. N. Zeilinger, and C. N. Jones. Quantization design for distributed optimization. *IEEE Transactions on Automatic Control*, 62(5):2107–2120, 2017.

B. S. Rao and H. F. Durrant-Whyte. Fully decentralised algorithm for multisensor Kalman filtering. In *IEE Proceedings D (Control Theory and Applications)*, volume 138, pages 413–420. IET, 1991.

C. R. Rao. *Linear statistical inference and its applications*. Wiley New York, 1973.

P. Rawat, K. D. Singh, H. Chaouchi, and J. M. Bonnin. Wireless sensor networks: A survey on recent developments and potential synergies. *The Journal of supercomputing*, 68(1):1–48, 2014.

F. F. C. Rego, A. P. Aguiar, and A. M. Pascoal. A packet loss compliant logic-based communication algorithm for cooperative path-following control. In *Proceedings of the 9th IFAC Conference on Control Applications in Marine Systems 2013*, volume 46, pages 262–267. Elsevier, 2013.

F. F. C. Rego, J. M. Soares, A. M. Pascoal, A. P. Aguiar, and C. N. Jones. Flexible triangular formation keeping of marine robotic vehicles using range measurements. In *Proceedings of the 19th IFAC World Congress*, 2014.

F. F. C. Rego, Y. Pu, A. Alessandretti, A. P. Aguiar, and C. N. Jones. A consensus algorithm for networks with process noise and quantization error. In *Proceedings of the 53rd Annual Allerton Conference on Communication, Control, and Computing*, 2015.

F. F. C. Rego, Y. Pu, A. Alessandretti, A. P. Aguiar, and C. N. Jones. Proofs of lemmas of the paper "Design of a distributed quantized Luenberger filter for bounded noise. Technical report, 2016a.

F. F. C. Rego, Y. Pu, A. Alessandretti, A. P. Aguiar, A. M. Pascoal, and C. N. Jones. Design of a distributed quantized Luenberger filter for bounded noise. In *Proceedings of the 2016 American Control Conference (ACC)*, pages 6393–6398, 2016b.

F. F. C. Rego, A. P. Aguiar, A. M. Pascoal, and C. N. Jones. A design method for distributed Luenberger observers. In *Proceedings of the 56th IEEE Conference on Decision and Control, CDC 2017*. IEEE, 2017.

J. Ribeiro. Motion control of single and multiple autonomous marine vehicles. Master's thesis, Instituto Superior Técnico, 2011.

J. Ribeiro, A. P. Aguiar, and A. M. Pascoal. Motion control design for the Medusa robotic vehicle with experimental results. Technical report, LARSyS, 2012.

W. Saab, M. M. Maaz, S. Bliudze, and J.-Y. Le Boudec. Quarts: Quick agreement for real-time control systems. Technical report, 2017.

C. Samson and K. Ait-Abderrahim. Feedback control of a nonholonomic wheeled cart in cartesian space. In *Proceedings of the 1991 IEEE International Conference on Robotics and Automation*, pages 1136–1141. IEEE, 1991.

G. S. Seyboth, D. V. Dimarogonas, and K. H. Johansson. Event-based broadcasting for multi-agent average consensus. *Automatica*, 49(1):245–252, 2013.

L. Shanbin and X. Bugong. Modified fault isolation filter for networked control system with send-on-delta sampling. In *2011 30th Chinese Control Conference (CCC)*, pages 4145–4150. IEEE, 2011.

J. Sijs and P. van den Bosch. Heterogeneous state estimation in dynamic networked systems. *Control Theory & Applications, IET*, 9(15):2232–2241, 2015.

R. Skjetne, T. I. Fossen, and P. V. Kokotović. Robust output maneuvering for a class of nonlinear systems. *Automatica*, 40(3):373–383, 2004.

D. Smith and S. Singh. Approaches to multisensor data fusion in target tracking: A survey. *IEEE transactions on knowledge and data engineering*, 18(12):1696–1710, 2006.

R. S. Smith and F. Y. Hadaegh. Distributed estimation, communication and control for deep space formations. *IET Control Theory & Applications*, 1(2):445–451, 2007.

C. Soares, J. Xavier, and J. Gomes. Simple and fast convex relaxation method for cooperative localization in sensor networks using range measurements. *IEEE Transactions on Signal Processing*, 63(17):4532–4543, 2015a.

J. M. Soares, A. P. Aguiar, A. M. Pascoal, and M. Gallieri. Triangular formation control using range measurements: An application to marine robotic vehicles. In *Proceedings of the IFAC Workshop on Navigation, Guidance and Control of Underwater Vehicles*, 2012.

J. M. Soares, A. P. Aguiar, A. M. Pascoal, and A. Martinoli. Joint ASV/AUV range-based formation control: Theory and experimental results. In *2013 IEEE International Conference on Robotics and Automation (ICRA)*, pages 5579–5585, 2013.

J. M. Soares, A. P. Aguiar, A. M. Pascoal, and A. Martinoli. A distributed formation-based odor source localization algorithm-design, implementation, and wind tunnel evaluation. In *2015 IEEE International Conference on Robotics and Automation (ICRA)*, pages 1830–1836. IEEE, 2015b.

D. Soetanto, L. Lapierre, and A. M. Pascoal. Adaptive, non-singular path-following control of dynamic wheeled robots. In *Proceedings of the 42nd IEEE Conference on Decision and Control*, volume 2, pages 1765–1770, 2003.

A. Speranzon, C. Fischione, K. Johansson, and A. Sangiovanni-Vincentelli. A distributed minimum variance estimator for sensor networks. *IEEE Journal on Selected Areas in Communications*, 26(4):609–621, 2008.

D. J. Stilwell and B. E. Bishop. Platoons of underwater vehicles. *Control Systems, IEEE*, 20(6):45–52, 2000.

S. Sun, J. Lin, L. Xie, and W. Xiao. Quantized Kalman filtering. In *IEEE 22nd International Symposium on Intelligent Control. ISIC 2007.*, pages 7–12. IEEE, 2007.

P. Tabuada. Event-triggered real-time scheduling of stabilizing control tasks. *IEEE Transactions on Automatic Control*, 52(9):1680–1685, 2007.

R. R. Tenney and Nils R. Sandell. Detection with distributed sensors. *IEEE Transactions on Aerospace and Electronic systems*, (4):501–510, 1981.

D. Thanou, E. Kokiopoulou, and P. Frossard. Progressive quantization in distributed average consensus. In *2012 IEEE International Conference on Acoustics, Speech and Signal Processing (ICASSP)*, pages 2677–2680. IEEE, 2012.

D. Thanou, E. Kokiopoulou, Y. Pu, and P. Frossard. Distributed average consensus with quantization refinement. *IEEE Transactions on Signal Processing*, 61(1):194–205, 2013.

R. M. Tifenbach. On an SVD-based algorithm for identifying meta-stable states of Markov chains. *Electronic Transactions on Numerical Analysis*, 38:17–33, 2011.

M. Todescato, A. Carron, R. Carli, and L. Schenato. Distributed localization from relative noisy measurements: A robust gradient based approach. In *2015 European Control Conference (ECC)*, pages 1914–1919. IEEE, 2015.

J. N. Tsitsiklis. Decentralized detection. *Advances in Statistical Signal Processing*, 2(2):297–344, 1993.

V. Ugrinovskii. Distributed robust filtering with consensus of estimates. *Automatica*, 47(1):1–13, 2011.

V. Ugrinovskii. Conditions for detectability in distributed consensus-based observer networks. *IEEE Transactions on Automatic Control*, 58(10):2659–2664, 2013.

J. K. Uhlmann. General data fusion for estimates with unknown cross covariances. In *Aerospace/Defense Sensing and Controls*, pages 536–547. International Society for Optics and Photonics, 1996.

J. K. Uhlmann. Covariance consistency methods for fault-tolerant distributed data fusion. *Information Fusion*, 4 (3):201–215, 2003.

F. Vanni, A. P. Aguiar, and A. M. Pascoal. Cooperative path-following of underactuated autonomous marine vehicles with logic-based communication. In *Proceedings of NGCUV'08-IFAC Workshop on Navigation, Guidance and Control of Underwater Vehicles*, pages 1–6, 2008.

F. V. Vanni. Coordinated motion control of multiple autonomous underwater vehicles. Master's thesis, Instituto Superior Técnico, 2007.

M. Velasco, J. Fuertes, and P. Marti. The self triggered task model for real-time control systems. In *Work-in-Progress Session of the 24th IEEE Real-Time Systems Symposium (RTSS03)*, volume 384, 2003.

M. Verhaegen and V. Verdult. *Filtering and system identification: A least squares approach*. Cambridge university press, 2007.

D. Viegas, P. Batista, P. Oliveira, and C. Silvestre. Decentralized observers for position and velocity estimation in vehicle formations with fixed topologies. *Systems & Control Letters*, 61(3):443–453, 2012.

C. Viel, S. Bertrand, H. Piet-Lahanier, and M. Kieffer. New state estimator for decentralized event-triggered consensus for multi-agent systems. *IFAC-PapersOnLine*, 49(5):365–370, 2016.

C. Viel, S. Bertrand, M. Kieffer, and H. Piet-Lahanier. Distributed event-triggered control for multi-agent formation stabilization. In *IFAC World Congress*, 2017.

R. Viswanathan and P. K. Varshney. Distributed detection with multiple sensors Part I. Fundamentals. *Proceedings of the IEEE*, 85(1):54–63, 1997.

N. G. Wah and Y. Rong. Comparison of decentralized tracking algorithms. In *Proceedings of the International Conference on Information Fusion*, pages 107–113, 2003.

S. Wang and W. Ren. On the convergence conditions of distributed dynamic state estimation using sensor networks: A unified framework. *IEEE Transactions on Control Systems Technology*, (99):1–17, 2017.

X. Wang and M. D. Lemmon. Self-triggered feedback control systems with finite-gain $\mathscr{L}_2$ stability. *IEEE Transactions on Automatic Control*, 54(3):452–467, 2009.

X. Wang and M. D. Lemmon. Event-triggering in distributed networked control systems. *IEEE Transactions on Automatic Control*, 56(3):586–601, 2011.

X. Wang, Y. Sun, and N. Hovakimyan. Asynchronous task execution in networked control systems using decentralized event-triggering. *Systems & Control Letters*, 61(9):936–944, 2012.

P. Willett, P. F. Swaszek, and R. S. Blum. The good, bad and ugly: Distributed detection of a known signal in dependent Gaussian noise. *IEEE Transactions on Signal Processing*, 48(12):3266–3279, 2000.

L. Xiao and S. Boyd. Fast linear iterations for distributed averaging. *Systems & Control Letters*, 53(1):65–78, 2004.

N. Xu. A survey of sensor network applications. *IEEE Communications Magazine*, 40(8):102–114, 2002.

Y. Xu and J. P. Hespanha. Communication logic design and analysis for networked control systems. In L. Menini, L. Zaccarian, and C. T. Abdallah, editors, *Current Trends in Nonlinear Systems and Control*, Systems & Control: Foundations & Applications, pages 495–514. Birkhäuser Boston, 2006.

M. E. Yildiz and A. Scaglione. Coding with side information for rate-constrained consensus. *IEEE Transactions on Signal Processing*, 56(8):3753–3764, 2008.

J. K. Yook, D. M. Tilbury, and N. R. Soparkar. Trading computation for bandwidth: Reducing communication in distributed control systems using state estimators. *IEEE Transactions on Control Systems Technology*, 10(4): 503–518, 2002.

M. M. Zavlanos. *Distributed control of robotic networks*. PhD thesis, University of Pennsylvania, 2008.

K. Zhang, X. R. Li, P. Zhang, and H. Li. Optimal linear estimation fusion - Part VI: Sensor data compression. In *Proceedings of the International Conference on Information Fusion*, volume 23, page 221, 2003.

W. Zhang, Z. Wang, Y. Liu, D. Ding, and F. E. Alsaadi. Event-based state estimation for a class of complex networks with time-varying delays: A comparison principle approach. *Physics Letters A*, 381(1):10–18, 2017.

F. Zhao, J. Shin, and J. Reich. Information-driven dynamic sensor collaboration. *IEEE Signal processing magazine*, 19(2):61–72, 2002.